Identification and characterisation of *Chlamydia psittaci* Inc proteins and mechanistic elucidation of doxycycline-induced persistence of *Chlamydia trachomatis*

Inaugural-Dissertation

to obtain the academic degree
Doctor rerum naturalium (Dr. rer. nat.)

submitted to the Department of Biology, Chemistry, Pharmacy
of Freie Universität Berlin

by

Jean-Marc Gensch

2022

Diese Arbeit wurde von Juni 2017 bis Januar 2021 im Fachgebiet "Sexuell übertragbare bakterielle Krankheitserreger" am Robert Koch-Institut, Berlin unter der Leitung und Betreuung von Dr. Dagmar Heuer angefertigt.

This work was realised from June 2017 until January 2021 in the Unit ‘Sexually Transmitted Bacterial Pathogens’ at the Robert Koch Institute, Berlin and was supervised by Dr. Dagmar Heuer.

First reviewer: Dr. Dagmar Heuer

Second reviewer: Prof. Dr. Markus Wahl

Date of thesis defense: 12.09.2022

Danksagung

Danke!

Ich bedanke mich bei allen, die ich während meiner Promotion kennenlernen durfte, für die gemeinsame,

aufregende

und tolle Zeit!

Ganz besonders möchte ich mich bei Dr. Dagmar Heuer bedanken, dass ich bei FG19 meine Arbeit anfertigen durfte. Das Brainstorming hat mir viel Spaß gemacht.

Auch mit Dr. Sebastian Banhart.

Henning!

Danke!

Selbstständigkeitserklärung

Hierdurch versichere ich, dass ich meine Dissertation selbstständig verfasst und keine anderen als die von mir angegeben Quellen und Hilfsmittel verwendet habe.

Berlin, März 2022 Jean-Marc Gensch

Zusammenfassung

Die obligat intrazellulären Pathogene *Chlamydia trachomatis* und *C. psittaci* können Menschen infizieren, wohingegen *C. psittaci* auch Vögel infiziert. Während der intrazellulären Infektion replizieren und entwickeln sich die Bakterien in einer Einschlussmembran, die sogenannte Inklusion. *Chlamydia* sekretieren Proteine in die Inklusionsmembran, sogenannte Inklusionsmembranproteine, kurz Inc Proteine. Mit Hilfe dieser Proteine modifizieren Sie die Inklusionsmembran und interagieren mit Wirtszellproteinen. Je nach Spezies und Serovar können sie bestimmte Krankheiten verursachen und zu Folgeschäden führen, sollte die Behandlung fehlschlagen. Patienten, die mit *C. trachomatis* serovar D infiziert sind, werden mit dem Translationsinhibitor Doxycyclin behandelt. Doxycyclin induziert bei *C. trachomatis* serovar D einen Zustand, genannt Persistenz, der es ihnen ermöglicht, die Behandlung zu überstehen und anschließend die Infektion fortzufahren. Diese Arbeit identifiziert und charakterisiert *C. psittaci* Inc Proteine, und klärt den Mechanismus der Doxycyclin-induzierten Persistenz von *C. trachomatis* serovar D auf.

C. psittaci, als zoonotischer Erreger von Vögeln und Menschen, wurde auf Wirtszellinteraktionen untersucht, um Spezies-übergreifende Ähnlichkeiten zu entschlüsseln und um die Grundlage der Fähigkeit, sich an verschiedene Wirte anzupassen, besser zu verstehen. Zur Untersuchung der Interaktionen zwischen Inc Proteinen und der Wirtszelle wurde eine neue Methode etabliert: Split-Inc Proteine. Die Split-Inc Proteine bauen auf das grün fluoreszierende Protein eGFP, welches die Membrandomäne der Inc Proteine ersetzt. Die Integration der *N*- und *C*-terminalen cytosolischen Domänen des Inc Proteins ermöglicht es, native Interaktionen zu imitieren. Mit Hilfe des eGFPs der Split-Inc Proteine können Proteininteraktionskomplexe co-immunopräzipitiert und einzelne Interaktionspartner in der Massenspektrometrie identifiziert werden.

In silico-Untersuchungen identifizierten 11 mögliche Inc Proteine in *C. psittaci*, wovon 8 weiter charakterisiert wurden. Die transkriptionelle Quantifizierung ihrer Genexpression ermöglichte die Zuordnung zu bestimmten Phasen der chlamydialen Entwicklung während der Infektion. Unter Verwendung der Split-Inc Proteine wurden für die Inc Proteine CP0355, CP0856, CP0857, CP0558 und CP0598 humane Interaktionspartner identifiziert, die mit der Wirtszellexpression, Cytokinese, Organisation des Cytoskeletts der Wirtszelle, Fettsäuremetabolismus und Aminosäureversorgung zusammenhängen. Für die Inc Proteine CP0534, CP0535 und CP0181 wurde eine Beteiligung an der Stabilität der Inklusion und Organisation von Inc Proteinen in sogenannten Mikrodomänen in der Inklusion vorhergesagt.

Die Untersuchung der Doxycyclin-induzierten Persistenz von *C. trachomatis* serovar D ergab, dass das Pathogen trotz Behandlung mit Doxycyclin translational aktiv ist. Es wurde vermutet,

dass die aktive Translation durch die Trans-translation ermöglicht wird. Die Trans-translation, bekannt aus *Escherichia coli*, ist ein Mechanismus, der die Dissoziation eines ins Stocken geratenen Translationskomlpex bewirkt. Transkriptionelle Quantifizierung ergab, dass *C. trachomatis* serovar D Komponenten des Mechanismus transkribiert, weshalb angenommen wird, dass die Trans-translation zur Persistenz beiträgt. Anschließend wurden Änderungen des chlamydialen Proteoms und der Inklusionsrekrutierten Wirtszellproteine während der Doxycyclin-Behandlung untersucht. Sogenannte markierungsfreie Proteomics wurden durch die Isolierung intakter Inklusionen ermöglicht. Die resultierenden Proteine wurden per Massenspektrometrie identifiziert und ergaben signifikante Anreicherung vom Inc Protein IncD und der Ras-related GTPase Rab12. Folgeuntersuchungen ergaben, dass IncD das Ceramid-Transportprotein CERT während der Persistenz zur Inklusion rekrutiert, was eine Bedeutung der Inklusionsstabilität durch angereicherte Ceramide hervorhebt. Der Knock-down von Rab12 ergab eine verbesserte Erholung von *C. trachomatis* serovar D nach der Doxycyclin-Behandlung, reduzierte allerdings die Nachkommenbildung während der akuten Infektion. Rab12 ist an der Autophagie und der Eisenhomöostase beteiligt. Dies ließ vermuten, dass die Rab12-Rekrutierung in der akuten Infektion die chlamydiale Eisenaufnahme unterstützt und während der Persistenz die Autophagie der Inklusion verhindert. Weiterhin wurde mit Hilfe der Proteome die chlamydiale Proteinregulation analysiert, um Veränderungen bestimmter Stoffwechselwege zu ermitteln. Während der Persistenz sind Enzyme des Citratzyklus leicht erhöht, sowie einige ABC-Transporter. Enzyme der Peptidoglykansynthese und Translation waren reduziert, während MreB, Teil des Divisoms und der Zellteilung, in der Persistenz erhöht vorkam. Anhand der Ergebnisse und vorhandener Publikationen konnte die chlamydiale Persistenz aufgeklärt werden. Somit ist chlamydiale Persistenz die Folge von angehaltener Zellteilung. Jeder Stimulus kann zur Persistenz führen, wenn der Zeitpunkt der Infektion und Behandlungsbeginn, und die Konzentration des Stimulus eine basale chlamydiale Aktivität ermöglichen. Zudem ist das Überleben von *C. trachomatis* serovar D während der Persistenz von der Stabilität der bakteriellen Membran und Inklusion abhängig.

Zusammenfassend konnten neue *C. psittaci* Inc Proteine identifiziert und charakterisiert werden. Die Ermittlung der humanen Wirtszellinteraktionspartner liefert neue und weitere Ansatzpunkte zur Untersuchung von *C. psittaci*. Die neu-etablierte Split-Inc Protein Methode ermöglicht die Imitation nativer Interaktionen und bietet somit eine verbesserte Möglichkeit zur Untersuchung von Interaktionen von Inc Proteinen, die bei zukünftigen Fragestellungen Anwendung finden kann. Zudem wurde die Doxycyclin-induzierte Persistenz von *C. trachomatis* serovar D aufgeklärt und weitere Faktoren identifiziert, die zur chlamydialen Entwicklung beitragen. Die Ermittlung aktiver Translation während der Doxycyclin-induzierten Persistenz bietet Ansätze für interessante Folgeuntersuchungen.

Abstract

The obligate intracellular pathogens *Chlamydia trachomatis* and *C. psittaci* can infect humans, while *C. psittaci* also infect birds. During the intracellular infection, the bacteria replicate and develop inside of a membrane component, called inclusion. *Chlamydia* secrete proteins into the inclusion membrane, so called inclusion membrane proteins (Inc proteins). Inc proteins modify the inclusion and interact with host cell proteins. Dependent on species and even serovar, they cause different diseases with consequential damage if treatment fails. Patients infected with *C. trachomatis* serovar D are treated with the translation inhibitor doxycycline. Doxycycline induces a state in *C. trachomatis* serovar D, called persistence, which enables to persist the treatment and continue infection afterwards. This work identifies and characterises *C. psittaci* Inc proteins, and elucidates the mechanism of doxycycline-induced persistence of *C. trachomatis* serovar D.

C. psittaci, as a zoonotic pathogen of birds and humans, was investigated according to host cellular interaction to decipher interspecies similarities and basics to understand the pathogens' capability to adapt to different hosts. A new method was established to study the interactions between Inc proteins and the host cell: split-Inc proteins. The split-Inc proteins are based on the enhanced green fluorescent protein eGFP, which replaces the membrane domain of Inc proteins. The integration of the N- and C-terminal cytosolic domains of an Inc protein enables mimicry of native interactions. The eGFP portion of split-Inc proteins allows the co-immunoprecipitation of protein interaction complexes and subsequent identification of single interaction partners by mass spectrometry.

In silico analyses identified 11 putative Inc proteins of *C. psittaci*, of which 8 were further characterised. The transcriptional quantification of their gene expression enabled categorisation according to the phase of chlamydial development during the infection. Using split-Inc proteins, human interaction partners were identified for the Inc proteins CP0355, CP0856, CP0857, CP0558 and CP0598. These human interaction partners are associated with host cell expression, cytokinesis, cytoskeletal rearrangements, fatty acid metabolism and amino acid supply. The Inc proteins CP0534, CP0535 and CP0181 were suggested to participate in inclusion stability and organisation of Inc proteins in so-called microdomains in the inclusion.

Investigation of doxycycline-induced persistence of *C. trachomatis* serovar D showed translational activity despite doxycycline treatment. It was assumed that trans-translation enables the active translation. The trans-translation, known from *Escherichia coli*, is a mechanism that dissociated a stalled translation complex. Transcriptional quantification showed that *C. trachomatis* serovar D transcribes components of the trans-translation

mechanism, indicating that trans-translation supports the persistence. Subsequently, differences in the chlamydial proteome and inclusion-recruited host cell proteins were analysed during doxycycline treatment. The isolation of intact inclusions allowed to perform so-called label-free proteomics. The resulting proteins were identified by mass spectrometry and showed significant abundant IncD and Ras-related GTPase Rab12. Follow-up investigations demonstrated that the Inc protein IncD recruits the ceramide transport protein CERT during the persistence, underscoring a role in inclusion stability by enriched ceramides. The knockdown of Rab12 displayed an enhanced recovery of *C. trachomatis* serovar D after doxycycline treatment and a reduced progeny formation during the acute infection. Rab12 is involved in autophagy and iron homeostasis. This let suggest that Rab12-recruitment in acute infection supports chlamydial iron uptake and impedes autophagy of the inclusion during persistence. Using the results of the proteomes, Furthermore, differences in chlamydial protein regulation was analysed to determine changes in metabolic pathways using the proteome data. During persistence, enzymes of the tricarboxylic acid cycle were slightly increased as well as ABC transporter. Enzymes according to peptidoglycan synthesis and translation were reduced, while MreB, part of the divisome and cell division, was abundant in persistence. Based on the results and available publications, chlamydial persistence was elucidated. Therefore, chlamydial persistence is the consequence of stalled cell division. Any stimulus can induce persistence, if time of infection, treatment timing and stimulus concentration allow a basal chlamydial activity. In addition, the survival of *C. trachomatis* serovar D during the persistence depends on the stability of bacterial membrane and inclusion.

In sum, new *C. psittaci* Inc proteins were identified and characterised. The determination of human host cell interaction partners provides new starting points to investigate *C. psittaci*. The newly established split-Inc protein method enables the mimicry of native interactions and serves a better opportunity to investigate interactions with Inc proteins, supporting future investigations. Finally, the doxycycline-induced persistence of *C. trachomatis* serovar D was elucidated and further factors were identified that help understanding the chlamydial development. The determination of translational activity during the doxycycline-induced persistence opens new starting points for interesting follow-up investigations.

Table of Contents

1 Introduction

Nature has challenged humanity with several pathogens that invade the body, replicate and get transferred to other individuals. One particular class of infectious pathogens are intracellular bacteria such as *Mycobacteria* spp. or facultative *Legionella* spp. (Fraser et al. 1977, McDade et al. 1977), *Salmonella* spp. (Gordon et al. 2008) and *Brucella* spp. (Vaughn & Abu Kwaik 2021). Phagocytic invasion is mediated by *Brucella* spp. in a broad range of phagocytes (Fernandez-Prada et al. 2003), *Mycobacterium* spp. in macrophages and monocytes (Clemens & Horwitz 1995) and *Legionella* spp. in alveolar macrophages (Albert-Weissenberger et al. 2007), whereas *Salmonella* spp. infect epithelial cells (Gordon et al. 2008) upon effector-mediated actin rearrangement (Ramos-Morales 2012). After the invasion, they replicate in isolated vacuolar membranous components to escape the endocytic pathway (Vaughn & Abu Kwaik 2021). One unique obligatory intracellular pathogen that follows this infectious strategy is the family *Chlamydiaceae* (Bayramova et al. 2018). In the genus *Chlamydia* of the family *Chlamydiaceae*, *Chlamydia pneumonia* causes the respiratory disease pneumonia (Lamoth & Greub 2010). The human pathogen *Chlamydia trachomatis* consists of three biovars characterised by specific serovars according to the type of disease. The serovars A-C cause the name-giving disease trachoma that leads to blindness (Wright et al. 2008). Members of serovar D-K, are sexually transmitted and can cause infections in the pharynx, rectum (E. P. F. Chow et al. 2016) and urogenital tract (C. Elwell et al. 2016). Sequelae associated with infection of these serovars are ectopic pregnancy, tubal factor infertility and pelvic inflammatory disease (Brunham et al. 1988, J. M. Chow et al. 1990, Ness et al. 2008, J. N. Robertson et al. 1987). Serovars L1-L3 of the third biovar lead to lymphogranuloma venereum (LGV) by invasive urogenital or anorectal infection (C. Elwell et al. 2016) that spread in lymph vessels (Bayramova et al. 2018). Asymptomatic infection with *C. trachomatis*, observed in 70%-80% of infected women and 50% of infected men, increases the risk of complications (Malhotra et al. 2013). The genus *Chlamydia* also contains zoonotic species. *Chlamydia abortus* initially infected cattle but adapted to humans (Bayramova et al. 2018). *Chlamydia psittaci* causes avian psittacosis and is also transferred to humans (Knittler & Sachse 2015).

1.1 The chlamydial developmental cycle

Although *Chlamydia* contain a plasma membrane, periplasm and a cell wall – and thus properties of gram-negative bacteria (Moulder et al. 1980, Schachter & Caldwell 1980) – they lack a sacculus made of peptidoglycan (Barbour et al. 1982, Garrett et al. 1974). However, *Chlamydia* do synthesise peptidoglycan but with a different function. Similar to the Z-ring of *E. coli* (Dewachter et al. 2018), *Chlamydia* produce a peptidoglycan ring to separate the

daughter cells during cell division (G. W. Liechti 2021). The duration of the developmental cycle varies and depends strongly on the *Chlamydia* species and serovar. The highest amount of progeny of *C. psittaci* emerges between 20 and 40 h post-infection (hpi) (Moulder 1985); similarly for *C. trachomatis* serovar L2 until 48 hpi (Dessus-Babus et al. 2008). In contrast, *C. trachomatis* serovar D has 1.5-times longer developmental cycle (Filardo et al. 2019, Todd & Caldwell 1985). Different phenotypes characterise the biphasic developmental cycle: the infectious non-replicative form, called the elementary body (EB), and the non-infectious replicative form, called the reticulate body (RB) (Lawn et al. 1973, Moulder et al. 1980, Tamura & Manire 1967). The EB is the smallest form with a diameter of 0.3 µm (Costerton et al. 1976), has a compact disulphide cross-linked cell wall (Bavoil et al. 1984, Christensen et al. 2019, T. P. Hatch 1976, Newhall & Jones 1983, Tamura & Manire 1967) and a condensed genome packed with histone-like proteins (Hackstadt et al. 1991, Kaul et al. 1997, Tao et al. 1991). EBs are filled with pre-synthesised effector proteins and enzymes (Saka et al. 2011) to interfere with host cell pathways during invasion (C. Elwell et al. 2016) and probably to direct metabolic activity to differentiate into RBs. They preferentially invade epithelial cells (Johnson & Kerr 2015, Maslow et al. 1988) but can also infect macrophages with a low infection efficiency and survive only temporarily, yielding reduced progeny formation (Herweg & Rudel 2016). One of the first contacts between bacteria and the host cell is the reversible electrostatic interaction of bacterial OmcB with heparan sulphate–containing glycosaminoglycans on the human cell surface (Fadel & Eley 2008, Stephens et al. 2001, Su et al. 1996, Su & Caldwell 1998, Taraktchoglou et al. 2001). This primary contact and many further interactions between the bacterium and host cell are species specific (reviewed in Gitsels et al. 2019). Upon binding to the cell surface (Fig. 1), the Type 3 Secretion System (T3SS) of *Chlamydia* injects the pre-synthesised (Saka et al. 2011) effector protein Tarp (translocated actin-recruiting phosphoprotein) into the host cell to promote actin rearrangement and endocytosis (Clifton et al. 2004). The chlamydial developmental cycle continues in the membranous vacuolar compartment called inclusion. During the first 0-2 h, the EB continues secretion of effector proteins, thereby escaping the endosomal-lysosomal degradation pathway (Eissenberg et al. 1983, Friis 1972, Lawn et al. 1973). The EB differentiates in the early phase from 2 to 8 hpi to the second phenotype, the replicative form: the RB (Christensen et al. 2019). During differentiation, the genome decondenses and transcription is activated, leading to *de novo* synthesis of early genes (Shaw et al. 2000). Inclusion membrane proteins, so-called Inc proteins, are secreted into the inclusion membrane to modify the membrane and to interact with host cell proteins (C. Elwell et al. 2016). The inclusion is bound to dynein and transported along microtubules to the microtubule-organising centre (MTOC), where it remains perinuclear (Clausen et al. 1997, S. S. Grieshaber et al. 2003). RBs are larger, with a diameter of 1 µm (Costerton et al. 1976). They replicate via binary fission (Friis 1972, Litwin 1959) in the growing

inclusion from 8 to 24 hpi and express mid-phase genes (Belland, Zhong, et al. 2003, Shaw et al. 2000). In this phase, *Chlamydia* spp. recruit cellular proteins and organelles via Inc proteins to modulate the host cell and provide the bacteria with nutrients for replication and development (Bugalhão & Mota 2019). They also modulate host cell survival by controlling host apoptosis in a complex manner (Sixt 2020). Around 24-36 hpi (Belland, Zhong, et al. 2003), RBs express late-phase genes and start to re-differentiate into EBs. They divide successive into smaller daughter cells (Chiarelli et al. 2020, G. W. Liechti 2021), forming intermediate bodies (IBs) before they finally re-differentiate into EBs. In the late phase of the developmental cycle, 40-60 hpi (Belland, Zhong, et al. 2003), the host cell with the EB-filled inclusion lyses, releasing EBs ready for a new infection round (AbdelRahman & Belland 2005). An alternative egress is extrusion of the complete inclusion, leaving an intact host cell behind. This yet unknown mechanism might aid transmission of *Chlamydia* over a greater distances to infect cells in remote places (Hybiske & Stephens 2007). Under stress situations (Harper et al. 2000, Raulston 1997) or treatment with inhibitors such as antibiotics (Skilton et al. 2009), RBs convert to a particular phenotype, the enlarged aberrant bodies (ABs) (Hammerschlag 2002). In this form, *Chlamydia* persists and recovers upon removing the stimulus, continuing the developmental cycle (Reveneau et al. 2005, Wolf et al. 2000).

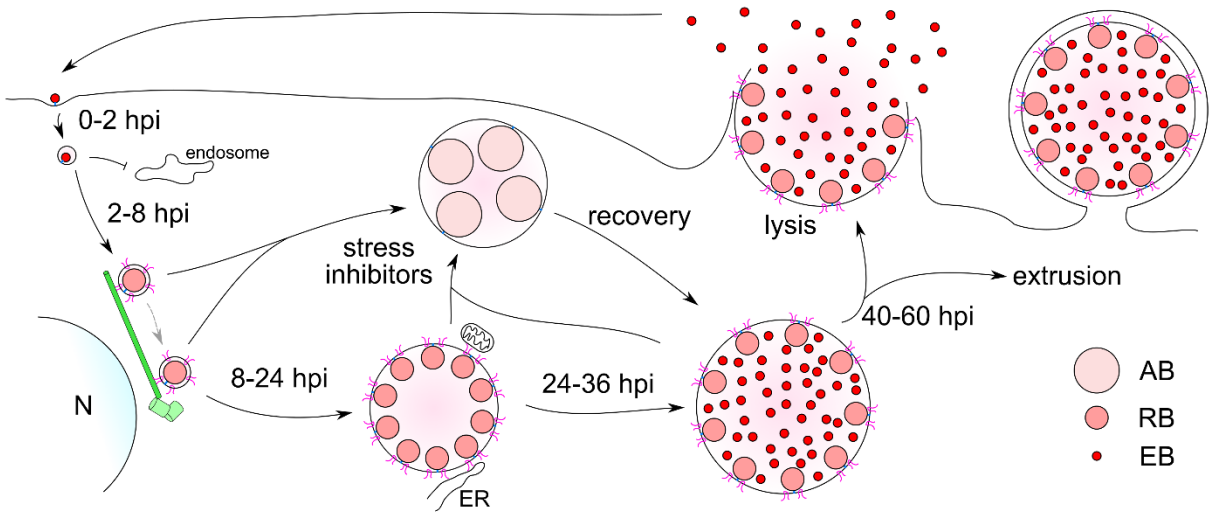

Fig. 1 Schematic overview of the chlamydial infection cycle and development.
Infection starts with an EB that injects effectors via T3SS (blue) into the host cell. The EB invades from 0-2 hpi and escapes fusion with the endosome. Between 2 and 8 hpi, the EB differentiates into the RB, expresses Inc proteins (magenta) and migrates to the MTOC (light green) along microtubules (dark green) close to the nucleus (N). Between 8 and 24 hpi, RBs replicate and rearrange cellular components and organelles. RBs re-differentiate into EBs from 24 to 36 hpi. RBs transform into ABs upon stress stimulus or inhibition. ABs recover upon removal of the stress factor into replicative and infectious life cycle. *Chlamydia* exits via extrusion formation or lysis 40-60 hpi, ready for reinfection.

1.2 The obligatory pathogen

Although metabolically active, the intracellular pathogen *Chlamydia* relies on the host's metabolism. The pathogen's genome is highly reduced. *C. trachomatis* serovar D, for example, has a genome of 1.04 Mb (NCBI reference sequence NC_000117.1), lacking several genes required for metabolism (Fig. 2). *Chlamydia* spp. cannot perform gluconeogenesis and therefore rely on importing host-derived glucose-6-phosphate. This metabolite is processed in glycolysis or the pentose phosphate pathway (Mehlitz et al. 2017) and serves in glycogen biosynthesis (Iliffe-Lee & McClarty 2000). *Chlamydia* must import host-derived amino acids because these species lack many enzymes for amino acid biosynthesis. L-glutamate is imported, converted into 2-ketoglutarate and feeds thus the tricarboxylic acid (TCA) cycle. The TCA cycle of *Chlamydia* is incomplete and proceeds only unidirectionally between 2-ketoglutarate and oxaloacetate over succinate, and thus is unable to metabolise citrate. Imported dicarboxylate is used for the TCA cycle and shuttling between malate and succinate. However, the partial TCA cycle can still generate NADH + H^+ using NAD (Mehlitz et al. 2017). NAD and the nucleotides ATP, GTP, CTP and UTP are actively imported (Fisher et al. 2013). Oxaloacetate from the TCA cycle can be converted into L-aspartate, which is used for peptidoglycan synthesis or proceeds unidirectionally into phosphoenolpyruvate for fatty acid biosynthesis. Taken together, the genome of *Chlamydia* lacks enzymes for biosynthesis of nucleotides and amino acids and harbours a partial unidirectional TCA cycle; hence, the species are dependent on the host's metabolism.

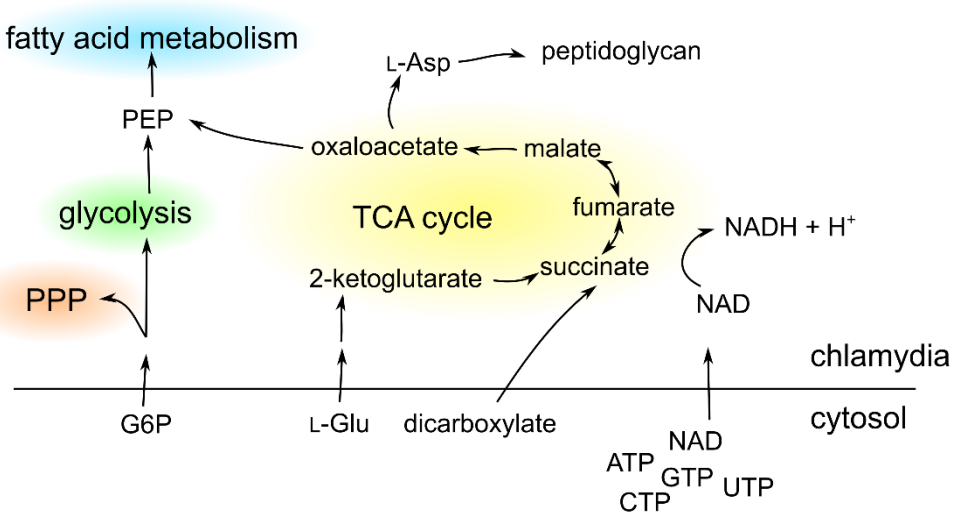

Fig. 2 Schematic overview of chlamydial metabolism and transport.

Glucose-6-phosphate (G6P), L-glutamate (L-Glu), dicarboxylate and nucleotides (ATP, GTP, CTP, UTP, NAD) are actively transported from the host cell into *Chlamydia*. G6P is processed in either the pentose phosphate pathway (PPP) or glycolysis. Glycolysis and the TCA cycle yield phosphoenolpyruvate (PEP) that is processed in fatty acid metabolism. L-glutamate is processed to 2-ketoglutarate. Dicarboxylate and NAD are metabolised in the TCA cycle, yielding NADH + H^+ and oxaloacetate. Oxaloacetate can be converted into L-aspartate (L-Asp) and used for peptidoglycan synthesis.

1.3 Interactions between host cell and *Chlamydia*

The chlamydial inclusion is decorated with secreted membranous chlamydial Inc proteins. They interact with host proteins and organelles to manipulate the host cell, thereby supporting the chlamydial developmental cycle. Inc proteins with distinct functions are expressed during specific phases of the chlamydial developmental cycle from the early to mid and late phase. In general, Inc proteins have at least a bi-lobed transmembrane (TM) domain (Rockey et al. 1995). Their signal peptide that drives secretion by T3SS lacks a consistent sequence, but computational investigations have identified a kind of pattern to predict secretion (Dehoux et al. 2011). The first identified Inc protein was IncA from *C. psittaci* (Rockey et al. 1995), followed by IncB and IncC (Bannantine et al. 1998). Orthologues have been found in different species, but they have low similarity according to the amino acid sequence (Dehoux et al. 2011, Lutter et al. 2012). To date, numerous Inc proteins of *C. trachomatis* have been identified and studied. The Soluble *N*-ethylmaleimide-sensitive factor attachment protein receptor (SNARE)-like domains of IncA interact homotypically to mediate fusion of separate inclusions within the same host cell (Ronzone & Paumet 2013), but IncA also interacts with vesicle associated membrane protein VAMP3/7/8 (Delevoye et al. 2008). Kumagai et al. (2018) recently showed that IncD recruits ceramide transport protein CERT, a phenomenon dependent on interaction with its C-terminus and N-terminus. IncE interacts with the Sorting-Nexin proteins SNX5 and SNX6, which participate in retrograde trafficking (C. A. Elwell et al. 2017, Paul et al. 2017, Sun et al. 2017). IncG was the first Inc protein demonstrated to interact with 14-3-3-β (Scidmore & Hackstadt 2001), whose role remains unknown (Bugalhão & Mota 2019) but is suggested to interact directly with lipid droplets (C. Elwell et al. 2016). The interaction between the endoplasmic reticulum (ER) and inclusion is driven by IncV and VAMPs (Stanhope et al. 2017), and even filamentous actin is remodelled around the inclusion by InaC (Kokes et al. 2015). Mirrashidi et al. (2015) identified interaction partners for 38 partially putative Inc proteins, reflecting the scale and complexity in host cell modulation by Inc proteins.

1.4 *Chlamydia* recruits Ras-related small GTPases

One family of the most recruited proteins is the Ras-related small GTPase (Rab) (Bugalhão & Mota 2019). Researchers have shown selective recruitment of certain Rabs (Rzomp et al. 2003), which are involved in intracellular organisation and trafficking amongst organelles. Rabs are molecular switches used in a regulatory manner. Hutagalung & Novick (2011) summarised the regulatory process as follows (Fig. 3). The inactive form bound to GDP interacts with a Rab escort protein (REP), aiding geranylgeranyl transfer to the C-terminus of Rab, leading to translocation to a target membrane via anchoring of the geranylgeranyl post-modification. The inactive Rab requires interaction with a guanine nucleotide exchange factor (GEF) to exchange GDP for GTP. The active Rab bound to GTP interacts locally with human effector proteins,

and this interaction proceeds downstream outcomes. The active Rab slowly hydrolyses GTP to GDP, but this speed is enhanced upon interaction with a GTPase activating protein (GAP), leading to the inactive Rab-GDP form. Interaction with a guanine nucleotide dissociation inhibitor (GDI) releases the inactive Rab from the membrane into a cytosolic form. A GDI dissociation factor (GDF) mediates GDI release and anchors the inactive Rab into the target membrane, and the cycle can repeat. This complex and highly regulated mechanism enables chlamydial interference at distinct points, allowing *Chlamydia* to take over and affect cellular trafficking. After invasion into the host cell, *Chlamydia* recruits Rab4 and Rab11 (Rzomp et al. 2003). At 18 hpi, the inclusion membrane of *C. trachomatis* was decorated with the secretory-related Rab6 and Rab1 (Rzomp et al. 2003). The knockdown of Rab6 and Rab11 inhibited the transport of ceramide to the inclusion that was correlated with the affected stability of the Golgi apparatus (Rejman Lipinski et al. 2009). Rab39a and Rab39b, which participate in vesicular transport (Gambarte Tudela et al. 2019), and Rab14, which is involved in vesicular sphingolipid delivery (Capmany et al. 2019), are recruited to the inclusion membrane (Capmany et al. 2019, Gambarte Tudela et al. 2019), demonstrating the necessity of *Chlamydia* to control Rab-mediated pathways.

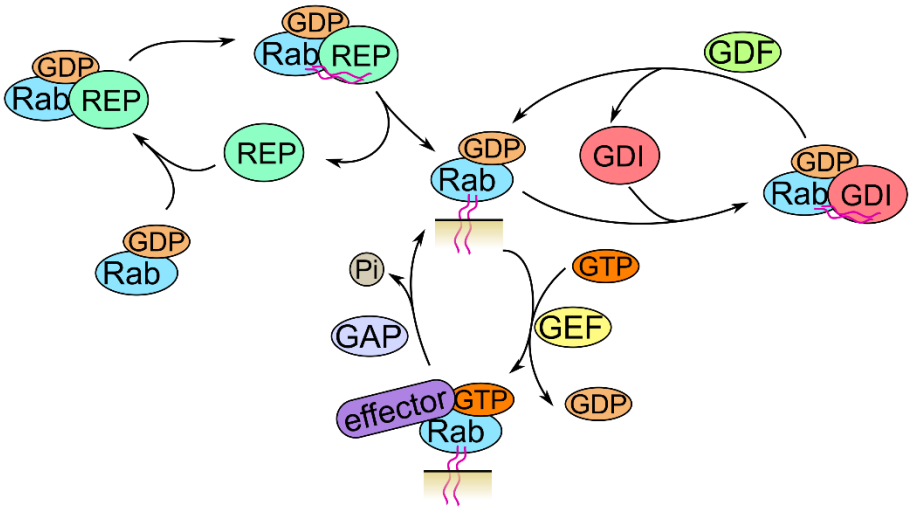

Fig. 3 Overview of Rab protein dynamics.

The inactive GDP-bound Rab requires REP for geranylgeranyl transfer (magenta) and anchoring to the target membrane. The GEF-mediated exchange of GDP for GTP converts Rab into the active form, which interacts with effector proteins. GAP enhances GTP hydrolysis. Interaction with GDI enables solubilisation of inactive Rab into the cytosol. GDF drives anchoring of the inactive soluble Rab into the target membrane. Abbreviations: Rab escort protein (REP), guanine nucleotide exchange factor (GEF), GTPase activating protein (GAP), guanine dissociation inhibitor (GDI), GDI dissociation factor (GDF).

1.5 Rab12 regulates autophagy

Autophagy is a eukaryotic process for the degradation of proteins aggregates, defective mitochondria or bacteria, and plays an important role for *C. trachomatis* (Witkin et al. 2017). In

brief, a membrane component, called autophagosome, encloses the target structure and fuses with the lysosome for final degradation (Witkin et al. 2017). The small GTPase Rab12 was shown to regulate autophagy (Matsui & Fukuda 2013). Rab12 interacts with proteins typical for the superfamily of small GTPases. One relevant GEF for Rab12 is Dennd3 (Matsui et al. 2014). This protein contains a PH-like domain that binds filamentous actin required for autophagy (J. Xu et al. 2018). Wojnacki & Galli (2018) summarised the mechanism as follows: the activated GEF Dennd3 binds Rab12 and is subsequently phosphorylated at Y940, leading to the interaction of the complex with filamentous actin. Myosin II catches the complex and transports it along the filament to elongating phagophores bound by Rab12. Efergan et al. (2016) deciphered a mechanism of microtubule-dependent retrograde transport of secretory granules in mast cells. This transport is performed by a protein complex consisting of GTP-bound Rab12, its effector RILP and dynein. They mentioned the accumulation of secretory granules by constitutively GTP-bound Rab12 in the perinuclear region. Wojnacki & Galli (2018) proposed transport of the autophagosome to the lysosome by the mechanism revealed by Efergan et al. (2016). Furthermore, Rab12 regulates membrane traffic pathways from recycling endosomes to lysosomes, thereby degrading the marker for recycling endosomes: transferrin receptor (Matsui et al. 2011). Puri et al. (2013) framed the correlation of recycling endosomes with autophagosomes. They depicted the source of the autophagosomal membrane derived from recycling endosomes. Rab12 KD inhibits autophagy and increases mTORC1 activity (Matsui & Fukuda 2013); this phenomenon highlights the central role of Rab12 as a positive regulator of autophagy (J. Xu et al. 2015). The role of autophagy in *C. trachomatis* was investigated. Yasir et al. (2011) showed increased progeny formation upon treatment with bafilomycin A1, an inhibitor of V-ATPase, which is necessary for lysosomal acidification. Bafilomycin A1 also inhibits sarco/endoplasmic reticulum Ca^{2+} ATPase (SERCA)-dependent autophagosome-lysosome fusion (Mauvezin & Neufeld 2015). Agaisse & Derré (2015) pinpointed the relevance of Ca^{2+} in chlamydial development by showing more ER contact sites with the inclusion membrane upon treatment with the SERCA inhibitor thapsigargin. These published results demonstrate the close correlation of the mentioned mechanisms and highlight the complexity of autophagy.

1.6 The zoonotic pathogen *C. psittaci*

Another focus of this work is investigation of the zoonotic pathogen *C. psittaci*. First reported in 1893 (Vanrompay et al. 1995), *C. psittaci* was originally an avian pathogen observed in *Psittacinae*, pigeons and poultry (Chen et al. 2020). This pathogen leads to psittacosis and ornithosis in birds and humans (Vanrompay et al. 1995) and manifests as pneumonia in humans (Balsamo et al. 2017, Hogerwerf et al. 2017). Ingestion of contaminated faeces or inhalation of dust from contaminated feathers or faecal material enables intraspecies or

zoonotic interspecies transmission of *C. psittaci* (Chen et al. 2020, Page 1959). Thus, people who are frequently in close contact with birds, such as owners or zookeepers, are more likely to be infected. Sequential genomic investigations have revealed that *C. psittaci* belongs to the genus *Chlamydia* (Knittler & Sachse 2015). Although *C. psittaci* has been investigated for a long time, little is known about its interaction with the host cell. A typical phenomenon of *Chlamydia* species is the lack of amino acid sequence similarities. Inc proteins that interact with the host cell differ distinctly according to the sequences. Lutter et al. (2012) screened different strains and serovars of *Chlamydia* to identify so-called core Inc proteins and species-specific non-core Inc proteins. Two well-known core Inc proteins, IncB and IncC, occur in all *Chlamydia* species (at least in *Chlamydia pecorum*, *C. pneumoniae*, *C. trachomatis*, *C. psittaci*, *C. muridarum*, *C. abortus*, *C. caviae* and *C. suis* according to NCBI) but have poor sequence similarities. Their interaction partners vary. For example, IncB of *C. psittaci* interacts with human Snapin, a protein involved in intracellular trafficking and the microtubule network (Böcker et al. 2014). In contrast, no interaction for IncB of *C. trachomatis* has been identified yet (Mirrashidi et al. 2015). Another example is IncA of *C. trachomatis* that interacts homotypically (Ronzone & Paumet 2013) and with VAMP3/7/8 (Delevoye et al. 2008), whereas IncA of *C. psittaci* interacts with Ras-GTPase activating protein SH3 domain-binding protein 1 (G3BP1) (Borth et al. 2011). It is fundamental for zoonotic pathogens to adapt to different hosts. *C. psittaci* challenges birds and humans with a genome that is similar to other members of the same genus that infect only humans or only birds (Hölzer et al. 2020). Identifying Inc proteins and their interaction partners is essential to understand the minimum interaction required for successful pathogenesis in humans, birds or both.

1.7 Clinical complications and chlamydial persistence

Based on the disease, *C. trachomatis* is clinically treated with either azithromycin, doxycycline or combination of both with varying recommended concentrations (Workowski et al. 2021). The widely used dose for doxycycline is around 200 mg or 100 mg twice per day for 7 days (Workowski et al. 2021). An oral dose of 200 mg doxycycline results in a serum concentration of 4.8 ± 0.3 µg/ml (Agwuh & MacGowan 2006). The clinical dose of azithromycin is 1 g. An alternative is the antibiotic levofloxacin given at 500 mg daily for 7 days, but this is only recommended as an exception (Workowski et al. 2021). Despite successful treatment of *C. trachomatis* with doxycycline and less effective treatment with azithromycin (Dombrowski et al. 2021, Dukers-Muijrers et al. 2019, Geisler et al. 2015, Kong et al. 2014, Páez-Canro et al. 2019), reports have emerged during the last decades of unsuccessful treatment and the return of disease symptoms (Dukers-Muijrers et al. 2019, Kong et al. 2014, Lau & Qureshi 2002, Molano et al. 2005, Páez-Canro et al. 2019, Suchland et al. 2017). Asymptomatic *C. trachomatis* infection is common amongst men and women (Workowski et al. 2021), and

treatment failures cumulatively and critically increase the subsequent damage of infected patients. Treatment failures are often correlated with antibiotic resistance. Bacteria can gain antibiotic resistance by horizontal gene transfer (HGT) of genomic islands, including efflux pumps, modifying enzymes and target mutations (Borel et al. 2016, Partridge et al. 2018). Unlike other bacteria, no clinical isolate of *Chlamydia* spp. carrying such a genomic island has been identified except for the zoonotic *Chlamydia suis* (Lenart et al. 2001). Tetracycline-containing feed was widely used in the 1950s in swine livestock, the host of *C. suis*, but was banned due to increasing resistance in the 1970s (Borel et al. 2016). Due to the circumstances, *C. suis* stably acquired resistant genomic islands through intraspecies HTG (Dugan et al. 2004). Cell culture experiments co-infecting cells with tetracycline-resistant *C. suis* and *C. trachomatis* or *Chlamydia muridarum* demonstrated successful intraspecies HGT. In contrast, there was no intraspecies HGT when using an artificially generated resistant strain of *Chlamydia caviae* as a donor (Suchland et al. 2009). Furthermore, genomic mosaicism by interspecies HGT was only reported for non-resistant clinical isolates of *C. trachomatis* (Harris et al. 2012, Jeffrey et al. 2010). However, resistant *C. trachomatis* emerge rarely in patients, and such clinical isolates with unstable mutations in drug targets that diminish as they are passaged in the laboratory (Mestrovic & Ljubin-Sternak 2018). Long-term investigations of patients have revealed that *Chlamydia* could survive and persist for 5 years without antibiotic resistance (Molano et al. 2005, Suchland et al. 2017). *Chlamydia* turned out to persist even in the presence of antibiotic and subsequently reactivated and continued the developmental cycle (Reveneau et al. 2005, Wolf et al. 2000). They are known to transform from RBs to an enlarged aberrant persisting form (Hammerschlag 2002), called ABs. The emergence of ABs in patients was proven by electron microscopy (EM) (Bragina et al. 2001, Lewis et al. 2014). Various persistence inducers are known and have been investigated – for example, quinolones such as nalidixic acid and ciprofloxacin (Dreses-Werringloer et al. 2000), azithromycin (Xue et al. 2017), penicillin (Skilton et al. 2009) and interferon gamma (IFN-γ) (Reveneau et al. 2005). IFN-γ, a cytokine, came into focus because it is part of the innate immune response and plays a role in inflammatory response and immunomodulation (Schroder et al. 2004). This kind of persistence induction has been well investigated and characterised. IFN-γ induces upregulation of human indoleamine 2,3-dioxygenase that degrades L-tryptophan to *N*′-formylkynurenine, which cannot be metabolised by *C. trachomatis*, thus leading to L-tryptophan starvation and subsequent persistence (Pokorzynski et al. 2019). Transcriptomic investigations of IFN-γ-treated *C. trachomatis* showed upregulation of the *trp*RBA operon that encodes the repressor (TrpR) and the α-subunit (TrpA) and β-subunit (TrpB) of tryptophan synthase (Belland, Nelson, et al. 2003). The chlamydial TrpA is not functional but binds to the catalytic active TrpB as an αββα heterotetramer, thereby enhancing the conversion from indole to L-tryptophan driven by TrpB (Michalska et al. 2021). Indole is supposed to be provided by

the microbial flora of the female genital tract as an additional source (Caldwell et al. 2003). Due to the identification of upregulated genes during persistence, a persistence stimulon with a complex mechanism has been proposed (Belland, Nelson, et al. 2003). Transcriptional investigation upon iron depletion, known to induce persistence (Thompson & Carabeo 2011), revealed a complex iron- and tryptophan-dependent repressive relationship between gene regulation of *trp*BA and *ytg*CR, which encodes the cleavable fusion protein ABC transporter permease YtgC and the iron-dependent repressor YtgR (Pokorzynski et al. 2020). Researchers recently showed that mimicking L-tryptophan depletion by distinct inhibition of the tryptophanyl-tRNA synthase resulted in chlamydial persistence but yielded a different transcriptional regulation of *euo* (N. D. Hatch & Ouellette 2020) than determined for IFN-γ-induced L-tryptophan depletion (Ouellette et al. 2006).

Another well-studied inducer is the group of β-lactam antibiotics, comprising penicillin and ampicillin, amongst others. Studies have revealed the peptidoglycan ring is stalled by inhibition of synthesis (Brockett & Liechti 2021) and interaction with penicillin-binding proteins (Haeusser & Margolin 2016). Detailed analysis of the peptidoglycan synthesis in persistence induced by different stimuli demonstrated the absence of peptidoglycan upon failure of replication, chromosome segregation and translation inhibition (Brockett & Liechti 2021). Less investigated is persistence driven by translation inhibitors, but several studies have revealed concentration-dependent persistence that relies on the time of infection (Marangoni et al. 2020, Xue et al. 2017). Natural infection is mostly unsynchronised, with multiple follow-up infections leading to a batch of *Chlamydia* at different developmental phases. In this circumstance, antibiotic treatment might not eliminate all chlamydial bacteria, leading to survival of persistence-induced *Chlamydia*. Overall, IFN-γ-dependent and IFN-γ-independent L-tryptophan starvation, iron-depletion and translation inhibition highlight that translation is a bottleneck for persistence, an area that is poorly understood and requires further investigation.

1.8 Prokaryotic translation and trans-translation

The ribosomal assembly for prokaryotic translation starts with the small ribosomal subunit 30S (reviewed by Rodnina 2018). The proteins IF1, IF3 and the GTP-bound IF2 bind to the 30S, which leads to the association of the fMet-tRNA^{fMet}. This complex allows binding and screening of an mRNA until the start codon AUG matches with the fMet-tRNA^{fMet}. In this state, the large ribosomal subunit 50S subunit joins the complex forming the 70S ribosome. The 50S has an A-site for aminoacyl-tRNA, a P-site for peptidyl-tRNA and an E-site for the exit. Upon joining, the fMet-tRNA^{fMet} is located in the P-site. The GTP in F2 is hydrolysed, leading to the release of GDP-F2 and F1, which starts the translation. An aminoacyl-tRNA that matches the mRNA codon enters the A-site, where the aminoacyl-residue is transferred to the elongating peptide. This tRNA moves thereby to the P-site, and the initial fMet-tRNA enters the E-site, where it

dissociates from the translation complex. A stop codon finishes the translation and leads to the dissociation of all components.

Trans-translation is a mechanism for dissociating ribosomes that are stalled due to translational interference or by reaching the 3' end of mRNAs lacking the stop codon (Giudice et al. 2014). The driving components of this mechanism are tmRNA and the tmRNA-binding protein SmpB. Recent work has shown that tmRNA increased in *E. coli* treated with ribosomal inhibitors (Andini & Nash 2011), making the mechanism as putative candidate for the driving force of doxycycline-induced persistence in *C. trachomatis* serovar D. In *E. coli*, the *SsrA* gene is transcribed into pre-tmRNA and processed into tmRNA. The tmRNA combines the tertiary structure shape of a tRNA with a short mRNA strand encoding a degradation signal peptide with a stop codon. The tRNA-mimicking part of tmRNA is charged with an alanyl residue. Together with SmpB, the elongation factor Tu and ribosomal protein S1, tmRNA is part of the ribonucleoprotein complex tmRNP. The tRNA-like portion of the complex enters the A site of a stalled ribosome. The alanyl-residue of the tmRNA is transferred to the current peptide in the peptidyl-transferase centre. After this initiation, the initial mRNA of the stalled ribosome is replaced by tmRNA during translation of the tmRNA open reading frame (ORF). The translated mRNA of tmRNA tags the degradation peptide to the current protein using regular aminoacyl-tRNAs. The stop codon of tmRNA leads to release of the tagged protein and dissociation of the translation complex. The tagged protein is degraded and the tmRNA-SmpB complex is re-used.

1.9 Aims of this thesis

The investigation of chlamydial interaction with the host cell is essential to understand the interspecies adaptation to different hosts and the ability to maintain intracellular survival. This fundamental interaction will be investigated in detail in the first part of this thesis. Putative Inc proteins of *C. psittaci* will be analysed and characterised. In addition, host cellular interaction partners of these Inc proteins will be identified. This information is predicted to support the understanding of chlamydial interactions necessary to maintain infection in human epithelial cells, indicating correlations with the human pathogen *C. trachomatis*.

Another central aspect of this thesis will be the investigation of the doxycycline-induced persistence of *C. trachomatis* serovar D. The chlamydial persistence is a critical factor in patients suffering from consequential damage, highlighting the relevance of this work. A basic persistence mechanism is presumed and therefore analysed morphological, translational, transcriptional, and proteomic, thereby focussing on chlamydial protein expression and interactions with host cellular proteins at the inclusion membrane.

The first aim of this work is to decipher a supposed interspecies consensus of interaction with host cellular proteins that might reveal the secret of chlamydial adaptation to different hosts. The second aim is the investigation of chlamydial persistence that will gather information suitable to generate hypotheses or even elucidate the mechanisms of persistence.

2 Materials & methods

2.1 Materials

2.1.1 Software

tool	publishers	online
BLAST	NCBI	https://blast.ncbi.nlm.nih.gov/Blast.cgi
Clustal Omega	Madeira et al. 2019	https://www.ebi.ac.uk/Tools/msa/clustalo
Jpred 4	Drozdetskiy et al. 2015	http://www.compbio.dundee.ac.uk/jpred4/index.html
Protter	Omasits et al. 2014	http://wlab.ethz.ch/protter/start/
ProtScale Hydrophobicity tool	Gasteiger et al. 2005	https://web.expasy.org/protscale/
Geneious® 11.1.5	Biomatters development team	https://www.geneious.com/
Cytoscape 3.8.2	Shannon et al. 2003	https://cytoscape.org/
ClueGO 2.5.7	Bindea et al. 2009	https://apps.cytoscape.org/apps/cluego
GraphPad Prism 8.4.0	GraphPad Software	https://www.graphpad.com/
Inkscape 0.92.3	Free Software Foundation, Inc.	https://www.inkscape.org/
PyMOL	The PyMOL Molecular Graphics System, Version 2.0 Schrödinger, LLC	https://pymol.org/2/

2.1.2 Antibodies, enzymes & proteins

antibody	manufacturers ID	manufacturer	dilution in IF	dilution in western blot
α-cHsp60(A57-B9)^{m}	MA3-023	Thermo Fisher Scientific	1:500	
α-IncA^{rb}		in-house production	1:500	
α-IncE$_{C}^{rb}$		in-house production		1:500
α-FLAG^{m}	F1804-50UG	Sigma-Aldrich	1:100	
α-c-myc(9E10)^{m}	sc-40	Santa Cruz Biotechnology	1:100	
α-myc(71D10)^{rb}	2278	Cell Signaling Tech.	1:50	
α-HA^{rb}	ab9110	abcam	1:250	
α-SNX5^{rb}	ab180520	abcam		1:500
α-GFP^{rb}	A-6455	Invitrogen		1:5000
α-mouse-Alexa Fluor® 488	115-545-146	Dianova	1:100	
α-mouse-Cy™3	115-165-146	Dianova	1:200	
α-mouse-Alexa Fluor® 647	115-605-146	Dianova	1:100	

α-rabbit-Cy™3	111-165-144	Dianova	1:200	
α-mouse-HRP	926-80010	Li-Cor Biosciences		1:5000
α-rabbit-HRP	926-80011	Li-Cor Biosciences		1:5000

enzyme	**manufacturers ID**	**manufacturer**
AscI	R0558S	NEB
NotI-HF	R3189S	NEB
T4 DNA Ligase 5 U/µl	EL0014	Thermo Scientific
BigDye®		Thermo Fisher Scientific Inc.
Trypsin (sequencing grade modified)	V5111	Promega
0.25% trypsin-EDTA 1x	25200072	Gibco
DNaseI (RNase-free)	M0303S	NEB
Antarctic phosphatase	M0289S	NEB
Proteinase K (20 mg/ml)	P8102	NEB
Phusion High-Fidelity PCR Master Mix with HF Buffer	F531L	Thermo Scientific

protein	**manufacturers ID**	**manufacturer**
BSA, Albumin fraction V	8076.2	Roth
Murine RNase Inhibitor	M0314S	NEB

2.1.3 Organisms

eukaryote	**origin**	**source**
HeLa cells	isolate from human cervical cancer cells	ATCC: CCL-2
HeLa CRISPR/Cas9 CTRL cell	Koch-Edelmann et al. 2017	
HeLa CRISPR/Cas9 CERT-KO cells	Koch-Edelmann et al. 2017	
HeLa CRISPR/Cas9 SNX5/6 double KO cells	Dissertation Laura Rose 2019	

prokaryote	**origin**	**manufacturers ID**	**manufacturer/source**
NEB® 5-alpha F'I^q Competent *E. coli* (High Efficiency)	*E. coli* DH5α	C2992H	NEB
Chlamydia trachomatis serovar D	human cervix isolate UW-3/Cx	VR-885	ATCC
Chlamydia psittaci 02DC15	bovine isolate		Schöfl et al. 2011

2.1.4 Buffers & media

Commercial buffers & media

product	manufacturers ID	manufacturer
6x DNA Loading Dye	R06F	Thermo Scientific
SOC Outgrowth Medium	C2992H	NEB
1x DMEM, +4.5 g/L D-Glucose, -L-Gln, -Pyruvate	R31053-028	Gibco
1x DMEM, +4.5 g/L D-Glucose, -L-Gln, -Sodium pyruvate, -L-Methionine and L-Cystine	R21013-024	Gibco
1x RPMI Medium 1640, + L-Glutamine	R21875-034	Gibco
10x CutSmart® Buffer	B7204	NEB
10x T4 DNA Ligase buffer	B69	Thermo Fisher Scientific
1x PBS pH 7.2, -$CaCl_2$, -$MgCl_2$	R20012-016	Gibco
1x OPTI-MEM® I Reduced Serum Medium	R31985-062	Gibco
10x DNase I buffer	B0303S	NEB

Self-prepared buffers

buffer	ingredients
1x HSMG	20 mM HEPES, 1.25 M sucrose, 7.5 mM $MgCl_2$, 2.5 mM EGTA, pH 7.4
TRIzol	38% Acid Phenol:Chloroform, 0.8 M guanidine thiocyanate, 0.4 M ammonium thiocyanate, 0.1 sodium acetate, 5% glycerol, pH 5.0
1x SDS separation gel buffer	1.5 M Tris, 0.4% SDS, pH 8.8
1x SDS stocking gel buffer	0.5 M Tris/HCl, 0.4% SDS, pH 6.7
1x SDS-PAGE running buffer	24.7 mM Tris, 191.8 mM glycine, 0.1% SDS
1x western blot buffer	24.7 mM Tris, 191.8 mM glycine, 20% methanol
4x Laemmli buffer	250 mM Tris/HCl, 32% glycerol, 6% 2-mercaptoethanol, 4% SDS, 0.02% bromphenol blue, pH 6.8
1x TBS buffer	100 mM Tris/HCl, 1.5 mM NaCl, pH 8.0
1x LB medium	10 g/L trypton, 5 g/L yeast extract, 5 g/L NaCl

2.1.5 Materials, kits & devices

kit	manufacturer
Plasmid Midi Kit	QIAGEN
Wizard® SV Gel and PCR Clean-up System	Promega
iST GFP-Trap Kit	Chromotek
Power SYBR® Green RNA-to-CT™ 1-Step Kit	Thermo Fisher Scientific Inc.

device	manufacturer
Carl Zeiss LSM 780	Carl Zeiss
NanoDrop™ 2000	Thermo Scientific
SDS-PAGE chambers	Bio-Rad

material	manufacturer
Whatman™ paper	VWR
Immobilon®-P Transfer Membrane	Millipore®
Amersham Hyperfilm™ ECL	GE Healthcare Limited

SDS-containing acrylamide gels

gel	ingredients
10% separation gel	5 ml 1x SDS separation gel buffer, 6.6 ml Rotiphorese®Gel30 (30% acrylamide, 0.8% bisacrylamide), 8.2 ml H_2O, 200 µl 10% APS, 20 µl TEMED
15% separation gel	5 ml 1x SDS separation gel buffer, 9.9 ml Rotiphorese®Gel30 (30% acrylamide, 0.8% bisacrylamide), 4.9 ml H_2O, 200 µl 10% APS, 20 µl TEMED
stacking gel	2.5 ml 1x SDS stacking gel buffer, 1.6 ml Rotiphorese®Gel30 (30% acrylamide, 0.8% bisacrylamide), 5.8 ml H_2O, 100 µl 10% APS, 10 µl TEMED

2.1.6 Solutions, compounds & chemicals

chemical	manufacturers ID	manufacturer
Agarose NEEO ultra-quality	2267.5	Roth
Midori Green Advance DNA Stain	MG04	NIPPON Genetics EUROPE GmbH
FBS (foetal bovine serum)	F7524	Sigma-Aldrich
L-Glutamine 200 mM (100x)	R25030-024	Gibco
Sodium pyruvate 100 mM (100x)	R11360-039	Gibco
Dimethylsulphoxide ROTISOLV®	HN47.1	Roth
L-Homopropargylglycin (L-HPG)	CLK-1067-25	Jena Bioscience
HiPerFect® Transfection Reagent	301705	QIAGEN
Lipofectamine® 2000 Reagent	52887	Invitrogen
Paraformaldehyde	0335.3	Roth
MitoTracker™ DeepRed FM	M22426	Invitrogen
Phalloidin iFluor-555	ab176456	abcam
DAPI	D9542	Sigma-Aldrich
Alexa Fluo®546 Azide	CLK-1283-1	Jena Bioscience
Triton X 100	3051.2	Roth
Mowiol® 4-88 granula	0713.2	Roth

Percoll® pH 8.5-9.5 (20°C)	P1644-500ML	Sigma-Aldrich
cOmplete™ Mini, EDTA-free protease inhibitor	R11836170001	Sigma-Aldrich
ROTI®Quant	K015	Roth
Water BioScience-Grade, nuclease-free, autoklaved, DEPC-treated	T143.3	Roth
Dithiothreitol (DTT)	6908.1	Roth
2-iodoacetamide (IAA)	I1149-5G	Sigma-Aldrich
Urea	U5128-500G	Sigma-Aldrich
Thiourea	HN37.1	Roth
Trifluoroacetic acid (TFA)	302031-100ML	Sigma-Aldrich
Water, ROTISOLV® ultra LC-MS	HN43.1	
ACN Acetonitrile LC-MS CHROMASOLV R	34967-250ML	Fluka
Methanol	8388.5	Roth
Acid Phenol:Chloroform 5:1 solution, pH 4.5 +/-0.2, MB Grade	AM9722	Ambion
Water with 0.1% Formic Acid (v/v), Optima™ LC/MS Grade	LS118-500	Fisher Chemical
Isopropanol ROTIPURAN®	6752.4	Roth
Trichloromethane/Chloroform ROTIPURAN®	3313.1	Roth
Ethylenediaminetetraacetic acid (EDTA)	8040.3	Roth
Ethylene glycol-bis(β-aminoethyl ether)-*N*,*N*,*N*′,*N*′-tetraacetic acid (EGTA)	3054.2	Roth
(+)-Sodium L-ascorbate, BioXtra	11140-50G	Sigma-Aldrich
Tri-sodium citrate dihydrate	4088.3	Roth
NaOH, Sodium hydroxide, BP as pellets	P031.1	Roth
HCl Hydrochloric acid	X896.1	Roth
HEPES PUFFERAN®, buffer grade	HN78.2	Roth
Rotiphorese® Gel 30 (37.5:1) (30% Acrylamide, 0.8% Bisacrylamide)	3029.2	Roth
APS (Ammonium persulphate)	A3678	Merck
Bromphenol blue	A512.1	Roth
Tetramethylethylenediamine (TEMED), for electrophoresis	2367.1	Roth
Milk powder	T145.3	Roth
TRIS-hydrochlorid PUFFERAN®	9090.2	Roth
$Cu(II)SO_4$	451657-10G	Sigma-Aldrich
Sodium dodecyl sulphate (SDS) pellets, for biochemistry	CN30.2	Roth
NonidetTM P 40 Substitute BioXtra, mixture of 15 homologues	74385-1L	Sigma-Aldrich

Sodium acetate, water-free	X891.1	Roth
NaCl, sodium chloride	3957.1	Roth
Ammonium thiocyanate	4477.1	Roth
Guianidine thiocyanate, for biochemistry	0017.1	Roth
Glycine, CELLPURE®	HN07.3	Roth
Glycerol	6962.1	Roth
Ethanol ROTIPURAN®	9065.3	Roth
2-Mercaptoethanol	4227.3	Roth
GeneRuler 1 kb DNA Ladder, ready-to-use	SM0313	Thermo Scientific
GeneRuler 100 bp DNA Ladder, ready-to-	SM0243	Thermo Scientific
Tween® 20	9127.1	Roth
Detection Reagent 2 *Luminol* Enhancer	1859697	Thermo Scientific
Detection Reagent 1 *Peroxide* Solution	1859700	Thermo Scientific
Tris	4855.2	Roth
$MgCl_2$	KK36.1	Roth
Trichloroacetic acid	3744.2	Roth

Antibiotics & inhibitors

chemical	manufacturers ID	manufacturer
Kanamycin	T832.3	Roth
Cycloheximide	8682.1	Roth
Azithromycin	J66740.06	Thermo Fisher
Doxycycline hyclate	D9891	Sigma-Aldrich

2.1.7 Oligonucleotides

Quantitative PCR

label	sequence 5’ → 3’	target	product length / bp
CP0355_for	GTCCCTGATGCCACTGTTCC	CP0355	150
CP0355_rev	TCCTCCTATCATGATCACAGCG	CP0355	150
CP0534_for	ACCGAAACATCGCTACCTCC	CP0534	136
CP0534_rev	TTGTTCCAGATGCTGTGCCC	CP0534	136
CP0535_for	CTGCTTCTCAATCCGTTGCC	CP0535	152
CP0535_rev	TGTGATTTGCCCGTGATTCG	CP0535	152
CP0558_for	TTCCTTTGGTGTGGCTCTCC	CP0558	150
CP0558_rev	GAAGCACTCACTTCTCCTTGC	CP0558	150
CP0598_for	TGGAGCAGATAAAAGTGCGG	CP0598	123
CP0598_rev	GCGCTGAAGCACCGAAAC	CP0598	123
CP0856_for	GCAGCTTGCGTATTTCTGGG	CP0856	134

CP0856_rev	ACCTGTTGTGGAGAACTGCTC	CP0856	134
CP0857_for	TCTCAGTCGCAGCGTTTCTC	CP0857	147
CP0857_rev	GCGCTCTTGCTCATGTTCTG	CP0857	147
CP0181_for	ATGGCTTCTTCAATACCAAACACC	CP0181	115
CP0181_rev	AGGATGATACCTCGCCTCTC	CP0181	115
16S rRNA CP_for	GAGCGTACCAGGTAAAGAAGC	16S rRNA CP	226
16S rRNA CP_rev	TATCTACGCATTTCACCGCT	16S rRNA CP	226

Short interfering RNAs (siRNAs)

siRNAs FlexiTube GeneSolution GS201475 for RAB12, QIAGEN (Rydell et al. 2014)

product name	**sequence 5' → 3'**	**target**	**cat.-no**	**lot.-no**
Hs_RAB12_4	ACCGTGGGTGTTGACTTCAAA	Rab12	SI04346447	20110301
Hs_RAB12_3	ATGATTGATAAGTATGCTTCA	Rab12	SI04300534	20110301
Hs_RAB12_2	AACCTAGTACTTCTAATATGA	Rab12	SI04233054	20120328
Hs_LOC201475_3	CAGCATTACCTCAGCTTATTA	Rab12	SI00486206	20110301

Cloning primers

label	**sequence 5' → 3'**	**target**	**description**
AscI-CP0355$_N$_for	ATCGGCGCGCCATGGCTT CTTCAATACCA	N-terminus CP0181	AscI extension
eGFP-CP0181$_N$_rev	CTTGCTCACAGAGGCTCT CTGACATTT	N-terminus CP0181	eGFP extension
CP0181$_N$-eGFP_for	AGAGCCTCTGTGAGCAAG GGCGAGGAG	eGFP	CP0181$_N$ extension
CP0181$_C$-eGFP_rev	CAAGTGCTGCTTGTACAG CTCGTCCATGCCGAGAGT	eGFP	CP0181$_C$ extension
eGFP-CP0181$_C$_for	CTGTACAAGCAGCACTTG TCAATGCGG	C-terminus CP0181	eGFP extension
NotI-CP01981$_C$_rev	TCTGCGGCCGCTTATAGA TCAATCGGAGG	C-terminus CP0181	NotI extension
AscI-CP0355$_N$_for	ATCGGCGCGCCATGACTC CGTCTAAACT	N-terminus CP0335	AscI extension
eGFP-CP0355$_N$_rev	CTTGCTCACTCTATTTTTTT GTGAGCT	N-terminus CP0335	eGFP extension
CP0355$_N$-eGFP_for	AAAAATAGAGTGAGCAAG GGCGAGGAG	eGFP	CP0355$_N$ extension
CP0355$_C$-eGFP_rev	TTTGGATGACTTGTACAGC TCGTCCAT	eGFP	CP0355$_C$ extension

eGFP-CP0355$_C$_for	CTGTACAAGTCATCCAAAC CACCTGTT	C-terminus CP0355	eGFP extension
NotI-CP0355$_C$_rev	TCTGCGGCCGCTTAATCT ATACAATGCAT	C-terminus CP0355	NotI extension
AscI-CP0534$_N$_for	ATCGGCGCGCCATGACCT CTGTAAGAACC	N-terminus CP0534	AscI extension
eGFP-CP0354$_N$_rev	CTTGCTCACTGCTGATAAA GCCATAGG	$_N$-terminus CP0534	eGFP extension
CP0534$_N$-eGFP_for	CCTATGGCTTTATCAGCAG TGAGCAAG	eGFP	CP0534$_N$ extension
CP0534$_C$-eGFP_rev	CAAGGGTTTGTTGTGACG CTTGTACAG	eGFP	CP0534$_C$ extension
eGFP-CP0534$_C$_for	CTGTACAAGCGTCACAAC AAACCCTTGCCTCTTGAAA CTA	C-terminus CP0534	eGFP extension
NotI-CP0534$_C$_rev	TCTGCGGCCGCTTAATTTC CTGTTAATCTAGTTTCAAG AGGCA	C-terminus CP0534	NotI extension
AscI-CP0535$_N$_for	ATCGGCGCGCCATGTCAA TAACAACGCCA	N-terminus CP0535	AscI extension
eGFP-CP0535$_N$_rev	CTTGCTCACTTTCGAACAA GTGGAGGG	N-terminus CP0535	eGFP extension
CP0535$_N$-eGFP_for	CCCTCCACTTGTTCGAAA GTGAGCAAG	eGFP	CP0535$_N$ extension
CP0535$_C$-eGFP_rev	GATTGCAGGTCTGCTTCT CTTGTACAG	eGFP	CP0535$_C$ extension
eGFP-CP0535$_C$_for	CTGTACAAGAGAAGCAGA CCTGCAATCTACATGGTAA ACAAT	C-terminus CP0535	eGFP extension
NotI-CP0535$_C$_rev	TCTGCGGCCGCTCAAGCT TCTATTTGAGAATTGTTTA CCATGTA	C-terminus CP0535	NotI extension
AscI-CP0558$_N$_for	ATCGGCGCGCCATGATAC CTTCTATATTA	N-terminus CP0558	AscI extension
eGFP-CP0558$_N$_rev	CTTGCTCACACTCACAGTC TTGCGACT	N-terminus CP0558	eGFP extension
CP0558$_N$-eGFP_for	AGTCGCAAGACTGTGAGT GTGAGCAAG	eGFP	CP0558$_N$ extension
CP0558$_C$-eGFP_rev	AGGCTTTTTAAGAATACGC TTGTACAG	eGFP	CP0558$_C$ extension

eGFP-CP0558$_C$_for	CTGTACAAGCGTATTCTTAAAAAGCCT	C-terminus CP0558	eGFP extension
NotI-CP0558$_C$_rev	TCTGCGGCCGCTTATGATTCTTCTTCTTT	C-terminus CP0558	NotI extension
AscI-CP0598$_N$_for	ATCGGCGCGCCATGACATCACCAGTAGAA	N-terminus CP0598	AscI extension
eGFP-CP0598$_N$_rev	CTTGCTCACATGAAAAATGCGCTGAAG	N-terminus CP0598	eGFP extension
CP0598$_N$-eGFP_for	CTTCAGCGCATTTTTCATGTGAGCAAG	eGFP	CP0598$_N$ extension
CP0598$_C$-eGFP_rev	AGAGGGGGTGCTATCCTGCTTGTACAG	eGFP	CP0598$_C$ extension
eGFP-CP0598$_C$_for	CTGTACAAGCAGGATAGCACCCCCTCT	C-terminus CP0598	eGFP extension
NotI-CP0598$_C$_rev	TCTGCGGCCGCCTAATCTGCCGTTTCTGT	C-terminus CP0598	NotI extension
AscI-CP0856$_N$_for	ATCGGCGCGCCATGAAATGTATGCAGACGA	N-terminus CP0856	AscI extension
eGFP-CP0856$_N$_rev	CTTGCTCACATGAGAGTTCGTTCTGTC	N-terminus CP0856	eGFP extension
CP0856$_N$-eGFP_for	GACAGAACGAACTCTCATGTGAGCAAG	eGFP	CP0856$_N$ extension
CP0856$_C$-eGFP_rev	AGAACTGCTCTGACAACACTTGTACAG	eGFP	CP0856$_C$ extension
eGFP-CP0856$_C$_for	CTGTACAAGTGTTGTCAGAGCAGTTCT	C-terminus CP0856	eGFP extension
NotI-CP0856$_C$_rev	TCTGCGGCCGCCTATATACTTGAAGATCG	C-terminus CP0856	NotI extension
AscI-CP0857$_N$_for	ATCGGCGCGCCATGAAATGTGTTTCTCCT	N-terminus CP0857	AscI extension
eGFP-CP0857$_N$_rev	CTTGCTCACAGTCGTAAGAACATGAAC	N-terminus CP0857	eGFP extension
CP0857$_N$-eGFP_for	CTTACGACTGTGAGCAAGGGCGAGGAG	eGFP	CP0857$_N$ extension
CP0857$_C$-eGFP_rev	AAAACATTTCTTGTACAGCTCGTCCAT	eGFP	CP0857$_C$ extension
eGFP-CP0857$_C$_for	CTGTACAAGAAATGTTTTTCTTGCCAC	C-terminus CP0857	eGFP extension
NotI-CP0857$_C$_rev	TCTGCGGCCGCTTATTCTCTAGATTCACC	C-terminus CP0857	NotI extension

2.2 Methods

2.2.1 *In silico* analysis of putative inclusion proteins

DNA and amino acid sequences were analysed with Geneious® 11.1.5 (Biomatters development team). Homologous sequences of nucleotides and proteins or only nucleotide-nucleotide queries were screened by using BLAST from NCBI (https://blast.ncbi.nlm.nih.gov/Blast.cgi). Single alignments of nucleotides or amino acids were done by using Clustal Omega (https://www.ebi.ac.uk/Tools/msa/clustalo/). The secondary structure of peptides, protein domains or amino acid sequences was characterised with Jpred (http://www.compbio.dundee.ac.uk/jpred4/index.html), and hydrophobicity analysis was done by using Protter (http://wlab.ethz.ch/protter/start/) and the ProtScale Hydrophobicity tool based on Kyte & Doolittle (https://web.expasy.org/protscale/).

2.2.2 Cloning strategy of split-Inc proteins

Cloning the constructs was based on overlap polymerase chain reaction (PCR). The split-Inc protein contains the N-terminal domain of an Inc protein, a centred enhanced green fluorescent protein (eGFP), and the C-terminal domain of an Inc protein. In detail, the nucleotide sequences of these domains were separately amplified and flanked with overlapping homologue sequences or with restriction enzyme (RE) sequences (Fig. 4 A). The fragment containing the nucleotide sequence of the N-terminal domain (nt-Inc$_N$) was flanked with the AscI RE sequence at the 5' that requires three extending nucleotides at the 5' end to enable digestion by RE. The 3' end of nt-Inc$_N$ was flanked with nine nucleotides homologous to the 5' end of the nucleotide sequence of eGFP (nt-eGFP). The fragment of nt-eGFP, excluding the stop codon, was extended at the 5' by nine nucleotides equaling the 3' end of nt-Inc$_N$ and flanked at the 3' end with nine nucleotides that are homologue to the 5' end of nt-Inc$_C$. The fragment of nt-Inc$_C$ was flanked at the 5' end with nine nucleotides according to the 3' end of nt-eGFP and was extended at the 3' end by the NotI RE sequence with additional three nucleotides for efficient digestion by RE. The final overlapping area of the extended nt-Inc$_N$ with nt-eGFP and nt-eGFP with nt-Inc$_C$ spanned exactly 18 nucleotides. The overlap PCR itself was performed in two steps (Fig. 4 B, Table 1): the first step without primers and an annealing temperature (T_a) based on overlapping region, and a second step with a T_a based on primers that amplify the fused construct. The second step was performed immediately after adding the primers. The first overlap PCR contained the nt-Inc$_N$ cassette and the nt-eGFP cassette. The product and the nt-Inc$_C$ cassette were used in the second overlap PCR, resulting in the final insert. The T_a equalled the lowest melting temperature +5 °C. The ratio of constructs for the overlap PCR relies on Equation 1, with 10 ng of the small construct and a final stoichiometry of 1:1.

The final construct was gel extracted (Wizard® SV Gel and PCR Clean-up System, Promega) after running on a 1% agarose gel (1:10000 Midori Green Advance DNA Stain), loaded with 1x DNA Loading Dye (Thermo Fisher Scientific), and re-amplified to yield an amount sufficient for downstream processes such as digestion. The re-amplified DNA was purified by using the Wizard® SV Gel and PCR Clean-up System (Promega) and digested by the AscI RE and NotI-HF RE (NEB) in 1x CutSmart Buffer (NEB) at 37 °C for 1 h. Plasmid pEGFP-C1 was modified by inserting AscI and NotI restriction sites. The modified plasmid was digested by AscI and NotI-HF in 1x CutSmart Buffer for 1 h at 37 °C and further incubated with 6 units of Antarctic Phosphatase (NEB) for 1 h at 37 °C to remove phosphate residues, to avoid re-ligation. The enzymes were inactivated at 80 °C for 20 min. The digested plasmid and constructs were purified by gel extraction after running a 1% agarose gel. The reaction mix for ligation of a 20 µl reaction consisted of 1 unit of T4 DNA Ligase (Thermo Fisher Scientific) and 1x T4 DNA Ligase buffer (Thermo Fisher Scientific). The amount of digested insert was calculated based on the digested insert length, the digested plasmid length and 50 ng of digested plasmid (Equation 2) with a ratio of 3:1 (insert:plasmid). After incubation for 20 min at room temperature (RT), the reaction was stopped by enzymatic inactivation for 5 min at 70 °C. Twenty-five microlitres of competent bacteria (section 2.1.3) was transformed with 5 µl of ligation solution. The transformed bacteria were plated on LB-medium agar with kanamycin (1.5% bacto agar supplemented). After incubation overnight at 37 °C, 10 colonies were picked to be re-plated on agar with kanamycin as backup and to perform colony-PCR (20 µl reaction volume with insert-flanking primers, section 2.1.7).

After PCR, 10 µl of the reaction mix was checked by agarose gel. The remaining 10 µl was purified and used as a template for Sanger sequencing (BigDye®, Thermo Fisher Scientific). The backup plate was incubated overnight at 37 °C and stored at 4 °C. The colony with the correct sequence was used for midi preparation (section 2.2.4).

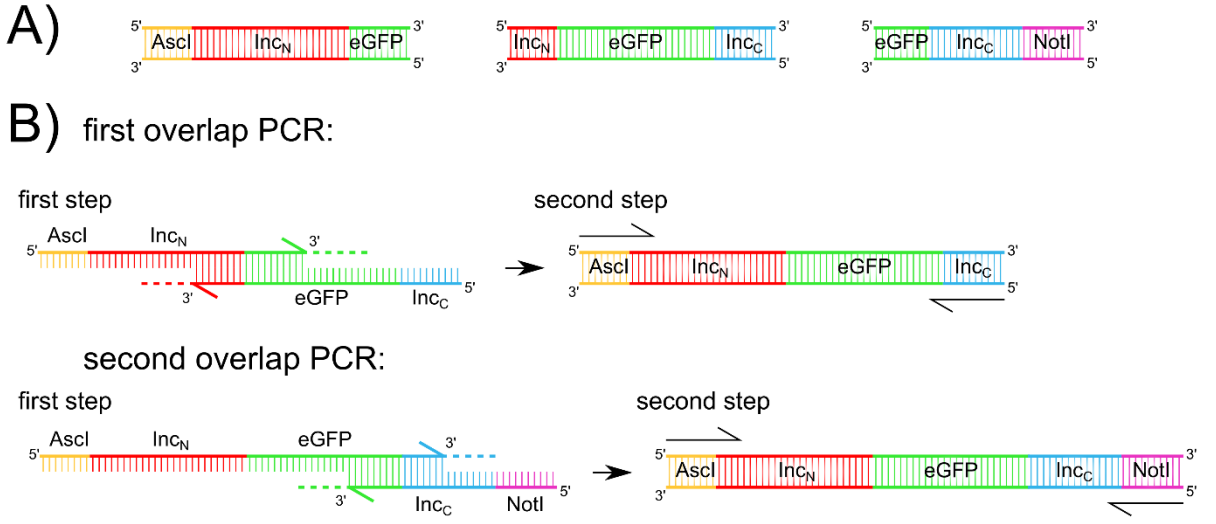

Fig. 4 Schematic overview of the cloning strategy.

A) Scheme of the initial PCR products with flanking sequences for overlap PCR and RE digestion. The nucleotide sequences of eGFP, the N-terminal domain of an Inc protein (Inc_N), the C-terminal domain of an Inc protein (Inc_C), and the RE sequences of AscI and NotI are indicated and highlighted with individual colours. B) Schematic overview of cloning process via overlap PCR. The Inc_N construct and eGFP construct are used in the first overlap PCR in the first step. Homologue regions allowed annealing and elongation at the 3' ends, indicated by half-arrows and dashed lines. Primers (black half-arrows) are added in the second step for amplification. The second overlap PCR uses the product of the first overlap PCR and the Inc_C construct. Primers are added in the second step of the second overlap PCR.

Table 1 PCR programmes using Phusion High-Fidelity PCR Master Mix with HF Buffer (Thermo Scientific).

Overlap PCR		
First step		
98 °C	2 min	
98 °C	10 s	15 cycles
T_a overlap	30 s	
72 °C	30 s/kb	
72 °C	10 min	
Second step	add primers	
98 °C	2 min	
98 °C	10 s	20 cycles
T_a primers	30 s	
72 °C	30 s/kb	
72 °C	10 min	
4 °C	hold	

Regular PCR		
98 °C	2 min	
98 °C	10 s	25 cycles
T_a primers	30 s	
72 °C	30 s/kb	
72 °C	10 min	
4 °C	hold	

Equation 1

$$\text{small construct} = \text{S}; \quad \text{large construct} = \text{L}; \quad m_{\text{L}}(m_{\text{S}} = 10\ \text{ng}) = MW_{\text{L}} \cdot n_{\text{S}} = \frac{MW_{\text{L}} \cdot m_{\text{S}}}{MW_{\text{S}}}$$

Equation 2

$$\text{digested plasmid} = \text{dp}; \quad \text{insert} = \text{i}; \qquad m_{\text{i}}\left(m_{\text{dp}} = 50\ \text{ng}\right) = m_{\text{dp}} \cdot \frac{3}{1} \cdot \frac{size_{\text{i}}\ [\text{bp}]}{size_{\text{dp}}\ [\text{bp}]}$$

2.2.3 Transformation

Transformation was performed according to the manufacturer's protocol. Competent *Escherichia coli* was thawed on ice for 5 min and subsequently supplemented with 5 µl ligation mix. After incubation on ice for 30 min, the bacteria were heat shocked for 30 s at 42 °C and

then chilled on ice for 5 min. Suspension was supplemented with 1 ml of SOC medium and shaken at 250 rpm for 1 h at 37 °C. Finally, the bacteria were pelleted by centrifugation for 5 min at 6000 *g*, resuspended in 100 µl LB medium plated on a kanamycin-containing agar plate and incubated for 24 h at 37 °C.

2.2.4 Midi preparation

A 2 ml culture with LB medium containing kanamycin was inoculated with a sequencing-validated colony and cultivated at 37 °C for 6 h. This 2 ml culture was used to inoculate 50 ml of LB medium (+kanamycin) overnight. The next day, the suspension was used to prepare the plasmid at midi scale according to the manufacturer's protocol (Plasmid Midi Kit, QIAGEN).

2.2.5 Cell culture

HeLa cells or CRISPR-Cas9 cells generated based on the HeLa cell line were stored in foetal bovine serum (FBS) supplemented with final 10% dimethyl sulphoxide (DMSO) in liquid nitrogen tanks. Cells were thawed and grown for 24 h in fresh growth medium at 37 °C and 5% carbon dioxide (CO_2); the medium was replaced after 24 h. The cells were split once 48 h post-thawing before they were used for seeding and experiments. In total, one thawed cell stock was passaged a maximum of nine times before being replaced.

2.2.6 Infection

Cultured cells were split 1:4 one day before infection to reach a confluency of about 80% on the next day. Cells were washed once with Dulbecco's Modified Eagle Medium (DMEM) (5% FBS, 2 mM L-glutamine, 1 mM sodium pyruvate) and incubated with *Chlamydia* spp. diluted with DMEM (half of the regular growth volume) for 30 min, centrifuged (30 min, 600 *g*, RT) and incubated for 60 min at 35 °C and 5% CO_2. The infectious solution was aspirated, and cells were washed once with DMEM before being incubated with a regular volume of DMEM.

2.2.7 Labelling *de novo* expressed proteins

Labelling with L-homopropargylglycine (L-HPG) was performed 2.5 h before the time point of interest. Growth medium was replaced with starvation medium (L-methionine and L-(-)-cystine depleted RPMI, 5% dialysed and sterile-filtered FBS, 2 mM L-glutamine, 1 mM sodium pyruvate, 0.5 µg/ml cycloheximide) supplemented with or without antibiotics, and the cells were incubated for 30 min. Cells were pulsed with starvation medium supplemented with 50 µM L-HPG for 2 h. After the pulse, cells were washed once with 1x phosphate-buffered saline (PBS) and used for subsequent experiments.

2.2.8 Click chemistry

The incorporated amino acid L-HPG was detectable by using the copper-catalysed click reaction. The copper-catalysed cycloaddition between alkyne and azido groups is called the click reaction and is widely used for diverse applications (Pickens et al. 2018). The cells were prepared by fixation with 2% paraformaldehyde (PFA) for 20 min at RT, washed once in 100 mM Tris (pH 8.55, 24 °C) for 10 min and blocked/permeabilised (0.2% Triton-X in Tris) for 20 min at RT. The click reaction solution was prepared during two more washing steps right after permeabilisation for a maximum of 5 min in that order and mixing between the addition of each component: $CuSO_4$ (final 1 mM) to 100 mM Tris-HCl (pH 8.55, 24 °C), Alexa Fluor® 546-Azide (final 20 µM) and sodium ascorbate (final 100 mM). The reaction mix was incubated with the cells for 30 min at RT, followed by washing twice with 0.5% Triton-X in 100 mM Tris for 10 min each. After washing twice in 1x PBS for 10 min, samples were blocked with 0.2% bovine serum albumin (BSA) in 1x PBS for 20 min at RT and proceeded further for immunofluorescence as described in section 2.2.12.

2.2.9 Read-out of expression intensity via immunofluorescence

HeLa cells were seeded in 12-well plates with 15 mm coverslips. After the cell culture experiment, cells were pulsed with L-HPG as described in section 2.2.7 and fixed with 2% PFA. Incorporated L-HPG was clicked with Alexa Fluor® 546-Azide as described in section 2.2.8, and the cells were immunostained against chlamydial Hsp60 (cHsp60) by using Alexa Fluor® 488 and DAPI (section 2.2.12). Twenty images per condition with 100x magnification were recorded manually with a laser scanning confocal microscope (Carl Zeiss LSM 780) and saved in easy-to-process 24-bit bitmap grayscale format. The cHsp60 signal was post-processed into a mask to identify individual bacteria and thus inclusions (Fig. 5 A). The mask layer was overlaid with the L-HPG signal to restrict the expression signal to chlamydial areas. The minimal threshold of cHsp60 was pre-analysed to eliminate the background. Hence, using ImageJ (https://imagej.nih.gov/ij/index.html), the type of a single image was set to 8-bit greyscale (values 0-255 for black to white) and the value 40 was determined as the minimum threshold. A batch-processing program was written in C++ to quantify the images. The cHsp60 image was read pixel by pixel, and pixels in a row that touched were grouped as row elements (Fig. 5 B). After reading, the rows were queried regarding whether they bordered other rows and clustered as areas. The areas contained information about the total size and single-pixel coordinates that referred to the coordinates of the L-HPG image. Reading the L-HPG image was facilitated by using the previously saved coordinates. The sum of the pixel intensity was divided by the area size, yielding the mean expression intensity per area (and thus per inclusion). The colour of a pixel in a 24-bitmap file contains the values for red, green and blue (0-255, 0-255, 0-255). All three values were equal since the images were saved in greyscale

format (red = green = blue). Therefore, the intensity value of a pixel refers to one channel (0-255). In the batch process, the value 40 was used as the minimum threshold (determined in the pre-analysis, as described above). If the process took more than 7 s per image, indicating a threshold too low for background elimination, the threshold was automatically loop-wise increased by 2. The arithmetic mean of the background was subtracted from the arithmetic mean of the expression value per area. The differences of all areas per condition are displayed as the arithmetic mean with the standard deviation. This newly developed algorithm increased the efficiency of reading the cHsp60 image to extraction of the quantified values. Depending on the complexity of the image, the processing time could be reduced to approximately 3 s per sample.

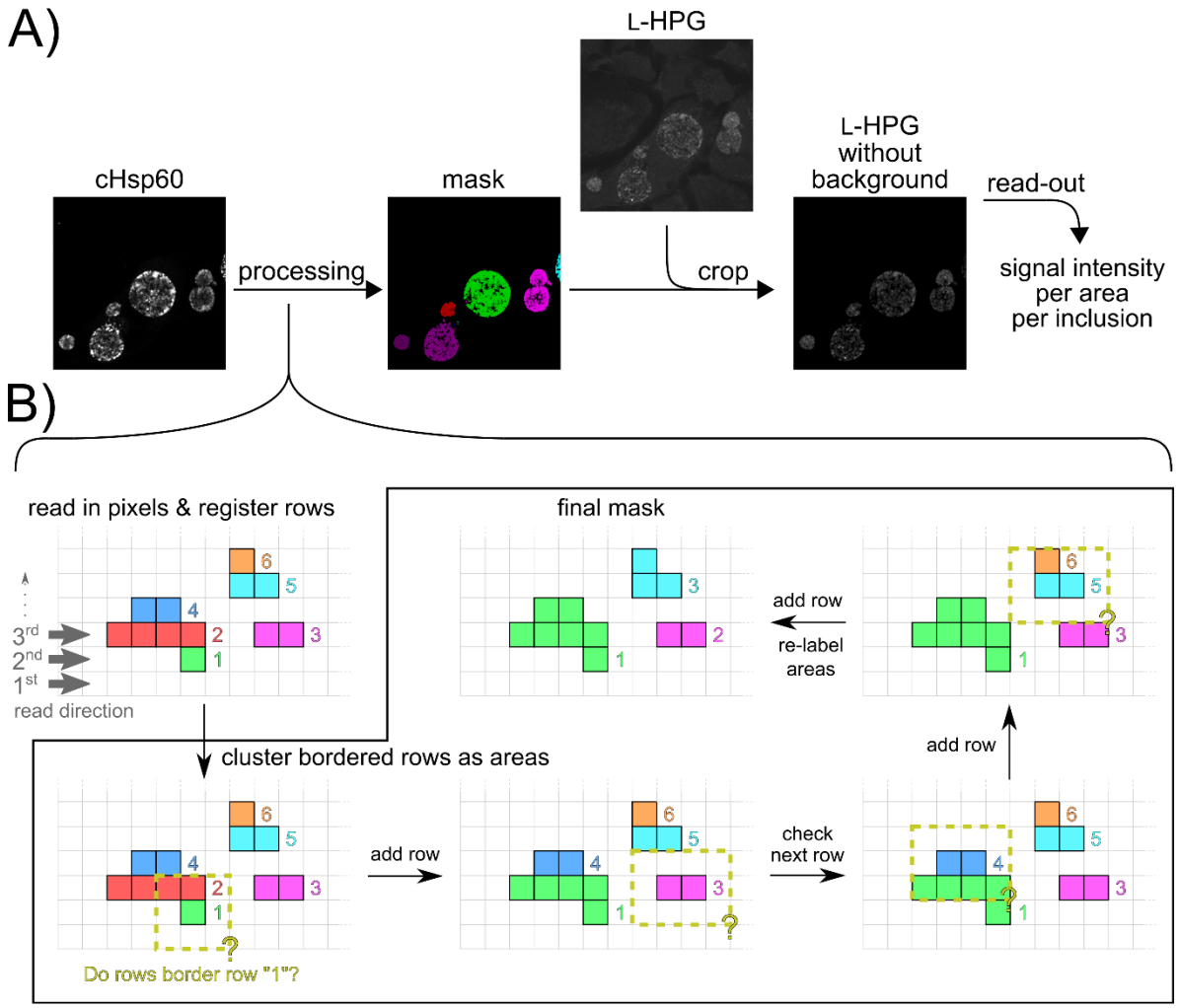

Fig. 5 Workflow of protein expression quantification in *C. trachomatis* serovar D using immunofluorescence images.

A) Simplified workflow scheme. Expression was monitored via incorporation of L-HPG and subsequent covalent binding to Alexa Fluor 488 via click chemistry. Immunofluorescent labelling of cHsp60 as chlamydial marker was used as a mask. The image yielding the cHsp60 signal was processed by using the described method to generate a mask containing indices of individual inclusions. The mask was overlaid with the L-HPG signal and cropped, yielding a *Chlamydia*-specific L-HPG signal without background noise. The signal intensity was read and aligned with individual inclusions, resulting in the mean signal intensity per area per inclusion. B) Image processing in detail. The image file of the cHsp60 channel was converted to a 24-bit bitmap and read pixel by pixel from left to right and from bottom to top (grey labelled directions). Pixels with a colour value below the set background threshold were referred to as negative pixels and displayed in white. Pixels with a colour value above the background threshold were designated as positive pixels and displayed in colour. Positive pixels that touched each other to the left or right were grouped and registered as rows with index, indicated with coloured index numbers. 'Row clustering as areas' indicates rows and their neighbourhood. Depending on the case, contiguous rows and existing areas were combined into a single area with the lowest index number of the elements involved. In the end, all indices were re-labelled with an increasing number from the left to the right and from the bottom to the top. The final file was saved as a mask file as a proof of concept.

2.2.10 Small interfering RNA (siRNA) knockdown

Four siRNAs with different sequences targeting the same gene of interest were pooled (section 2.1.7, Rydell et al. 2014). The transfection mix consisted of 6 µl of HiPerFect, 2 µl of 10 µM siRNA #1 (Hs_LOC201475_3), 2 µl of 10 µM siRNA #2 (Hs_RAB12_2), 2 µl of 10 µM siRNA #3 (Hs_RAB12_3) and 2 µl of 10 µM siRNA #4 (Hs_RAB12_4) in 100 µl of OptiMEM, pre-incubated for 20 min at RT. Cells at 80% confluency in one well of a 12-well plate were washed once with medium. Six-hundred microlitres of medium was placed on cells before adding 100 µl of transfection mix dropwise. 24 hours post-transfection, cells were split 1:8 into 6-well or 12-well plates. Cells were infected at 48 h post-transfection and then processed as necessary.

2.2.11 Plasmid transfection

Unless otherwise noted, 1 µg of plasmid DNA and 2 µl of Lipofectamine 2000 were used per 1×10^6 cells. DNA was pre-incubated in 100 µl OptiMEM for 5 min, and Lipofectamine 2000 was also incubated in OptiMEM for 5 min. The DNA solution was added to the Lipofectamine 2000 solution and incubated for 20 min at RT. Cell culture supernatant was removed, and 200 µl of the final transfection mix was added dropwise to cells. The transfection mix was filled up to half of the growth volume by medium for at least 4 h. Subsequently, the mix was replaced with fresh medium or adjusted to the regular growth volume. Finally, the medium was replaced by fresh medium 24 h after transfection.

2.2.12 Immunofluorescence (IF)

Cells were seeded in either 12-well plates with coverslips (15 mm diameter), or 24-well plates with coverslips (12 mm diameter). After cell culture experiments, cells were either fixed in 2% PFA for 30 min at RT or in pre-cooled methanol for 20 min at -20 °C. Fixable live dyes, such as MitoTracker™ DeepRed FM (Invitrogen), were incubated for 30 min right before fixation. The coverslips were washed three times with 1x PBS for approximately 8 min after each of the following steps: fixation, blocking/permeabilisation and incubation with primary and secondary antibodies. Slides were blocked with 0.2% BSA in 1x PBS and, in the case of PFA-fixed cells, permeabilised with 0.2% Triton-X for 20 min at RT. In a wet chamber, the cells were immunostained with primary and secondary antibodies (in 0.2% BSA, 1x PBS) for 1 h. Slides were mounted in Mowiol® and dried overnight.

2.2.13 Quantification of progeny formation

Cells were seeded in one 6-well per condition and infected with *Chlamydia* spp. Infected cells were detached and lysed in their supernatant by glass beads and shaking movements. Subsequently, this solution was homogenised in a 15-ml tube with glass beads by vortexing

for 3 min. The infectious solution was diluted serially (a dilution factor of 5) and used for infection as described in section 2.2.6. Cells that were infected by the dilution series were seeded 1:3 in 24-well plates with coverslips one day before the experiment. Titrations of *C. trachomatis* serovar D were fixed in 2% PFA at 30 hpi. The slides were stained against chlamydial Hsp60 (1:500) and DNA using DAPI (1:5000). The arithmetic mean of counted inclusions (marked by Hsp60 signal) of 10 fields of view was used and converted to inclusion forming units (IFU)/ml (Equation 3).

Equation 3

$$\text{dilution factor} = \text{DF};\ \text{mean counted inclusions [IFU]} = \overline{\text{M}};\ \ \text{progeny formation} \left[\text{IFU} \cdot \text{ml}^{-1}\right] = \text{pf}$$

$$\text{pf}\ (V = 0.25\ \text{ml}) = \frac{\overline{\text{M}}}{V} \cdot\ \text{DF}\ \cdot\ 412$$

2.2.14 Preparation of EM samples

Cells were seeded in 6-well plates, infected the next day with *C. trachomatis* serovar D (multiplicity of infection [MOI] of 2) and fixed at indicated times with the following order: glutaraldehyde was pre-warmed at RT 1 h before use, medium was aspirated and 3 ml of glutaraldehyde was added per well and incubated for 2 h at RT. The cells were stored in glutaraldehyde at 4 °C and further processed by the EM facility. The samples were harvested by scraping and embedded in low-melting-point agarose. Post fixation was performed in osmium tetroxide (1% in distilled water), followed by block contrasting with tannic acid (0.1% in 50 mM HEPES) and uranyl acetate (2% in distilled water; Merck, Darmstadt, Germany). Subsequent incubation in a stepwise-graded ethanol series, infiltration with propylene oxide and embedding in epon dehydrated the samples. Incubation for 48 h at 60 °C allowed polymerisation of epon. Approximately 60 nm ultrathin sections were prepared using an ultramicrotome (ZC7; Leica, Germany). Further staining with uranyl acetate (2% in distilled water, 20 min) and lead citrate (2 min) increased the contrast. A Tecnai12 transmission electron microscope (FEI, Thermo Fisher, Netherlands) operated at 120 kV was used to examine the samples. Digital images of the samples were recorded using a Megaview III Camera (OSIS, Germany).

2.2.15 Inclusion preparation

Cells were seeded in six T75 flasks per condition and infected the next day with an MOI of 5. As described in section 2.2.6, infection was performed except for a relative centrifugal force of 800 *g* during centrifugation. Flasks were cooled on ice and washed with ice-cold 1x HSMG buffer (20 mM HEPES, 250 mM sucrose, 1.5 mM $MgCl_2$, 0.5 mM EGTA, pH 7.4) at the indicated time points post-infection. Cells of all six flasks were scraped with a 30-cm cell scraper into 6 ml of Percoll solution (33.3% Percoll®, 1 tablet of EDTA-free cOmplete™

protease inhibitor per 20 ml, 1x HSMG). A pre-cooled ball homogeniser with a ball (7.984 mm diameter) and a 16 µm clearance was used on ice to homogenise the cells (13 strokes). The homogenate was transferred to centrifugal tubes and adjusted to 16 ml using the Percoll solution. After centrifugation (30 min, 35,000 *g*, 4 °C), a needle was used to reach the bottom of the centrifugation tube to harvest either single fractions from the bottom for counting inclusions (section 2.2.15.1) or 6 ml (equal to the first six fractions from the bottom) for proteomic analyses. In the latter case, the 6 ml was diluted by adding 30 ml 1x HSMG (1:6), thus reducing the Percoll concentration. After centrifugation (10 min, 1200 *g*, 4 °C), the supernatant was gently removed by pipetting, avoiding loss of the inclusion containing pellet. The remaining pellet was processed for proteomic analyses as described in section 2.2.18.

2.2.15.1 Counting inclusions per fraction

The number of inclusions per fraction that derived from the inclusion preparation (section 2.2.15) was counted in a Neubauer counting chamber. The samples were diluted 1:10 in 1x HSMG to reduce the Percoll concentration-dependent density. This resulted in sedimentation of inclusions to the bottom, thereby facilitating counting. One subfield with a volume of 0.0111 µl out of five fields was counted, and the arithmetic mean with standard deviation was used to determine the inclusions per ml.

2.2.16 Mitochondria preparation

HeLa cells in two 6-wells were co-transfected with 4 µl of Lipofectamine2000, 1 µg of plasmid DNA encoding mitochondrial anchored fusion protein of interest and 1 µg of plasmid DNA encoding myc-BirA-SNX5 per 6-well (section 2.2.11). The following steps were performed on ice. Twenty-four hours post-transfection, cells were washed once with 1x PBS and once with 1x HSMG. Two 6-wells of the same condition were scraped with a cell scraper, pooled in 2 ml of 1x HSMG buffer and resuspended with a 1000 µl pipette tip. The cell suspension was lysed and homogenised as described in the inclusion preparation (section 2.2.15). Forty-eight microlitres of the lysate was saved as lysate control and supplemented with 16 µl of 4x Laemmli buffer. The remaining lysate was split equally between two 1.5 ml tubes. After centrifugation (3 min, 1500 *g*, 4 °C), the pellets containing nuclei were pooled in 2x Laemmli buffer (nucleus fraction control), whereas the supernatant was transferred to fresh 1.5 ml tubes and centrifuged (17 min, 13000 *g*, 4 °C). Twenty-four microlitres of the supernatant was saved and supplemented with 8 µl of 4x Laemmli buffer as the mitochondria-cleared fraction control. The pellets containing intact mitochondria were pooled in a total of 21 µl of 1x PBS and supplemented with 7 µl of 4x Laemmli buffer. All samples and fraction controls were incubated for 5 min at 95 °C. Thirteen microlitres of each sample was loaded on a sodium dodecyl

sulphate (SDS)-containing acrylamide gel (section 2.2.23) and subjected to western blot (section 2.2.24).

2.2.17 Mild digestion of isolated mitochondria for import analysis

Two 6-wells of HeLa cells were co-transfected with plasmids encoding a mitochondria-targeting fusion protein and myc-BirA-SNX5 as described in section 2.2.11. Twenty-four hours post-transfection, the mitochondria were isolated as described in section 2.2.16, and the pellets with intact mitochondria of the same condition were pooled in 110 µl of Tris buffer (100 mM Tris/HCl, pH 8.5). Twenty-five microlitres of mitochondria was transferred to a 96-well with a V-bottom placed on ice. Two microlitres of proteinase K (125 µg/ml in Tris buffer) was added to each well of a 96-well plate with a V-bottom; 2 µl Tris buffer served as the negative control. The digestion started by transferring 23 µl of mitochondria to the pre-pipetted 2 µl of proteinase K or Tris buffer. After 0 s (only Tris buffer), 30 s, 60 s and 5 min incubation on ice, the digestion was stopped by transferring the 25 µl digestion solution to a 1.5 ml tube on ice, containing 25 µl 40% trichloroacetic acid, and allowed to precipitate for 10 min. The precipitated proteins and peptides were pelleted (5 min, max speed, 4 °C) and washed twice by resuspending in 200 µl ice cold acetone (pre-incubated at -20 °C) and centrifuging for 5 min (max speed, 4 °C). The pellet was dried by heating at 95 °C for 10 min. The pellet was resuspended in 15 µl of 2x Laemmli buffer and incubated for 10 min at 95 °C. Fourteen microliters of each sample were loaded on a 15% SDS-containing acrylamide gel and subjected to SDS-polyacrylamide gel electrophoresis (PAGE) (section 2.2.23) and western blot (section 2.2.24).

2.2.18 Proteomics

The protein-containing pellet was resuspended in a freshly prepared urea solution. Five freeze-thaw cycles were performed by freezing in liquid nitrogen and thawing for 3 min in a water bath at 37 °C. Samples were then mechanically disrupted with a sonicator at 4 °C (3x 1 min, 50% cycles, 50%-60% power). According to the manufacturer's protocol, the protein amount was determined by the Bradford assay using the ROTI®Quant (Carl Roth GmbH + Co. KG) microassay. Fifty micrograms of protein was used, trying not to exceed a volume of 30 µl. After adding dithiothreitol (DTT, final 3 mM), disulphide bonds in the samples were reduced for 45 min at 37 °C. The DTT concentration was diluted 1:6 with 100 mM Tris-HCl (pH 8.55, 24 °C). Samples were alkylated with a final concentration of 6 mM 2-iodoacetamide (IAA) for 20 min at 37 °C in the dark. Unreacted IAA was quenched by adding DTT (final concentration of 3 mM) for 15 min at RT in the dark. The remaining urea in the samples was diluted below 1 M with 100 mM Tris-HCl; the solution was then ready for digestion with trypsin. Trypsin was added at a 1:20 (trypsin:protein) ratio and incubated overnight at 37 °C. Digestion was stopped

by acidification with trifluoroacetic acid (TFA, final concentration ~2%) with pH ~2. After centrifugation (60 min, 13,000 *g*, 24 °C), the supernatant was desalted with C18-StageTips (non-autoclaved 100 µl pipette tips from Eppendorf with 3x C18 discs, Empore). The StageTip was equilibrated with 100 µl methanol and washed once with 100 µl of 0.2% TFA in liquid chromatography–mass spectrometry (LC-MS) water, centrifuging for 1 min (2000 *g*, RT) between steps. Samples were loaded in 200 µl steps and washed three times with 200 µl of 0.2% TFA. Purified peptides were eluted in 20 µl of 80% acetonitrile (ACN) in 0.1% formic acid and dried with a SpeedVac. Samples were resuspended in 0.1% formic acid, and the concentration was measured via NanoDrop™ 2000 (Thermo Scientific) at 280 nm (AU 1.1/µg) with a purity ratio at 260/280 < 1.3. Samples were run via matrix-assisted laser desorption/ionization-time of flight (MALDI-TOF) LC-MS.

2.2.19 GFP-Trap samples

Three 6-wells of HeLa cells per condition were transfected (section 2.2.11) with 2 µg of plasmid DNA per well and harvested 24 h post-transfection. GFP-Trap was performed with magnetic agarose beads and magnetic separation according to the manufacturer's protocol of the iST GFP-Trap Kit (Chromotek). The purified magnetic beads enriched in split-Inc protein (section 3.2.5) and putative interaction partners were resuspended in 30 µl of a urea solution (8 M urea, 2 M thiourea, 5 mM DTT, 50 mM Tris/HCl, pH 8.5). While incubating for 1 h at 37 °C, shaking at 1400 rpm, disulphide bonds were reduced and proteins were denatured. The proteins in the urea-bead mix were alkylated by supplementation with 3.33 µl of 150 mM IAA and then incubated in the dark for 30 min at RT with shaking at 1400 rpm. The mix was diluted 1:8.5 with 50 mM Tris/HCl (pH 8) and digested overnight at 37 °C after adding 0.5 µg of trypsin. The choice of the 62:1 (protein:trypsin) ratio was based on prediction of the maximum binding capacity of the beads (8 µg protein), putative interaction partners (8 µg for stoichiometric 1:1 interactions) and the nanobodies covering the beads (8 µg), for a total of 32 µg. The beads were centrifuged the next day (5 min, 2000 *g*, 4 °C) and the supernatant was transferred to a new 1.5 ml tube. The digestion was stopped by adding TFA (final 2%, pH ~2). As described in section 2.2.18, the peptides were further desalted, resuspended in 0.1% formic acid and their concentration measured by NanoDrop™ 2000 at 280 nm (AU 1.1/µg) with a purity ratio of 260/280 < 1.3. Samples were run via MALDI-TOF LC-MS.

2.2.20 Quantitative PCR (qPCR)

qPCR was performed according to the manufacturer's protocol of the Power SYBR® Green RNA-to-CT™ 1-Step Kit (Thermo Fisher Scientific Inc.). The primers were designed to amplify a product of the gene of interest with a length of 150 bp and a T_a of 60 °C using 50 ng of extracted RNA (section 2.2.21) or DNA (section 2.2.22) per sample. The controls were no-

reverse transcriptase controls (RNA or DNA template but without reverse transcriptase) and one with water as a template (with reverse transcriptase). Two technical replicates per sample were performed.

2.2.21 RNA extraction

The cell pellet was resuspended in 1 ml of TRIzol. After incubation for 5 min at RT, 200 µl of chloroform was added and the tube was gently inverted for 15 s. The samples were chilled for 5 min at RT before centrifugation (15 min, 12,000 *g*, 4 °C). Approximately 500 µl of the upper aqueous, polar phase that contained RNA was transferred to a new tube. The DNA-containing intermediate phase was saved for DNA extraction (section 2.2.22). Isopropanol (70% of the volume of the aqueous phase) was added (e.g. 350 µl isopropanol for 500 µl aqueous phase) and the tube was briefly inverted. RNA precipitated during 10 min at RT and was pelleted for 15 min (max speed, 4 °C). The RNA pellet was washed three times with 700 µl of ice-cold 70% ethanol in RNase-free water by vortexing and then centrifuging (5 min, max speed, 4 °C). After the last wash, the supernatant was removed carefully by pipetting and the pellet was dried for 3 min at RT (the lid of the tube was left open). The pellet was redissolved in 12 µl of RNase-free water. Next, 1 µl of DNase (NEB), 1.5 µl of 10x DNase buffer and 0.5 µl of murine RNase inhibitor were added and the mixture was incubated for 45 min at 37 °C to degrade DNA contamination. The DNase reaction was stopped by adding 0.15 µl of 500 mM EDTA (final concentration of 5 mM EDTA), which chelates bivalent metal ions and also prevents autocatalytic self-splicing of the RNA. Enzymes were deactivated by incubating at 70 °C for 10 min. The DNA-decontaminated RNA was then extracted and eluted in 15 µl of RNase-free water as described above to remove proteins and EDTA that interfere with downstream applications such as qPCR. The concentration was measured by NanoDrop™ 2000.

2.2.22 DNA extraction

DNA was extracted from the intermediate phase of RNA extraction (section 2.2.21). After removing the upper aqueous phase, the organic bottom phase and DNA interphase were supplemented with 300 µl of ice-cold 98% ethanol per 1 ml of TRIzol. The sample was inverted several times and incubated for 3 min at RT. DNA was pelleted by centrifugation (5 min, 2000 *g*, 4 °C) and washed twice as follows: the pellet was resuspended in 1 ml of 100 mM sodium citrate (in 10% ethanol, pH 8.5), incubated for 30 min at RT while gently inverting every 10 min and then centrifuged (5 min, 2000 *g*, 4 °C); the supernatant was discarded. The pellet was further resuspended in 1.5 ml of 75% ethanol and incubated for 10 min at RT (inverting every 5 min). After centrifugation (5 min, 2000 *g*, 4 °C), the supernatant was discarded and the pellet was air-dried for 5 min. The pellet was re-dissolved in 300 µl of 8 mM NaOH, centrifuged (10 min, 12,000 *g*, 4 °C) and the supernatant was transferred to a new 1.5 ml tube. The pH

was adjusted to ~7 by the addition of 55 µl of 100 mM HEPES (pH 7). The concentration was measured with a NanoDrop™ 2000.

2.2.23 SDS-PAGE

Before western blotting, proteins were separated by SDS-PAGE. Considering the size of the target proteins, gels with 10%-15% acrylamide (higher concentration for smaller proteins) were prepared and used in SDS-PAGE chambers (Bio-Rad). The gels were covered with SDS running buffer (section 2.1.5) before loading with samples and pre-stained protein ladder (Thermo Scientific PageRuler Prestained Protein Ladder 10 kDa-180 kDa). The samples were mixed with 2x or 4x Laemmli buffer, incubated for 10 min at 95 °C and then immediately loaded on the gel. SDS-PAGE was first run at 70 V, allowing the formation of an accumulated dye front within the stacking gel. The proteins were subsequently separated at 140 V until the dye front reached the bottom of the gel. The separated protein was then immediately transferred to a membrane via western blot.

2.2.24 Western blot

The transfer apparatus consisted of ice pads pre-cooled at -20 °C, equilibration of sandwich components in 1x western blot buffer (stored and pre-cooled at 4 °C) and activation of polyvinylidene fluoride (PVDF)-membrane (Immobilon®-P Transfer Membrane, Millipore®) by rinsing in methanol. The transfer sandwich was built from anode to cathode in the following order: sponge, Whatman™ paper, SDS-PAGE gel, activated membrane, Whatman™ paper, sponge. The chamber with the sandwich, stirrer and ice-pads was filled with cold 1x western blot buffer and quickly moved to a cold room (4 °C), where the transfer was performed stirring for 2 h at 200 mA. After the transfer, the membrane was washed once for 15 min at RT in 1x TBS-T (0.05% Tween20, 1x Tris-buffered saline) and blocked for 1 h at 4 °C (3% milk powder, 1x TBS-T). The membrane was incubated with primary antibody diluted in blocking solution overnight at 4 °C. The next day, the membrane was washed three times with 1x TBS-T for 10 min and incubated with horseradish peroxidase (HRP)-conjugated secondary antibody in blocking solution for 1 h at RT. After three more washes, the membrane was incubated with detection solution (mixing A and B 1:1 before pipetting on the membrane) for at least 2 min and covered by a plastic sheet in an X-ray cassette. The film (Amersham Hyperfilm™ ECL, GE Healthcare Limited) was incubated on that sheet in the dark for 10 s to 30 min depending on the antibody and developed using CP1000 automatic film processor (Agfa-Gevaert N.V.). The developed film was labelled and scanned using a scanner and the appropriate software.

3 Results

In this work, two aspects were investigated. In the first part, a new method was established that support the identification of putative human interaction partners with putative *C. psittaci* Inc proteins by transient expression, co-immunoprecipitation and subsequent MS: the split-Inc protein (section 3.1). Subsequently, *C. psittaci* Inc proteins were identified and characterised (section 3.2). *In silico* analysis revealed putative *C. psittaci* Inc proteins, which were further characterised based on their gene expression. Using the newly established split-Inc protein method, human interaction partners of the *C. psittaci* Inc proteins were identified. The second aspect focussed on the elucidation of the doxycycline-induced persistence of *C. trachomatis* serovar D (section 3.3). The translation during antibiotic treatment was analysed, and transcripts of the trans-translation components were quantified. Recruitment of ectopically expressed human proteins to the inclusion was determined in IF. Finally, label-free proteomics of isolated inclusions revealed altered proteins during the doxycycline treatment, which role during the acute and persistent infection was subsequently investigated.

3.1 Design of solubilised and fluorescent Inc proteins: split-Inc proteins

As obligate intracellular pathogens, *Chlamydia* spp. rely on nutrients derived from its hosts. *Chlamydia* can hijack cellular organelles, components and proteins by recruiting them to the inclusion membrane via Inc proteins. Inc proteins have at least two bi-lobed TM helices (Dehoux et al. 2011, Rockey et al. 1995). In the 1990s (Bannantine et al. 1998, Rockey et al. 1995, Scidmore-Carlson et al. 1999), the process to identify and characterise Inc proteins comprised prediction of the TM domain, generation of antibodies against the Inc protein for the validation of the localisation in the inclusion membrane via immunofluorescence, interaction studies by co-immunoprecipitation of the tagged Inc protein and analysis of motifs or binding sites that drive the interaction. However, the generation of antibodies is expensive, time-consuming and resource-intensive. An alternative is the genetic modification of *Chlamydia*. Dickinson et al. (2019) modified IncB by genetic transformation of *C. trachomatis* serovar L2. Although the protocol of the authors seems to be promising, it requires further optimisation for *C. psittaci* and time-consuming selection. Another disadvantage is the required permission for genetic modification of human pathogens. These factors limit the fast investigation of numerous Inc proteins. So, instead of visualising native Inc proteins during infection, transiently expressed Inc proteins could be used to visualise cellular host targets and vice versa. This approach has one issue: the TM domain. Experiments of transiently expressed terminally tagged full-length Inc proteins have shown co-translation into the ER membrane that depends on the hydrophobic characteristics of the TM domain (Basovskiy et al. 2008, Shkarupeta et al.

2008). A workaround to avoid misdirection and local impact on the interactome is depletion of the TM domain. Therefore, single N- or C-terminal cytosolic domains have been expressed for interaction studies based on co-immunoprecipitation (Böcker et al. 2014, Mirrashidi et al. 2015). The expression of a single domain and omitting the remaining cytosolic domains might affect the native folding of the Inc protein or change its physicochemical properties, which are probably involved in protein interaction. For example, the tertiary structure of an Inc protein may rely on a combination of cytosolic subdomains separated by TM domains. Depleting or omitting one cytosolic domain could disturb its native folding and subsequent function. Moreover, single cytosolic domains of an Inc protein may differ in functions or targets that, in sum, form a regulative interaction complex.

The new approach developed in this study addresses the aforementioned challenge and characterises all cytosolic domains with fluorescence labelling and co-immunoprecipitation. To overcome the problem of transiently expressed Inc proteins from being stuck in membranes, the TM domains of Inc proteins are replaced by eGFP, which solubilises the Inc proteins and provides a fluorescent label. This new fusion protein is called ‘split-Inc’ because the cytosolic domains are separated and thus split by eGFP. eGFP has similar proportions to a bi-lobed TM domain (Fig. 6). The most important aspect is its *cis*-directed and flexible termini. Their proximity mimics the distance of TM helices, supporting native folding of the cytosolic domains of the Inc protein. The final construct renders its cellular targets (organelles or cellular components) fluorescent. A further advantage is the ability to perform co-immunoprecipitation. Split-Inc protein can be isolated by using GFP-Trap targeting eGFP and thus co-immunoprecipitate its interaction partners. These immunoprecipitated proteins can be determined downstream via western blotting or MS. Split-Inc proteins were investigated and demonstrated as an approach to determine interaction partners by using immunofluorescence and co-immunoprecipitation.

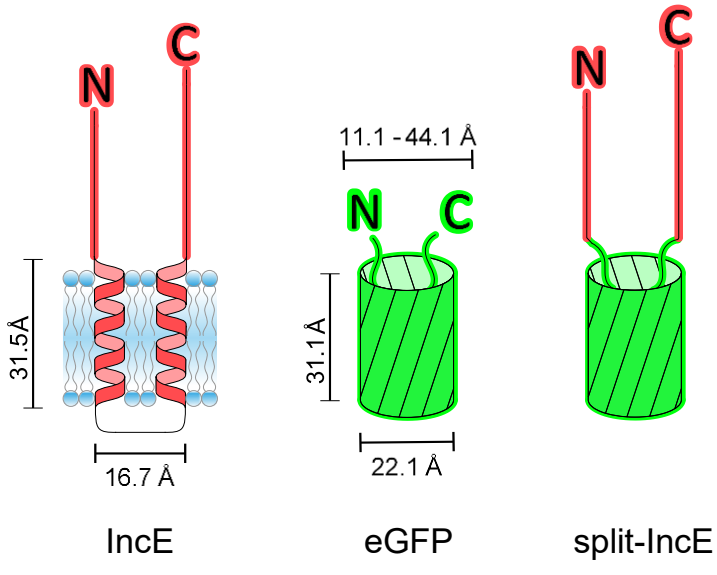

Fig. 6 Schematic overview.

The topologies and proportions of IncE from *C. trachomatis* serovar D, eGFP and the fusion protein split-IncE are shown. The TM helices of IncE ($IncE_{41-61}$ and $IncE_{66-86}$) were predicted by uniprot.org (P0DJI4) and used to calculate their lengths. The width is based on the sum of the TM domain diameters and the peptide length of $IncE_{62-65}$. The sequence lengths of the IncE cytosolic domains (red) are displayed as a scheme normalising the small to the large domain. Distances between CA atoms of eGFP were determined using PyMol (PDB: 2Y0G). The range above the termini describes the minimum and maximum calculated distances between the flexible N-terminus and C-terminus.

3.1.1 Immunofluorescence validation of split-Inc proteins

The design of split-Inc proteins is predicted to support the visualisation of interactions with host cellular proteins in immunofluorescence. To verify this postulation, the well-established interaction of IncE from *C. trachomatis* with human SNX5 and SNX6 (C. A. Elwell et al. 2017, Mirrashidi et al. 2015, Paul et al. 2017, Sun et al. 2017) was reconstructed by split-Inc proteins. Therefore, the cytosolic N-terminal and C-terminal domains of IncE were determined by Protter and used to design the protein $IncE_N$-eGFP-$IncE_C$ (split-IncE). Restriction-free overlap PCR avoided adding amino acids and generated the final construct used for *in vitro* analysis of the interaction with human SNX5. Because both SNX5 and SNX6, interact with IncE, depletion of only one SNX probably interferes with direct interaction analysis. Thus, HeLa cells lacking SNX5 and SNX6 were co-transfected with plasmids encoding split-IncE and myc-SNX5, whereas the expression of eGFP with myc-SNX5 and split-IncE, respectively, served as controls (Fig. 7). The overexpressed myc-SNX5 co-localised with split-IncE (upper panels) and appeared as spread dots when co-expressed with eGFP without co-localisations (middle panels). Split-IncE in the bottom panels appears like puncta. SNX5 is involved in retrograde trafficking and forms a retromer complex with multiple SNX proteins. Myc-SNX5 overexpression enhances the signal of those complexes bound by split-IncE. Although SNX5 and SNX6 were absent in the bottom panel, split-IncE was still punctate, indicating accumulation of homooligomerised split-IncE or binding to an unknown structure. However, transient expression of split-IncE highlighted its distinct destinations within the cell, in contrast to expressed eGFP that remained diffusely cytosolic (middle panel). In these experiments, the interaction between SNX5 and IncE was reconstructed successfully by using the new split-Inc protein method. Furthermore, the postulated capability to visualise interaction targets by split-Inc proteins in immunofluorescence was demonstrated. In the next step, the predicted usage of split-Inc proteins for co-immunoprecipitation was investigated in detail.

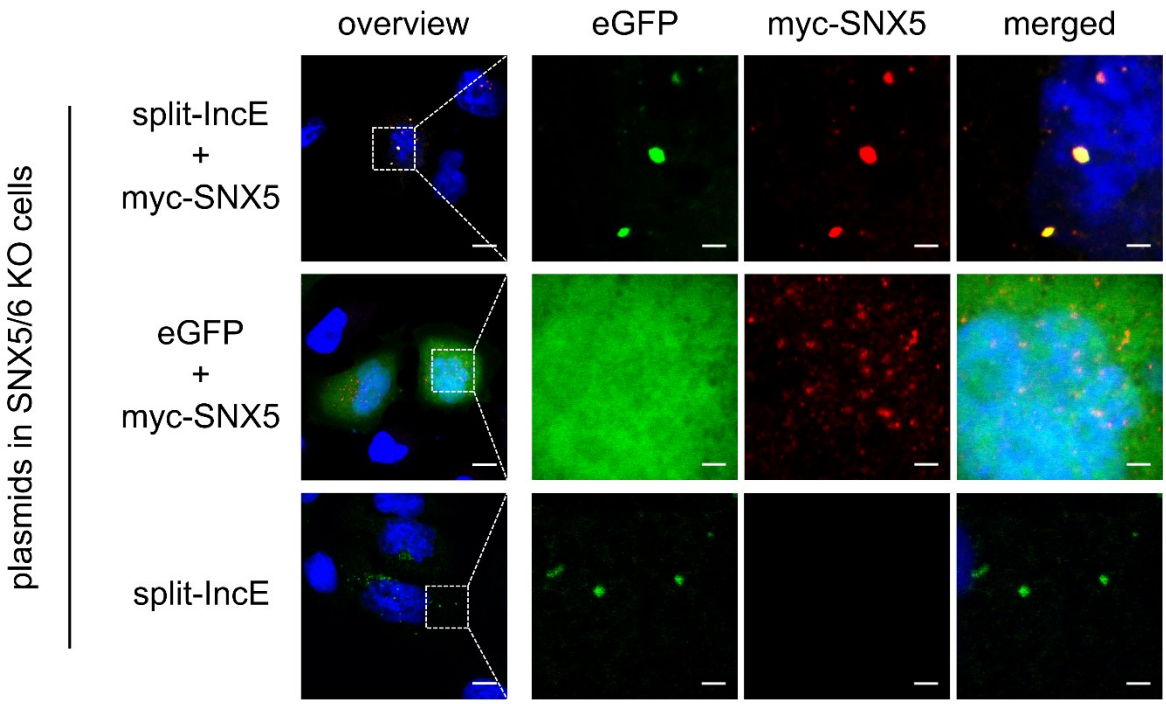

Fig. 7 Localisation of split-IncE *in vivo*.

HeLa cells with SNX5 and SNX6 double-knockout were (co-)transfected with constructs as indicated. The merged overview displays a dash-bordered area that is enlarged and separated into its channel and merged on the right. The scale bar is 10 µm in the overview and 2 µm in the zoom. DNA is stained by DAPI (blue), myc-SNX5 is stained by α-myc^{m} followed by α-mouse-Cy3 (red) and eGFP is displayed in green.

3.1.2 Determination of interaction partners using split-Inc proteins

Identifying human proteins that interact with *C. psittaci* Inc proteins is one aim of this work. Using split-Inc proteins as a tool to determine interaction partners requires establishing and validating the method. Hence, the previously introduced interaction of IncE with SNX5 and SNX6 was analysed further by using split-IncE. Cells expressing split-IncE were gently lysed 24 h post-transfection (Fig. 8). The lysate was incubated with agarose bead–linked micro-antibodies with a high affinity for GFP, known as GFP-Trap (Chromotek). Proteins were digested directly on beads by trypsin to yield peptides. These peptides were further desalted and detected via LC-MS. The spectral counts of identified proteins were used for the Significance Analysis of INTeractome (SAINT) algorithm to determine significant hits (Olson et al. 2020). Amongst 1040 identified proteins, SNX5 and SNX6 yielded the highest SAINT scores (Fig. 9). Therefore, the interaction between SNX5 and SNX6 and IncE was demonstrated successfully by using split-Inc proteins as a new strategy for interaction studies. These results indicate the great advantage of using split-Inc proteins as a method to visualise solubilised Inc proteins and their targets in immunofluorescence and the detailed identification of interaction partners by co-immunoprecipitation and subsequent MS.

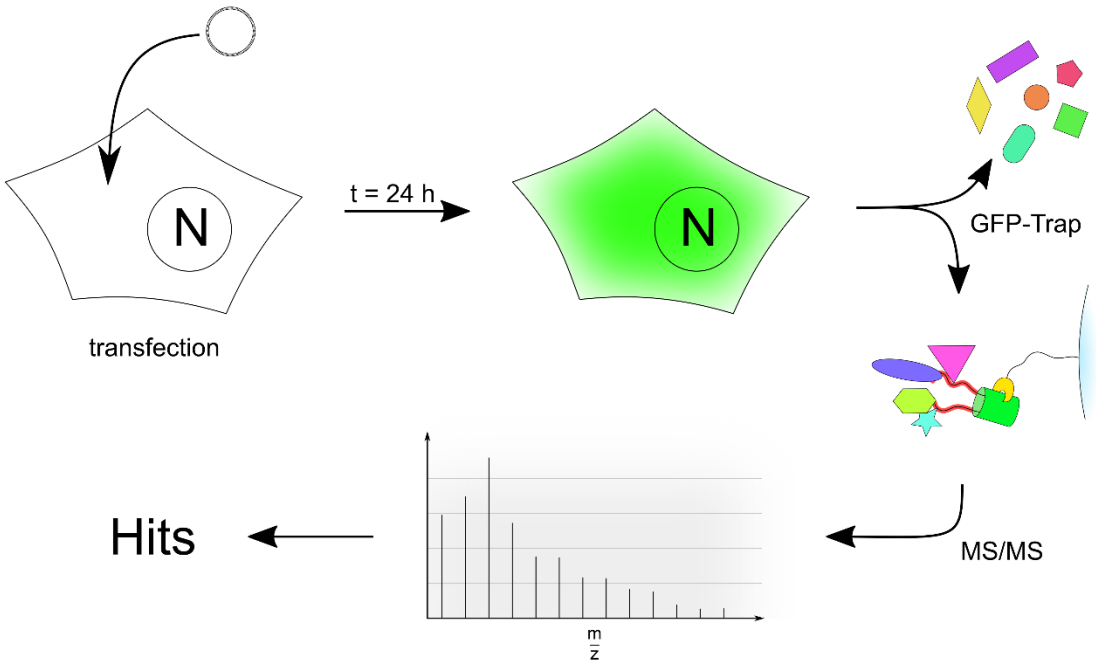

Fig. 8 Schematic workflow.

HeLa cells were transfected with a plasmid encoding split-Inc. Twenty-four hours post-transfection, the cells were gently lysed, and proteins were separated from the fusion protein with its interaction partners using GFP-Trap (Chromotek). The enriched proteins were digested directly on beads with trypsin. The resulting peptides were desalted by Stage-Tips and measured by LC-MS. Statistically enriched hits were determined by SAINT (Olson et al. 2020).

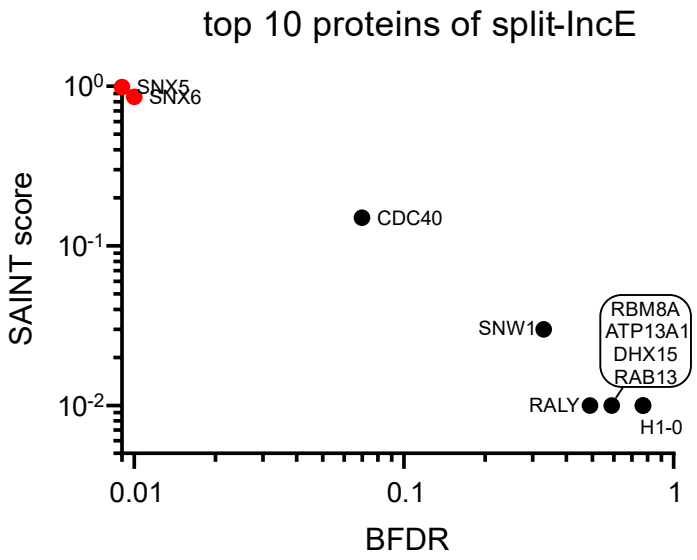

Fig. 9 SAINT scores of split-IncE co-purified targets.

The split-IncE interaction partners were determined as described in the workflow (Fig. 8). SAINT scores were determined by using the controls eGFP and split-CP0534 with n = 1. The 10 proteins with the highest SAINT scores are displayed in the plot of SAINT score versus the Bayesian false discovery rate (BFDR) on a log10-scale. The top two proteins are highlighted as red dots. The BFDR of SNX5 is 0 but was set as 0.009 so it could be displayed.

3.1.3 The synergy of both cytosolic domains of IncE regulates the interaction with SNX5

The concept of split-Inc proteins relies on the hypothesis that the interplay of all cytosolic domains is necessary to mimic native interactions. So split-Inc proteins are designed to mimic the native state of Inc proteins as close as possible using the N-terminal and C-terminal cytosolic domains of an Inc protein. However, the relevance of a short terminal sequence in interaction dynamics and native folding remains unclear. Paul et al. (2017) and Sun et al. (2017) showed that the interaction of IncE with SNX5 and SNX6 depends on the C-terminus of the Inc protein. Herein, the effect of the N-terminal domain on the interaction of the C-terminal IncE with SNX5 was examined. The C-terminus or N-terminus of IncE or full-length IncE was translocated into the outer membrane (OM) of mitochondria with cytosol-facing chlamydial domains. This mitochondrial approach was predicted to mimic the membrane-bound interaction of *Chlamydia* and to facilitate quantification of bound interaction partners. Thus, mitochondria were isolated, purified and analysed via western blot (Fig. 10 A). The full-length construct corresponds to the split-Inc protein but with interposed TM domains that translocate proteins into the OM of mitochondria. The N-terminal TM domain is from a predicted alternate exon of Protein spire homolog 1, called ExonC. Manor et al. (2015) showed correct integration into the OM when tagged with GFP at the N- or C-terminus. The C-terminal TM domain corresponds to the first 33 N-terminal amino acids of human Tom20 ($Tom20_{N33}$). Kanaji et al. (2000) showed sequence-dependent N-terminal-directed translocation of rat $Tom20_{N33}$ into the OM. They demonstrated the relevance of the C-terminal amino acid motif DRKRRSD for successful import. The herein used *Homo sapiens* orthologue differed in the motif at R26H. The difference was assumed not to impair the translocation because the change still yields a basic amino acid. Kanaji et al. (2000) showed that even a mutation in this position facilitates successful transport into mitochondria. The eGFP portion of the final full-length construct $IncE_N$-ExonC-eGFP-$Tom20_{N33}$-$IncE_C$-myc was predicted to reside in the mitochondrial intermembrane space (IMS). The IncE full-length protein was compared with $IncE_N$-ExonC-eGFP (N-term) and $Tom20_{N33}$-$IncE_C$-FLAG (C-term). The constructs were transiently expressed in HeLa cells and analysed via immunofluorescence (Fig. 10 B). All three constructs were located in the mitochondria. SNX6 co-localised with the IncE C-term and IncE full-length, whereas no co-localisation was observed in IncE N-term expressing cells, demonstrating functional interaction and targeting into mitochondria. The mitochondria of HeLa cells expressing IncE C-term were isolated, and purification steps were investigated by western blot (Fig. 10 C). IncE C-term was detected in the lysate and in the purified mitochondria. The nuclei fraction contained smeared bands of different heights that might correlate with improper denaturation. The mitochondria-cleared supernatant was absent of

IncE C-term. These results demonstrate successful isolation of mitochondria. The isolated mitochondria containing the translocated IncE N-term or IncE full-length constructs were subjected to mild digestion by proteinase K for 0, 30, 60 s or 5 min to determine the correct translocation (Fig. 10 D). The C-terminal IncE signal of the IncE full-length construct vanished after 30 s, whereas the GFP signal decreased more slowly. Moreover, the IncE N-term construct showed only a slight reduction in GFP signal with emerging degradation bands. These results specified correct integration into the OM as predicted and allowed the analysis to proceed. Interaction of the IncE constructs with SNX5 was analysed via western blot. Due to the low, barely detectable endogenous SNX5 expression, myc-BirA-SNX5 was co-expressed to enhance the signal intensity (Fig. 10 E). All three constructs were translocated successfully into the mitochondria, as confirmed by the antibody against the C-terminus of IncE (Fig. 10 E, left) and anti-GFP (Fig. 10 E, right). The IncE full-length construct was translocated less intensely compared with the IncE C-term and IncE N-term constructs.

The SNX5 signal was detected only in the IncE C-term and IncE full-length constructs (Fig. 10 E, upper left panel). On the contrary, no SNX5-signal was detected in the negative control N-term construct. This observation demonstrated successful co-purification of interacting SNX5 and confirmed the dependence of the interaction on the C-terminus of IncE. The SNX5 signal intensity was similar for mitochondria that contained the IncE C-term or IncE full-length constructs, although the IncE C-term construct signal was more intense than the full-length construct signal. Overall, more SNX5 was recruited per IncE full-length molecule than per IncE C-term construct. This enrichment indicated that the additional N-terminus might enhance or stabilise the interaction between the C-terminus of IncE and SNX5. Therefore, the N-terminus of IncE seems to act as a stabiliser. The results demonstrate that the presence of both cytosolic domains affects the interaction.

In sum, the synergistic effect of both cytosolic domains of IncE enhanced and stabilised the interaction with SNX5, a finding consistent with the hypothesis of this work. It is recommended that future interaction studies of Inc proteins consider using all cytosolic domains. Finally, the split-Inc protein method is a powerful tool for *in vivo* and *in vitro* interaction studies.

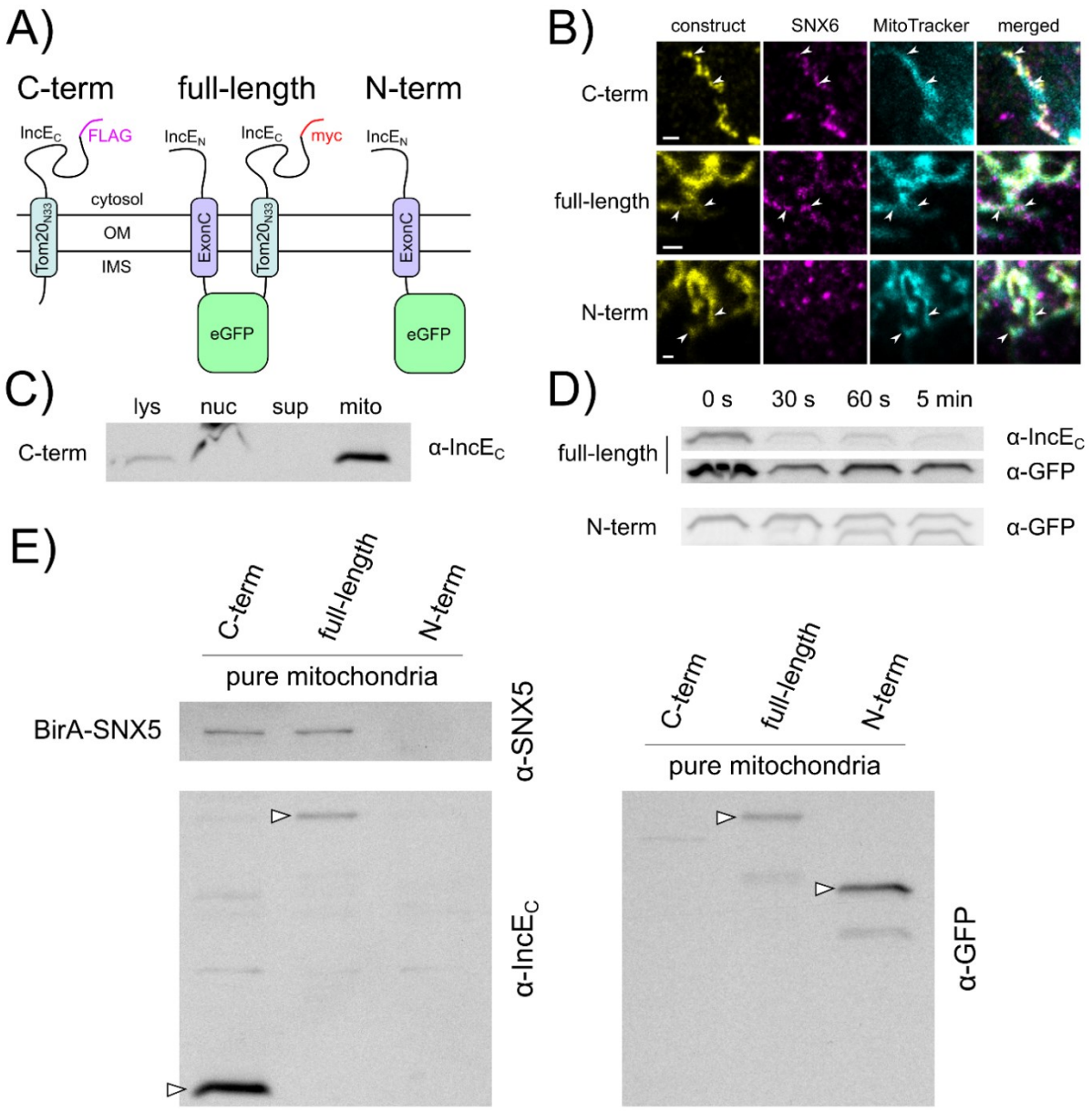

Fig. 10 Investigation of translocation and interactions of mitochondrial split-IncE.

A) Scheme of split-IncE variants that are anchored in the mitochondria. OM, outer membrane; IMS, intermembrane space. B) Immunofluorescence of transiently expressed constructs. Full-length and N-term are visualised by eGFP (construct, yellow) and SNX6 with a specific antibody via Cy3 (magenta). C-term is visualised by α-FLAG^m at Cy3 (construct, yellow) and SNX6 with a specific antibody at 488 nm (magenta). Mitochondria were visualised by MitoTracker™ DeepRed FM (cyan). Arrowheads indicate co-localisations. The scale bar is 1 µm. C) Isolation of mitochondria. HeLa cells transiently expressing C-term were lysed, and mitochondria were isolated (section 2.2.16). Western blot with fractions of lysate (lys), nuclei (nuc), mitochondria-cleared supernatant (sup) and purified mitochondria (mito) were stained by α-IncE$_C$. D) Time-dependent digestion of isolated mitochondria with split-IncE inserted. Isolated mitochondria with N-term or full-length constructs were digested with proteinase K for 0 s, 30 s, 60 s or 5 min. Samples were analysed via western blot. C) SNX5-co-purification by mitochondrial isolation. Cells were transfected with BirA-SNX5 together with the C-term, full-length or N-term construct. Mitochondria were isolated and western blot was performed. The arrowheads show split-IncE that successfully anchored in mitochondria.

3.2 Characterisation and interaction studies of *C. psittaci* Inc proteins

3.2.1 *In silico* analysis of predicted *C. psittaci* Inc proteins

One of the most common zoonotic pathogens amongst the *Chlamydiae* is *C. psittaci*. Its ability to infect and replicate successfully and to form infectious progenies in both humans and birds makes it a fascinating subject for interspecies pathogenesis from an evolutionary point of view. With the aid of Inc proteins, *Chlamydia* can hijack cellular organelles and recruit components and proteins to the inclusion membrane. Lutter et al. (2012) screened putative Inc proteins of different *Chlamydia* spp. based on hydrophobicity for the TM domain and amino acid sequence similarities. They did PSI-BLAST of the identified Inc proteins to analyse similarities. Inc proteins that showed similar Inc proteins in all investigated species (*Chlamydia felis*, *C. trachomatis*, *C. muridarum*, *C. caviae* and *C. pneumoniae*) were declared as core-Inc proteins, whereas unique proteins were categorised as non-core Inc proteins. Although they are similar, core Inc proteins lack conserved amino acid patterns. The concept of core Inc proteins to form a basis for infection, enabling adaptation to different hosts, is an essential element to investigate the zoonotic pathogen *C. psittaci*. The identification of *C. psittaci* Inc proteins and their potential interaction partners is predicted to clarify interspecies basic functions and host-specific adaptation. One aim of this work is to identify *C. psittaci* Inc proteins *in silico* by annotation screening and TM domain prediction. Furthermore, the Inc proteins will be functionally characterised by transcriptional analysis and interaction studies *in vivo*. The results may facilitate understanding how *Chlamydia* adapt to different hosts using species-specific and core Inc proteins. Hence, *in silico* analysis of *C. psittaci* was performed to identify and predict putative Inc proteins.

The genomic analysis of *C. psittaci* using the widely accepted reference genome *C. psittaci* VS225 (Accession: CP003793) (Van Lent et al. 2012) revealed 12 Inc-annotated proteins with terms like ‘inclusion membrane (domain) protein’, ‘IncA family protein’, ‘IncB’ or ‘IncC’ (Table 2). Comparison with the genome of the lab strain *C. psittaci* 02DC15 used in this study revealed an insertion at the 3' end of CPS0B_0181 that leads to a frameshift and abolishes the stop codon. Therefore, the protein covers the sequences of the referring gene B600_0189 and immediately follows B600_0190 without harming the latter amino acid sequence. Due to the fusion of the coding sequences, CPS0B_0181 is likely a combination of B600_0189 and B600_0190.

A total of 11 Inc proteins of *C. psittaci* 02DC15 were investigated regarding their TM domains by using Protter (Omasits et al. 2014) and by hydrophobicity scoring according to Kyte & Doolittle using ProtScale from Expasy on https://web.expasy.org/protscale/ (Fig. 11). *In silico*

prediction analysis of all 11 Inc proteins revealed bi-lobed TM domains typical for Inc proteins (Rockey et al. 1995). The TM domain of CP0181 is highly hydrophobic and separated a small N-terminal cytosolic domain from a large C-terminal cytosolic domain (Fig. 12 A). The latter displays a consistent mix of residues with slightly higher polarity in the middle and slightly increased hydrophobicity at the C-terminus. CP0355 has a small polar N-terminus and a larger polar C-terminus. IncC (Fig. 12 A) and IncB (Fig. 12 B) have a large N-terminus with an average hydrophobicity score of 0 and a small C-terminus. In addition, both share an enlarged linkage between the TM helices. The small N-terminal and the large C-terminal cytosolic domains of CP0558 are overall polar with a highly polar pattern at the end of the C-terminus (Fig. 12 B). The TM domain of IncA has an N-terminal hydrophobic increase deriving from the small N-terminal cytosolic domain that is separated only diffusely from the TM domain compared with the other Inc proteins. Its C-terminal domain consists of distinct polar and hydrophobic patterns followed by a variable region of hydrophobic and polar residues. The large C-terminal domain of CP0849 shows five repeating patterns of high polarity followed by moderate hydrophobicity (Fig. 12 C). The Inc proteins CP0850, CP0855, CP0856 and CP0857 (Fig. 12 D) have a very polar, large C-terminal domain with single hydrophobic residues. In addition, CP0855 and CP0857 display a small hydrophobic N-terminus. The N-termini of IncB and IncC are longer than their C-termini, in contrast to the other nine Inc proteins, which have longer C-termini than N-termini.

In summary, the *in silico* analysis comparing *C. psittaci* 02DC15 with the pre-annotated reference genome of *C. psittaci* VS225 revealed 11 putative Inc proteins. Two unrelated online tools revealed typical bi-lobed TM domains in all predicted Inc proteins, although there are different size ratios of the terminal cytosolic domains. The chlamydial expression of these hypothetical Inc proteins during infection of HeLa cells was analysed by using transcriptional quantification.

Table 2 Comparison of annotated Inc proteins in *C. psittaci* VS225 with orthologues in *C. psittaci* 02DC15

C. psittaci VS225		*C. psittaci* 02DC15		
ID	**length / bp**	**ID**	**length / bp**	**Difference in 02DC15**
B600_0189	330	CPS0B_0181	3039	1 insertion shifted the stop codon
B600_0190	2697			
B600_0375	675	CPS0B_0355	675	
B600_0569	555	CPS0B_0534	555	
B600_0570	609	CPS0B_0535	609	
B600_0596	1119	CPS0B_0558	1119	
B600_0636	993	CPS0B_0598	1149	1 point mutation changed the stop codon
B600_0904	717	CPS0B_0849	729	Computational 5′ extension of annotation but no sequence change
B600_0905	1059	CPS0B_0850	1059	
B600_0910	1431	CPS0B_0855	2433	1 insertion shifted the stop codon
B600_0911	1029	CPS0B_0856	1062	Computational 5′ extension of annotation but no sequence change
B600_0912	1440	CPS0B_0857	1440	

A)

CP0181

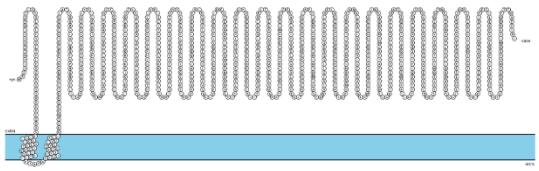

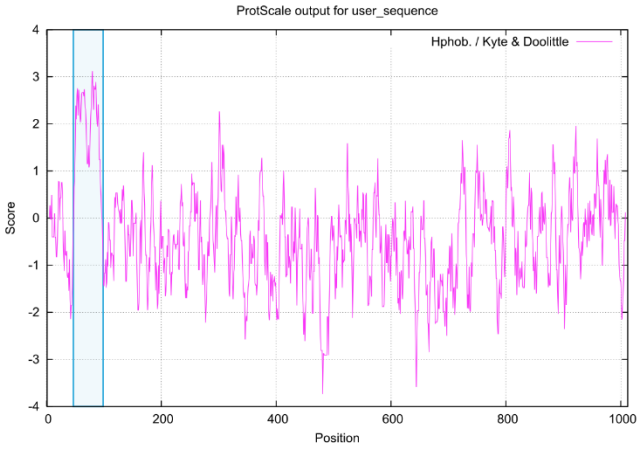

CP0355

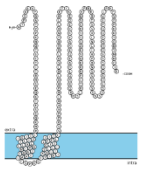

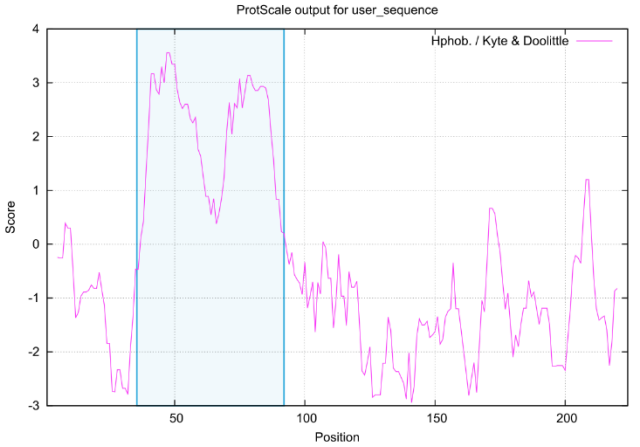

CP0534 (IncC)

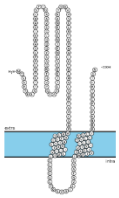

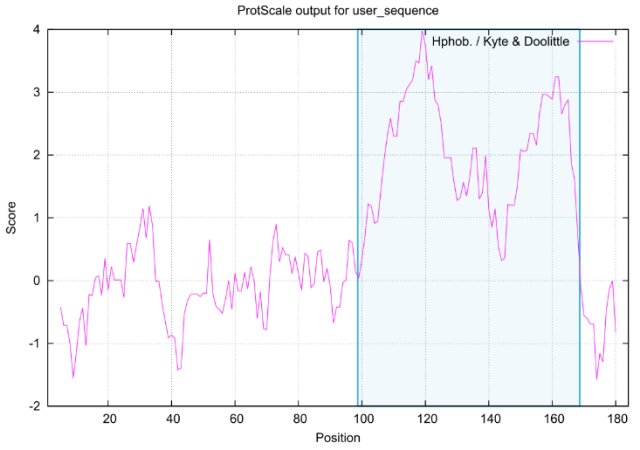

B)

CP0535 (IncB)

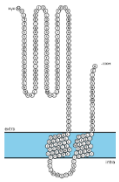

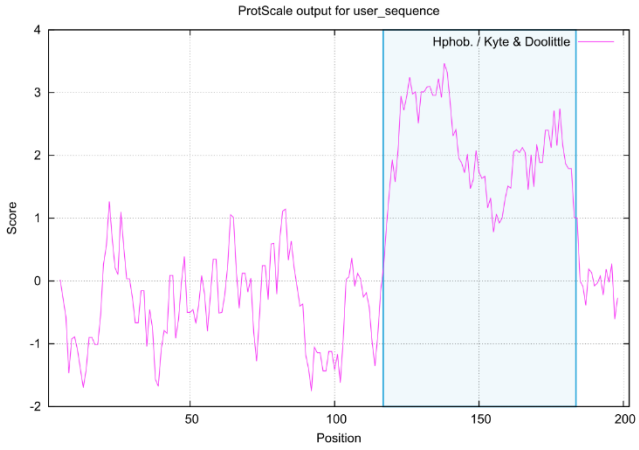

CP0558

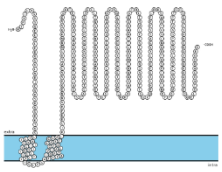

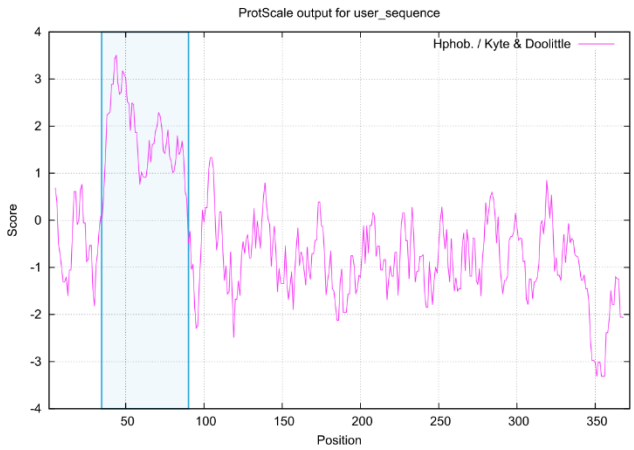

CP0598 (IncA)

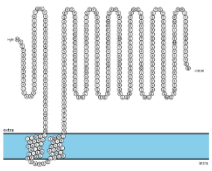

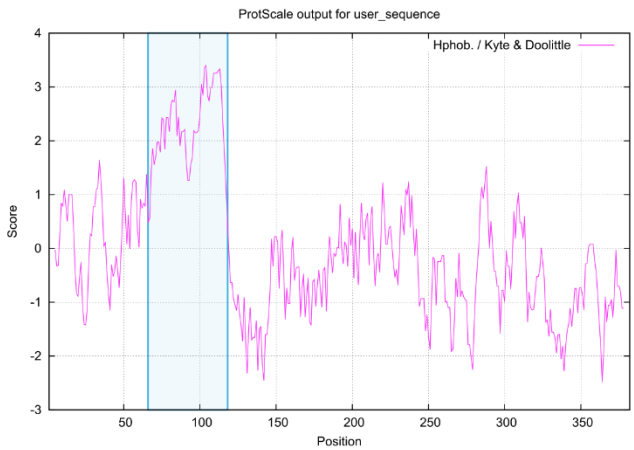

C)

CP0849

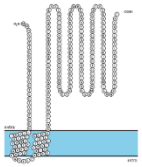

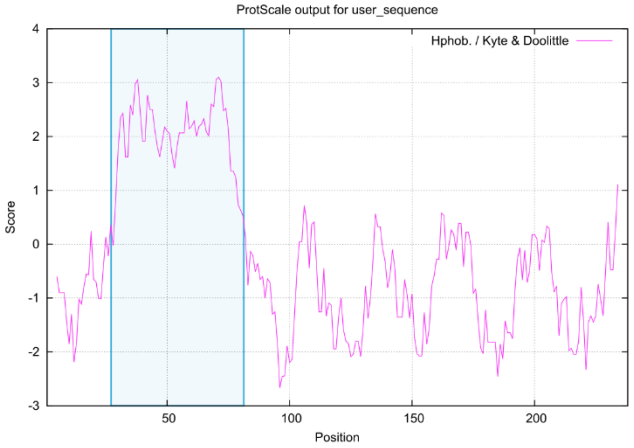

CP0850

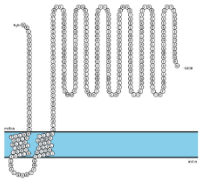

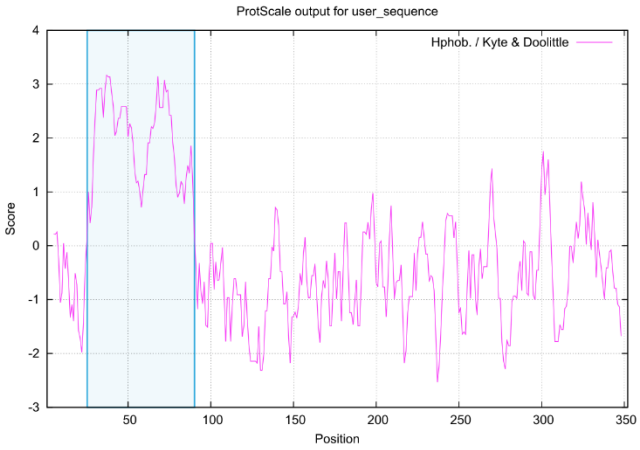

CP0855

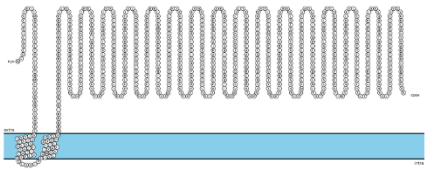

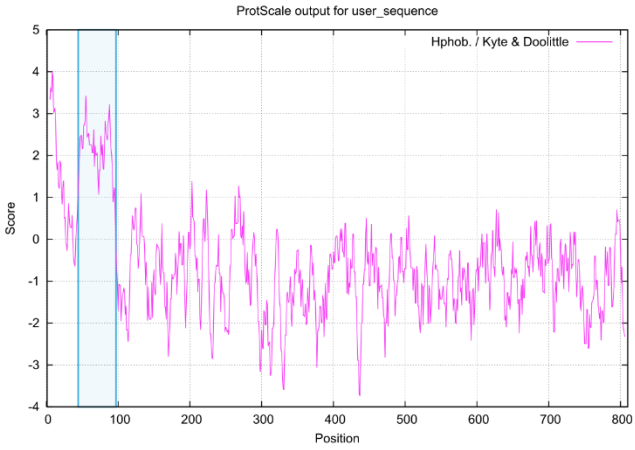

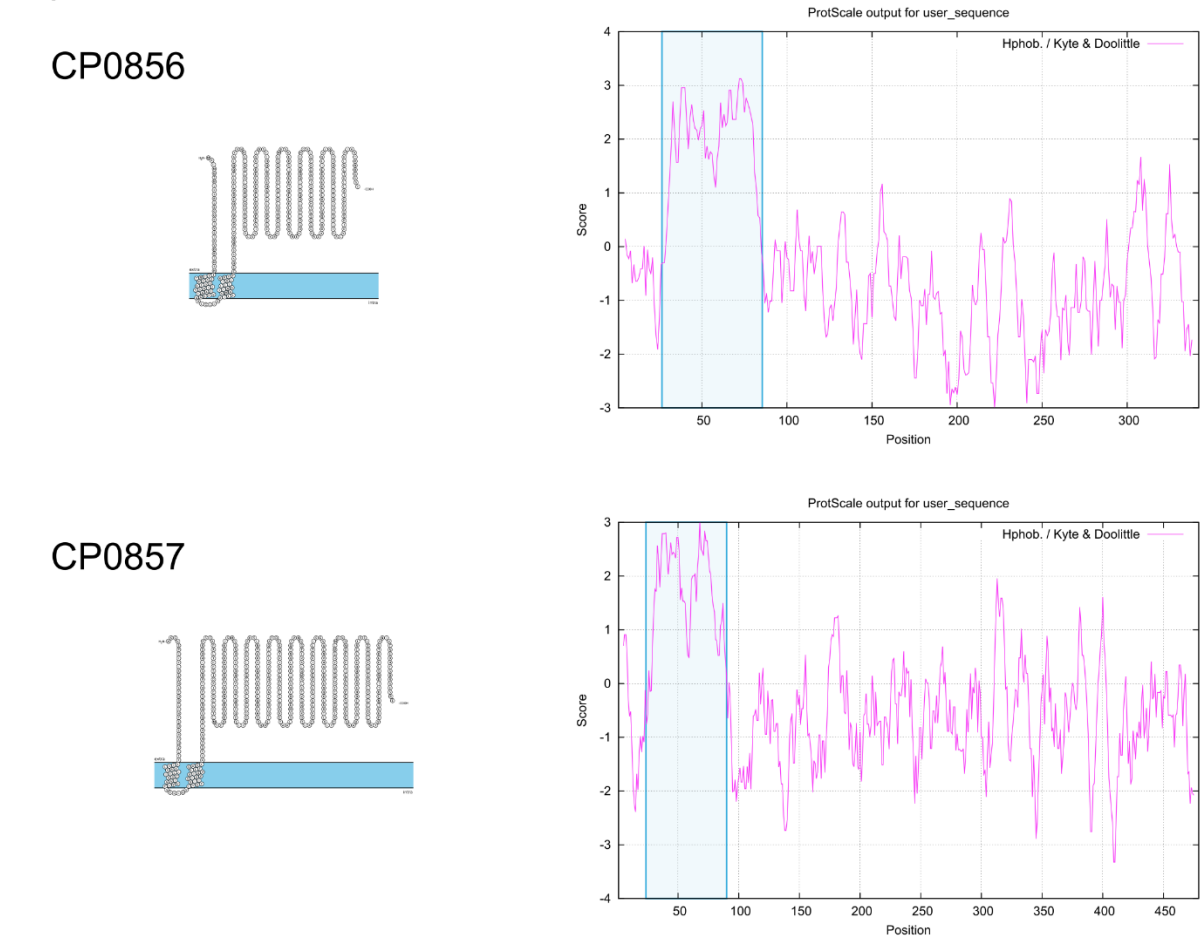

Fig. 11 *In silico* analysis and prediction of the TM domain of *C. psittaci* Inc proteins.
The topologic view of cytosolic and TM determination (left) was generated by Protter and hydrophobicity was calculated by using the Kyte & Doolittle scale (from the ProtScale website https://web.expasy.org/protscale/). The predicted TM domain in the hydrophobicity plot is highlighted in light blue. *C. psittaci* Inc proteins are shown in the following order: A) CP0181, CP0355, CP0534 (IncC); B) CP0535 (IncB), CP0558, CP0598 (IncA); C) CP0849, CP0850, CP0855; and D) CP0856, CP0857.

3.2.2 Quantification of *C. psittaci* Inc gene expressions

The developmental cycle of *Chlamydia* is complex and comprises several stages. Proteins are expressed at certain times based on their mode of action – for example, EB ↔ RB conversion, replication, metabolism, maintaining inclusion constitution or cellular component recruitment. Eight of 11 previous highlighted Inc proteins were characterised by investigating their transcript level at times from the early to the late phase of infection (Fig. 12). HeLa cells were infected with *C. psittaci*, and total RNA was extracted at the indicated times via phenol-chloroform extraction using self-made TRIzol (section 2.2.21). The genes and the level of the endogenous 16S ribosomal RNA (rRNA) were quantified via qPCR (section 2.2.20) using the 1-Step Kit Power SYBR® Green RNA-to-CT™ (Thermo Fisher Scientific Inc.) with gene-specific primers.

The resulting C_T values were normalised to the C_T values of the 16S rRNA, yielding a relative transcript level that was displayed as log2 fold change. Several Inc genes shared a similar transcriptional pattern. *IncC*, *incB* and *cp0558* were expressed early or immediately early with decreasing levels until 24 or 32 hpi and an increase again during the very-late phase of infection (32 or 48 hpi). *cp0181* was also expressed immediately early with a high transcript level at 2 hpi and decreased until 16 hpi. Interestingly, *cp0181* was again transcribed in the mid-late phase between 16 and 48 hpi, represented as a small peak. The *cp0355* and *cp0856* transcript levels reached a maximum at the early-mid phase transition of around 8 and 16 hpi, respectively. *incA* and *cp0857* displayed a bi-phasic transcriptional profile. They decreased initially from the beginning of the infection until 8 hpi but were transcribed highly at 16 hpi, reaching a level close to that seen at 2 hpi. Their levels decreased immediately after 16 hpi. These results demonstrated the transcription of the hypothetical Inc genes during *C. psittaci* infection in HeLa cells. Furthermore, they showed different transcriptional profiles related to distinct expression phases of *C. psittaci*: immediate-early (*incC*, *incB*, *cp0558*), mid (*cp0355*, *cp0856*), a bi-phasic combination of immediate-early and mid-late (*cp0181*) and a bi-phasic combination of early and mid (*incA*, *cp0857*). The transcriptional characterisation helps to narrow down the individual function of each Inc protein. Hence, these Inc proteins were characterised functionally *in vivo* by using the new established split-Inc protein method.

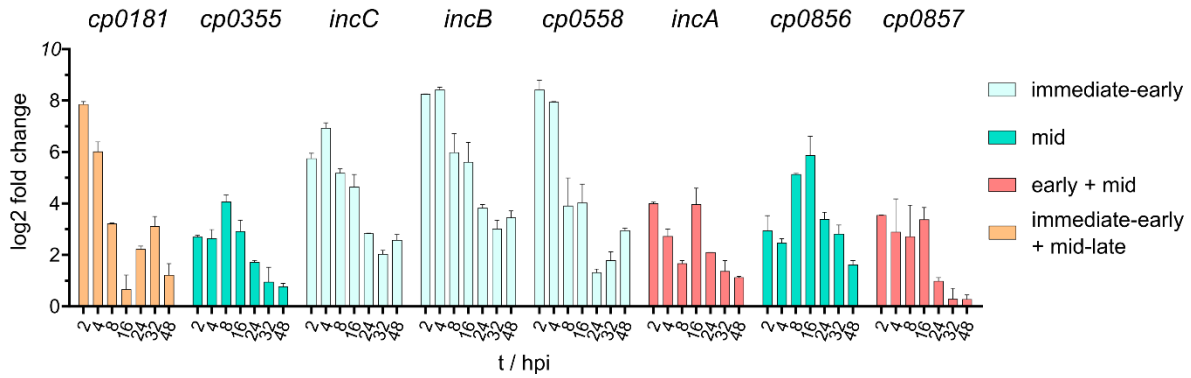

Fig. 12 Relative transcript levels of *C. psittaci* Inc genes during infection.

HeLa cells (approximately 80% confluent) were infected with *C. psittaci* 02DC15 (MOI = 2). At the indicated time (hpi, x-axis), total RNA was extracted for qPCR. The C_T values of the samples were normalised to the time-related C_T values of 16S rRNA and adjusted to the smallest $-\Delta C_T$ value of the data. $-\Delta\Delta C_T$ is displayed as the mean log2 fold change with the standard deviation. The related Inc genes are labelled above the bars. The bars are coloured according to the infection phases (see the legend). The experiment was performed with two biological replicates and two technical replicates.

3.2.3 *In vivo* investigations of *C. psittaci* Inc proteins using split-Inc proteins

The previous analysis revealed the transcription of the hypothetical putative Inc genes. These Inc proteins were investigated by immunofluorescent cell culture experiments that were expected to show interactions with host cellular structures. Therefore, the newly established split-Inc protein method was applied to generate eight split-Inc proteins: split-CP0181, split-CP0355, split-IncC, split-IncB, split-CP0558, split-IncA, split-CP0856 and split-CP0857. Uninfected HeLa cells were transfected with plasmids encoding the split-Inc proteins. The eGFP portion of the ectopically expressed split-Inc protein displayed the cellular localisation of the protein (Fig. 13). The cells were stained with phalloidin-555 to visualise F-actin and DAPI to visualise nuclei. All split-Inc proteins localised in the cytosol except for split-CP0355, which strongly accumulated in the nucleus (see arrowhead). In remarkable contrast to split-CP0355, both split-CP0856 and split-CP0857 showed much stronger accumulation in the cytosol (arrowheads pointing on nucleus and cytosol as comparison). In addition, split-IncB co-localised with actin at distinct areas (see arrowheads), whereas the small punctate accumulations of split-CP0181 were not related to actin (see arrowheads). Overall, only split-IncC, split-CP0558 and split-IncA displayed a cytosolic localisation, whereas split-CP0181, split-CP0355, split-IncB, split-CP0856 and split-CP0857 localised to distinct areas inside the eukaryotic cell. These results showed the cytosolic distribution of *C. psittaci* split-Inc proteins, suggesting cytosolic interaction partners, while split-CP0355 seems to interact with nuclear proteins. The localisation of the split-Inc proteins during the infection with *C. psittaci* could provide further information. Hence, the next experiments addressed this issue.

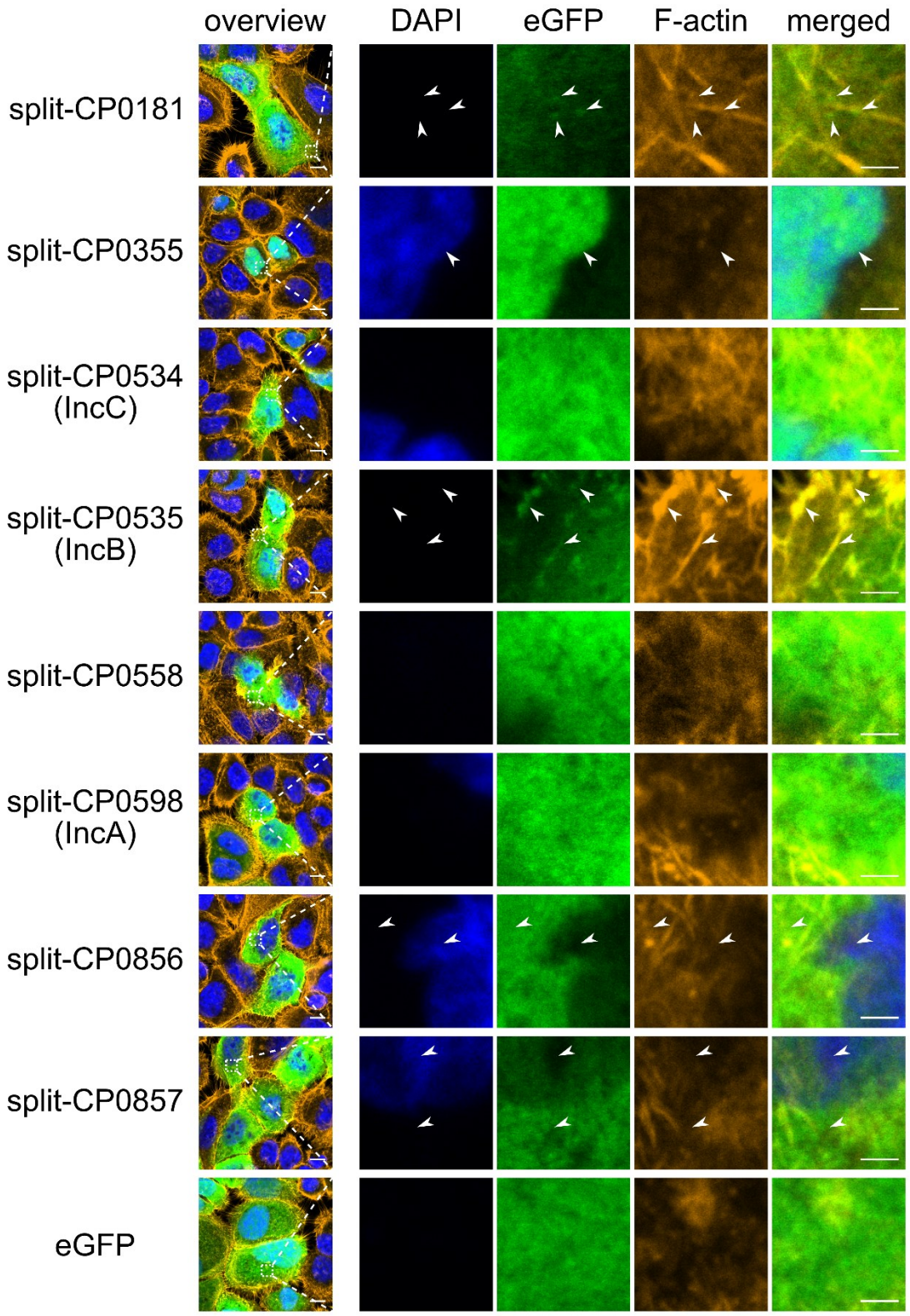

Fig. 13 *In vivo* localisation of *C. psittaci* split-Inc proteins.

Cells were transfected with the construct indicated at the left for 24 h and then fixed with 2% PFA. The inlay of the overview (left) was zoomed (right). Filamentous actin (F-actin) and DNA were stained with phalloidin-555 and DAPI, respectively. The eGFP portion of the expressed construct is displayed in green. Arrowheads indicate special localisations of the split-Inc protein. The scale bar is 10 µm in the overview and 2 µm in the zoom.

3.2.4 Cellular distribution of *C. psittaci* split-Inc proteins during infection

The immunofluorescence of *C. psittaci* split-Inc proteins in cells infected with *C. psittaci* was predicted to reveal information about recruitment and cellular distribution. When expressed during infection, split-Inc proteins might bind to host proteins recruited by Inc proteins to the inclusion membrane. This sandwich-like binding may highlight the inclusion membrane via bound split-Inc proteins. Thus, *C. psittaci* split-Inc proteins were investigated during infection with *C. psittaci*. Cells were infected with *C. psittaci*, transfected at 2 hpi with plasmids encoding the split-Inc protein as indicated and fixed at 24 hpi (Fig. 14). All split-Inc proteins showed relatively intense accumulation at the inclusion membrane except for split-CP0857, which remained cytosolic and did not accumulate at the inclusion membrane. In addition, split-CP0181 was localised only diffusely along the inclusion membrane. Split-CP0355 showed reduced nuclear localisation compared with uninfected cells and accumulated slightly at the inclusion membrane. Actin filaments are recruited by *C. psittaci* and form a cage-like structure around the inclusion (Chin et al. 2012). These filaments co-localised strongly with split-CP0558 and less intensely with split-IncB. Split-IncA covered the complete inclusion and appeared less diffuse. Split-IncC and split-CP0856 accumulated at distinct regions of the inclusion membrane with different intensities. This observation indicates specific binding to recruited proteins. In sum, all *C. psittaci* split-Inc proteins located at the inclusion membrane except for split-CP0857, which remained cytosolic. Moreover, split-CP0558 and split-IncB co-localised with actin filaments. These results supported the participation of the putative Inc proteins in the interaction surface between the host cell and the inclusion membrane. The results also indicate that split-Inc proteins could serve as a tool for *in vivo* interaction studies. The subsequent experiments aimed to identify cellular interaction partners.

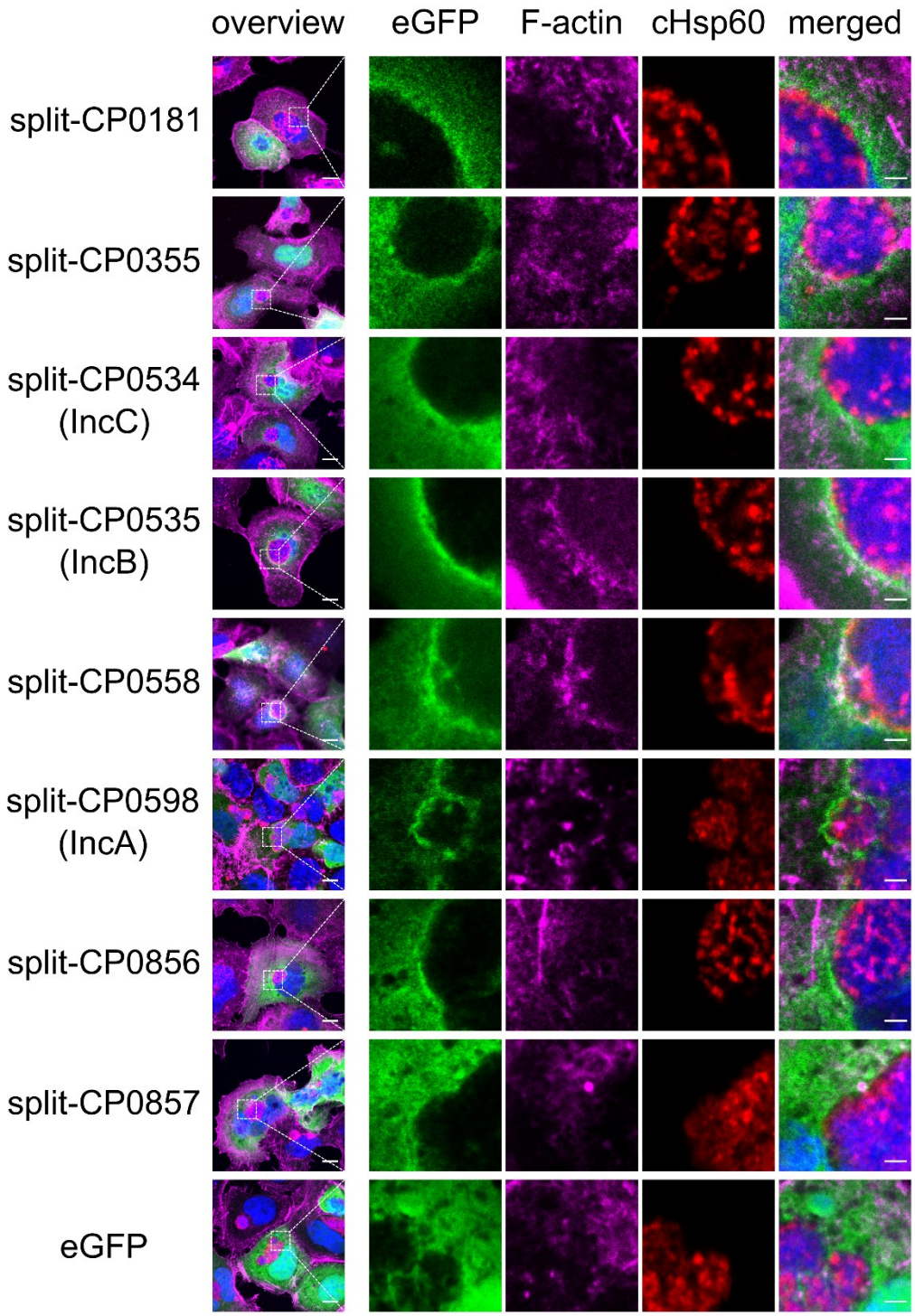

Fig. 14 *In vivo* localisation of *C. psittaci* split-Inc proteins during infection.

Cells were infected with *C. psittaci* and subsequently transfected at 2 hpi with the construct indicated to the left. eGFP expression was used as control. Slides were fixed with 2% PFA at 24 hpi. The inlay of the overview (left) was zoomed (right). Filamentous actin (F-actin) and DNA were stained with phalloidin-555 and DAPI, respectively. The bacteria were stained with α-cHsp60^{m} and α-mouse conjugated to Alexa Fluor® 647. The scale bar is 10 µm in the overview and 2 µm in the zoom.

3.2.5 Determining interaction partners of *C. psittaci* split-Inc proteins

The previous results revealed that the chosen *C. psittaci* Inc proteins bind to proteins. Next, *C. psittaci* split-Inc proteins were used to identify interaction partners using GFP-Trap followed by MS (see section 3.1.2, Fig. 8). Hence, cells were transfected with plasmids encoding the split-Inc protein and lysed 24 h post-transfection. The split-Inc protein and its putative bound interaction partners were co-immunoprecipitated and purified using GFP-Trap. The proteins were further digested into peptides by trypsin, desalted via C18-StageTips and detected with LC-MS (section 2.2.19). The significance of 520 identified proteins was determined using the SAINT algorithm based on spectral count comparison amongst all samples (Olson et al. 2020). Proteins with a SAINT score ≥ 0.9 and a Bayesian false discovery rate (BFRD) < 0.01 were considered to be significantly enriched. The SAINT enrichment analysis yielded 120 mammalian proteins, representing 22.56% of the total identified host proteins (Fig. 15 A). These 120 proteins were sorted considering their intensity-based absolute quantification (iBAQ) values (Fig. 15 B) to highlight the most enriched proteins. Another sorting approach involved identifying protein sub-complexes that were predicted to have similar iBAQ values but yielded no results. The top 20 significantly enriched proteins of each split-Inc protein were visualised as an interaction network (Fig. 15 C) using CytoScape (Shannon et al. 2003). These proteins were investigated further via Gene Ontology (GO) term enrichment analysis according to biological processes, cellular components and molecular functions to associate the function of the Inc protein. The analysis relied on the CytoScape-plugin ClueGO (Bindea et al. 2009) without term restriction but with a p-value ≤ 0.05 (Fig. 16). GO terms were clustered with at least one gene and linked to the associated gene, except for the hits of CP0355: its 104 interaction proteins and correlated GO terms exceed the amount for a clear overview. Therefore, the interaction proteins of CP0355 were not shown, but the resulting clusters were displayed as groups according to their parental clusters. The only representative of the immediate-early group is the CP0558 target acyl-CoA dehydrogenase family member 11 (ACAD11), which is involved in a cluster of medium-chain-acyl-CoA dehydrogenase activity. Members of the mid-phase group are CP0355 and CP0856. Interaction proteins of CP0355 bind different types of RNA, such as rRNA or mRNA. Consequently, the resulting GO terms are about ribosomal biogenesis and negative regulation of mRNA metabolic process. As part of ribosomes, some proteins are also involved in translational elongation. Most proteins are localised in the nucleus and some in intracellular organelles or are part of membranes, including the plasma membrane and cell junctions. The largest cluster with the most highly enriched GO terms of CP0856 interacting proteins is the positive regulation of protein insertion into the mitochondrial membrane involved in apoptotic signalling. The interaction proteins are

also part of the anchoring junction and are involved in cadherin binding and anatomical structure development. Besides protein C-terminus binding, several proteins are enriched for protein kinase C inhibitor activity and negative regulation of biological processes. The last group consists of *C. psittaci* Inc proteins whose transcript levels doubled in the early and mid phases: CP0857 and IncA. The interaction partners of CP0857 are part of processes like cognition, corpus callosum morphogenesis and dendritic spine maintenance. One interaction partner of IncA is related to dendritic microtubules, but both targets of IncA share ubiquitin-protein transferase activity. In summary, the immediate-early Inc protein CP0558 targets ACAD11 in the context of lipid metabolism; the mid-phase Inc proteins CP0355 and CP0856 are associated with nuclear function and intracellular signalling, respectively, whereas the bi-phasic Inc proteins CP0857 and IncA are involved in cellular morphology and protein degradation. These experiments have revealed new interaction partners of four novel Inc proteins and IncA by using the newly established split-Inc protein method.

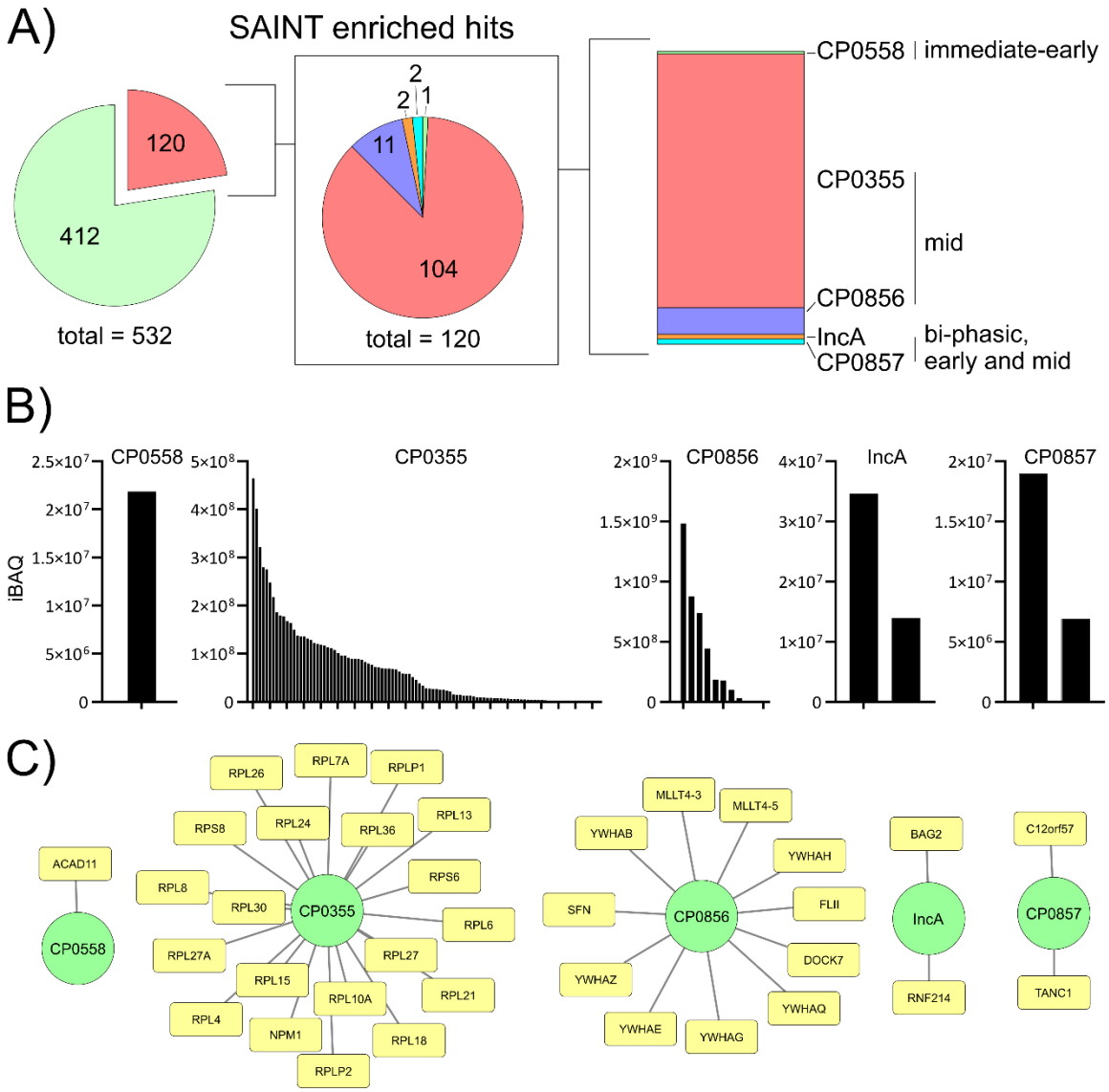

Fig. 15 *In silico* analysis of GFP-Trap MS results.

A) The number of significantly enriched proteins by SAINT. Significant proteins (hits) were determined using the SAINT algorithm (SAINT score ≥ 0.9 and BFDR < 0.01). Targets were aligned to *C. psittaci* Inc proteins that were categorised by their expression profile (Fig. 12). B) iBAQ distribution of significant proteins, which are sorted with respect to their iBAQ value beginning with the highest value. C) Interaction network of *C. psittaci* Inc proteins. The top 20 proteins deriving from B) (yellow) are connected to their corresponding interaction Inc protein (green). The networks were created with CytoScape.

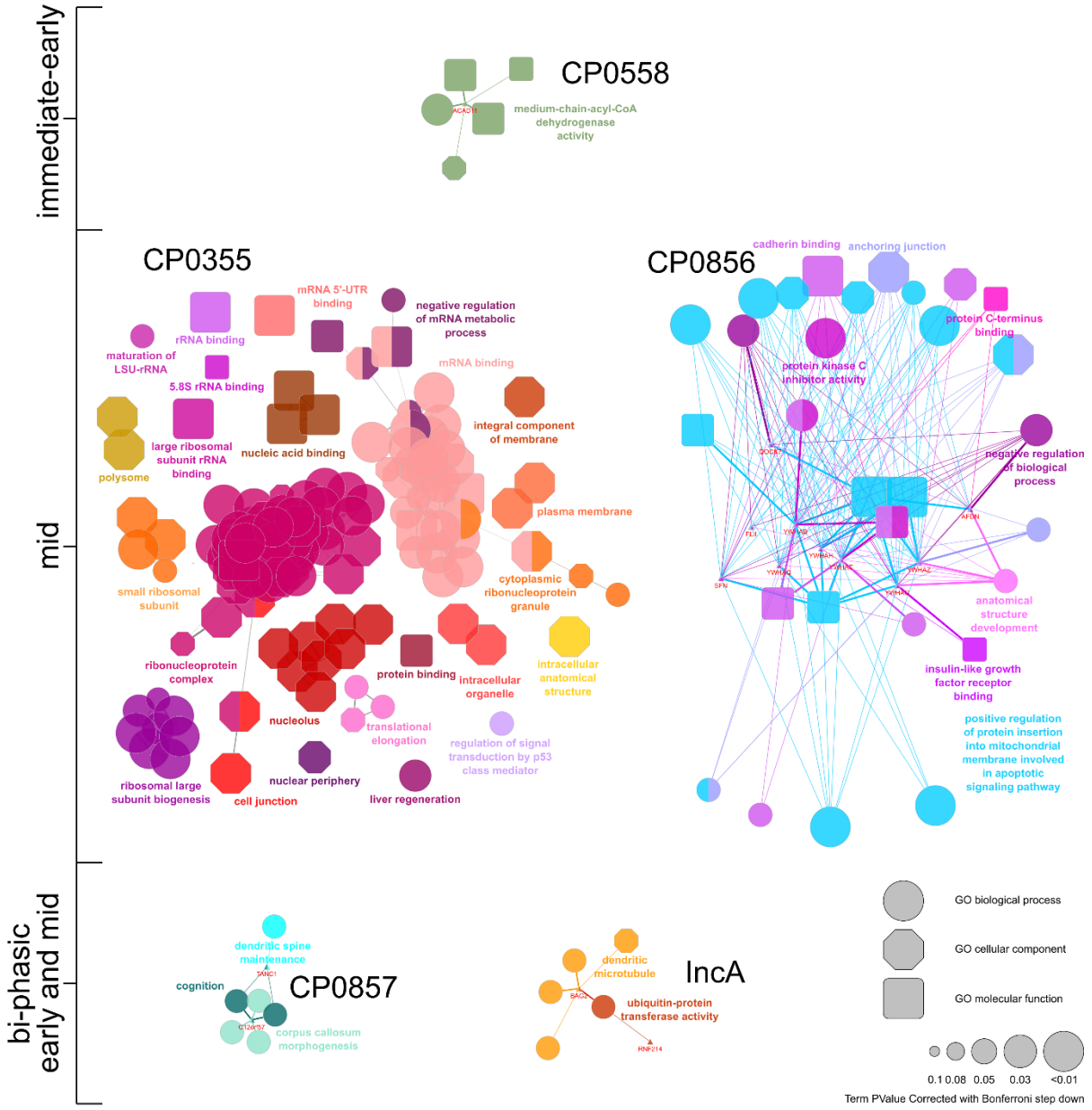

Fig. 16 GO term analysis of interaction proteins.

GO terms of biological processes, cellular components and molecular functions for *C. psittaci* lnc protein interaction partners were identified by using the CytoScape plugin ClueGO with a p-value < 0.05. The hits for each *C. psittaci* lnc protein were analysed as one batch. GO terms sharing at least one gene were clustered. GO terms were linked to associated genes except for CP0355. *C. psittaci* lnc proteins and associated GO terms are coloured and categorised based on the transcriptional profile of the lnc protein (Fig. 12).

3.3 Investigations of chlamydial and host cellular mechanisms during doxycycline-induced persistence of *C. trachomatis* serovar D

Pathogenic bacteria withstand clinical treatment by acquiring resistance. They escape the bactericidal or bacteriostatic pressure by inactivating enzymes or altering ribosomes, metabolism or protein target sites via decreasing antibiotic permeability or counteracting the antibiotic concentration via efflux pump (Chopra & Roberts 2001, van Hoek et al. 2011). Unlike other bacteria, *Chlamydia* spp. also can survive antibiotic treatment by a mechanism called persistence. They form non-infectious and enlarged ABs originating from RBs (Wyrick 2010). In that form, *Chlamydia* spp. persist in the presence of antibiotics and reactivate after antibiotics are removed, fulfilling the developmental cycle (Marangoni et al. 2020). The persistence of *Chlamydia* reflects a clinical issue and requires further investigation. Hence, the following work focussed on the mechanism of doxycycline-induced persistence, beginning with its characterisation *in vivo* and proceeding with proteomic analysis.

3.3.1 Morphology of treated *C. trachomatis* serovar D

In the literature, the differentiation of RBs into EBs occurs between 24 and 36 hpi during the developmental cycle of *C. trachomatis* serovar D (Belland, Zhong, et al. 2003). Because only RBs enlarge to ABs upon antibiotic treatment (W. L. Beatty et al. 1994), an experimental setup was chosen in which the treatment (0.5 µg/ml doxycycline) started early at 16 hpi (Fig. 17 A), a time when EB maturation was assumed not to interfere with persistence induction. Images of persistent and acute bacteria were obtained with EM (Fig. 17 B). During acute infection, the light and large spherical RBs decreased from 20 to 28 hpi. At 24 hpi, small IBs emerged, recognisable by bacteria with a light cytosol and a dark centre (Costerton et al. 1976). Consistently with the literature (Belland, Zhong, et al. 2003), dark and very small EBs (Costerton et al. 1976) were observable at 28 and 32 hpi. After 4 h of doxycycline treatment, the bacteria looked similar to RBs. *Chlamydia* enlarged and lightened 8 h after the start of treatment; they did not appear spherical and lacked clear boundaries. The bacteria with this asymmetric and bulging morphology were designated ABs. At 28 hpi, smaller bacteria emerged between the enlarged ABs. These smaller bacteria and the ABs continued to enlarge at 32 hpi. No EBs or IBs were observed during the antibiotic treatment. These results support that RBs asynchronously start differentiating into EBs at 24 and 28 hpi. Aberrant bacteria were observed after 8 h of doxycycline treatment, a finding that supports the induction of persistence. This treatment regimen was used for expression analysis to understand the doxycycline-induced persistence in the cell culture *C. trachomatis* serovar D infection model.

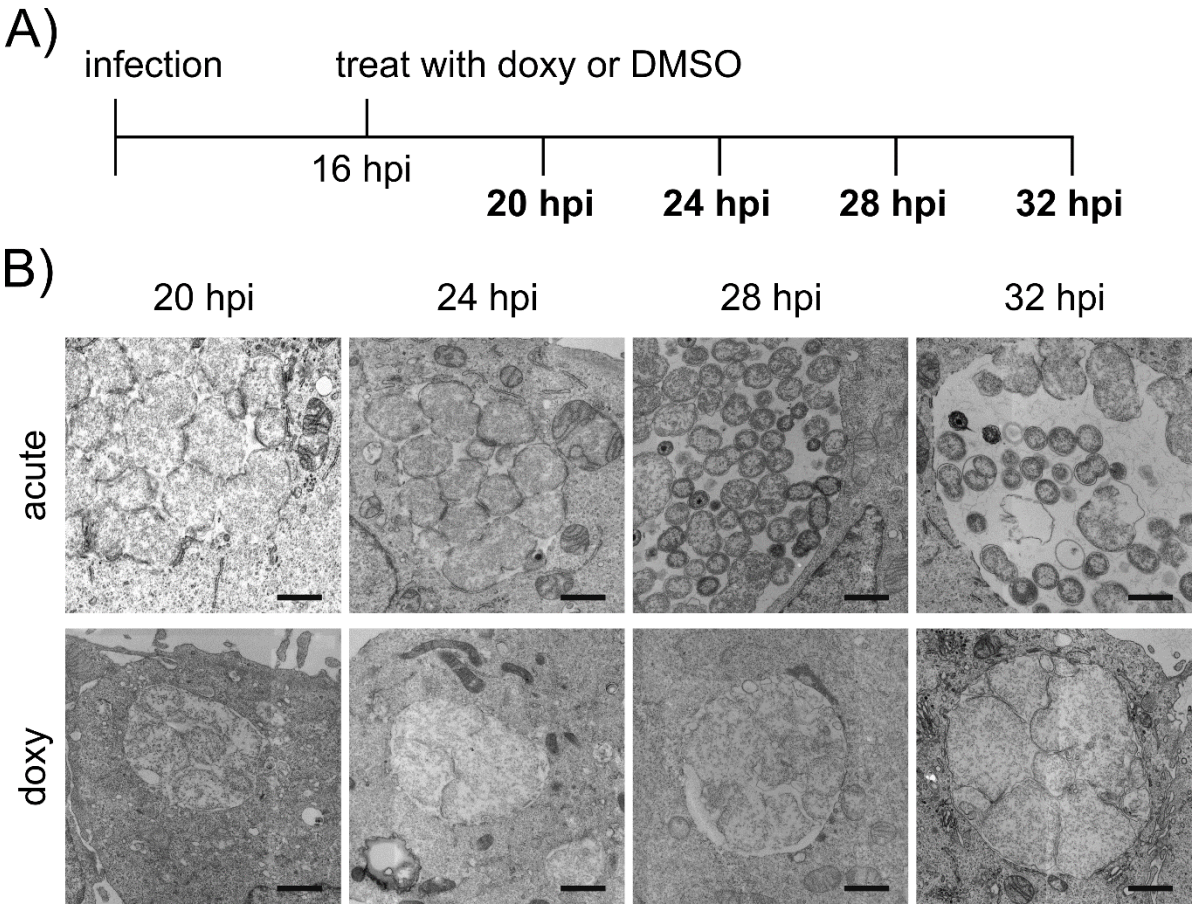

Fig. 17 Electron micrographs of acute and persistent *C. trachomatis* serovar D.

A) Treatment scheme. Cells infected with *C. trachomatis* serovar D (MOI = 2) were treated with DMSO (acute infection) or 0.5 µg/ml doxycycline (doxy, persistence) at 16 hpi. Samples were collected at the indicated times (bold text). B) Electron micrographs of acute and persistent *C. trachomatis* serovar D according to the treatment. Samples were treated according to A). The scale bar is 1 µm.

3.3.2 *C. trachomatis* serovar D continues protein expression despite doxycycline treatment

Chlamydia spp. persist in the presence of antibiotics and recover after treatment, continuing their developmental cycle (Marangoni et al. 2020). The mechanisms underlying persistence and the ability to recover remain unknown. Hence, the protein expression activity of *C. trachomatis* serovar D was monitored during antibiotic treatment (persistence) and after the treatment (recovery). *De novo* protein expression is recordable by incorporating the artificial amino acid L-HPG mimicking L-methionine. L-HPG contains an alkyl moiety that can be easily covalently linked to an azide moiety of Alexa Fluor® 546-Azide (K. E. Beatty et al. 2006, S. Grieshaber et al. 2018). The amino acid L-HPG was incorporated specifically in prokaryotic proteins by using a high dosage of cycloheximide (0.5 µg/ml), which selectively inhibits eukaryotic expression (Chesnokov & Mertvetsov 1990, Ennis & Lubin 1964, Schneider-

Poetsch et al. 2010). Past experiments of Agacfidan et al. (1993) determined the minimum inhibitory concentration (MIC) of doxycycline and azithromycin correlating with persistence induction. Both antibiotics are used in clinical treatment of patients infected with *Chlamydia* (Mpiga & Ravaoarinoro 2006). They inhibit translation by different mechanisms. Doxycycline binds reversibly to the 30S ribosomal subunit and blocks binding of aminoacyl-tRNA to the A-site of the translation complex (Chopra & Roberts 2001, Semenkov et al. 1982). In contrast, the macrolide azithromycin binds to 23S rRNA close to the peptidyl-transferase centre of the large subunit, interfering with peptide elongation (Parnham et al. 2014). Of note, Agacfidan et al. (1993) reported a MIC of 0.015-0.06 µg/ml for doxycycline, approximately two orders of magnitude smaller than the clinical serum concentration of 4.8 ± 0.3 µg/ml after an oral dose of 200 mg (Agwuh & MacGowan 2006). For comparison, concentrations around the MIC of doxycycline and azithromycin were used in addition to 0.5 µg/ml doxycycline. *C. trachomatis* serovar D–infected cells were treated with antibiotics at 16 hpi for 8 h (Fig. 18 A). At 24 hpi, the antibiotics were removed. The doxycycline-treated *C. trachomatis* serovar D subsequently recovered, as indicated by enlarged inclusions (Fig. 18 B). The acute control also showed enlarged inclusions, demonstrating chlamydial development. In contrast, no morphological differences were estimated during the recovery time of azithromycin-treated *C. trachomatis* serovar D. The expression intensity in the acute control decreased from 0 to 48 h recovery time, which is equivalent to 24 and 72 hpi, respectively. In contrast, at 24 h doxycycline-recovered *C. trachomatis* serovar D showed increased protein expression. During the recovery of azithromycin-treated *C. trachomatis* serovar D, there was no apparent increase in protein expression.

The software described in section 2.2.9 was used to quantify the immunofluorescence intensity to estimate the effects of different concentrations of doxycycline and azithromycin. The expression intensity was determined and normalised to the acute expression level of *Chlamydia* at 16 hpi + 8 h, equal to 24 hpi (Fig. 19). The first result cluster (Fig. 19 A) contains expression values of bacteria treated with low concentrations of azithromycin (0.001 µg/ml) and doxycycline (0.001-0.060 µg/ml). Expression was reduced linearly over time, comparable with the acute control (ctrl). Higher doxycycline concentrations (0.5 and 4 µg/ml) showed a unique pattern (Fig. 19 B): the level during treatment (0 h recovery) was 27% and 30.5% and increased up to 65% and 64% after 24 h recovery but decreased after 48 h recovery to 23% and 43% for 0.5 and 4 µg/ml doxycycline, respectively. In contrast, all azithromycin concentrations between 0.06 and 4 µg/ml led to levels between 15.3% and 23.6% (Fig. 19 C). At 1 and 4 µg/ml azithromycin, the expression decreased from 20.3% to 15.3% and from 20.7% to 18.4%, respectively. Only treatment with 0.06 µg/ml azithromycin produced an increase after

24 h recovery, from 19.5% to 23.6%, but it subsequently decreased to 18.4% after 48 h recovery.

In summary, the time-saving high-throughput quantification of immunofluorescence images was realised successfully using the described software. The results revealed that treatment with 0.001 µg/ml azithromycin or ≤ 0.06 µg/ml doxycycline did not alter protein expression. *Chlamydia* treated with ≥ 0.06 µg/ml azithromycin were unable to recover because there was no inclusion growth and protein expression remained low, between 15.3% and 23.6%. Notably, *C. trachomatis* serovar D showed relatively high protein expression (27%-30.5%) during treatment with ≥ 0.5 µg/ml doxycycline. Recovery after treatment with high doxycycline concentrations was reflected by growing inclusions and increased protein expression after 24 h. These results indicate the ability of *C. trachomatis* serovar D to persist in high concentrations of doxycycline and still perform translation, whereas high concentrations of azithromycin seemed to be bactericidal. Doxycycline and azithromycin differ mechanistically in translational inhibition. There appears to be a distinct mechanism for doxycycline that leads to persistence and recovery. Next, the remarkable ability of *C. trachomatis* serovar D to withstand translational inhibition was investigated.

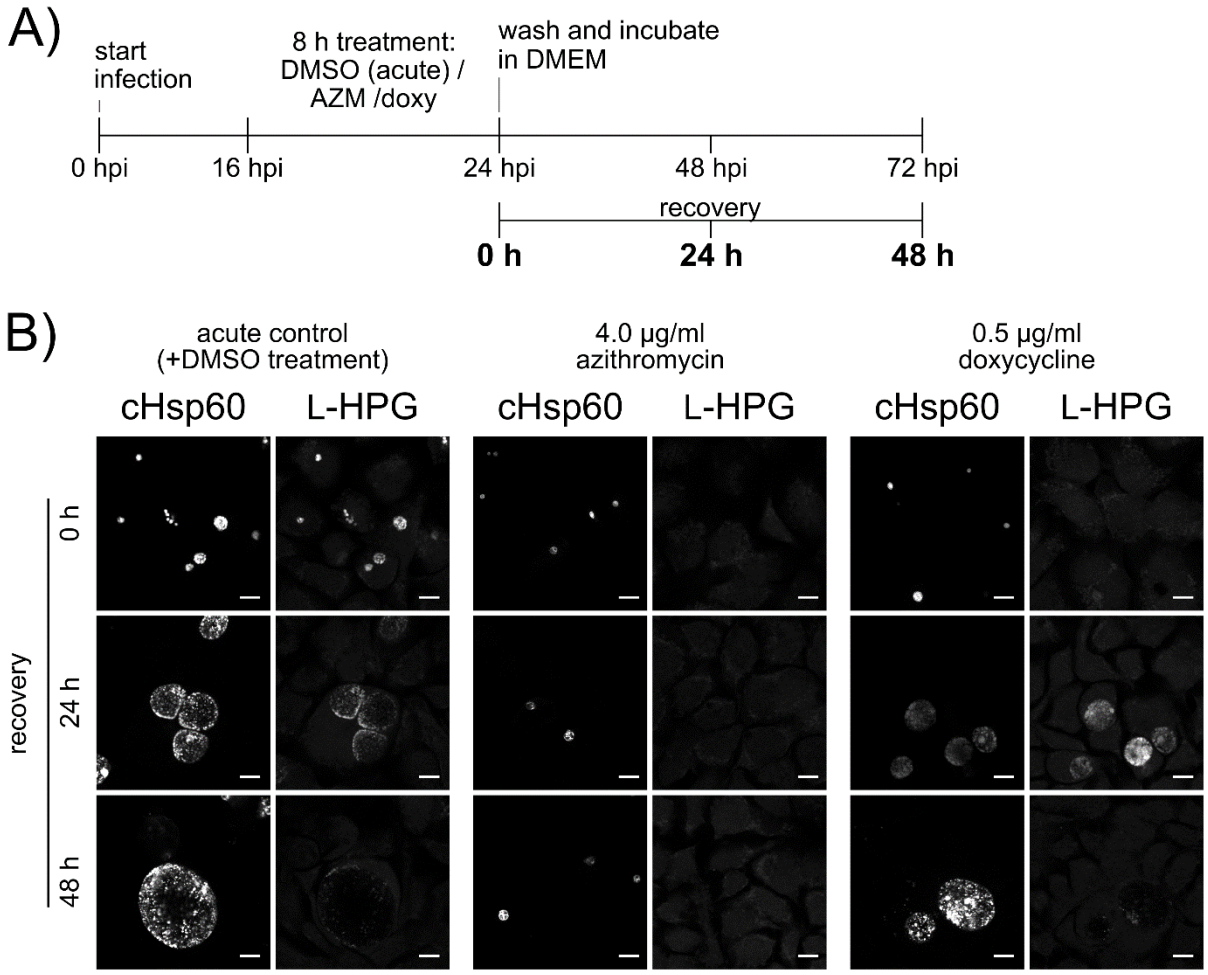

Fig. 18 *De novo* expression of *C. trachomatis* serovar D during antibiotic treatment and recovery. A) Treatment scheme. *C. trachomatis* serovar D was treated with either azithromycin (AZM), doxycycline (doxy) or DMSO for the acute control (ctrl) at 16 hpi for 8 h. Initial 0 h recovery equals 24 hpi relative to values during the treatment. Infected cells were washed with DMEM and further incubated for recovery. As described in the methods, cells were pulsed for 2.5 h in the presence of 0.5 µg/ml cycloheximide before fixation at 24, 48 or 72 hpi for recovery values of 0, 24 or 48 h, respectively. B) Immunofluorescence assay of expressing *C. trachomatis* serovar D. Infected cells (MOI = 0.5) were treated with DMSO (acute control), 4.0 µg/ml AZM or 0.5 µg/ml doxy according to the scheme in A). *De novo* protein expression was visualised by L-HPG clicked to Alexa Fluor® 546. *C. trachomatis* serovar D was stained with α-cHsp60^{m} and α-mouse Alexa Fluor® 488. Images were recorded at 0, 24 or 48 h recovery. The scale bar is 10 µm.

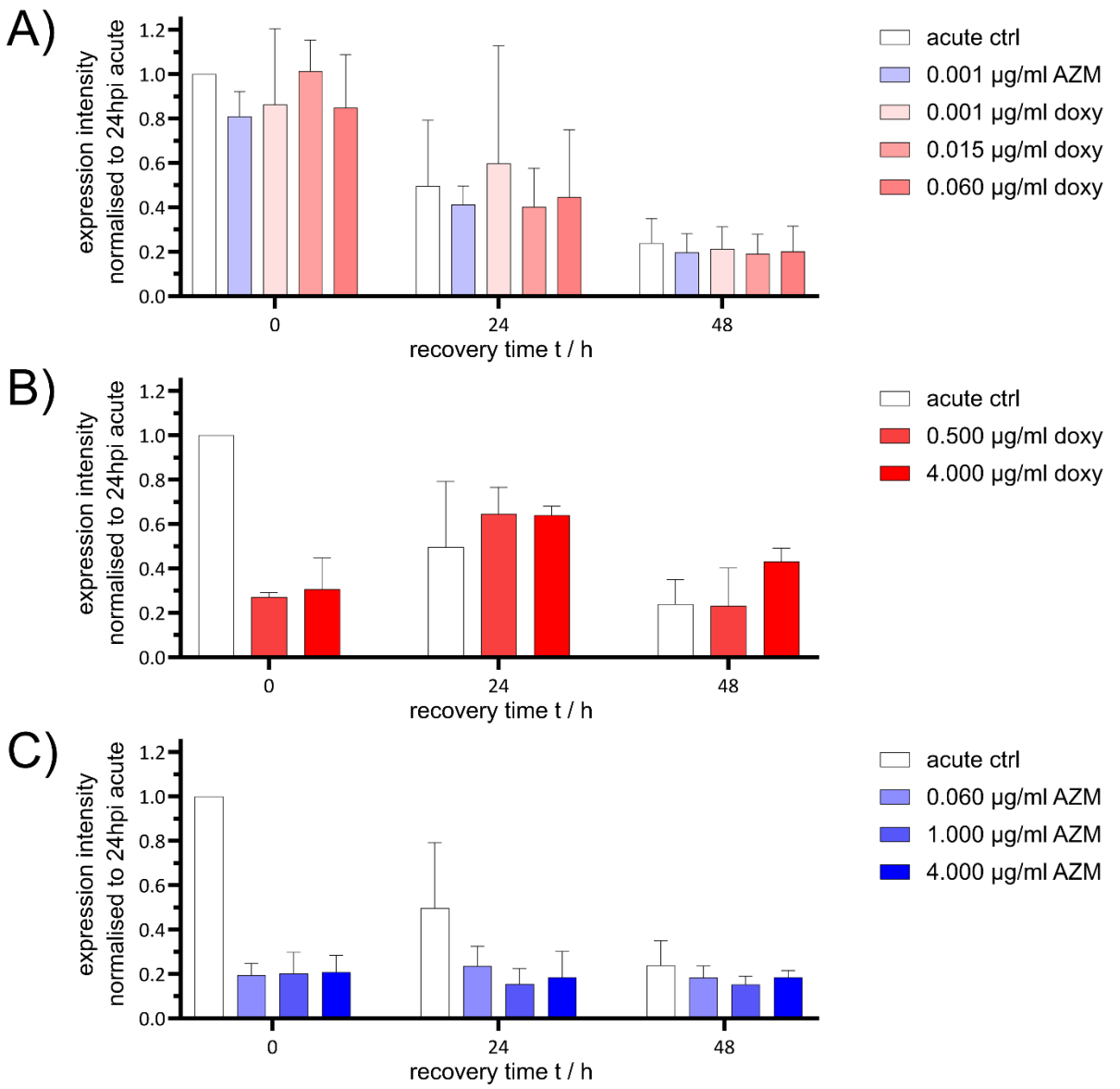

Fig. 19 The effects of antibiotics on chlamydial expression.

HeLa cells infected with *C. trachomatis* serovar D (MOI = 0.5) were treated according to Fig. 18 A and quantified as described in 2.2.9. All values were normalised to 24 hpi acute control and separated into three clusters: A) low treatment concentration of AZM and doxy (0-0.06 µg/ml), B) high concentrations of doxy (0.5-4 µg/ml) and C) high concentrations of AZM (0.06-4 µg/ml). Ten images per condition were recorded (n =2 biological replicates). Values are displayed as the mean with the standard deviation.

3.3.3 *C. trachomatis* serovar D counteracts doxycycline treatment via dynamic equilibrium of trans-translation

The previous results showed that *C. trachomatis* serovar D still translates proteins during doxycycline treatment. Therefore, it was assumed that there is a mechanism that competes with the antibiotic to overcome the inhibitory effect and continue translation. Translation of mRNA lacking a proper stop codon leads to stalling of the ribosome at the 3′ end of the mRNA (Giudice et al. 2014). Bacteria perform so-called trans-translation that replaces the mRNA and

tags the current polypeptide with a degradation sequence, leading to dissociation of the ribosome (Giudice et al. 2014). The essential components of this mechanism are transfer-mRNA (tmRNA) and the tmRNA-binding protein Small Protein B (SmpB). In the genome of *C. trachomatis* serovar D/UW-3/CX (GenBank: AE001273.1), locus CT_s01 produces '10Sa RNA', which is annotated as tmRNA, and locus CT_076 produces 'Small Protein B', indicating that *C. trachomatis* serovar D might also perform trans-translation. It is also known that the putative tmRNA of *C. trachomatis* serovar D encodes the proteolytic tag AEPKAECEIISFADLEDLRVAA (UniProt: V6CEP7). Based on this information, the levels of the putative tmRNA and *smpB* transcripts in *C. trachomatis* serovar D were quantified to identify whether they are transcribed and upregulated in doxycycline-induced persistence, thus indicating that trans-translation occurs as part of persistence. In this experiment, the treatment began 12 hpi to ensure absolutely no conversion from RB to EB that might interfere with the results. The *ssrA* and *smpB* transcript levels were recorded from 4 to 50 hpi and normalised to the expression of each gene at 4 hpi as log2 fold change (Fig. 20). In acute infection, the total level of both *ssrA* and *smpB* increased strongly from 4 to 12 hpi. *ssrA* transcripts increased only slightly from 12 to 16 hpi but the rose abruptly until 20 hpi. *smpB* transcription also increased slightly from 12 hpi but started rising later than *ssrA* at 18 hpi. Starting from 20 hpi, slope of *ssrA* and *smpB* transcription was reduced similarly until 32 hpi. At this point, *smpB* transcripts decreased until 50 hpi, whereas *ssrA* transcripts reached a plateau between 32 and 50 hpi. The transcriptional pattern of doxycycline-treated *Chlamydia* differed from acute infection. Immediately after starting the treatment, *smpB* transcripts increased strongly until 14 hpi, then decreased until 18 hpi and then increased again at 20 hpi. Conversely, *ssrA* transcription increased slightly until 18 hpi but rose until 20 hpi in the same time-slope manner as seen for *smpB* transcripts in persistence. *ssrA* and *smpB* transcripts decreased from 20 to 50 hpi after doxycycline treatment. Although *ssrA* increased from 32 hpi for 4 h, at later times its level decreased again.

These results revealed different transcriptional profiles of *ssrA* and *smpB* in acute infection and during doxycycline treatment. The increase in both transcripts during acute infection until 32 hpi correlated with dividing bacteria. The subsequent stabilised *ssrA* level and decreased *smpB* evidenced the previously determined differentiation of RBs into EBs between 24 and 32 hpi. This reduced *de novo* transcription indicates metabolic shutdown because *smpB* is no longer translated, although at that time K remains unaffected. These results further support active expression in doxycycline-treated *C. trachomatis* serovar D and indicate a dynamic equilibrium of trans-translation to counteract translational inhibition.

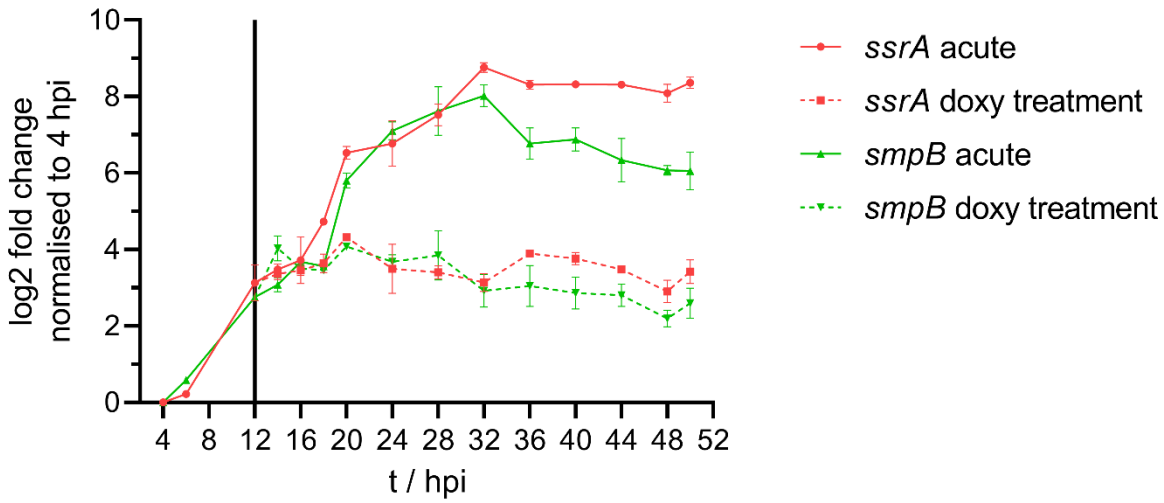

Fig. 20 Relative transcript levels of trans-translation genes.

Total RNA of infected cells was extracted at different times (4-50 hpi). The levels of *smpB* (green) and *ssrA* (red) transcripts were determined by qPCR from acute infection (solid line) and persistent infection (dashed line). Persistence of *C. trachomatis* serovar D was induced at 12 hpi with 0.5 µg/ml doxycycline (doxy, black line in plot). Expression was normalised to the value at 4 hpi. The means with SD of technical replicates from one biological replicate are displayed as the log2 fold change on a linear scale.

3.3.4 Ectopically expressed host proteins are recruited to the persistent inclusion

As described earlier, *Chlamydia* express so-called Inc proteins that can recruit host proteins, protein complexes or organelles to the inclusion membrane to enhance survival in multiple ways. Due to reduced protein expression in persistent *Chlamydia*, the composition of the proteome from persistent *Chlamydia* is predicted to differ from the proteome of acute *Chlamydia*, leading to different recruitment. Using proteomics, Aeberhard et al. (2015) determined inclusion-associated host proteins and analysed them using immunofluorescence upon ectopic expression in *C. trachomatis* serovar L2–infected cells. These host proteins were used as a starting point for investigations in *C. trachomatis* serovar D–infected cells. Hence, 20 host proteins and eGFP as a negative control were ectopically expressed in HeLa cells during acute and persistent *C. trachomatis* serovar D infection (Fig. 21). Because early treatment of *Chlamydia* with doxycycline resulted in small inclusions that were assumed to limit proper visualisation of recruitment, the treatment regimen was changed. Cells infected with *C. trachomatis* serovar D were treated at 24 hpi for 8 h with 0.5 µg/ml doxycycline or DMSO for persistent or acute infection, respectively (scheme in Fig. 22 A). The ectopically expressed proteins displayed different phenotypes. Rab35, Tfr, Rac1, Stim1 and Fli covered the complete inclusion in acute and persistent infection (Fig. 21 A). The mitochondrial protein Fis1 translocated into enlarged mitochondria surrounding the inclusion. Only a few mitochondria were attached tightly to the acute and persistent inclusion. There was a unique punctate

accumulation around the inclusion membrane in acute and doxycycline-treated infection for the human proteins Yth, Syntaxin-4 and Arginase (Fig. 21 B). The proteins Syntaxin-7 and Rab8a were recruited extensively to the acute inclusion but accumulated only diffusely in the proximity of the persistent inclusion (Fig. 21 C). DHCR7 and Stm2 accumulated around the acute inclusion but remained cytosolic during persistence (Fig. 21 D). There was a similar phenotype for Ubxd1 and ilk. These proteins accumulated diffusely around the acute inclusion but were not recruited to the inclusion after doxycycline treatment (Fig. 21 E). Cofilin and Rootlein displayed rod-like formations and distinct localisations in the cytosol independently of the inclusion (Fig. 21 F). Hspb1, Hspba8, Vsp and eGFP were distributed cytosolically without recruitment to the inclusion.

These results demonstrated consistent or reduced recruitment upon treatment with doxycycline. The proteins recruited during acute infection appeared less intensely recruited during persistence. Fli, Syntaxin-7 and Rab8a were less recruited to the inclusion membrane after doxycycline treatment. Interestingly, the intensely recruited proteins DHCR7 and Stm2 and the diffusely recruited proteins Ubxd1 and ilk were not recruited during doxycycline treatment, demonstrating a drastic effect on the recruitment behaviour in persistent *C. trachomatis* serovar D. Recruited proteins that appeared as puncta showed equal intensity for acute infection and persistence, indicating a fundamental relevance for *C. trachomatis* serovar D infection.

In summary, the treatment with doxycycline showed different recruitment of ectopic expressed individual host proteins to the inclusion membrane. The expressed host proteins consistently covered the inclusion or displayed reduced co-localisation. These results indicate a dynamic interaction at the inclusion membrane of persistent *C. trachomatis* serovar D. Immunofluorescence is limited in its quantification ability, making stochiometric interpretation of reduced or increased protein amounts at the inclusion membrane difficult due to variable expression intensity and the different inclusion sizes caused by the treatment. Correct estimation of protein quantities, especially for persistent inclusions, requires another approach. Hence, proteomic analysis was performed for widescale protein identification and quantification.

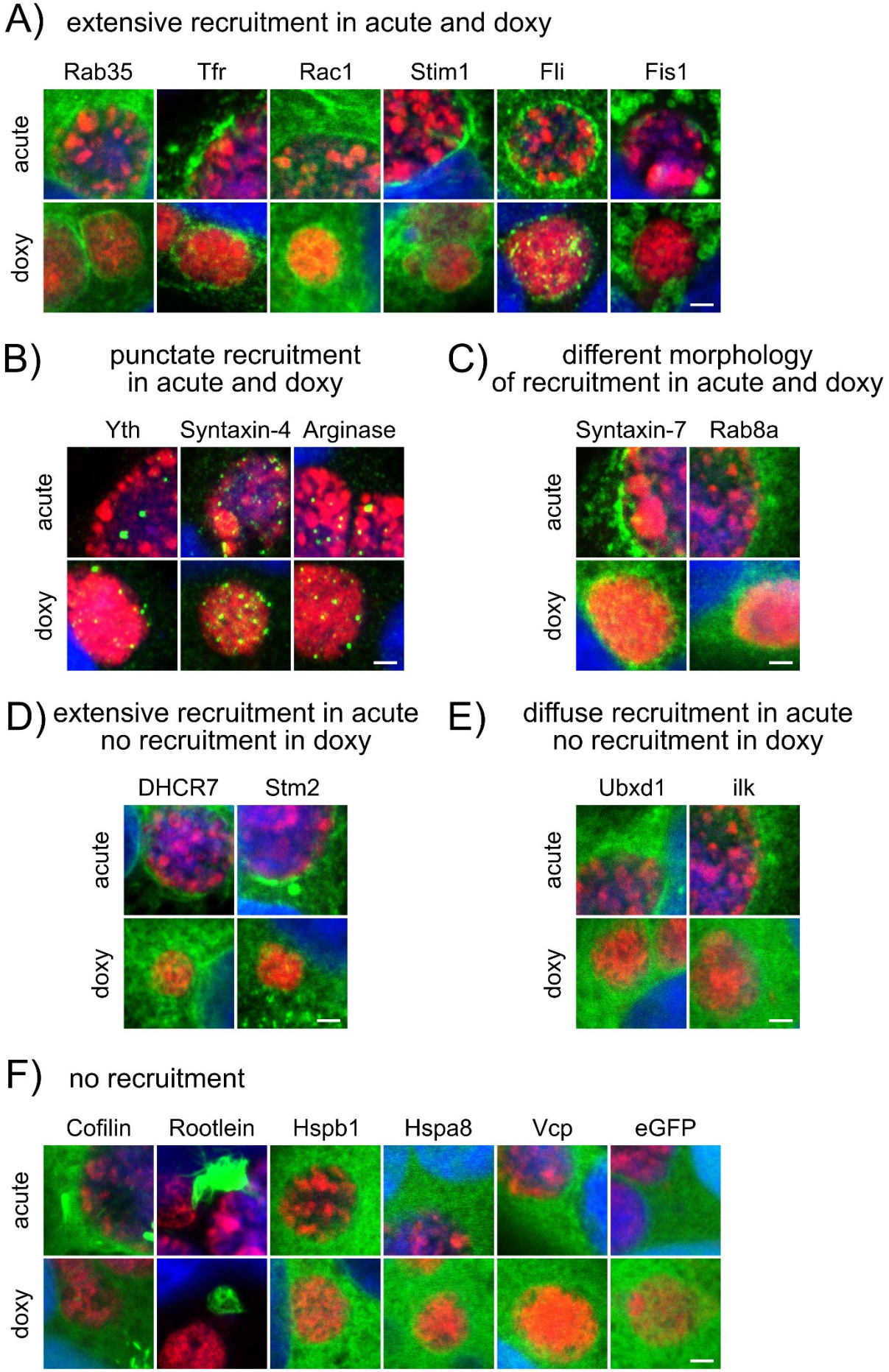
A) extensive recruitment in acute and doxy
Rab35
Tfr
Rac1
Stim1
Fli
Fis1
acute
doxy
B) punctate recruitment in acute and doxy
Yth
Syntaxin-4
Arginase
acute
doxy
C) different morphology of recruitment in acute and doxy
Syntaxin-7
Rab8a
acute
doxy
D) extensive recruitment in acute no recruitment in doxy
DHCR7
Stm2
acute
doxy
E) diffuse recruitment in acute no recruitment in doxy
Ubxd1
ilk
acute
doxy
F) no recruitment
Cofilin
Rootlein
Hspb1
Hspa8
Vcp
eGFP
acute
doxy

Fig. 21 Localisation of ectopically expressed, tagged human proteins in acute and persistent *C. trachomatis* serovar D infection.

Cells were infected with *C. trachomatis* serovar D (MOI = 2) and transfected with plasmids expressing human proteins (green) at 3 hpi. Persistence was induced 24 hpi by treatment with 0.5 µg/ml doxycycline. Cells were fixed at 32 hpi, and then stained for chlamydial Hsp60 as a chlamydial marker (red) and DAPI for DNA (blue). Transiently expressed proteins with a HA-tag were stained with primary antibody α-HA^{rb} and proteins with myc-tag with α-myc^{rb}. The subsequent secondary antibody was α-rabbit-Cy™3. The merged images were grouped according to the phenotype of recruitment or non-recruitment: A) extensive recruitment in acute and persistent infection, B) punctate recruitment in acute and persistent infection, C) different morphology of recruitment in acute and persistent infection, D) extensive recruitment in acute infection but no recruitment in persistent infection, E) diffuse recruitment in acute infection but no recruitment in persistent infection and F) no recruitment. The following constructs were expressed: Rab35-eGFP, Fli-HA, mEmerald-ilk, Vcp-eGFP, DHCR7-eYFP, eYFP-Stm2, Cofilin-eGFP, eGFP-Rootletin, Hspb1-eGFP, Fis1-eGFP, Ubxd1-mCherry, eGFP-Syntaxin-7, Tfr-eGFP, eGFP-Rac1, HA-Yth, Hspa8-eGFP, Syntaxin-4-myc, Arginase-HA, Stim1-eYFP, Rab8a-eGFP and eGFP. The scale bar is 2 µm.

3.3.5 Interactomics to study mechanisms of persistence

In the context of *Chlamydia*, interactomics describes the proteomic investigation of proteins recruited to the inclusion surface that interact with chlamydial proteins. Aeberhard et al. (2015) isolated and purified intact inclusions without disturbing the interaction with host proteins. That isolation involved a purification step via magnet-assisted cell sorting (MACS) targeting IncA with high affinity. Previous purification work has been insufficient due to the less abundant IncA in persistent inclusions. Therefore, the current study employed label-free proteomics of isolated acute and persistent inclusions, omitting the last purification step.

3.3.5.1 Inclusion preparation

Aeberhard et al. (2015) isolated inclusions of *C. trachomatis* serovar L2 at 24 hpi using a Percoll® density gradient. The success of proper inclusion isolation depends on the size and density of the inclusion. The developmental cycle of *C. trachomatis* serovar D is longer compared with *C. trachomatis* serovar L2. Therefore, there are inclusions of different sizes, densities and morphologies. In addition, treatment with antibiotics alters these properties. The inclusion preparation is necessary for label-free proteomics, and an optimised setting requires validation before subsequent proteomic examination. Three conditions were analysed for label-free proteomics (Fig. 22 A): 24 hpi (acute, before treatment, abbreviated as ‘acute’), 24 hpi + 8 h doxy (doxycycline induced persistence, abbreviated as ‘doxy-treated’) and 32 hpi (mock-treated acute, abbreviated as ‘mock-treated’). Gradient purification was performed as

described in section 2.2.15. Fifteen millilitres of the gradient was separated into 1 ml fractions with a needle from the bottom to the top with increasing fraction numbers. Those fractions were blotted and stained for chlamydial Hsp60 (cHsp60) as a marker for the bacteria and for bacterial IncE as a marker for the inclusion membrane (Fig. 22 B). The cHsp60 signal was found in all acute and mock-treated fractions but was most intense in the bottom fractions (f1 to f8). Doxy-treated *C. trachomatis* serovar D showed only cHsp60 signal in the bottom fractions but displayed the most intense IncE signal of all conditions, also in the bottom fractions. The bottom fractions of acute and mock-treated also showed IncE signal. Weak IncE signals was observed in the top fractions of acute and mock-treated *C. trachomatis* serovar D. Furthermore, the inclusions of single fractions were quantified by manual counting using Neubauer counting chambers (Fig. 22 C). The most inclusions were quantified in the bottom fractions of all three conditions, demonstrating the successful separation of inclusions by Percoll density gradient. Both western blot and counting proved the successful gradient separation of acute and doxy-treated inclusions similarly to mock-treated at 32 hpi. Because fractions 1-6 contained the most inclusions, these fractions were pooled together and processed for proteomics.

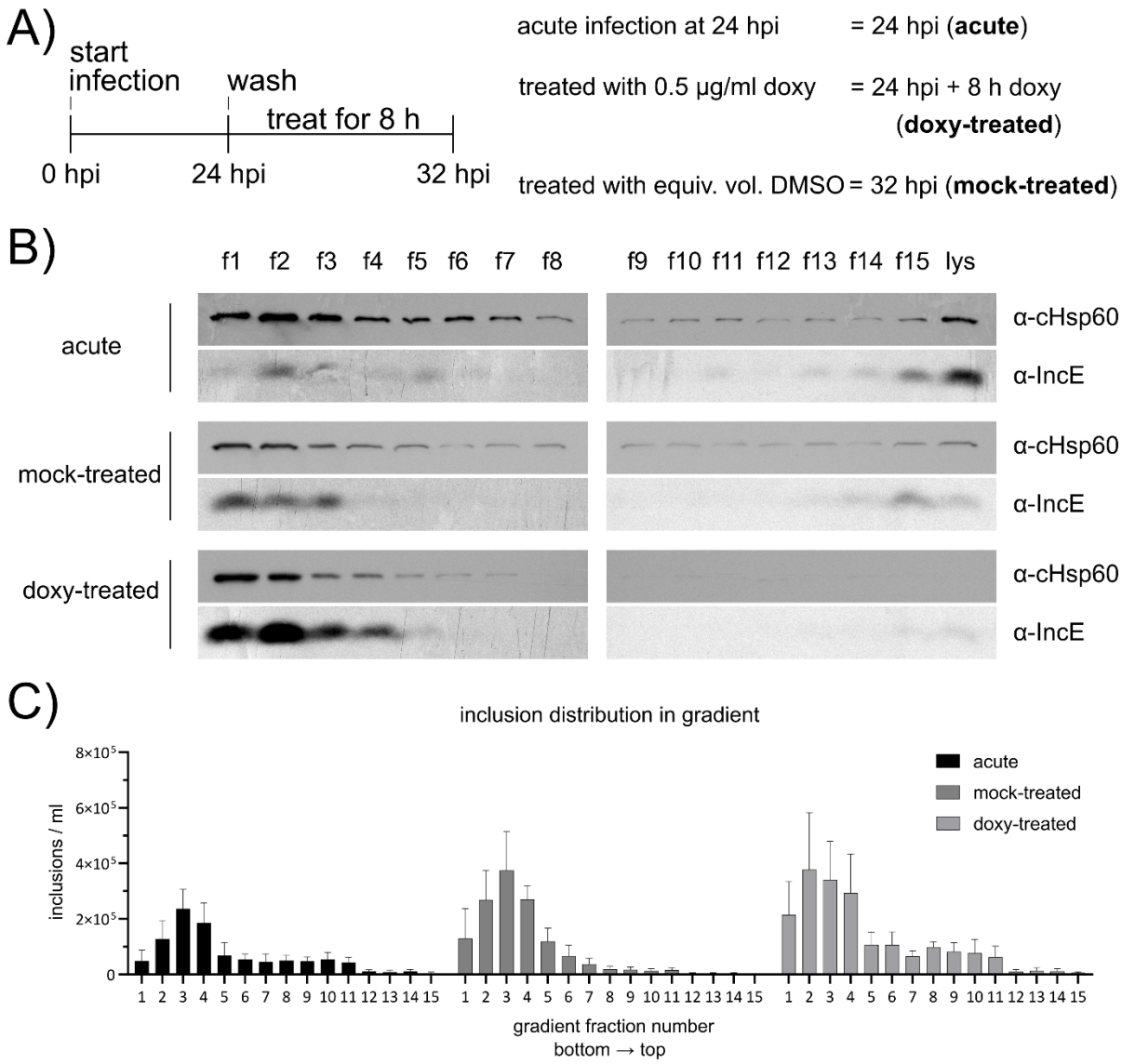

Fig. 22 Fraction analysis of inclusion preparation.

A) Treatment scheme. Cells were infected with *C. trachomatis* serovar D and treated at 24 hpi (acute) with either 0.5 µg/ml doxycycline (= 24 hpi + 8 h doxy = doxy-treated) or with an equivalent volume of DMSO (32 hpi = mock-treated) for 8 h. B) Western blot of fractions. Lysate (lys) and all 15 fractions (f1 to f15) from the inclusion preparations of 24 hpi, 24 hpi + 8 h doxy and 32 hpi were subjected to SDS-PAGE and blotted against chlamydial Hsp60 and IncE. C) Inclusion distribution in gradient. Inclusions of each fraction were counted in a Neubauer counting chamber.

3.3.5.2 Proteomics

Proteomics was performed by using full lysates and isolated inclusions. The in-home MS service kindly measured and identified the resulting peptides by using LC-MS. Subsequently, Katharina Baum (Hasso Plattner Institute, Digital Engineering Faculty, University of Potsdam) performed proteomic-based bioinformatic analyses. In full lysate samples, 463 chlamydial proteins and 4033 host proteins were identified. In isolated inclusions, 734 chlamydial proteins and 3398 host proteins were identified. Differential expression of these proteins was analysed

by using a bootstrap approach (Fig. 23). There were similar altered host proteins in the full lysate, with 84-98 upregulated and 96-102 downregulated proteins. The inclusion proteome of doxy-treated *C. trachomatis* serovar D was compared with the proteome of acute as a control and revealed 7 up- and 12 downregulated host proteins, and 8 up- and 10 downregulated chlamydial proteins. The inclusion proteome of doxy-treated *C. trachomatis* serovar D compared to the proteome of mock-treated as a control, showed 14 up- and 4 downregulated host proteins, and 3 up- and 52 downregulated chlamydial proteins. The inclusion proteome of mock-treated *C. trachomatis* serovar D compared to the proteome of acute as a control, displayed 50 up- and 3 downregulated host proteins. The full lysate proteomes presented only a few significant differences for chlamydial proteins. The full lysate proteome of doxy-treated *C. trachomatis* serovar D compared to the full lysate proteome of mock-treated *C. trachomatis* serovar D as a control showed 13 downregulated chlamydial proteins. The comparison of the full lysate proteome of mock-treated *C. trachomatis* serovar D with the full lysate proteome of acute as a control revealed 16 upregulated chlamydial proteins. The comparison of the proteomes of doxy-treated *C. trachomatis* serovar D with acute as a control revealed expression despite antibiotic treatment. The almost equal upregulation and downregulation underlined the previously stated expression equilibrium (section 3.3.3). Interestingly, the inclusion proteome of the doxy-treated compared to the inclusion proteome of mock-treated as a control revealed accumulation of human proteins, while the human proteins decreased using the inclusion proteome of acute as a control. However, there was an almost equal number of upregulated and downregulated proteins in all three full lysate proteomes.

These results gave rise to two hypotheses regarding persistence: 1) selectively upregulated chlamydial proteins lead to increased accumulation or distinct recruitment of human proteins that aid in survival and thus persistence in the presence of antibiotics and 2) chlamydial expression counteracts the antibiotic treatment in a dynamic equilibrium that allows the bacterium to survive and persist. The first hypothesis will be addressed in the follow-up analysis focussed on human and chlamydial proteins of the inclusion proteome (described in separate sections).

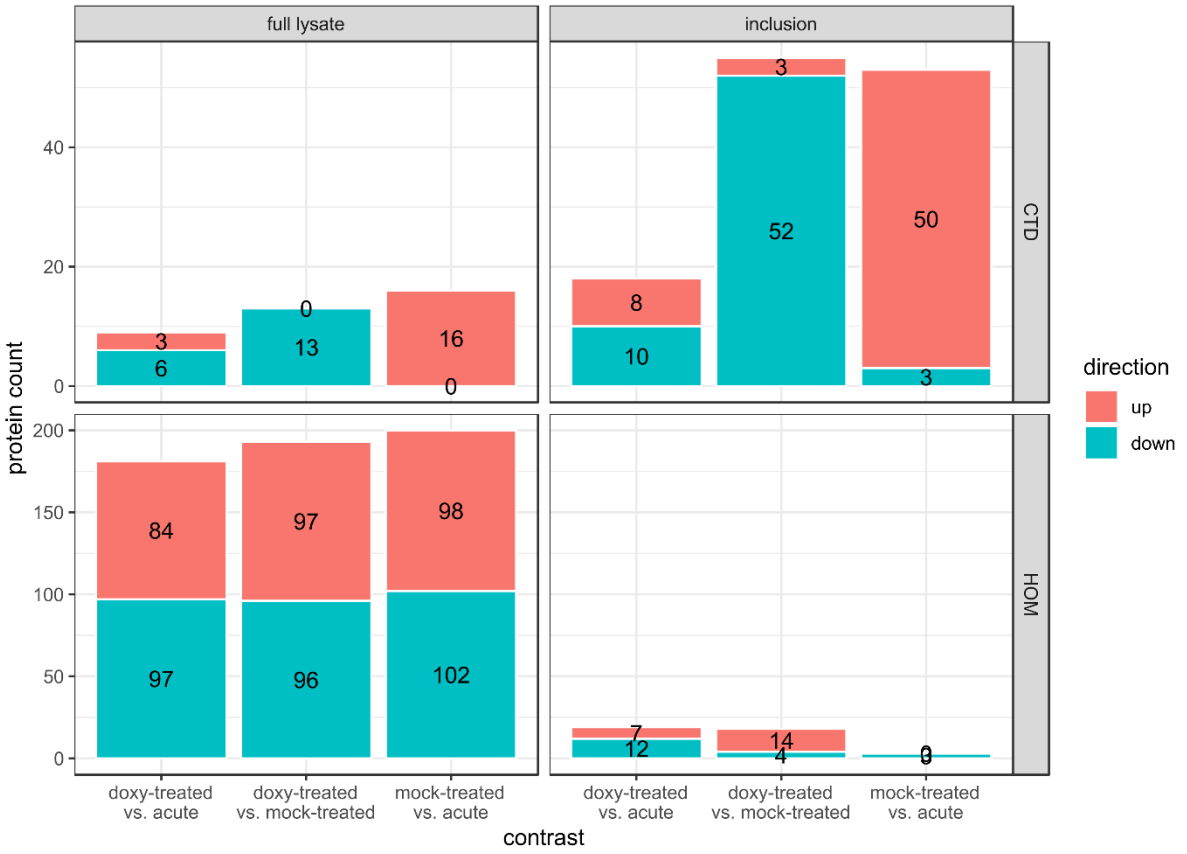

Fig. 23 The number of significantly altered proteins.

Proteins were analysed for differential expression that had at least one condition without NA measurement. Missing values were imputed by using a bootstrap approach. CTD, proteins of *C. trachomatis* serovar D; HOM, human proteins.

3.3.5.2.1 Deciphering the function of upregulated host proteins in persistence

The previous analysis of human proteins in the inclusion proteome (section 3.3.5.2) demonstrated differentially regulated proteins after antibiotic treatment. The differences in these human proteins were analysed qualitatively and visualised with a volcano plot using over 100 imputations (Fig. 24). High p-values resulted from imputations with less stringent significance regarding the full lysate proteome. In contrast, analysis of inclusion proteomes yielded fewer differences. Most human proteins differed significantly in the inclusion proteome of doxy-treated *C. trachomatis* serovar D when compared to acute (7 enriched, 12 reduced). Interestingly, the most altered host proteins appeared in the inclusion proteome of doxy-treated *C. trachomatis* serovar D when compared to the inclusion proteome of mock-treated *C. trachomatis* serovar D (12 out of 16), indicating a response to the doxycycline treatment. The temporal difference between the mock-treated and acute infection was predicted to show more enriched host proteins in the inclusion proteome of mock-treated *C. trachomatis* serovar D. However, no proteins were significantly increased, but three host proteins were reduced.

The results showed that regulated proteins that were qualitatively strongly separated from the background, as demonstrated with the volcano plots.

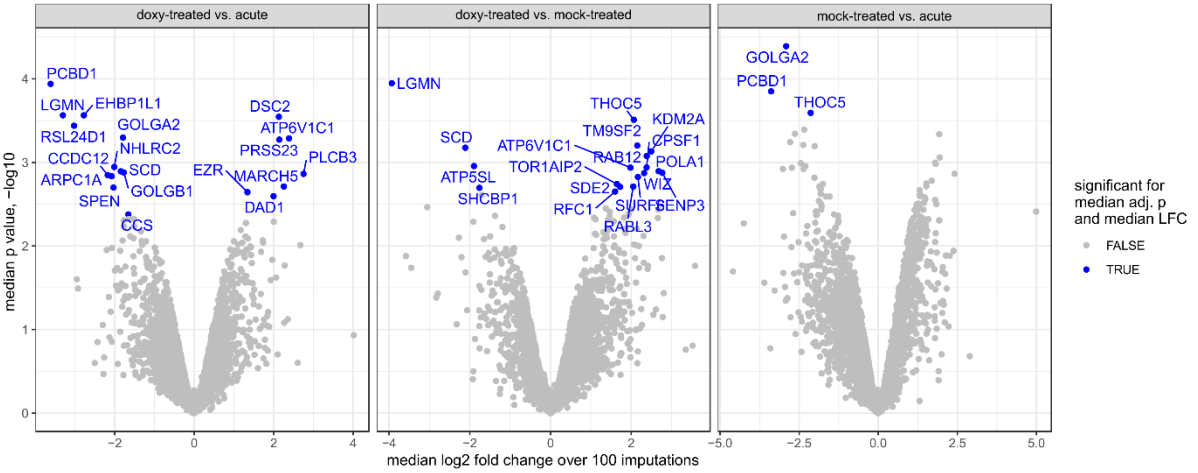

Fig. 24 Differentiation of significantly altered human proteins based on a proteomic comparison. The median log2 fold change over 100 imputations of human proteins was plotted against the median p-value on a -log10 scale from the human inclusion proteome. The doxy-treated vs. acute, doxy-treated vs. mock-treated and mock-treated versus acute comparisons are shown. Significantly altered proteins in the inclusion proteome are labelled with the gene name in blue.

3.3.5.2.1.1 Autophagy-related accumulation at persistent inclusions

The upregulated host proteins of the inclusion proteome of doxy-treated *C. trachomatis* serovar D using the mock-treated inclusion proteome as a control, were subjected to GO analysis to characterise the functions of the identified hits. The screening yielded six significant GO terms covering retrograde transport, transport of amino acids and proteins and autophagy (Table 3). The investigated proteins were enriched significantly in the relevant GO terms. Therefore, the linkages of these proteins with the GO terms were evaluated by using abundancy and p-values from the previous analysis.

In the positive control, all proteins of this data set were aligned to the GO terms (Fig. 25). There were no significant hits for single GO terms except for Rab12, which was upregulated and occurred in ‘autophagy’ (GO:006914) with an enrichment p-value of 0.10. Rab12 is known to be involved in autophagy (Omar et al. 2021, J. Xu et al. 2015), validating the identified GO term. Additional full analysis of all GO terms, Kyoto Encyclopedia of Genes and Genomes (KEGG) pathways and Reactome pathways revealed three enriched Reactome pathways with an adjusted p-value of 0.0406 and 2 of 11 significantly altered proteins of the terms ‘Polymerase switching on the C-strand of the telomere’, ‘Polymerase switching’ and ‘Leading Strand Synthesis’. Because autophagy plays an important role in infection with *C. trachomatis* (Witkin et al. 2017), the relevance of Rab12 in persistence was analysed.

Table 3 Relevant GO-terms for human proteins

ID	GO term	GO ID
1	Amino acid transport	GO:0006865
2	Autophagy	GO:0006914
3	Protein transport	GO:0015031
4	Retrograde protein transport, ER to cytosol	GO:0030970
5	Retrograde transport, endosome to Golgi	GO:0042147
6	Retrograde transport, endosome to plasma membrane	GO:1990126

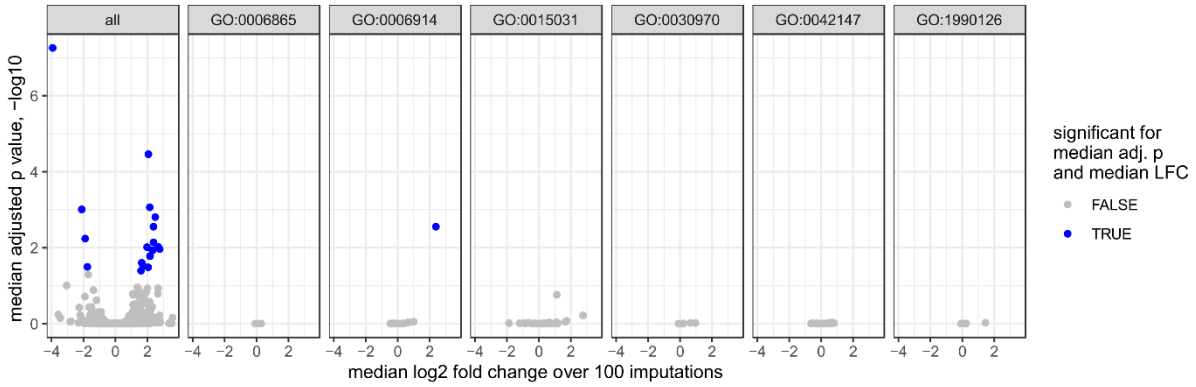

Fig. 25 Human inclusion proteome abundance of proteins for the GO terms identified from the doxy-treated versus mock-treated comparison.

The abundance of proteins from the human inclusion proteome according to the doxy-treated versus mock-treated comparison and their p-values were plotted against the chosen GO terms from Table 3.

3.3.5.2.1.2 *C. trachomatis* serovar D interferes with regular Rab12 dynamics

The Ras-related protein Rab12 is involved in membrane trafficking and autophagy (Omar et al. 2021, J. Xu et al. 2015). Rab12 is a small GTPase that binds with high affinity for guanine nucleotides. When bound to GDP, Rab12 is inactive and requires GEFs to catalyse the exchange of GDP to GTP, thus switching to its active, GTP-bound form. When activated, Rab12 interacts with effector proteins that mediate signalling. Rab12 hydrolyses GTP to GDP with the assistance of GAPs, a process that returns Rab12 to the inactive, GDP-bound form. Based on the current data availability, Rab12, as a part of autophagy, could be involved in degradation of the inclusion. Of note, Rab12 might function differently in this process depending on whether it is in the active or inactive state. There is the possibility that *C. trachomatis* serovar D recruits Rab12 and stabilises it in a distinct state to block proper host-derived autophagy. Hence, the function of Rab12 was analysed with respect to chlamydial infection and persistence. In a recent study, authors investigated the function of Rab12 by using mutations to generate Rab12 constitutively bound to GDP, a dominant-negative form (T56N), and Rab12 constitutively bound to GTP, a dominant-active form (Q101L) (J. Xu et al.

2015). The dominant-negative mutation prevents GTP binding, whereas the activating mutation eliminates the ability to hydrolyse GTP to GDP (McCray et al. 2010). Localisation of FLAG-tagged Rab12 wild-type (wt) and its dominant-active and negative forms was evaluated during acute and persistent infection by ectopic overexpression (Fig. 26). The overexpressed Rab12-wt covered the inclusion in acute and persistent infection. The dominant-active form, Rab12-Q101L, was predicted to be membrane-bound but occurred diffusely in the cytosol. The protein accumulated at the proximity of the inclusion. The dominant-negative form, Rab12-T56N, seemed to be recruited more strongly to acute inclusions rather than persistent inclusions and showed several overlaps with IncA-clusters in the acute infection. In persistent infection, Rab12-T56N was predicted to occur both in the cytosol and bound to the membrane but it accumulated at a distinct cluster of the persistent inclusion that was also highly IncA positive. In acute infection, as expected Rab12-T56N was dispersed around the inclusion independent of IncA-clusters.

In summary, the observed phenotypes differed according to acute or persistent infection, without a clear indication of whether host-driven degradation is involved. The diffuse or membrane-bound state of active, inactive and wild-type Rab12 indicates specific *C. trachomatis* serovar D–interfering mechanisms that require further analysis.

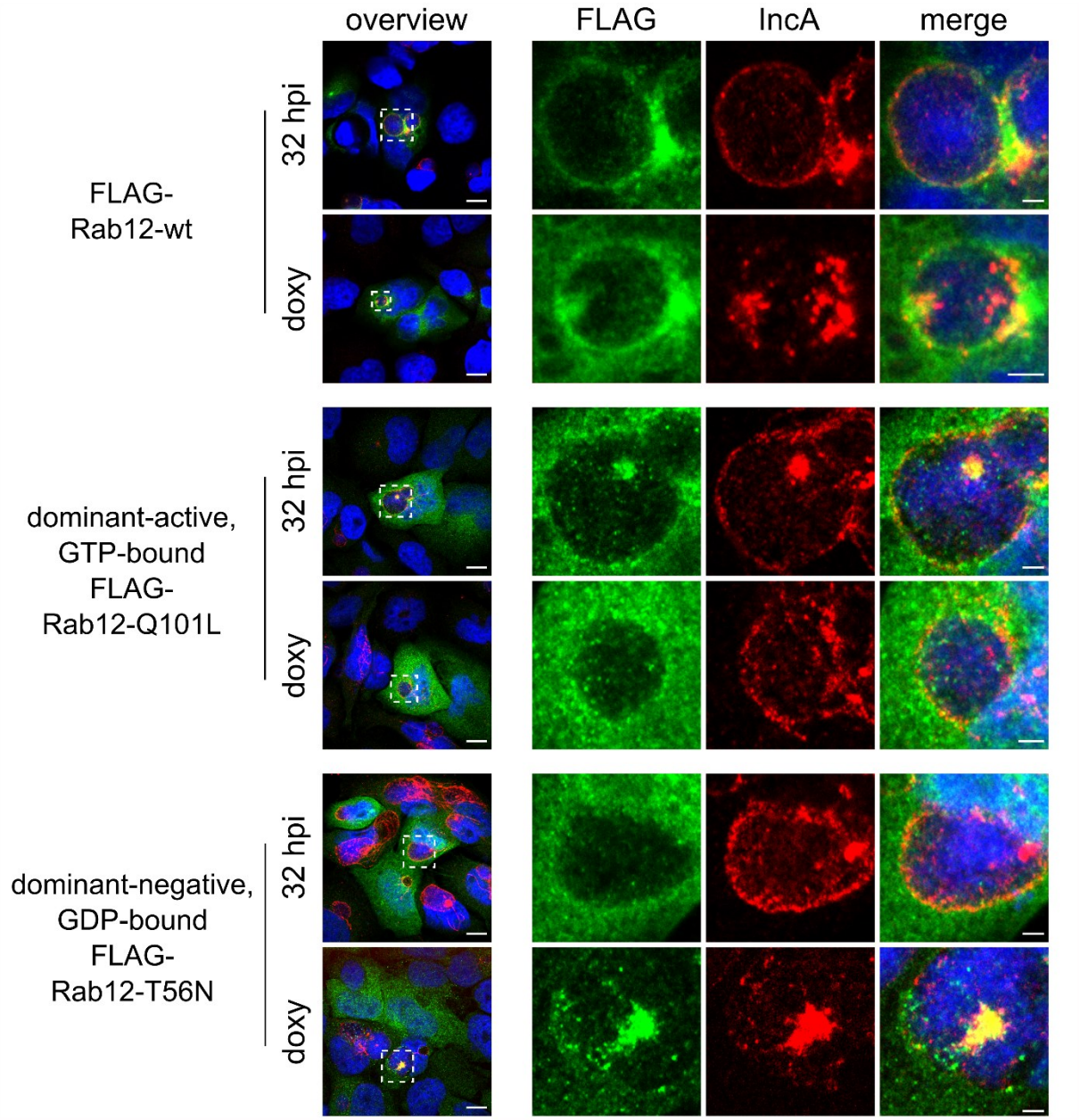

Fig. 26 Localisation of ectopically expressed Rab12 variants in acute and persistent infection. At 3 hpi, *C. trachomatis* serovar D–infected cells were transfected with plasmids encoding FLAG-Rab12-wt, FLAG-Rab12-Q101L or FLAG-Rab12-T56N. The infected cells were treated according to the treatment regimen in Fig. 22 A, resulting in acute infection (32 hpi) or persistent infection (doxy). The constructs were visualised by staining with α-FLAG^{m} and α-mouse-Alexa Fluor® 488 (green), the chlamydial inclusion was visualised by staining for IncA (red), and DNA was visualised with DAPI (blue). The dashed area in the overview is displayed as a zoom in the three panels to the right. The scale bar is 10 µm in the overview and 2 µm in the zoom.

3.3.5.2.1.3 Rab12 KD supports persistence and recovery of *C. trachomatis* serovar D

The previous results highlighted that Rab12 is recruited to the inclusion of acute and persistent *C. trachomatis* serovar D. Quantification of chlamydial progeny formation is a suitable tool to demonstrate the influence of cellular changes on chlamydial development. Hence, endogenous Rab12 expression of HeLa cells was reduced by siRNA (Rydell et al. 2014) 48 h before infection and compared with the knockdown (KD) control AllStars. Progeny formation was monitored at 48, 72 and 96 hpi during acute infection, doxycycline treatment (beginning at 24 hpi) and recovery for 24 h treatment starting from 48 hpi (Fig. 27). Recovery from doxycycline treatment showed a small increase in AllStars KD with a subsequent slight decrease. In contrast, recovered *C. trachomatis* serovar D in Rab12 KD cells showed enhanced progeny formation at 72 hpi that increased further at 96 hpi. Doxycycline-treated *C. trachomatis* serovar D in the AllStars KD control showed stable progeny formation at all time points, which differed only a little in Rab12 KD cells. Whereas persistent *C. trachomatis* serovar D showed a slightly higher progeny formation at 48 hpi in Rab12 KD than AllStars KD, progeny formation was reduced slightly at 72 and 96 hpi. These variations seemed not to indicate a distinct effect on persistent *C. trachomatis* serovar D in Rab12 KD cells. Progeny formation of acute *C. trachomatis* serovar D in Rab12-depleted cells was reduced slightly compared with the AllStars KD control, indicating an effect on acute chlamydial development. Taken together, Rab12 KD reduced progeny formation in acute infection and during doxycycline treatment, whereas progeny formation of recovering *C. trachomatis* serovar D was enhanced slightly. The enhanced recovery in Rab12 KD indicates that Rab12 affects *C. trachomatis* serovar D during doxycycline treatment leading to a minored recovery. Rab12 is involved in the regulation of autophagy which could play a role during the doxycycline treatment. The complex regulation of autophagy and the different states of active or inactive Rab12 underscores the difficulty in these investigations. Future cell biological investigations of Rab12 during infection with *C. trachomatis* serovar D could extend the understanding of the role of Rab12 in chlamydial development and persistence.

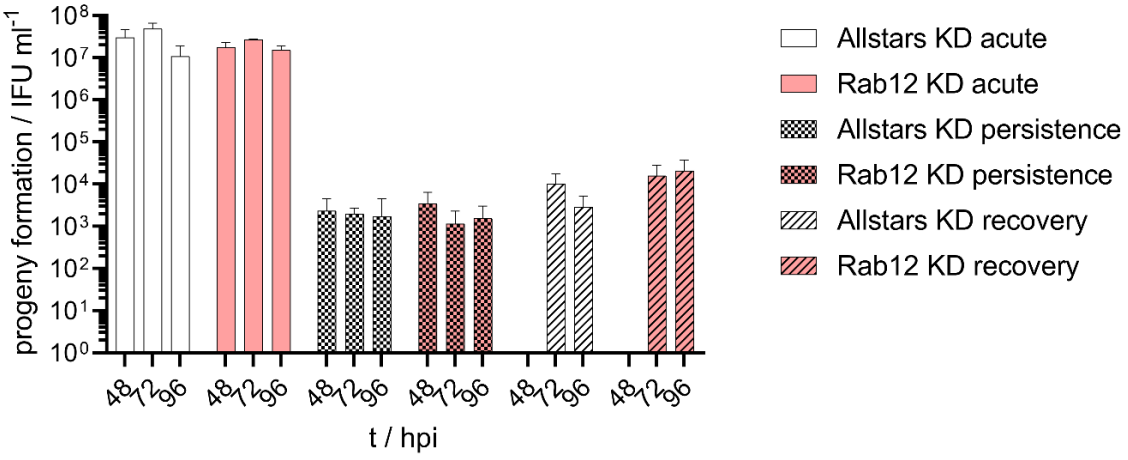

Fig. 27 Effect of Rab12 KD on progeny formation during acute and persistent infection.
Rab12 KD (and AllStars KD as a control) was performed with gene-specific siRNAs 48 h before infection (section 2.2.10). Progeny formation was determined for acute infection, persistence and recovery at the indicated times by quantifying the inclusion forming units as described (section 2.2.13). Persistence was induced by treatment with 0.5 µg/ml doxycycline at 24 hpi. Recovery was allowed for 48 hpi, 24 h after doxycycline treatment, upon replacing the doxycycline-containing medium with doxycycline-free DMEM. The progeny formation in Rab12-depleted cells is displayed as a fold change relative to AllStars KD (mean ± standard deviation; n = 3; ordinary one-way analysis of variance followed by Dunnett's multiple comparisons test, *p < 0.05).

3.3.5.2.2 The inclusion proteome surpasses the full lysate proteome

The inclusion proteome (section 3.3.5.2) yielded 734 identified chlamydial proteins. The inclusion proteome contained more individual proteins than the full lysate proteome, which contained only 463 (Fig. 28). The mock-treated acute infection at 32 hpi displayed 267 additional proteins in the inclusion proteome compared with the full lysate proteome. Interestingly, the full lysate proteome of doxycycline-treated *Chlamydia* at 32 hpi showed fewer individual proteins (314) than the full lysate proteome of the acute infection at 24 hpi (351), despite the additional 8 h of infection. This indicated reduced *de novo* protein expression in persistent *C. trachomatis* serovar D. The isolation and enrichment of inclusions yielded more identified proteins than the full lysate. This outcome might be due to the increased amount of host proteins in the full lysate. They technically cover chlamydial proteins and thus hinder their identification. In summary, these results demonstrate that the inclusion preparation highly enriches chlamydial proteins, suitable for proteomics. The subsequent analysis aimed to characterise the functions of these proteins.

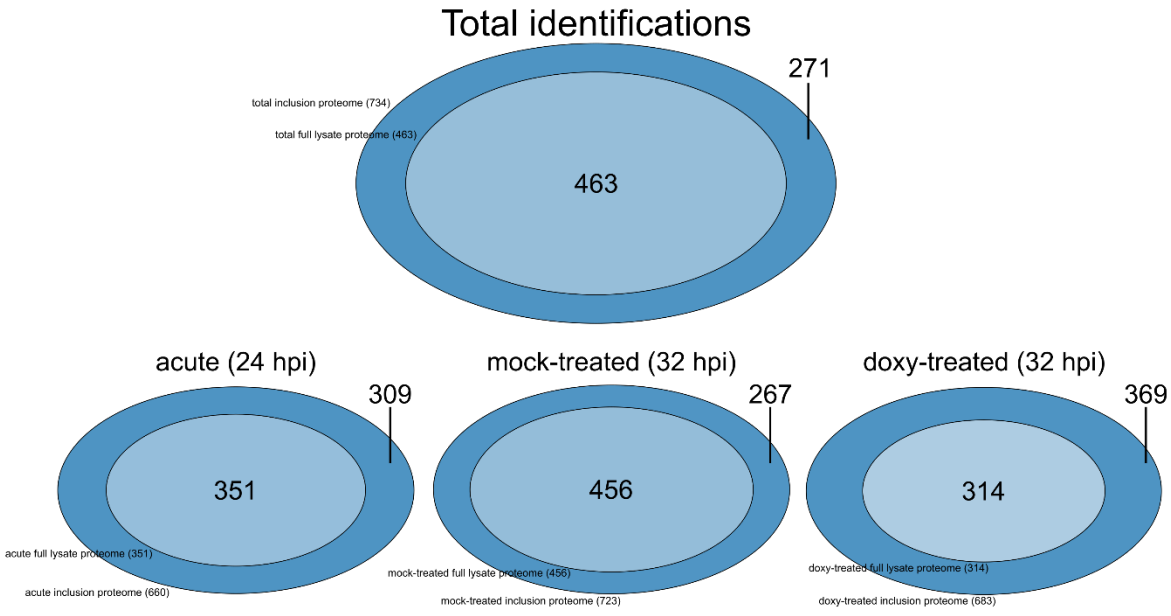

Fig. 28 Overlap of identified chlamydial proteins between isolated inclusions and full lysate measurements.

3.3.5.2.2.1 RB- and EB-related markers are unaffected in persistence

Saka et al. (2011) categorised chlamydial proteins according to EBs, RBs or both. Based on these criteria, proteins of all three conditions were assigned to the categories (Fig. 29). There was a relatively small but equal number of RB markers in all three conditions. Far more proteins were associated with RBs and EBs, which occurred equally in acute, doxy-treated and mock-treated conditions. The number of EB markers in doxy-treated and acute were similar, whereas mock-treated showed more proteins. Unquantifiable proteins increased in the following order: acute, doxy-treated and mock-treated, with 82, 85 and 95, respectively. Saka et al. (2011) were unable to detect a large number of proteins, and thus they could not be aligned. These proteins also increased in the same order mentioned above and at the time increased from 24 hpi (acute) to 32 hpi (doxy-treated, mock-treated), but doxycycline treatment attenuated this increase. Overall, the distribution of RB and EB markers was similar in all three conditions but was shifted slightly, as expected, to EBs in mock-treated at 32 hpi. The ABs of persistent *C. trachomatis* serovar D originate from RBs (Panzetta et al. 2018) expecting an increase of RB markers. Nevertheless, RB markers did not change during persistence compared with acute infection at 24 hpi. Instead, doxycycline treatment led to an enrichment of EB markers, unquantifiable and unlisted proteins similar to mock-treated *C. trachomatis* serovar D but in a reduced manner. These results gave rise to two hypotheses: 1) the constitution of RB- and EB-related proteins of *C. trachomatis* serovar D at 24 hpi is sufficient to survive and persist in the presence of antibiotic or 2) the unquantifiable and unlisted proteins that increased in doxy-treated are necessary for survival and persistence. The functional characterisation of the identified proteins is indispensable and might reveal the mechanistic background of persistent *C. trachomatis* serovar D. Hence, this aspect was analysed.

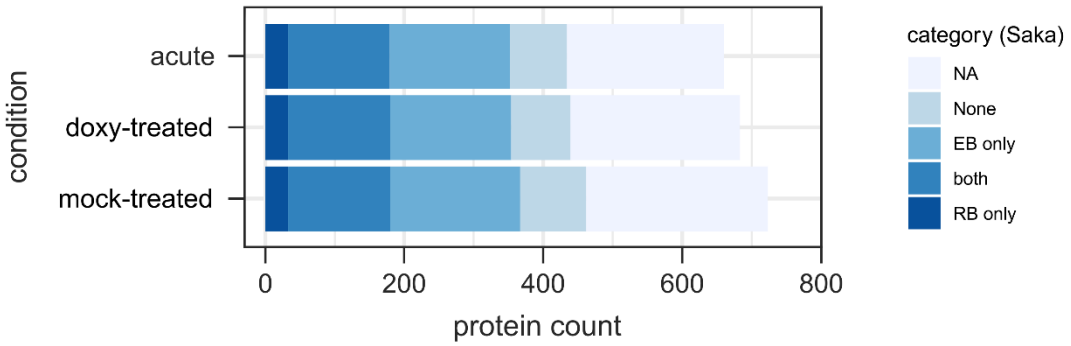

Fig. 29 EB/RB categorisation of identified proteins.

The identified proteins of the inclusion proteomes were categorised according to the criteria from Saka et al. (2011). EB/RB only, quantified only in EB or RB samples; both, quantified in both EB and RB samples; none, not quantifiable or not detected but listed; NA, not listed.

3.3.5.2.2.2 Altered chlamydial proteins in persistent *C. trachomatis* serovar D are involved in metabolism, transport, binding and cellular processes

The previous analyses revealed an equal distribution of EB and RB markers and slightly enriched proteins in doxy-treated and mock-treated *C. trachomatis* serovar D at 32 hpi. The abundance of these proteins was investigated to identify altered and thus regulated proteins that might participate in distinct correlating functions. Comparing the inclusion proteomes of doxy-treated with acute, doxy-treated with mock-treated, and mock-treated with acute resulted in log2 fold changes that were visualised with volcano plots (Fig. 30). The median log2 fold change over 100 imputations was plotted against the median p-value on a negative log10 scale. According to the previous analyses, most proteins were identified in mock-treated *C. trachomatis* serovar D at 32 hpi. As expected, the comparison of mock-treated with acute shows many upregulated proteins and three downregulated proteins in the volcano plot. The proteome of doxy-treated *C. trachomatis* serovar D revealed numerous downregulated proteins compared to mock-treated, reflecting the lack of expression during doxycycline treatment. Despite the reduced expression during persistence, three membranous proteins were upregulated significantly: O84417 (pmpA), P0DJI3 (IncD) and O84061 (CT_058).

When comparing the proteome of doxy-treated *C. trachomatis* serovar D with acute, 8 upregulated and 10 downregulated proteins were shown, indicating a treatment-specific alteration of protein regulation. These altered proteins were categorised functionally according to Østergaard et al. (2016). The proteins of the proteome of mock-treated *C. trachomatis* serovar D that were altered compared to acute as a control were also categorised (Fig. 31) to understand the biological function of the doxycycline-specific alteration. The most prominent categories are cell envelope, cellular processes, central intermediary metabolism, energy metabolism, regulatory functions, transport and binding, and translation with decreasing proportion. It is worth mentioning that about 47% of altered proteins were uncharacterised or not listed by Østergaard et al. (2016), demonstrating a myriad of unknown functions. The downregulated proteins of the doxy-treated proteome compared to acute showed that only 10% of the proteins are related to cell envelope or cellular processes. 40% of the proteins are either uncharacterised or not listed. On the contrary, upregulated proteins are evenly distributed in the categories of cellular processes, central intermediary metabolism, transport and binding and unlisted, reflecting consistent metabolic activity. Taken together, persistent *C. trachomatis* serovar D increased the expression of at least three membranous proteins and several proteins that correlate with metabolism. These results indicate a direct interaction with the host cell via membranous proteins and metabolic processing. The subsequent downstream analyses focussed on the membrane proteins and metabolism.

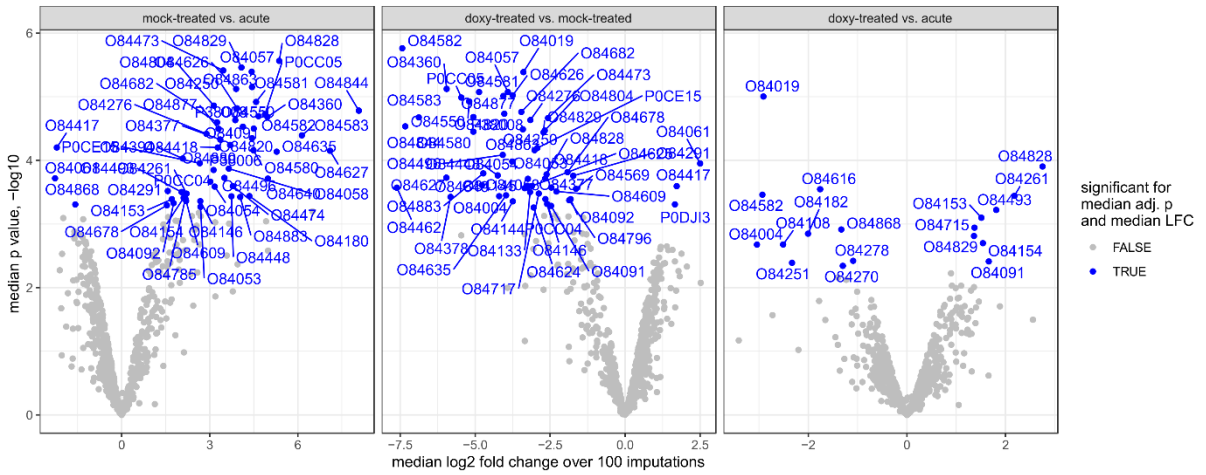

Fig. 30 Proteomic comparison of significantly altered chlamydial proteins.

The median log2 fold change over 100 imputations of chlamydial proteins was plotted against the median p-value on a -log10 scale from chlamydia inclusion proteomes in volcano plots. The mock-treated versus acute, doxy-treated versus mock-treated and doxy-treated versus acute comparisons are shown. Significant proteins are labelled with the uniport.org protein ID (in blue).

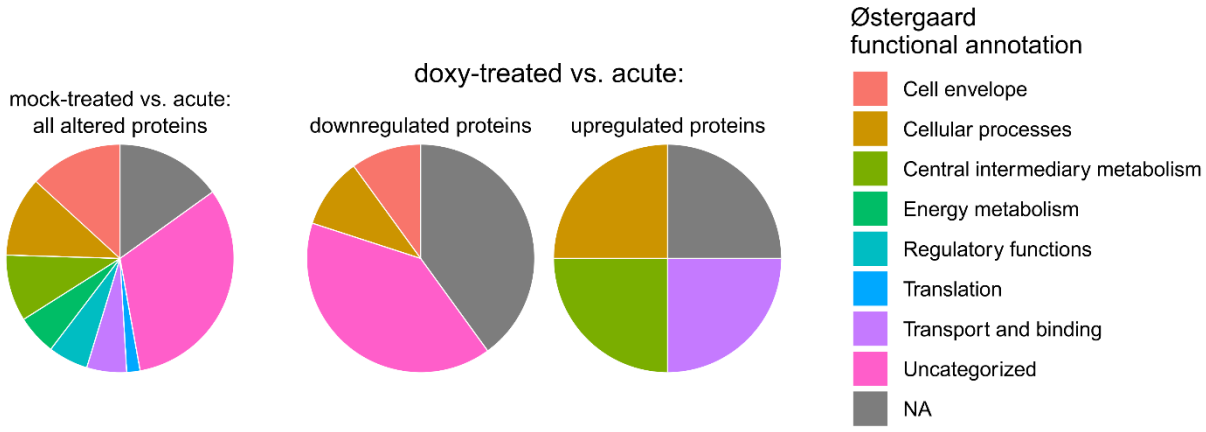

Fig. 31 Functional annotation of significantly altered proteins.

Significantly altered proteins of the mock-treated versus acute and doxy-treated versus acute (separately for downregulated and upregulated proteins) were annotated functionally according to the categories of Østergaard et al. (2016).

3.3.5.2.2.3 Increased IncD recruits CERT in persistence

The previous analysis revealed upregulation of the membrane proteins pmpA, IncD and CT_058 during doxycycline treatment. The protein pmpA localises in the OM of the bacterium apart from host contact sites, whereas the inclusion membrane proteins IncD and CT_058 are

exposed directly to the host cytosol. Due to its localisation, pmpA is assumed to stabilise the chlamydial membrane during persistence and does not interact with the host cell.

IncD recruits the human ceramide transferase protein CERT to the inclusion membrane of *C. trachomatis* serovar D, thus interfering with ceramide transport (Agaisse & Derré 2014, Banhart et al. 2019, Derré et al. 2011, Kumagai et al. 2018). Therefore, IncD was hypothesised to affect the lipid composition of the inclusion membrane, thereby stabilising and protecting it from host-driven degradation and reducing permeability to doxycycline. To test this hypothesis, cells were transfected with CERT-eGFP and analysed during acute and persistent infection to clarify whether CERT is recruited in persistence. In the acute infection at 48 hpi, CERT was recruited to the inclusion membrane (Fig. 32). The immunofluorescence of recruited CERT was reduced at 72 hpi but was still visible and vanished slightly at 98 hpi. During persistence, CERT was recruited to the inclusion membrane for up to 72 h of doxycycline treatment, with only traces of CERT being visible in distinct areas of the inclusion membrane. The decreased intensity correlated with the reduced expression of CERT-eGFP 72 h post-transfection. These results confirmed the recruitment of CERT during doxycycline treatment by probably upregulated IncD.

CT_058 has been reported to interact with proteins from the mitochondrial OM and proteins associated with the immune response (Mirrashidi et al. 2015). The published interactome of CT_058 was considered critically because the truncated protein has still an N-terminal hydrophobic TM domain (amino acids 57-367) that might affect its translocation and the resulting interactome. Due to the lack of information, subsequent investigations were not continued. To determine the role of CERT during persistence, the effect of CERT KO on doxycycline-treated *C. trachomatis* serovar D was determined.

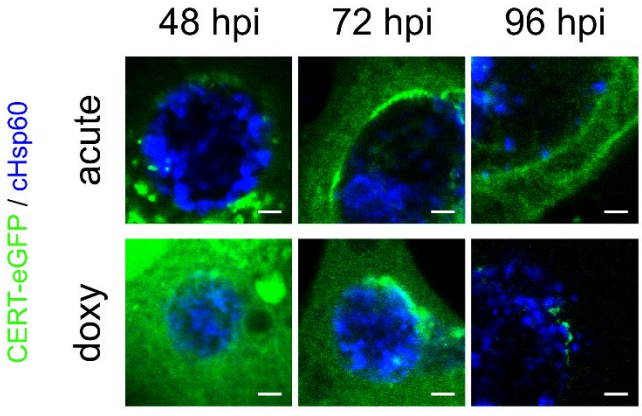

Fig. 32 Recruitment of CERT-eGFP during acute and persistent infection.
Cells were infected with *C. trachomatis* serovar D and treated or not treated with 0.5 µg/ml doxycycline at 24 hpi. The expression plasmid of CERT-eGFP (green) was transfected at 24 hpi. *C. trachomatis* serovar D within the inclusion was stained with α-cHsp60^{m} and α-mouse-Alexa Fluor® 647 (blue, cHsp60). The scale bar is 2 µm.

3.3.5.2.2.4 CERT is necessary for proper entry into persistence

Previous studies of ceramide acquisition in *C. psittaci* and *C. trachomatis* serovar L2 revealed a species specificity (Koch-Edelmann et al. 2017). While the KO of CERT resulted in increased uptake of fluorescent ceramide in *C. psittaci* infection, infection with *C. trachomatis* serovar L2 displayed a reduced ceramide acquisition in CERT-KO cells compared to control cells (Figure 4b, Koch-Edelmann et al. 2017). The progeny formation of acute, persistent and recovering *C. trachomatis* serovar D infection was determined in CERT-KO cells and CRISPR CTRL-KO cells to investigate the effect of CERT. Remarkably, the recovery of *C. trachomatis* serovar D from persistence was enhanced in CERT KO cells. After 24 h of recovery, the progeny formation peaked and then decreased. In contrast, *C. trachomatis* serovar D recovered more slowly in CRISPR CTRL KO cells, peaking after 48 h of recovery. Acute *C. trachomatis* serovar D infection displayed a constant but slightly reduced level of progeny formation in CERT KO cells compared to CRISPR CTRL KO cells (Fig. 33). Doxycycline-treated *C. trachomatis* serovar D infection of CERT KO cells displayed a slightly higher and constant level of progeny formation compared to the control cell line. The overall increased progeny formation in CERT KO cells agrees with the published observation of acute *C. trachomatis* serovar E infection during inhibition of sphingolipid biosynthesis (D. K. Robertson et al. 2009). Those authors showed an early increase with subsequent decrease, suggesting early redifferentiation into EBs, and thus early egress. The increased infectivity of inclusion-forming units of persistent *C. trachomatis* serovar D in CERT KO cells indicates continued EB formation despite treatment with doxycycline. This 'improper' persistence might lead to immediate recovery, as indicated by the marked increase in progeny formation after 24 h of recovery. The subsequent decrease in progeny formation after 48 h of recovery might reflect that chlamydial development has

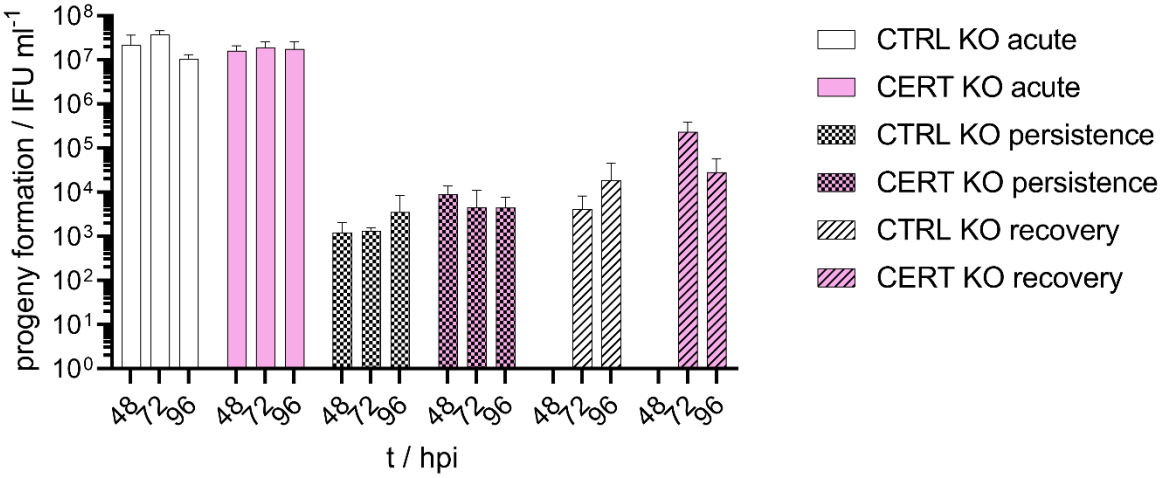

Fig. 33 Effect of CERT-knockout on progeny formation.

Cells with CERT KO and CRISPR CTRL KO (control) cells were infected with *C. trachomatis* serovar D (MOI = 2) and treated as described in Fig. 27. Progeny formation was determined for acute infection, persistence and recovery (data presented as the mean ± standard deviation; n = 3).

finished with early egress and host cell lysis. These results indicate improper entry into the persistent state in CERT KO cells, underscoring the necessity of CERT-mediated sphingolipid acquisition for persistence.

3.3.5.2.2.5 SNX5 and SNX6 KO enhances recovery from persistence

Proteomics revealed that IncE was unaffected in persistence (Fig. 30). IncE has been well studied and is known to interact with SNX5 and SNX6, which are involved in retrograde trafficking (C. A. Elwell et al. 2017, Mirrashidi et al. 2015, Paul et al. 2017, Sun et al. 2017). It was hypothesised that stable IncE expression is sufficient for SNX5 and SNX6 recruitment to support doxycycline-induced persistence. Hence, the effect of SNX5 and SNX6 double KO on progeny formation was investigated (Fig. 34). Progeny formation of the acute infection of *C. trachomatis* serovar D in SNX5/6 KO cells was slightly higher compared with CRISPR CTRL KO cells. These results agree with the increasing IFU of acute *C. trachomatis* serovar L2 and *C. trachomatis* serovar D upon SNX5/6 KD (Aeberhard et al. 2015, Mirrashidi et al. 2015), demonstrating the relevance of interfering with the host cellular retrograde trafficking. Progeny formation of doxycycline-treated *C. trachomatis* serovar D in SNX5/6 KO cells peaked after 48 h and then decreased after 72 h to a similar level as 24 h. Persistent *C. trachomatis* serovar D in the CRISPR CTRL KO cells displayed slightly increased progeny formation after 72 h of doxycycline treatment. Progeny formation of persistent *C. trachomatis* serovar D in both cell lines showed a similar variation, thus impeding estimation of a correlation with SNX5/6. *C. trachomatis* serovar D recovered similarly in both cell lines after 24 h. Progeny formation increased in both cell lines after 48 h of recovery and was enhanced in SNX5/6 KO cells. This observation indicates SNX5/6 KO enhances recovery of doxycycline-treated *C. trachomatis* serovar D.

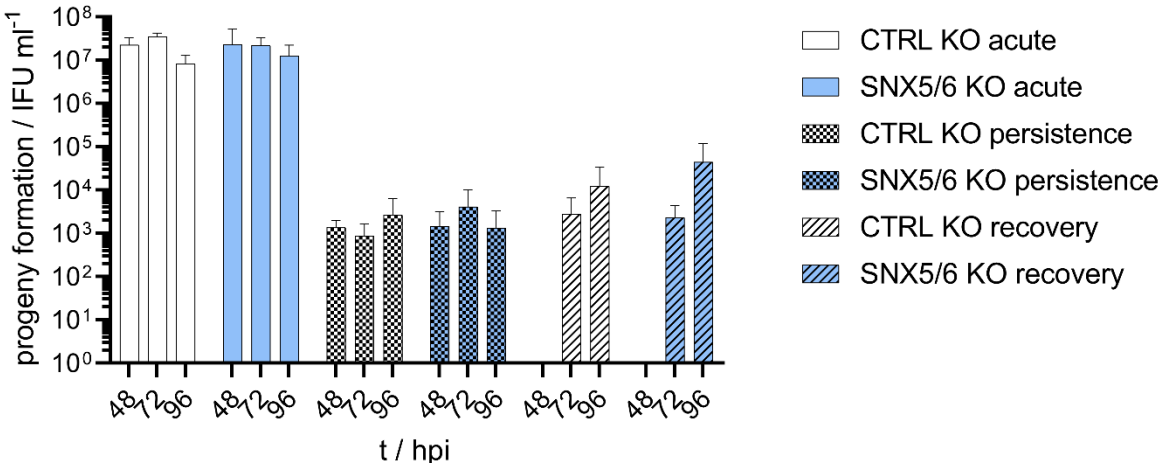

Fig. 34 Effect of SNX5 and SNX6 double KO on progeny formation.

SNX5 and SNX6 double KO cells and CRISPR CTRL KO (control) cells were infected with *C. trachomatis* serovar D and treated as described in Fig. 27. Progeny formation was determined for acute infection, persistence and recovery (data are presented as the mean ± standard deviation; n = 3).

3.3.5.2.2.6 Metabolic enzymes are slightly upregulated in persistent *C. trachomatis* serovar D

Significantly differentially regulated chlamydial proteins identified from the proteomes of mock-treated and doxy-treated *C. trachomatis* serovar D compared to acute as a control, were subjected to KEGG pathway analysis and clustered into functional groups (Table 4). Five categories were identified: transporter, TCA cycle, glucose and starch metabolism, peptidoglycan and translation. As described previously for the mock treatment, most upregulated proteins are involved in metabolism (TCA cycle, glucose and starch metabolism) followed by transporters. In persistence, transport proteins for the two-component system were not differentially expressed. Both subunits of succinyl-CoA ligase, α and β, were upregulated, whereas the remaining enzymes of the TCA cycle were unaffected. Moreover, there was no apparent regulation for glucose and starch metabolism. In contrast to acute infection (mock-treated), proteins involved in peptidoglycan metabolism and translation were regulated in persistence. tRNA pseudouridine synthase A, relevant for processing tRNA in translation, was decreased strongly. Interestingly, CT_268, relevant for peptidoglycan synthesis, was downregulated, while MreB (CT_709), involved in chlamydial cell division, was upregulated.

In summary, the most highly upregulated proteins in acute infection relied on metabolism and transport. Only a few of those proteins were also altered in persistence. Translation- and peptidoglycan-associated proteins were downregulated upon doxycycline treatment. Interestingly, one member of the cell division machinery, MreB, was increased during persistence. This observation might explain the morphology of enlarged ABs, which are ready for division. These results indicate moderately activate metabolism that might be sufficient to persist and survive antibiotic treatment.

Table 4 Functional clustering of regulated proteins.

Significantly regulated proteins from the inclusion proteomes of mock-treated versus acute (acute) and doxy-treated versus acute (doxy) treatments were subjected to KEGG pathway analysis and clustered. Regulation of acute and doxy are displayed as log2 fold changes. Unaltered proteins were left blank.

Transporter

Acute	Doxy	Protein	Name	Sub-function
1.710	1.510	CT_151	lipoprotein releasing system ABC transporter permease	
2.110	1.540	CT_152	lipoprotein releasing system ABC transporter ATP-binding protein	
2.040	1.810	CT_486	ABC transporter substrate-binding protein	
3.460		CT_467	two component system sensor histidine kinase	
3.790		CT_468	two component system response regulator	

TCA cycle

Acute	Doxy	Protein	Name	Sub-function
4.430		CT_054	2-oxoglutarate dehydrogenase subunit E1	
3.650		CT_055	2-oxoglutarate dehydrogenase complex subunit dihydrolipoyllysine-residue succinyltransferase	
5.365	2.750	CT_821	succinyl-CoA ligase subunit β	binds succinate (and GTP/ATP)
4.080	1.360	CT_822	succinyl-CoA ligase subunit α	binds CoA and phosphate
4.440		CT_855	fumarate hydratase	

glucose starch metabolism

Acute	Doxy	Protein	Name	Sub-function
3.930		CT_248	glycogen phosphorylase	
3.500		CT_489	glucose-1-phosphate adenylyltransferase	
3.140		CT_798	glycogen synthase	

Peptidoglycan

Acute	Doxy	Protein	Name	Sub-function
	-1.300	CT_268	*N*-acetylmuramoyl alanine amidase	
	1.370	CT_709	rod shape-determining protein MreB	

Translation

Acute	Doxy	Protein	Name	Sub-function
	-2.510	CT_106	tRNA pseudouridine synthase A	

4 Discussion

4.1 Identification and characterisation of *C. psittaci* Inc proteins

4.1.1 Split-Inc proteins are a powerful tool for interaction studies

In this work, a new approach was established to facilitate the investigation of interactions between host cell proteins and *C. psittaci* Inc proteins: split-Inc proteins. The split-Inc protein was designed to solubilise Inc proteins by replacing the TM domain with eGFP. Cytosolic split-Inc proteins bind unhampered and directly to host targets. The involvement of both cytosolic domains is predicted to influence the protein folding, thus allowing mimicry of native interactions. Due to the eGFP portion in split-Inc, the protein enables visualisation via immunofluorescence and allows co-immunoprecipitating interacting protein complexes by using GFP-specific antibodies. The IncE from *C. trachomatis* serovar D interacts with the human proteins SNX5 and SNX6 (C. A. Elwell et al. 2017, Mirrashidi et al. 2015, Paul et al. 2017, Sun et al. 2017), thus offering the opportunity to prove the concept. Interaction of split-IncE and SNX5 was shown by co-localisations of split-IncE and SNX5 clusters (Fig. 7). Another advantage of split-Inc proteins is the possibility to determine interaction partners by MS. Indeed, split-Inc protein and its interaction partners were isolated via GFP-Trap and further purified for MS. This application was demonstrated by successful detection of SNX5 and SNX6 using split-IncE as a well-known interaction partner.

The new split-Inc protein method described here is a promising tool to investigate interactions of Inc proteins with host cell proteins. Split-Inc proteins could be used to visualise interactions via immunofluorescence. Furthermore, split-Inc proteins and their potential interaction partners can be co-immunoprecipitated and identified by MS or western blot. Split-Inc proteins mimics native Inc proteins in a solubilised form without misdirected translocation, capable of identifying potential interaction partners through the natural binding of host cell proteins.

4.1.2 Hypothesis proven: the interplay of all cytosolic domains of Inc proteins is necessary to mimic native interactions

In previous studies, single cytosolic domains, either the N-terminus or C-terminus, had been tagged and expressed for interaction studies. Omitting a cytosolic domain might lead to misfolding of the complete Inc protein, weaken its physicochemical properties or dysregulate the efficacy of interacting with host proteins. Both *cis*-faced cytosolic domains of Inc proteins with a bi-lobed TM domain are integrated into the split-Inc protein method without excluding either one. The C-terminus of IncE interacts with human SNX5 and SNX6 by complementing the β-sheet folding of both host cell proteins (C. A. Elwell et al. 2017, Paul et al. 2017, Sun et al. 2017). In contrast, the N-terminus of IncE is not involved in direct interaction with SNX5/6.

The interaction intensity between split-IncE and transiently expressed SNX5 was analysed via western blot and compared with split-IncE lacking the N-terminus (split-Inc$E_{\Delta N}$). There was reduced interaction with split-Inc$E_{\Delta N}$, indicating that the N-terminus enhances the interaction. Kumagai et al. (2018) showed that both the N-terminal and C-terminal regions of *C. trachomatis* IncD are necessary to bind the CERT pleckstrin homology (PH) domain.

In summary, the results from the current study and from published investigations (Kumagai et al. 2018) prove the hypothesis of this work that the interplay of all cytosolic domains is necessary to mimic native interactions. Interaction studies using single domains might produce misleading results. The herein newly established method of split-Inc proteins offers the simultaneous usage of both cytosolic domains of an Inc protein. It is recommended to use split-Inc proteins as a method to consider the simultaneous integration of all cytosolic domains in future investigations to mimic possible physiological native interactions as closely as possible.

4.1.3 Host interaction partners of *C. psittaci* Inc proteins

In recent decades, investigations of chlamydial Inc proteins have intensified (Delevoye et al. 2008, Kokes et al. 2015, Rockey et al. 1995, Scidmore & Hackstadt 2001, Stanhope et al. 2017, Tang et al. 2021). They interact with host proteins and mediate host cell rearrangement to support chlamydial development. Lutter et al. (2012) performed *in silico* analysis of Inc proteins from different *Chlamydia* species and strains and determined so-called core and non-core Inc proteins. Identification and prediction of Inc proteins is based on the hydrophobicity of the amino acid sequence, considering that Inc proteins contain a unique bi-lobed TM domain (Rockey et al. 1995). This TM domain is identified by hydrophobicity plots (Fig. 11). In this work, the hydrophobicity of 11 annotated putative Inc proteins from *C. psittaci* 02DC15 was investigated by Protter (Omasits et al. 2014) and ProtScale according to Kyte & Doolittle. All 11 putative Inc proteins displayed a bi-lobed TM domain pattern (Fig. 11). Further functional and cell biological investigations were carried out by ectopically expressing Inc proteins in HeLa cells. Kostryukova et al. (2005) expressed full-length Inc proteins in uninfected HeLa cells and determined different membranous localisations in the cell. Basovskiy et al. (2008) and Shkarupeta et al. (2008) determined that full-length Inc proteins, expressed in uninfected HeLa cells, were localised either in the ER, plasma membrane or organelles. The location depends on the physicochemical properties of the TM domain.

Eight of eleven putative Inc proteins from *C. psittaci* 02DC15 were investigated their gene expression was quantified. These Inc proteins were cloned as split-Inc proteins and were investigated in immunofluorescence of uninfected and *C. psittaci* infected HeLa cells. Moreover, targets of the split-Inc proteins were detected by MS after GFP-Trap. Chosen

targets were cloned, FLAG-tagged and transiently expressed in uninfected and infected HeLa cells to investigate interactions *in vivo*.

4.1.4 CP0355 interferes with host protein expression and cytokinesis

Ectopically expression of Split-CP0355 was highly enriched in the nucleus, particularly in the nucleoli. This localisation was unique among the tested split-Inc proteins. When infected with *C. psittaci* 02DC15, the nuclear localisation of split-CP0355 decreased and it diffused through the cell but was not recruited to the inclusion membrane (Fig. 14). Consistently with the localisation, all interacting targets that were determined by MS after GFP-Trap relate to the nucleus: nucleases, nucleic acid–binding proteins and ribosomal proteins, amongst others. Kebbi-Beghdadi et al. (2020) expressed the effector protein CT_460 from *C. trachomatis* and showed distinct localisation in the host nucleus. CT_460 contains a SWIB/MDM2 domain that is involved in chromatin remodelling. Although the free online prediction tool DNABIND (https://dnabind.szialab.org/) displayed DNA-binding elements with a score of 4.091 and a probability of 0.9835, subsequent *in silico* analysis of the CP0355 amino acid sequence was insufficient to predict properties known for transcription factors. Regarding the distribution of charged amino acids, there is a large accumulation of positively charged residues at the N-terminal region of the C-terminus. With a positive net charge (six positive versus three negatively charged amino acids at the N-terminus and 33 positive versus 17 negatively charged amino acids at the C-terminus, Fig. 35), CP0355 resembles nuclear proteins that bind negatively charged DNA or RNA via positively charged residues.

Furthermore, ScanProsite identified a bipartite nuclear localisation signal (NLS) in the C-terminus of CP0355 (Fig. 35). The bipartite NLS of CP0355 might recruit proteins of the nuclear import machinery such as importin α, importin β1 or RanGTPase, amongst others (Lu et al. 2021). Reduced nuclear RanGTP inactivates the nuclear transport machinery and leads to the accumulation of NLS-containing proteins in the cytosol by binding to importin α and importin β (Wong et al. 2009). As a membrane-bound Inc protein, CP0355 could therefore reduce nuclear import by binding to related proteins. Consequently, the import of histones, cell cycle regulators and transcription factors would be limited.

There are multiple ways CP0355 could interfere with the expression of host proteins: 1) positively charged residues could bind RNA and thereby dysregulate translation; 2) upon phosphorylation, CP0355 might bind ribosomal proteins, disturbing ribosome assembly and inhibiting translation; and 3) the bipartite NLS could snatch proteins of the nuclear import machinery, hindering gene expression at a fundamental level. Overall, CP0355 might reduce host transcriptional or translational activity, changes that enable greater availability of metabolites and nutrients for chlamydial development. The nuclear import blockade could disturb cytokinesis and impair the host cell cycle, favouring chlamydial development. It is worth mentioning that a membrane-anchored split-CP0355 might indicate cytosolic interaction partners by counteracting nuclear import, absent of nuclear proteins that otherwise covers the interactome. Rockey et al. (1997) demonstrated that IncA from *C. psittaci* is phosphorylated by host cell phosphatases. Future investigations should include post-translational phosphorylation of CP0355 to determine putative phosphorylation-dependent interactions.

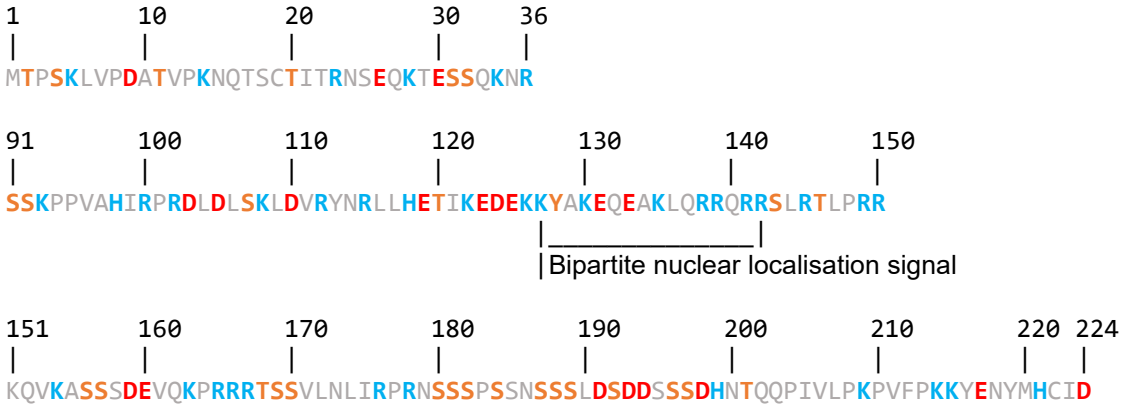

Fig. 35 Amino acid sequence analysis of CP0355.

The cytosolic sequences of CP0355 (N-terminus 1-36, C-terminus 91-224) were screened for motifs via ScanProsite (marked below sequence) and for phosphorylation sites (highlighted orange) via the NetPhos 3.1 Server. Physiologically charged acidic amino acids are labelled in red, basic amino acids are labelled in blue and the remaining amino acids are in grey.

4.1.5 CP0856 and CP0857 contribute to cytoskeletal arrangements

Amongst all analysed putative Inc proteins, the gene *cp0856* was the predominantly transcribed at mid-phase and *cp0857* at early and mid-phase (Fig. 12). The ectopic expression of split-CP0856 during infection highlighted the inclusion membrane (Fig. 14), in contrast to the diffuse expression of split-CP0857. MS of co-immunoprecipitated split-CP0857 revealed the scaffold proteins C12orf57 and TANC1. Split-CP0856 revealed 11 interaction partners: seven members of the 14-3-3 protein family, two isoforms of Afadin, FLII and dedicator of cytokinesis protein 7 (DOCK7) (Fig. 15). Remarkably, four of these interaction partners seem to be relevant to the cytoskeleton: Afadin (MLLT4-3, MLLT4-5) connects nectin to the actin

cytoskeleton (Reymond et al. 2000); DOCK7, a Rac GEF (Watabe-Uchida et al. 2006), may be involved in cytoskeletal dynamics (O'Loughlin et al. 2018); and FLII (Protein flightless-1 homologue) plays a role in the regulation of cytoskeletal rearrangements (Lee et al. 2004). The members of the 14-3-3 family are involved in cell signalling and bind phosphoserine or phosphothreonine in proteins (Angrand et al. 2006).

In silico prediction (http://www.compbio.dundee.ac.uk/1433pred/) showed a recognition pattern for 14-3-3 proteins at the C-terminus of CP0856. Interestingly, four 14-3-3 proteins (SFN [14-3-3 protein sigma], YWHAB [14-3-3 protein beta/alpha], YWHAE [14-3-3 protein epsilon] and YWHAZ [14-3-3 protein zeta/delta]) bind cadherin (cell-cell adhesion) and one directly binds actin (YWHAH [14-3-3 protein eta]). In *C. trachomatis*, IncG interacts with 14-3-3-beta (Scidmore & Hackstadt 2001). *In silico* analysis revealed a recognition motif in IncG for the 14-3-3 protein, but IncG does not share physicochemical properties with CP0856. Further, cofilin leads to the depolymerisation of actin filaments and can be phosphorylated at Ser3. This phosphorylation inhibits depolymerisation and is bound by 14-3-3-zeta that stabilises the post-translationally modified state (Gohla & Bokoch 2002). The overexpressed 14-3-3-zeta protein was not recruited to the inclusion membrane (data not shown). Proteins involved in cell signalling are highly dynamic and can be post-translational dephosphorylated or phosphorylated. These dynamics might impede proper interaction between 14-3-3-zeta protein and split-CP0856, thus reducing the likelihood to visualise co-localisations in immunofluorescence. These results indicate that CP0856 might indirectly regulate polymerisation of actin filaments via 14-3-3 proteins. The genes around *cp0856* and *cp0857* encodes the proteins CP0855 and CP0852. Investigation of the amino acid sequences of these proteins yielded tropomyosin domains in CP0855 and CP0852. Tropomyosin stabilises actin filaments in a Ca^{2+}-dependent manner (Hitchcock-DeGregori & Barua 2017). As mentioned before, CP0857 binds scaffold proteins. Wasylnka et al. (2008) determined the role of myosin II for the intracellular and vacuolar pathogen *Salmonella enterica*. *C. trachomatis* also manipulate actin filaments (Caven & Carabeo 2019), supported by the recruitment of myosin phosphatase pathway elements through CT_228 in a regulatory manner (Lutter et al. 2013). The tropomyosin-like proteins CP0855 and CP0852 might interact with actin filaments, whose polymerisation depends on 14-3-3-zeta recruitment by CP0856. Furthermore, recruitment of the scaffold proteins CC12orf57 and TANC1 by CP0857 could stabilise actin filaments. CP0856 and CP0857 are theoretically not transcribed from the same operon. However, the complete locus might be necessary for actin stabilisation and might lead to proper extrusion formation or directed transport of organelles, proteins or nutrients to the inclusion membrane. Because actin filaments are large and only indirect targets, actin was not co-purified in the GFP-Trap.

4.1.6 CP0181 seems to have a role in microdomain organisation

The putative Inc protein CP0181 (CPS0B_0181) was expressed immediately early in *C. psittaci* 02DC15, with a small and brief peak from 24 to 32 hpi (Fig. 12). The split-Inc protein variant (split-CP0181) remained cytosolic in uninfected cells and displayed no accumulation at the inclusion membrane during infection (Fig. 14). The cytosolic distribution of split-CP0181 might depend on its cytosolic interaction partner. Ectopically expressed split-CP0181 during *C. psittaci* infection could stoichiometrically saturate interactions with a potential cytosolic host protein. This competition with the native CP0181 probably hinders accumulation of split-CP0181 around the inclusion during infection. In addition, the MS data revealed no significant interaction partners. The lack of significant interaction partners might be because there were only weak interactions that were lost during the purification protocol. Another possibility might be that CP0181 is only relevant for avian cells and thus interaction partners would not appear in experiments performed in a human cell line. *C. psittaci* is a zoonotic pathogen that originates from birds. So, CP0181 might interact with avian host proteins to support chlamydial development. The CP0181 gene is the only one within its locus, genetically surrounded by anti-directed genes that provide no further indication of its function. Finally, pattern prediction of InterPro (http://www.ebi.ac.uk/interpro/result/InterProScan/iprscan5-R20210806-174116-0303-4357690-p2m/) displayed many coiled regions in the C-terminus. The C-terminus of IncA from *C. trachomatis* contains two coiled-coil domains necessary for multimerisation and homotypic membrane fusion (Ronzone & Paumet 2013). In contrast to *C. trachomatis*, the inclusions of *C. psittaci* do not fuse (Rockey et al. 1996). The coiled domains of CP0181 could lead to homooligomers or heterooligomers with different Inc proteins during the early phase of infection. Therefore, the function of CP0181 could be the organisation of microdomains that contains Inc proteins. Immunofluorescence of ectopically expressed split-CP0181 in *C. psittaci*–infected cells was performed at 24 hpi, a phase beyond the peak of natively expressed CP0181. This late phase might explain the absence of putative interactions between split-CP0181 and native CP0181 or other early Inc proteins during infection.

To summarise, the lack of human interaction partners indicates a possible species-depended interaction with avian proteins. Furthermore, it is proposed that the *in silico* predicted coiled domains of CP0181 form homo- and heterooligomers with early expressed Inc proteins. However, further investigations are required to confirm or exclude one of the previously mentioned expectations, including comparison with infection and interaction studies in avian cells.

4.1.7 CP0534 and CP0535 support inclusion membrane integrity

Both CP0534 (IncC) and CP0535 (IncB) are conserved Inc proteins amongst *Chlamydia* spp. They are transcribed immediately early (Fig. 12) from one operon (Bannantine et al. 1998). Their TM domain is highly conserved, despite having different amino acid sequences. Structural prediction of the TM domain of IncB and IncC from *C. trachomatis*, *C. pneumoniae* and *C. psittaci* by Robetta (Baek et al. 2021) yielded two TM α-helices that are clearly separated in IncB by an amphipathic α-helix (Fig. 36 D-F) and separated in IncC by a proline-nicked amphipathic α-helix (Fig. 36 A-C). In this study, there were no significantly enriched interaction partners. In contrast, Böcker et al. (2014) identified the direct interaction partner Snapin and the indirect interaction partner Dynein for IncB from *C. psittaci*, indicating a role in organising microtubules. Böcker et al. (2014) immunoprecipitated glutathione *S*-transferase (GST)-tagged purified proteins that were incubated with cell lysates and proved the interaction by western blot and immunofluorescence of Snapin and dynein at the inclusion membrane. However, the current study employed a GFP-Trap of transiently expressed split-IncB or split-IncC in cell lysates followed by MS. Ectopically expressed split-IncB and split-IncC were recruited to the inclusion membrane during infection, indicating interactions with recruited host proteins or native Inc proteins (Fig. 14). Split-Inc proteins might 1) homooligomerise with the cytosolic domain of native IncB/IncC, 2) heterooligomerise via the cytosolic domain with different Inc proteins, 3) interact with IncB/IncC-recruited proteins in a sandwich manner or 4) interact with proteins recruited by different Inc proteins. Researchers have shown that the TM domain of IncD from *C. trachomatis* is necessary to form homooligomers (Kumagai et al. 2018). It has not yet been excluded that IncB and IncC also use their TM domain to homooligomerise or to form specific or nonspecific heterooligomers with several Inc proteins. However, because both Inc proteins are conserved, their function must be fundamental or extended by non-conserved cytosolic domains. The role of IncB or IncC might rely on selective clustering of Inc proteins based on their TM domain. These clustered Inc proteins could recruit host proteins and thereby increase the local concentrations of host proteins. These clusters could be relevant for regional interactomes that have distinct functions. Dickinson et al. (2019) performed proximity proteomics of *Chlamydia*-expressed IncB fused to APEX2 at different times during infection. They detected several host proteins and certain Inc proteins from *C. trachomatis* serovar L2 early (8 hpi). They did not find IncC amongst these proteins. Therefore, it is presumed that IncB and IncC accumulate in different clusters with certain Inc proteins in a kind of collective to act in different functional categories. Mital et al. (2010) showed that IncB of *C. trachomatis* serovar L2 co-localises with CT_101, CT_222 and CT_850 in so-called microdomains that are also enriched with cholesterol (Carabeo et al. 2003).

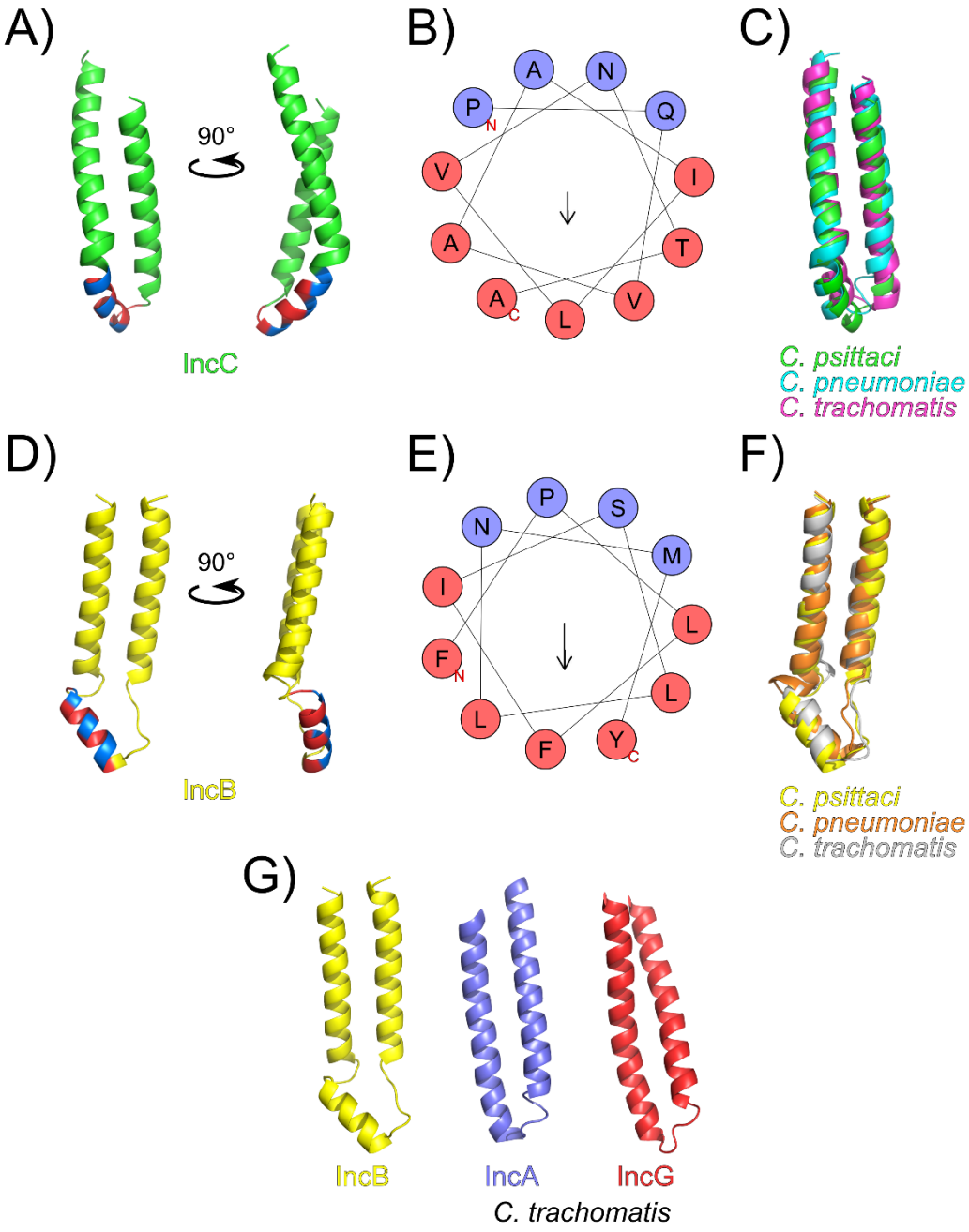

Fig. 36 Structural investigations of the TM domains of IncB and IncC.

The TM domains of IncB and IncC from *C. psittaci* 02DC15, *C. trachomatis* serovar D and *C. pneumoniae*, and IncA and IncG from *C. trachomatis* serovar D were predicted by using Robetta (Baek et al. 2021). The structural diagrams were created by using PyMol. The front view and 90° rotation on the y-axis of the TM domain of IncC and IncB are displayed in A) and D), respectively. Amino acids of the putative amphipathic helix are coloured according to B) for IncC and according to E) for IncB. The hydrophobicity of the amphipathic helix type 3-10 of B) IncC and E) IncB was determined via HeliQuest. The hydrophobic side (red) faces downward and the polar side (purple) faces upward. Structural alignment of TM domains of C) IncC and F) IncB from *C. psittaci* 02DC15, *C. trachomatis* serovar D and *C. pneumoniae* have been coloured. G) Comparison of the TM domain front view of IncB (*C. psittaci* 02DC15) with IncA and IncG from *C. trachomatis* serovar D.

As mentioned earlier, IncB and IncC seem to have a TM domain consisting of two α-helices connected by an amphipathic α-helix. This is atypical for Inc proteins because their TM α-helices are connected by a short peptide (Fig. 36 G). At high concentrations, IncB and IncC might affect the inclusion membrane, yielding a concave curvature (Fig. 37 A). The high concentration of cholesterol in IncB microdomains (Mital et al. 2010) might counteract the effect of IncB, leading to an equilibrated membrane curvature (Fig. 37 B). *Chlamydia* spp. are unable to synthesise sphingomyelin *de novo* (Stephens et al. 1998). *C. trachomatis* scavenge cholesterol (Carabeo et al. 2003), sphingomyelin (Wylie et al. 1997) and precursors like ceramide (Koch-Edelmann et al. 2017). Inhibition of sphingolipid biosynthesis at the serine palmitoyltransferase step halts the replication of *C. trachomatis*, whereas inhibition of sphinganine and sphingosine *N*-acetyltransferases leads to AB formation (van Ooij et al. 2000). Furthermore, inhibition of ceramide precursor biosynthesis disrupts homotypic inclusion fusion and interferes with the reactivation of INF-γ-induced persistent *C. trachomatis* (D. K. Robertson et al. 2009). Hence, sphingolipids are necessary for *C. trachomatis*, but their relevance for *C. psittaci* remains unknown. Proximity labelling by IncB-APEX2 (Dickinson et al. 2019) identified IncD in *C. trachomatis* that is known to recruit CERT (Agaisse & Derré 2014, Derré et al. 2011), a factor that correlates with the sphingomyelin increase in the inclusion membrane. On the contrary, CERT KO increased sphingomyelin uptake in *C. psittaci* by an unknown mechanism (Koch-Edelmann et al. 2017), though *C. psittaci* lacks an IncD orthologue. Furthermore, cholesterol associates with sphingomyelin (Massey 2001). It might be possible that microdomains containing IncB and enriched cholesterol also harbour sphingomyelin that probably forces the inclusion membrane to take on a convex curvature (Fig. 37 C). Furthermore, these microdomains might relate to lipid rafts. The lipid rafts of the host cell membrane consist of glycosphingolipids, sphingomyelins and cholesterol (Thomas et al. 2004). They can accumulate specific TM proteins but exclude most integral proteins (Alonso & Millán 2001). Hence, distinct Inc proteins could accumulate in the microdomains, leading to local and perhaps synergetic enhancement. Cholesterol in the inclusion microdomains increases hydrophobicity and decreases fluidity. These stabilised regions (possibly organised by IncB) withstand strong forces that could originate indirectly from the interaction between IncB and the microtubule organising proteins Snapin and Dynein (Mital et al. 2010). Taken together, IncB and IncC might be relevant for inclusion stability, functional Inc protein organisation and clustering by cytosolic interaction and recruitment of host proteins.

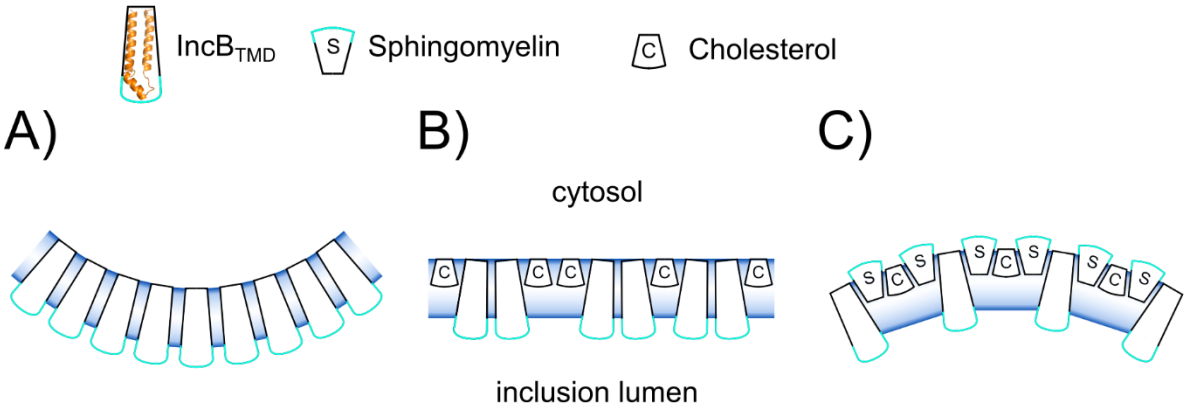

Fig. 37 Theoretical scheme of inclusion membrane curvature depending on its constitution. A) Concave curvature with a high IncB concentration. B) Equilibrated membrane curvature by counteracting cholesterol integration. C) Convex curvature due to integration of sphingomyelin. The TM domain of IncB, sphingomyelin (S) and cholesterol (C) are indicated. The membranous parts are outlined in black and the cytosolic parts are outlined in cyan. The lipid bilayer of the inclusion membrane is coloured dark blue.

4.1.8 CP0558 is involved in fatty acid metabolism

Like the genes *incB* and *incC*, *cp0558* is transcribed immediately early (Fig. 12), but it is also transcribed late. During the infection cycle of *C. psittaci*, ectopically expressed split-CP0558 localised to the inclusion membrane (Fig. 14). MS of co-immunoprecipitated proteins via GFP-Trap revealed one significantly enriched interaction partner: ACAD11, which has been described to localise in mitochondria (M. He et al. 2011) but in the current study accumulated strongly in cellular homogeneously distributed rod/punctate structures when transiently overexpressed (data not shown). *C. trachomatis* requires Acyl-CoA synthases (Recuero-Checa et al. 2016) and interacts with human acyl-CoA binding protein hACBD6 in a synergetic fashion to buffer the acyl-CoA concentration (Soupene et al. 2015). During *C. trachomatis* infection, hACBD6 is recruited to lipid droplets that translocate to the inclusion (Soupene et al. 2015), indicating a role for lipid droplets for *C. psittaci*. Because nothing is known regarding the relevance of lipid droplets in the *C. psittaci* development, host-derived lipid precursors might be involved and follow mechanisms similar to those observed for *C. trachomatis*. The fact that split-CP0558 was localised at the inclusion membrane might indicate binding of acyl-CoA precursors or analogue metabolites. Therefore, the Inc protein CP0558 recruits metabolites that share human binding proteins or enzymes to establish fatty acid metabolism or β-oxidation. The immediate-early expression of CP0558 probably highlights its relevance in fatty acid metabolism to compensate for the repertoire of fatty acids required by the fast-growing and dividing bacteria.

4.1.9 CP0598 provides a larger reservoir of amino acids

The gene *cp0598* (*incA*) was transcribed in a bi-phasic manner: early and mid (Fig. 12). When ectopically expressed during infection, split-IncA localised weakly to the inclusion membrane (Fig. 14). This pattern indicates that either the interaction partners are already occupied by natively expressed IncA or IncA has a low affinity for Inc proteins in general. The GFP-Trap of split-IncA yielded the interaction partners BAG family molecular chaperone regulator 2 (BAG2) and RING finger protein 214 (RNF214). Overexpression of either target during infection did not lead to recruitment to the inclusion membrane (data not shown). RNF214 consists of a RING-type zinc finger domain (type C3HC4) associated with ubiquitin-protein transferase activity (UniProt: Q8ND24) that remains to be studied. In contrast, BAG2 has multiple known functions. The protein is a co-chaperone and nucleotide-exchange factor for ADP release of Hsp70/Hsc70. It promotes Hsp70-mediated protein refolding, drives ubiquitin-independent degradation via the proteasome and inhibits the Hsp70-binding E3 ubiquitin ligase CHIP that mediates ubiquitylation of misfolded proteins (Qin et al. 2016). BAG2 is responsible for shifting the folding machinery from ubiquitin-dependent degradation to refolding or ubiquitin-independent degradation.

Borth et al. (2011) employed a yeast two-hybrid system and identified that G3BP1 interacts with IncA from *C. psittaci*. They extrapolated its role in chlamydial development by focussing on c-myc. Researchers recently published a complete mechanism involving G3BP1 (Meyer et al. 2020). G3BP1 participates in the recycling of stalled ribosomes in stress granules, where mRNA that failed to be translated or misfolded proteins are recycled. Ribosomes that stall or collide during translation of the same mRNA are recognised by ZNF598, which encodes an E3 ubiquitin ligase RING domain (C2H2-type zinc finger). This protein ubiquitylates the 40S ribosomal subunit. Furthermore, several proteins induce dissociation of the complex into the large subunit and small subunit bound to mRNA. G3BP1 binds the small subunit and recruits Ubiquitin carboxyl-terminal hydrolase 10 (UPS10). This protein complex leads to deubiquitylation of the small subunit that in turn will be available for regular translation. Consequently, G3BP1 rescues the 40S subunit from ubiquitin-dependent degradation.

IncA seems to scavenge BAG2 and/or G3BP1 to affect host degradation via ubiquitylation, making more amino acids available for *Chlamydia*. RNF214, which has not yet been characterised, might be interchangeable with ZNF598 because *in silico* prediction indicated RNA-binding elements that were also predicted for ZNF598 using the same tool (DNA, RNA, protein binding via disorder-prediction tool DisoRDPbind). This work identified different interaction partners than Borth et al. (2011), probably due to the difference in the methods. Borth et al. (2011) performed yeast two-hybrid screening and investigated direct interactions. Furthermore, purified GST-IncA (C-terminal) was incubated with a cell lysate whose interaction

partners were visualised via western blot. The identification of interaction partners in this work was based on the overexpression of split-Inc proteins, followed by GFP-Trap and subsequent MS. Split-IncA overexpression might exhaust the cell and induce stress granule formation. The ribosomal translation complex of the elongating split-IncA peptide could be directed to those stress granules, leading to ribosome recycling. Thereby, split-IncA could interact with RFN214 that is putatively involved in the granular ribosome recycling. Alternatively, BAG2 could accumulate to support refolding of misfolded proteins due to the exhausting overexpression. This accumulation would increase the likelihood of BAG2 interacting with split-IncA, thereby competing with G3BP1. However, a commonality of these hypotheses is that IncA is associated with increased ubiquitylation of host proteins, thus feeding the bacteria with available amino acids for chlamydial development. The transcriptional peaks of IncA in the early and mid-phase support the hypotheses and highlight the requirement of amino acids for initial and later increasing protein expression.

4.1.10 The role of interactions for successful zoonosis

Little is known about the Inc proteins of *C. psittaci*, whereas Inc proteins of several other *Chlamydia* spp. have been identified and studied during the last decades. In addition to the three common Inc proteins – IncA, IncB and IncC – new Inc proteins have been validated recently: CPSIT_0844 (≙CPS0B_0852) and CPSIT_0846 (≙CPS0B_0854) (Tang et al. 2021, Wu et al. 2016), as well as CPSIT_0842 (≙CPS0B_0850) and CPSIT_0556 (≙CPS0B_0559) (Z. He et al. 2021). Dehoux et al. (2011) listed several putative Inc proteins for *C. caviae*. BLASTing (Altschul et al. 1997) those predicted Inc proteins against *C. psittaci* 02DC15 revealed an additional 61 individual orthologues annotated as ‘uncharacterised’ (data not shown).

In this work, CPS0B_0850, CPS0B_0849 and CPS0B_0855 were investigated according to the hydrophobicity and the cytosolic domains displaying the bi-lobed TM domain. The transcriptional profiles of *cp0181*, *cp0355*, *incC* (*cp0534*), *incB* (*cp0535*), *cp0558*, *incA* (*cp0598*), *cp0856* and *cp0857* were investigated, as well as their split-Inc protein analogues for cytosolic destination and behaviour during infection. The split-Inc protein method revealed interaction partners of CP0355, CP0558, IncA, CP0856 and CP0857. These interactions seem to interfere with host cytokinesis and protein expression (CP0355), scavenge metabolites or proteins for fatty acid metabolism (CP0558), provide a large reservoir of amino acids (IncA) and contribute to cytoskeletal arrangements (CP0856 and CP0857). The Inc proteins without significant enrichment of interaction partners seem to perform different functions. IncC and IncB seem to stabilise the inclusion membrane and organise clustered microdomains. CP0181 likely participates in microdomain organisation during the early phase of infection and could probably interact with avian host cell proteins.

C. psittaci is a zoonotic pathogen of birds and can be transmitted to humans. Adaptation to humans requires successful entry into human cells, proper interaction with host proteins and metabolite scavenging. Based on the results, the combination of specific and unspecific interactions presumably achieves successful zoonosis. *C. psittaci* Inc proteins with distinct amino acid patterns or motifs are proposed to specifically bind to avian proteins since birds are the original host. Human proteins that differ only little from the avian orthologue can be recognised as well by specific binding motifs of Inc proteins. However, interactions based on physicochemical properties are predicted to be essential for zoonosis. Physicochemical-driven interactions are less specific and are herein postulated to maintain interactions with cellular proteins independent of the kind of host. This reduced specificity might facilitate adaptation to different hosts and underscore successful zoonosis.

It is essential to determine the localisation of Inc proteins either by antibody-mediated methods or by tagged protein expression of genetically transformed *C. psittaci*. An alternate method might be the secretion system reported by Dehoux et al. (2011). Those authors demonstrated the secretion of predicted Inc proteins via T3SS. Furthermore, split-Inc proteins offer the opportunity to investigate binding motifs that are relevant for interactions with host cell proteins. Simple site-directed mutagenesis of split-Inc proteins could substitute amino acids putatively involved in the interaction. These follow-up investigations could reveal whether the interactions are based on physicochemical properties or distinct amino acid motifs.

There has been relatively limited information revealed about *C. psittaci* in the last decades. This work has provided essential information that extends the current knowledge about how this bacterium interacts with its human host cell. The newly established split-Inc protein method has the ability to investigate native physiological interactions of Inc proteins. Investigations using split-Inc proteins proved the hypothesis that the interplay of all cytosolic domains of Inc proteins are required to mimic native interactions with host cell proteins. The results have enabled the formulation of hypotheses that remain to be investigated but are predicted to clarify the mechanisms of *C. psittaci* infection and replication. A fascinating aspect will be analysis of *C. psittaci* Inc proteins in avian cells. These experiments could help researchers understand the success of the chlamydial zoonosis. These future investigations could also inspire follow-up investigations of other *Chlamydia* species.

4.2 Doxycycline-induced persistence of *C. trachomatis* serovar D

C. trachomatis is known to survive different antibiotics during clinical treatment (Dukers-Muijrers et al. 2019, Kong et al. 2014, Lau & Qureshi 2002, Molano et al. 2005, Páez-Canro et al. 2019, Suchland et al. 2017). Its survival might lead to consequential damage of women's reproductive health (Workowski et al. 2021). Bacteria typically acquire genomic islands of antibiotic resistance through HGT (Partridge et al. 2018). Although interspecies HGT is possible in clinical *C. trachomatis* (Harris et al. 2012, Jeffrey et al. 2010), no clinical isolate has been identified harbouring a genomic island of antibiotic resistance until now (Benamri et al. 2021). In rare cases, resistant *C. trachomatis* occur, containing single mutations in drug targets (Mestrovic & Ljubin-Sternak 2018). It is more common for *Chlamydia* to enter a state called persistence under antibiotic stress. In recent decades, several persistence stimuli of *C. trachomatis* serovar D have been reported and investigated (N. D. Hatch & Ouellette 2020, Ouellette et al. 2016, Reveneau et al. 2005, Skilton et al. 2009, Thompson & Carabeo 2011, Xue et al. 2017). Penicillin, an inhibitor of bacterial cell wall synthesis, blocks the ability of *C. trachomatis* serovar D to divide and form progeny. The weakened or incomplete bacterial cell wall fails to stabilise the osmotic pressure leading to lysis of the bacteria. *Chlamydia* lack an overall peptidoglycan sacculus in the cell wall; they only synthesise peptidoglycan component during cell division (G. W. Liechti 2021). Consequently, such a bacteriocidic osmotic pressure does not affect *Chlamydia*. Instead, the bacteria enlarge to ABs. Another form of persistence is induction by IFN-γ: treatment with this cytokine depletes the amino acid L-tryptophan in mammal cells (Ouellette et al. 2016). Starvation of this amino acid forces *Chlamydia* into persistence, a state denoted by enlarged bacteria. A similar persistence mechanism underlies iron depletion (Thompson & Carabeo 2011). Less investigated are translational inhibitors that also induce persistence. *C. trachomatis*–infected patients are clinically treated with azithromycin or doxycycline (Mpiga & Ravaoarinoro 2006). Therefore, doxycycline-treated *C. trachomatis* serovar D was investigated to elucidate mechanisms of doxycycline-induced persistence of *C. trachomatis* serovar D.

4.2.1 *C. trachomatis* serovar D continues *de novo* protein expression during doxycycline-induced persistence

The morphology of doxycycline-treated *C. trachomatis* serovar D was investigated to identify persistence upon doxycycline treatment. Electron micrographs revealed early enlarged bacteria during treatment with 0.5 µg/ml doxycycline, known as ABs, with the absence of EBs (Fig. 17). These ABs are limited in number and represent the morphology of chlamydial persistence. The same treatment regimen was used for doxycycline and azithromycin as a

comparison to quantify translation during treatment and recovery as an indicator of persistence. The results revealed basal translational activity of *C. trachomatis* serovar D during treatment with 0.5 and 4 µg/ml doxycycline (Fig. 19). The ability to recover 24 h after doxycycline removal proved the persistent state. However, bacteria subjected to azithromycin treatment ≥ 0.06 µg/ml showed no translational activity or recovery, implicating a bactericidal effect on *C. trachomatis*. Due to the translational activity in doxycycline-treated *C. trachomatis* serovar D, transcription of genes related to the trans-translation was quantified to investigate this mechanism as a putative driving force for persistence. Analyses showed a stable transcriptional level of *smpB* and tmRNA (*ssrA*) in doxycycline-treated *C. trachomatis* serovar D (Fig. 20).

The morphologic investigation of doxycycline-treated *C. trachomatis* serovar D showed ABs in limited numbers. Electron micrographs of persistent *C. trachomatis* from patients also showed fewer ABs within the inclusion compared with acutely developed inclusions (Lewis et al. 2014). During persistence, chlamydial development is halted; consequently, inclusion growth is reduced. The limited space of the inclusion seems to restrict the size and numbers of ABs. Furthermore, fewer ABs reflects the inability of the bacteria to divide during antibiotic pressure (Panzetta et al. 2018). The enlarged phenotype might also contribute to dilute antibiotics, thus decreasing their concentration. Osmolarity-related gene expression drives the Donnan potential, a membrane potential of the OM of gram-negative bacteria, which affects the susceptibility to antibiotics during bacterial infection (Alegun et al. 2021). Investigations of this effect in *C. trachomatis* correlating with antibiotic treatment suggest a putative role in chlamydial persistence. However, *C. trachomatis* serovar D displayed translational activity in doxycycline treatment and was able to recover, while treatment with azithromycin was bactericidal. These results are in contrast to published observations of azithromycin-induced persistence (Reveneau et al. 2005, Xue et al. 2017). Xue et al. (2017) emphasised that the azithromycin concentration, the chlamydial developmental phase and the treatment duration are relevant to induce persistence successfully. Therefore, it is likely that the chosen azithromycin treatment regimen in this work was insufficient to induce persistence. ABs have been reported to be transcriptionally active (Panzetta et al. 2018). This observation is consistent with the results of the chlamydial trans-translation analysis. This mechanism seems to be involved in counteracting the effect of doxycycline during persistence. It is likely that the protein-RNA complex between SmpB and tmRNA had been stabilised and reached a sufficient saturated concentration. Treatment with 0.5 µg/ml doxycycline led to an early plateau of both transcripts. This transcriptional profile probably reflects impaired cell division. After 32 hpi, both *ssrA* and *smpB* had stabilised. Unlike in acute infection, *smpB* transcripts did not markedly decrease in persistence. The half-life of mRNA in *E. coli* is short, ranging from a few seconds

to 30 min (Lenz et al. 2011), and requires stabilising factors or continued transcription to keep the relative level of transcripts. Therefore, the comparatively high transcription of *smpB* in persistence indicates active expression. Hence, the SmpB protein level might be insufficient for trans-translation, or the translational elongation of SmpB is incomplete due to the interference of doxycycline. The low SmpB protein concentration may stimulate repeated transcription of *smpB* to maintain trans-translation. Persistent *Chlamydia* counteract translational inhibition by using trans-translation but are unable to remove doxycycline. Due to this dynamic equilibrium, *C. trachomatis* serovar D may persist, thus surviving the antibiotic treatment. This mechanism might underly a certain dynamic equilibrium to counteract antibiotic-induced stalling of ribosomes indefinitely such as described for resistance mechanisms (Griffin et al. 2010). In contrast to treatment with azithromycin, *Chlamydia* showed *de novo* protein expression during treatment with doxycycline.

Doxycycline binds reversibly to the 30S ribosomal subunit and blocks the entry of aminoacyl-tRNA to the A-site (Chopra & Roberts 2001, Semenkov et al. 1982). At the A-site, doxycycline could be replaced by tmRNA. Trans-translation continues, resulting in dissociation of the stalled ribosome. In the worst case, doxycycline could re-interfere during translation of the degradation peptide, a phenomenon that could lead to a reset and repetition of trans-translation. Therefore, the success of trans-translation depends on the concentration of doxycycline and the competing binding kinetics of aminoacyl-tRNAs and doxycycline.

Azithromycin acts differently than doxycycline: it inhibits translation by binding to 23S rRNA close to the peptidyl-transferase centre of the large subunit (Parnham et al. 2014). In the case of azithromycin-induced stalling of the translation complex, trans-translation is blocked in the peptidyl-transferase centre and cannot proceed. Hence, the stalled ribosome remains stalled. Presumably, only a low azithromycin concentration could induce chlamydial persistence, which allows some basal translation. At 12 hpi, treatment of *C. trachomatis* serovar F with ≥ 0.08 µg/ml azithromycin had almost completely inhibited inclusion formation (Xue et al. 2017). These authors showed chlamydial recovery upon treatment with 0.08-2.56 µg/ml azithromycin at 18 hpi. In the current work, at 16 hpi *C. trachomatis* serovar D treated with ≥ 0.06 µg/ml azithromycin could not reactivate translation during the recovery phase. These observations support the hypothesis that persistence depends on the treatment timing, the inhibitory or antibiotic concentration and the serovar.

IFN-γ-induced persistence might underscore that persistence depends on the treatment timing and inducer concentration. Treatment with IFN-γ activates host cell expression of indoleamine 2,3-dioxygenase that degrades L-tryptophan to *N*′-formylkynurenine. *C. trachomatis* serovar D is unable to process this metabolite (Pokorzynski et al. 2019). The resulting tryptophan

depletion leads to reduced expression in *C. trachomatis*, allowing a basal translation (N. D. Hatch & Ouellette 2020). Therefore, L-tryptophan depletion and low azithromycin concentrations enable basal translation, similarly to doxycycline that competes with trans-translation. All three cases lead to chlamydial persistence, supporting the hypothesis.

The actual participation of trans-translation in doxycycline-inhibited translation remains unknown. The transcriptional analysis provided an insight into the *smpB* mRNA level but was restricted to the actual level of tmRNA because the results cannot distinguish between pre-tmRNA and processed mature tmRNA. The RNA secondary structure represents a challenge to designing primers that anneal to either pre-tmRNA or mature tmRNA. However, the ability to perform translation despite translational inhibition highlights a mechanism that counteracts the inhibitory effect of doxycycline. Trans-translation facilitates survival under antibiotic pressure in other bacteria (Li et al. 2013). It might be interesting to compare binding affinities to gauge the competitive capacity of antibiotics versus the tmRNA-SmpB complex. This competitive mechanism might drive ribosomal recycling or enable continued translation at higher doxycycline concentrations. The limitation of genetic investigation and modification of *C. trachomatis* serovar D impedes sufficient investigation of this mechanism. In trans-translation, proteins that are not completely translated are tagged with a degradation signal with subsequent dissociation of the translation complex. Altering the degradation signal into a non-degrading peptide might facilitate future quantification and investigation of the mechanism. Roche & Sauer (1999) performed this kind of modification. Investigations of *Legionella pneumophila* revealed that trans-translation is essential (Brunel & Charpentier 2016). The outcome of these future investigations would clarify the mechanism by which translation continues in *Chlamydia* despite apparent translational inhibition.

Overall, the results demonstrated that *C. trachomatis* serovar D successfully enters persistence when treated with doxycycline. Electron micrographs showed AB formation in a few numbers. Furthermore, the experiments showed that *C. trachomatis* serovar D performs translation during doxycycline treatment. Transcriptional analysis revealed that doxycycline-treated *C. trachomatis* serovar D is still transcriptional active. The transcript levels of the components for the trans-translation are stabilised, suggesting the mechanism as a strategy to counteract the doxycycline-inhibition. Comparison with azithromycin revealed that the herein used treatment regimen for azithromycin was lethal. These results showed that persistence depends on treatment timing and inducer concentration that must allow a basal translation for successful persistence.

4.2.2 Persistent *C. trachomatis* interacts with the host cell

The doxycycline treatment reduces *de novo* protein expression, thereby limiting the potential to respond to the stimulus. In this form, expressed Inc proteins that target or recruit distinct human proteins were assumed to be essential for survival during persistence. Aeberhard et al. (2015) determined inclusion-associated host proteins using proteomics and analysed them via immunofluorescence upon ectopic expression in *C. trachomatis* serovar L2–infected cells. These host proteins served as a starting point for investigating the persistence of *C. trachomatis* serovar D. Twenty different human proteins were expressed transiently during chlamydial infection with or without doxycycline treatment (Fig. 21). Fifteen human proteins were differentially recruited by *C. trachomatis* serovar D upon treatment. Notably, the human proteins Rab35, Tfr, Rac1, Stim1, Fli, Fis1, Syntaxin-7 and Rab8a were recruited less intensely by persistent *C. trachomatis* serovar D. The recruitment intensity of these proteins presumably depends on the concentration of the corresponding Inc protein. During doxycycline treatment, the reduction of *de novo* Inc proteins could decrease the recruitment of host proteins.

GO term analysis of these proteins (https://string-db.org) revealed the terms ‘Clathrin-coated vesicle’ (GO:0030136, strength 1.58, FDR 0.0127 of Rab8a, Tfr and Rab35) and ‘Recycling endosome’ (GO:0055037, strength 1.85, FDR 1.04×10^{-5} of Rac1, Rab8a, Tfr, Rab35 and Syntaxin-7). The human protein Fli acts as a transcription factor in response to hormonal signal transduction and is involved in cytoskeletal rearrangements via inhibition of Rac1-dependent paxillin phosphorylation (Lee et al. 2004). Interestingly, Fis1 recruits the mitochondrial fission mediator dynamin-related protein 1 (DMN1L) to the mitochondrial surface (Yoon et al. 2003) but plays a minor role in mitochondrial fission (Koirala et al. 2013). The latter observation might explain why only a fraction of mitochondria was recruited to the inclusion membrane. These proteins demonstrate a reduction in endosomal and vesicular management, cytoskeletal rearrangement, the involvement of mitochondria and interference of ER-Ca^{2+} homeostasis via the Ca^{2+} sensor Stim1 (Liou et al. 2005).

The recruited human proteins that showed a punctate signal – Yth, Syntaxin-4 and Arginase – were slightly enhanced upon doxycycline treatment. These results indicate that Inc proteins are responsible for recruiting them and highlight a distinct role for Inc proteins in persistence. Recruitment of Yth, a regulator of alternative splicing (C. Xu et al. 2014) and nuclear export of m6A-containing mRNA (Roundtree et al. 2017), might disturb host cell protein expression. The recruitment of the plasma membrane t-SNARE protein Syntaxin-4 might inhibit the docking of transport vesicles to the plasma membrane (Pooley et al. 2008), and Arginase seems to supply L-arginine (Gokmenoglu et al. 2018) for chlamydial translation or metabolism. The human proteins DHCR7 (cholesterol biosynthesis [Luu et al. 2015]), Stm2 (a Ca^{2+} sensor for the ER [Brandman et al. 2007] and inhibitor of STIM1-mediated Ca^{2+} influx [Soboloff et al. 2006]),

Ubxd1 (mediating lysosomal transport for degradation [Ritz et al. 2011] and ER-associated degradation [ERAD] of misfolded proteins [Nagahama et al. 2009]) and ilk (a kinase involved in integrin-mediated cell migration [Dedhar 2000, Hannigan et al. 1996]) were recruited in acute infection but showed cytosolic localisation upon doxycycline treatment. Hence, there seems to be distinct protein recruitment during persistence: *Chlamydia* seem to recruit distinct human proteins that might support survival during antibiotic treatment. However, the function of these proteins in *C. trachomatis* serovar D persistence is until now not clarified. Endosomal and vesicular trafficking to the inclusion seem to be reduced in persistent *C. trachomatis* serovar D as well as cytoskeletal rearrangement, whereas integrin-mediated cell migration and degradation of host cell proteins are not influenced. Most importantly, persistent *C. trachomatis* serovar D putatively requires amino acids like L-arginine for metabolism and interferes in host cell expression.

In summary, these results show that *C. trachomatis* serovar D still relies on host cell nutrients during persistence and manages to scavenge via manipulation and misdirecting host trafficking. The expression of single human proteins is sufficient to investigate host interaction with *Chlamydia* when the interactions of particular proteins are of interest. However, this method is limited to the choice of human proteins and thus impractical for global large-scale analysis. Therefore, a proteomic approach was applied to identify persistence-related proteins.

4.2.3 Optimisation and preparation for proteomics

In 2015, our group (Aeberhard et al.) established a method to isolate and purify intact inclusions for proteomic analysis. The limitation of the published gradient separation relies on the particle size, density and surface. Thus, in this work, a protocol to isolate small inclusions at 24 hpi, persistent inclusions treated with doxycycline for 8 h and large inclusions of acute infection (32 hpi) was implemented successfully (Fig. 22). The subsequent purification step of Aeberhard et al. (2015) relies on MACS targeting IncA. The expression of chlamydial proteins is reduced in persistence due to the translation inhibitor doxycycline (Fig. 19). Previous experiments to isolate persistent inclusions with IncA and MACS was inefficient and insufficient for further analysis by MS. In this work, the isolation of inclusions without an additional enrichment step was successful and exceeded the requirements for proteomics. According to the original method of Aeberhard et al. (2015), determining the difference in abundant proteins in persistent or acute infection was planned to proceed via stable isotope labelling by amino acids in cell culture (SILAC). While performing these SILAC experiments, there was increased expression upon replacing the medium, suggesting a nutrient boost for host cells and *Chlamydia* despite translational inhibition. This artificial effect was observable in proteomics independently of the doxycycline treatment; hence, this procedure was not used for subsequent experiments. Therefore, label-free proteomics, without the requirement of using a

different medium, was performed to quantify the total chlamydial proteome and the inclusion–host cell interface covered with interacting host proteins. The label-free proteomics required the untreated control 24 hpi for relative quantification and exclusion of background proteins. The endeavour successfully identified 3398 host proteins and 734 chlamydial proteins of isolated inclusions (section 3.3.5.2).

4.2.4 Accumulation of Rab12 in persistence might support iron acquisition

The proteomic analysis revealed 18 altered host proteins in doxycycline-treated samples (Fig. 24). The most enriched protein in the doxycycline-treated sample was Rab12 (Fig. 25) associated with the GO term 'Autophagy' (GO:006914). Immunofluorescence investigation of Rab12 during acute and persistent infection with *C. trachomatis* serovar D showed strong recruitment of the Rab12 wildtype to the inclusion membrane and slightly recruitment of the constitutive GTP-bound dominant-active mutant (Q101L), whereas the latter also appeared more cytosolic (Fig. 26). The constitutively GDP-bound dominant-negative mutant (T56N) surrounded the acute inclusion diffusely but accumulated strongly at distinct areas of the persistent inclusion. The role of Rab12 on progeny formation in acute infection, persistence and recovery was investigated by siRNA-mediated KD (Fig. 27). The Rab12 KD led to enhanced recovery compared to the negative control (AllStars KD). The progeny formation of acute *C. trachomatis* serovar D was slightly reduced in the Rab12 KD. Doxycycline-treated *C. trachomatis* serovar D revealed a minor but similar level of progeny formation in Rab12 KD.

Rab12 is involved in autophagy (Matsui & Fukuda 2013, Omar et al. 2021, J. Xu et al. 2015) and regulates trafficking from the recycling endosomes to lysosomes (Matsui & Fukuda 2014). This regulation affects the degradation of the transferrin receptor Tfr (Matsui & Fukuda 2014). Iron-bound transferrin interacts with the Tfr, which induces endocytic uptake into endosomes. Rab11-positive vesicles containing the Tfr complex are transported to the lysosome, where the proteins are degraded, and iron is provided for the host cell. *Chlamydia* requires iron for development and enters persistence upon iron depletion (Thompson & Carabeo 2011). It was shown that *C. trachomatis* hijacks iron-loaded Rab11-positive vesicles from the slow recycling pathway (Ouellette & Carabeo 2010), suggesting a correlation with the iron dependence of *Chlamydia*. Rab11 and Rab4, involved in Tfr recycling, are recruited to the inclusion membrane (Rzomp et al. 2003). Investigations of Rab4 in *C. trachomatis* infection using dominant-active and negative Rab4 mutants showed no effect on chlamydial development (Rzomp et al. 2006). The stable KD of Rab11 led to a reduction of the progeny formation of *C. trachomatis* (Rejman Lipinski et al. 2009). Due to the involvement of Rab4 and Rab11 in the slow recycling pathway, Ouellette & Carabeo (2010) co-expressed dominant-negative Rab4 and dominant-negative

Rab11, showing reduced growth of *C. trachomatis* inclusions. Detailed investigations of Rab4 in *C. trachomatis* infection using dominant-negative and active Rab4 revealed different phenotypes (Rzomp et al. 2006). The dominant-active Rab4 (Q67L) was recruited to inclusion and occurred cytosolic, similar to the wildtype. The dominant-negative Rab4 (S22N) was not recruited to the inclusion and remained cytosolic. In contrast, transiently overexpressed dominant-negative Rab11 was recruited to the inclusion of *C. trachomatis* and occurred cytosolic (Leiva et al. 2013). Brumell & Scidmore (2007) proposed that some Rabs are anchored to the membrane and recruited selectively to the inclusion for different functions. These authors mentioned that decoration of the inclusion with human Rabs supports the escape of endo-lysosomal degradation. Rabs consists of a C-terminal amino acid pattern of CAAX with two cysteine residues that are covalently post-translationally modified with geranylgeranyl-moieties, allowing them to be anchored to the membrane (Hutagalung & Novick 2011).

The diffuse phenotype of GDP-bound Rab12 at the acute inclusion might be explained by dynamic equilibrium between membrane-anchored and cytosolic forms. Hutagalung & Novick (2011) described anchoring of cytosolic GDP-bound Rab in a complex with GDI to the membrane via GDF, thus releasing GDI. The membranous GDP-bound Rab is then reversely detached from the membrane by GDI diffusing into the cytosol. This mechanism would lead to a dense but diffuse ring of GDP-bound Rab12 around the inclusion. The punctate accumulation of GDP-bound Rab12 at the persistent inclusion membrane indicates the disequilibrium of GDI and GDFs. The GEF Dennd3 binds GDP-bound Rab12 to enhance GTP exchange (Matsui et al. 2014). The constitutively GDP-bound Rab12 mutant might permanently bind to Dennd3, whose protein complex would consequently be transported along actin filaments or bound to the filaments itself. One could assume that the Rab12(T56N)-positive intense accumulation at persistent inclusions also consists of actin filaments, a phenomenon that would explain the distinct directed localisation. Furthermore, the less clear recruitment of the active GTP-bound Rab12 indicates an indirect interaction with the inclusion. However, the recruited dominant-negative Rab12 displays the same phenotype as the dominant-negative Rab4 and the dominant-active Rab12 equals the cytosolic distribution of the dominant-active Rab4. In contrast, the dominant-negative Rab11 is recruited to the inclusion membrane. These contrasting observations demonstrate that the mutations used in the studies are no clear evidence of preferred recruitment but rather display that the recruitment of Rab12 might be a more complex mechanism.

The correlation between Rab4, Rab11 and Rab12 according to Tfr regulation highlights a putative role in iron acquisition for chlamydial development. As a regulator of trafficking from the recycling endosomes to lysosomes, Rab12 is predicted to affect Tfr degradation. Rab12

recruitment in persistence might enable chlamydial control of this process, leading to continuous hijacking of Rab11-positive vesicles. Iron might be essential in doxycycline-induced persistence, but its actual role remains unclear because iron depletion also induces persistence.

The siRNA-mediated KD of Rab12 led to a reduced progeny formation in acute infection of *C. trachomatis* serovar D. Since Rab12 regulates the degradation of Tfr, the Rab12 KD could negatively affect chlamydial iron acquisition, which is essential for chlamydial development. This might explain the reduced progeny formation of acute infection in Rab12 KD cells. The progeny formation during doxycycline treatment is slightly reduced in Rab12 KD. The progeny formation of persistent *C. trachomatis* serovar D does not increase during the treatment with doxycycline in Rab12 KD and AllStars KD, demonstrating that doxycycline stalls further EB formation in general. So, the initial minor level of progeny formation at the start of treatment is already affected by the Rab12 KD. Therefore, Rab12 plays an important role in chlamydial development and EB formation, indicating that Rab12 is involved in iron acquisition, which is essential for chlamydial development.

However, the recovery of *C. trachomatis* serovar D in Rab12 KD cells was enhanced after 24 h and increased further from 24-48 h. These results underscore the role of Rab12 in autophagy. Rab12 regulates autophagy which is assumed to drive degradation of the inclusion. The Rab12 KD impedes autophagy and thereby ensures greater survival of *C. trachomatis* serovar D during the persistence and recovery, demonstrated by the enhanced progeny formation in the recovery. Doxycycline reduces chlamydial translation, which diminishes the chlamydial counteracting of host cellular degradation of the inclusion and chlamydial proteins. The recruitment of Rab12 during the doxycycline-induced persistence might interfere with Rab12-mediated autophagy. This disruption might reduce autophagy events and supports the survival of the persistent *C. trachomatis* serovar D.

These results show that Rab12 plays a role in the chlamydial development and EB formation of acute *C. trachomatis* serovar D. Its correlation with the regulation of Tfr degradation indicates involvement in chlamydial iron uptake. The increased recruitment of Rab12 during the persistence supports chlamydial survival. This recruitment is hypothesised to impede and reduce Rab12-regulated autophagy to ensure chlamydial survival. However, the mechanism of recruitment and interactions with Rab12 require further investigations. The substitution of the C-terminal cysteines produces a Rab12 mutant incapable of being post-translationally modified with geranylgeranyl residues (necessary for membrane anchoring). This mutant might help to understand whether membrane anchoring is necessary for recruitment. Another method to identify direct and indirect interaction partners is the BioID. During the infection,

chlamydial proteins that are close to Rab12 could be labelled with a biotin moiety via the promiscuous Biotin ligase BirA* (Cronan 2005, Roux et al. 2012). These and other in-depth analyses might clarify the mechanisms and role of Rab12 in persistent and acute *C. trachomatis* serovar D.

4.2.5 CERT is essential for chlamydial development and persistence in *C. trachomatis* serovar D infection

The proteome of doxycycline-treated *C. trachomatis* serovar D showed an increase in IncD and the putative Inc protein CT_058 (Fig. 30). Since IncD recruits the ceramide transport protein CERT to the inclusion in *C. trachomatis* (Kumagai et al. 2018), the role of CERT in doxycycline-induced persistence of *C. trachomatis* serovar D was investigated in more detail. The transiently expressed CERT-eGFP was shown to be recruited to the inclusion of *C. trachomatis* serovar D during doxycycline treatment. Since CERT was recruited to the inclusion of persistent *C. trachomatis* serovar D, its effect on progeny formation of acute infection, persistence and recovery was analysed in CERT-KO cells compared to CRISPR CTRL-KO cells. The CERT-KO led to a reduced and plateauing progeny formation in acute infection, whereas the progeny formation was slightly increased during the persistence, compared to CTRL-KO cells. 24 h after doxycycline removal, the progeny increased strongly in CERT-KO cells with a subsequent decrease after 48 h. In contrast, the progeny formation in CRTL-KO slightly increased after 24 h and further after 48 h, demonstrating a different chlamydial development during the recovery in CERT-KO cells.

The early expressed IncD homodimerises via disulphide bonds across the TM domain, forming higher homooligomers via its cytosolic domains (Kumagai et al. 2018) and potentially increasing the concentration of recruited CERT. Both cytosolic domains are necessary for interacting with the PH domain of the ceramide transport protein CERT (Fig. 38), even though the single domains consist of binding patterns for PH domains (Kumagai et al. 2018). CERT consists of a PH domain (Lemmon 2008), relevant for binding phosphatidylinositol-4-phosphate (PI4P) at the *trans*-Golgi network (Balla & Balla 2006, Hanada et al. 2009), the amino acid motif FFAT (Loewen et al. 2003) for binding VAP-A and VAP-B in the ER (Lev et al. 2008) and the C-terminal START domain for binding and extracting ceramide from the ER (Ponting & Aravind 1999). IncD binds the PH domain of CERT and thereby forms a complex with ER-localised VAP-A/B. This complex is also referred to as ER-inclusion membrane contact sites (MCS), which also include the Ca^{2+} sensor Stim1 (Agaisse & Derré 2015). Comparative analysis revealed that the Inc protein IncV interacts directly and strongly with VAP-A, thus forming a more efficient and stable MCS than CERT (Stanhope et al. 2017). However, transfer of ceramides from the ER to the *trans*-Golgi network is necessary to convert

ceramides into sphingomyelins by the *trans*-Golgi protein SMS2 (Hanada et al. 2009). SMS2 is recruited and integrated into the inclusion membrane (C. A. Elwell et al. 2011), where it converts the hijacked ceramides into sphingomyelin. Ceramides that cannot be processed accumulate around the inclusion, whereas ceramides that can be converted into sphingomyelins intercalate into RBs (Banhart et al. 2014, Hackstadt et al. 1995). Alternatively, sphingolipids from multivesicular bodies (MVB) (Gambarte Tudela et al. 2019), *trans*-Golgi network (Capmany et al. 2019) and Golgi ministacks (Banhart et al. 2019) can be vesicularly transported via Rabs to the inclusion membrane. SMS2 synthesises sphingomyelin in Golgi minstacks and the *trans*-Golgi network. MVB contain sphingomyelin from the plasma membrane. Interestingly, SMS2 is also located in the plasma membrane, where it produce sphingomyelin (Turpin-Nolan & Brüning 2020). Interference of chlamydial sphingolipid acquisition reduces chlamydial replication and growth (Heuer et al. 2009, D. K. Robertson et al. 2009, van Ooij et al. 2000). Derré et al. (2011) showed that depletion of CERT or VAP-A/B reduces infectivity of *C. trachomatis*. HPA-12 is an inhibitor of the START domain and hinders the transport of ceramide. The treatment with HPA-12 reduces the progeny formation of *C. trachomatis* serovar L2 to a similar level of infection in CERT-KO cells (Koch-Edelmann et al. 2017). Investigations with depleted CERT showed only a 50% reduction in sphingomyelin, demonstrating another yet unknown CERT-independent pathway directing ceramides to the Golgi apparatus (Derré et al. 2011). Experiments with inhibitors that block previous steps of ceramide synthesis revealed early differentiation from RBs into EBs with a strongly reduced IFU arguing premature egress (D. K. Robertson et al. 2009).

These observations are in line with the results of this work. The lack of CERT is supposed to impair the chlamydial ceramide and sphingomyelin homeostasis leading to an early EB formation. As a result, the progeny formation in acute infected CERT-KO cells reached already a plateau at 48 hpi. The early EB formation is supposed to shift the RB/EB ratio in the direction of EBs displayed by the results during the doxycycline treatment. In CERT-KO cells, the progeny formation during the doxycycline treatment is higher than in CTRL-KO cells. This can be explained by the early increased EB formation. At the start of treatment, the EBs that are already formed determine the inclusion forming units during the doxycycline treatment. The number decreases only slightly during the 72 h of doxycycline treatment, demonstrating their stability inside the inclusion. In CERT-KO cells, the initial amount of RBs at the start of treatment is predicted to be reduced compared to the CRTL-KO cells. Doxycycline induces the conversion from RBs to ABs. Due to the reduced amount of RBs, the amount of ABs in the CERT-KO cells during the doxycycline treatment is also predicted to be reduced. In the recovery phase, RBs bud from the ABs and re-differentiate further into EBs. In turn, this means

that fewer ABs should yield fewer EBs. In contrast, the progeny formation strongly increases in the CERT-KO after 24 h recovery. What does this mean?

The recovery from the doxycycline treatment starts with RB progeny deriving from ABs. These RBs must re-differentiate further into EBs. As demonstrated by the results from the CRTL-KO cells, this process requires some time. In the first 24 h, the progeny formation increases slightly and increases further after 48 h recovery. So, the recovery phase could be interpreted as a kind of re-started infection cycle. The strong increase of progeny formation in CERT-KO cells after 24 h with a subsequent decrease indicates a different mechanism of chlamydial development. Unlike the time-consuming recovery phase in the CRTL-KO cells, EBs are formed in the CERT-KO cells immediately after removing doxycycline. This leads to the assumption that at the start of doxycycline treatment, a significant number of IBs must be already available that are as stable as EBs during the doxycycline treatment. In the recovery phase, these IBs can continue re-differentiation into EBs, demonstrated by the peak of progeny formation after 24 h. The subsequent decrease of progeny formation after 48 h in CERT-KO cells might be explained by early egress, thus cell lysis. During 24-48 h of the recovery phase, the released EBs are predicted to infect neighbouring cells. In this new round of infection, the EBs differentiate into RBs inside the newly infected cell and continue chlamydial development. These formerly EBs that are now RBs can not be detected anymore in the progeny formation assay that relies on infectious EBs. This reduction of EBs results in a decrease of IFU, as shown for 48 h recovery in CERT-KO cells.

At the bottom line, these results show that CERT is essential for the development of *C. trachomatis* serovar D since the CERT-KO leads to early EB formation. The impaired chlamydial ceramide and sphingomyelin homeostasis by CERT-KO is suggested to alter the integrity of the inclusion membrane and the cell wall of RBs. The imbalanced sphingolipid uptake might affect the growth of RBs and ABs, which in turn limits the number of persistent bacteria and consequently the progeny formation. CERT is recruited to the inclusion membrane during doxycycline treatment, underlining the hypothesis that *C. trachomatis* serovar D requires sphingolipids for RB and AB growth.

It is worth mentioning that, unlike EBs, RBs and ABs lack a disulphide cross-linked, stabilised membrane. Based on the results and previous publications, the acquisition of sphingolipids is hypothesised to be an important key factor to stabilise the membrane of RBs and ABs. Interference of the chlamydial sphingolipid homeostasis increases the fragility of RBs/ABs, which impedes chlamydial development and leads to early egress by early EB formation.

The abundant IncD in the proteome of persistent *C. trachomatis* serovar D led to analysis of CERT, which revealed that CERT is essential for chlamydial development and persistence in

C. trachomatis serovar D infection. Finally, the CERT-correlated acquisition of sphingolipids led to the hypothesis that sphingolipids are a membrane-stabilising component for RBs and ABs. Future investigations are required to address this hypothesis.

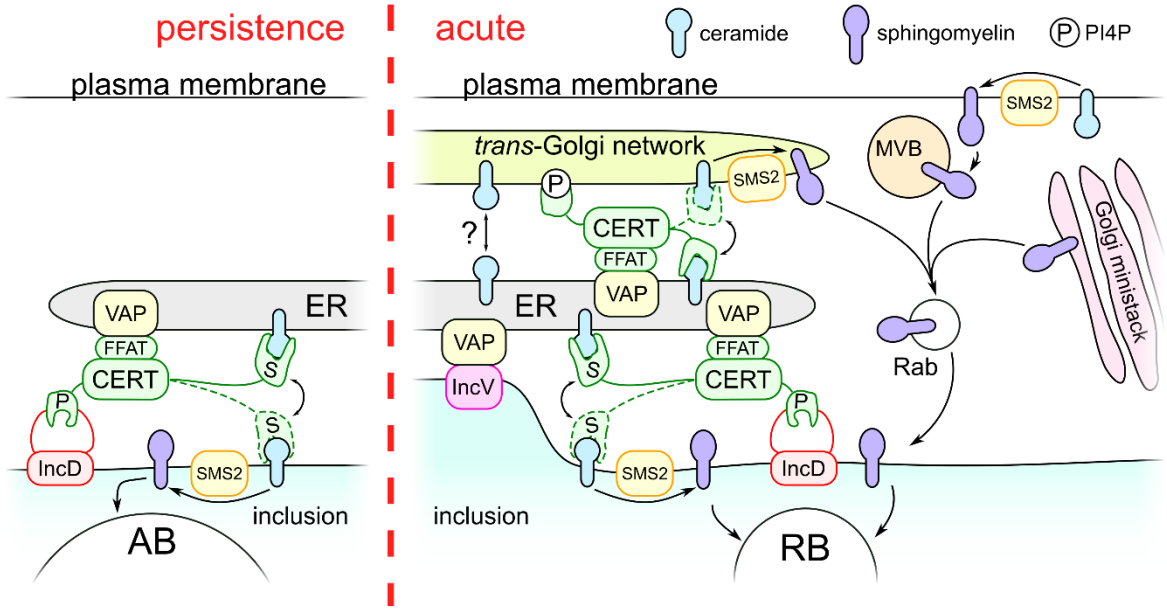

Fig. 38 Acquisition model of sphingolipids in *C. trachomatis*

The acquisition of sphingolipids in persistent *C. trachomatis* serovar D (left) depends on CERT (green). The PH domain of CERT (P) is bound by N- and C-terminus of IncD, whereas the FFAT motif of CERT binds to VAP in the ER. The START domain (S) transports ceramide (light blue) to the inclusion membrane. The recruited SMS2 converts ceramide to sphingomyelin (SM), which is further transferred to ABs. SM increases the stability of the inclusion membrane and ABs. Acute *C. trachomatis* serovar D (right) uses multiple opportunities to acquire sphingolipids. The first way is equal to the persistent acquisition, whereas the MCS formation via IncV and VAP enhances the transfer. The host cellular transfer of ceramide from ER to *trans*-Golgi network is CERT-independent (?) and CERT-dependent. The PH domain of CERT binds to phosphatidylinositol-4-phosphate (PI4P) in the *trans*-Golgi network, thereby transferring ceramide. SMS2 in the *trans*-Golgi network converts ceramide into sphingomyelin. Ceramide that was acquired at the plasma membrane is locally converted into sphingomyelin via SMS2 and transported to MVB. SM is Rab-mediated transported from *trans*-Golgi network, MVB and Golgi ministacks to the inclusion membrane that further integrates into RBs and increases stability.

4.2.6 *C. trachomatis* serovar D interferes with host cellular retrograde trafficking to enhance recovery from persistence

C. trachomatis serovar D enters persistence when treated with doxycycline. The translation inhibitor limits the bacterial protein expression capacity, demonstrated by the proteome of doxycycline-treated *C. trachomatis* serovar D. Eighteen proteins were altered in persistence, whereas 665 proteins remained stoichiometrically similar compared with untreated *C. trachomatis* serovar D at 24 hpi (Fig. 30). Based on these data, the repertoire of proteins at

24 hpi is hypothesised to be sufficient for *C. trachomatis* serovar D to persist under antibiotic pressure. One Inc protein, the early expressed IncE (Scidmore-Carlson et al. 1999), displayed intense abundance on western blot when detecting persistent inclusions in fractions of gradient separation (Fig. 22). In contrast, IncE was unaltered by persistence according to the proteomic analysis (Fig. 30). Quantification of IFU in CRISPR-Cas9-generated SNX5/6 double KO cells showed a slight increase of progeny formation in the acute infection with *C. trachomatis* serovar D (Fig. 34). SNX5/6 KO does not seem to affect persistent *C. trachomatis* serovar D because the progeny formation did not vary upon SNX5/6 silencing. However, most remarkably, *C. trachomatis* serovar D showed enhanced progeny formation after 48 h recovery in SNX5/6 KO cells. This increase was also shown in the acute infection depending on SNX5/6 KO.

IncE has been well characterised, with a role in interaction with the cellular retromer components SNX5 and SNX6 (C. A. Elwell et al. 2017, Mirrashidi et al. 2015, Paul et al. 2017, Sun et al. 2017). IncE complements and augments β-strands of SNX5/6 in a hydrophobic groove by two looped β-strands in its C-terminus (Paul et al. 2017, Sun et al. 2017). Further investigations revealed that IncE interferes with the regular interaction between SNX5 and the cation-independent mannose-6-phosphate receptor (CI-MPR), suggesting a suppressive effect on retrograde trafficking mediated by *C. trachomatis* (C. A. Elwell et al. 2017). siRNA-mediated depletion of SNX5/6 increases the progeny formation of *C. trachomatis* serovar L2 and D in acute infections (Aeberhard et al. 2015, Mirrashidi et al. 2015). Mirrashidi et al. (2015) quantified the IFU of *C. trachomatis* serovar D at 24 hpi in cells with simultaneous siRNA-mediated KD of SNX5 and SNX6, resulting in an approximately 10-fold increase compared with the control. Aeberhard et al. (2015) quantified the IFU of *C. trachomatis* serovar L2 in either SNX5- or SNX6-depleted cells at 48 hpi and reported a 5-fold and 1.8-fold increase, respectively, compared with control. Although the results agree with these published findings, they are difficult to compare due to the methodically different SNX5/6 depletion (stable KO versus transient KD). Furthermore, Aeberhard et al. (2015) depleted only individual SNX proteins that might function redundantly, because SNX-BAR dimers occur in pairs, namely SNX1/5, SNX1/6, SNX2/5 and SNX2/6 (Trousdale & Kim 2015).

The recovery of *C. trachomatis* serovar D from persistence can be regarded as a kind of rebooted differentiation from AB to RB further to EB. Therefore, the KO must support RB replication, leading to enhanced EB formation (Fig. 39). These results demonstrate the importance of recruiting SNX5/6 to the inclusion for the chlamydial development. IncE is expressed early in the chlamydial development and recruits SNX5/6 to the inclusion (C. A. Elwell et al. 2017, Mirrashidi et al. 2015, Paul et al. 2017, Sun et al. 2017). RBs replicate during the early and early-mid phases. The requirement of IncE to recruit SNX5/6 in the early and

early-mid phases supports the hypothesis that chlamydial interference with the host cellular retrograde trafficking enhances RB replication and subsequently leads to increased EB formation (Fig. 39). Investigations of IncE expression and SNX5/6 recruitment during recovery from doxycycline-induced persistence might address the role of IncE and SNX5/6 in RB replication.

Taken together, these results show that the interference with the SNX5/6-mediated retrograde trafficking of host cells enhances RB replication in recovery from doxycycline-induced persistence and in acute infection. In contrast, KO of both proteins does not affect the infectivity of persistent *C. trachomatis* serovar D. Future studies that disrupt the interaction between IncE and SNX5/6, and thereby stabilise the host retrograde trafficking, may provide additional insights into the need for SNX5/6-recruitment to the inclusion during recovery from persistence.

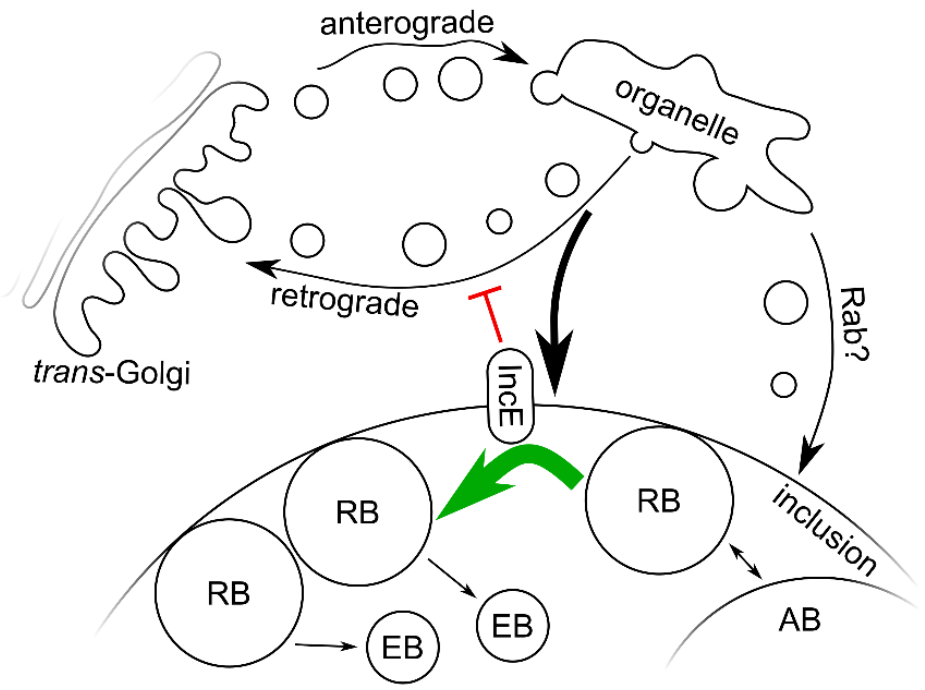

Fig. 39 Interference in retrograde trafficking supports RB replication

During the recovery from persistence, ABs re-differentiate into RBs. The replication of re-differentiated and acute RBs is enhanced (bold green arrow) through the interference of retrograde trafficking by IncE (red stamp), while the host cellular anterograde trafficking unaffectedly proceeds. The enhanced RB replication leads to increased progeny formation. The recruitment of SNX5/6 by IncE might re-direct vesicles to the inclusion membrane (bold arrow), thereby supporting the growth of the inclusion membrane and providing bacteria with nutrients that could be alternatively carried out by chlamydial control over Rab-mediated vesicular trafficking.

4.2.7 Basal metabolism prepares persistent *C. trachomatis* D for recovery

Comparing the inclusion proteomes of acute and doxycycline-treated *C. trachomatis* serovar D revealed several upregulated chlamydial proteins that are not associated with the inclusion membrane (Fig. 30, Fig. 31). These proteins are predicted to function in stabilising the bacterial metabolism and cell cycle to persist under antibiotic pressure. *In silico* analysis (Table 4) revealed altered proteins in the categories transporter (CT_151, CT_152, CT_486, CT_467, CT_468), TCA cycle (CT_054, CT_055, CT_821, CT_822, CT_855), glucose and starch metabolism (CT_248, CT_489, CT_798), peptidoglycan (CT_268, CT_709) and translation (CT_106). In acute infection, proteins that correlated with metabolism and transport were upregulated, while proteins of peptidoglycan and translation remained unchanged. Similarly, transport proteins and proteins of the TCA cycle are minor upregulated during persistence, while translation is downregulated and glucose starch metabolism remains unchanged. Proteins of the peptidoglycan are up- (CT_709) and downregulated (CT_268) during the doxycycline treatment. *C. trachomatis* expresses a Na^+-translocating NADH-quinone reductase (CT_278, CT_279, CT_280, CT_281, CT_634, CT_740, https://chlambase.org/) that enables the generation of a Na^+ gradient (Fig. 40) and activates the respiratory chain by reduction of quinone to quinol (Liang et al. 2018). The activated respiratory chain leads to the reduction of cysteines forming disulphide-bonds, which cross-links membrane proteins (Christensen et al. 2019). The cross-linked and compacted membrane is a property of EBs. The Na^+ gradient enhances the import of metabolites such as dicarboxylate or amino acids by Na^+ symporter (Liang et al. 2018). Although the Na^+ gradient, cross-linked membrane of EBs and enhanced import of amino acids seem to correlate, translation and transcription are downregulated in EBs (S. Grieshaber et al. 2018). Nevertheless, inhibition of tRNA synthetase was shown to lead to persistence in *C. trachomatis* serovar L2 (N. D. Hatch & Ouellette 2020). Recently, investigations of chlamydial cell division highlighted a cascade of dividing bacteria into smaller bacteria with proposed concentration-dependent (Chiarelli et al. 2020) and size-dependent signals that initiate differentiation into EBs with a decreased peptidoglycan signal (G. W. Liechti 2021). MreB (CT_709), an ortholog of FtsZ from *E. coli*, is involved in coordinating cell division (G. W. Liechti 2021).

The proteome of acute *C. trachomatis* serovar D infection at 32 hpi compared with 24 hpi reflects the differentiation from RB to EB. The abundance of proteins involved in the TCA cycle is greatly increased during acute infection. This enhanced TCA cycle might process the metabolites more frequently, yielding more abundant substrates available for fatty acid biosynthesis and glucose starch metabolism. The enhanced TCA cycle also increases the Na^+ gradient, which drives further metabolite-import and cross-links the cell wall by the activated

respiratory chain for EB formation. Furthermore, the unaltered repertoire of the translational machinery and peptidoglycan seems to be sufficient for infectious progeny formation. As infection progresses, smaller bacteria emerge that, in turn, synthesise a smaller peptidoglycan ring for cell division. This size-dependent decrease might explain why peptidoglycan-correlated proteins are unchanged. The results of the proteome in acute *C. trachomatis* serovar D at 32 hpi support this explanation.

Similar but less intense is the regulation of proteins correlated with metabolism in the persistence. Protein levels of some transporter proteins were increased to the same extent compared to 32 hpi. Only a few proteins of the TCA cycle were slightly increased in persistence and no difference in the abundance of enzymes of the glucose starch metabolism were detected. Succinyl-CoA ligase (CT_821, CT_822) in the TCA cycle is assumed to be a minimum requirement to generate a Na^+ gradient sufficient for importing metabolites. However, this gradient would be insufficient to increase respiratory chain activity and membrane cross-linkage. This unfavourable Na^+ gradient restricts growth and metabolism, but the sustained import of metabolites appears to be essential for survival during persistence.

Levels of the tRNA pseudouridine synthase A (CT_106), part of translation, was markedly downregulated in persistence. This alteration might indicate reduced fluctuation of tRNAs due to the translation inhibition by doxycycline. On the contrary, persistent *C. trachomatis* serovar D showed regulation of two proteins related to peptidoglycan synthesis. *N*-acetylmuramoyl-L-alanine amidase CT_268, a hydrolase that degrades peptidoglycan in the final step of cell division (EC 3.5.1.28), was downregulated, while MreB was upregulated. Electron micrographs of ABs showed only a few bacteria within an inclusion. The regulation of the proteins might be explained by cells ready for cell division (increased MreB) but that cannot proceed with final cell division (decreased CT_268), leading to a small number of enlarged ABs. Overall, many chlamydial proteins were not regulated during persistence. It cannot be excluded that the unaffected abundance of a protein indicates no fundamental requirement for the persistence. However, the consequence of a putative stable protein relies on its half-life and function. Chlamydial proteins within the bacteria might be more stable than a protein exposed to the host interface. Future proteomics of long-term persistent *C. trachomatis* serovar D might display stable proteins that are unregulated but required for maintenance and proteins with a longer half-life that independently of the persistence degrade after a while.

Overall, investigating the proteomes of acute and persistent *C. trachomatis* serovar D yielded different altered protein abundances. The subsequent analysis revealed the TCA cycle as a core element in acute and persistent *C. trachomatis* serovar D. In acute infection, the TCA cycle drives fatty acid biosynthesis, glucose starch metabolism, peptidoglycan synthesis and

cell wall cross-linkage via Na^+ gradient for EB formation. The Na^+ gradient is also the driving force for metabolite import via Na^+ symporter. A minor level of active TCA cycle is essential for persistent *C. trachomatis* serovar D. The TCA cycle maintains a Na^+ gradient that drives the import of metabolites necessary for translation and metabolism. Although the tRNA pseudouridine synthase A is downregulated, a basal level of translation is predicted to produce and accumulate MreB in preparation for cell division upon doxycycline removal.

These results support the explanation of EB formation in acute infection and explain the phenotype of ABs and the survival in persistent infection of *C. trachomatis* serovar D. However, the lack of metabolic information restricts proper investigation of these hypotheses. Future analytical metabolomics of persistent *C. trachomatis* serovar D might address the hypothetical model. Metabolomics combined with the proteomic results of this work might reveal even more information to understand the role and state of metabolism in persistence.

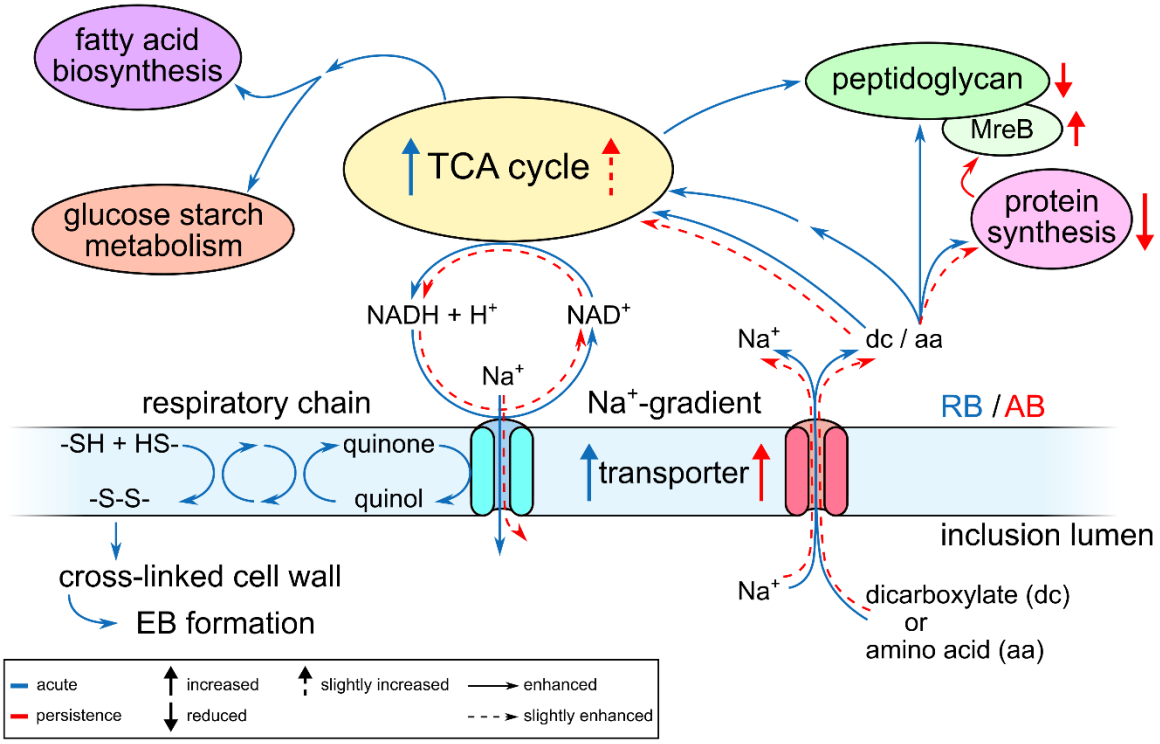

Fig. 40 Model of altered metabolism in acute and persistent *C. trachomatis* D

The increased abundance of transporters (red) enables the transport of metabolites and amino acids that are used for protein synthesis, peptidoglycan synthesis or the TCA cycle. The TCA cycle generates metabolites that are used for peptidoglycan and fatty acid biosynthesis, and that are involved in glucose and starch metabolism, thereby producing NADH + H^+. NADH is used to generate the Na^+ gradient (blue) required for Na+-dependent symporter (red). In the membrane, the fuelled respiratory chain reduces cysteine residues to disulphide-bonds that forms a cross-linked cell wall, a property of EBs. The regulation of pathways and transport (thin arrows), and proteins (vertical thick arrows) of acute (mock-treated versus 24 hpi comparison, blue) and persistent CTD (doxy-treated versus 24 hpi comparison, red) are confronted. The legend panel is located in the lower-left corner and shows elements of the regulation.

4.2.8 Chlamydial persistence as a consequence of stalled cell division

The aim of the work was to identify mechanisms of doxycycline-induced persistence of *C. trachomatis* serovar D. In the first steps, persistent *C. trachomatis* serovar D infections were characterised phenotypically and morphologically, followed by application of methods to determine bacterial transcription and translation characteristics. Finally, proteomics of gradient-separated inclusions revealed changes in the proteome of isolated inclusions during persistence. Together with published information, these results have enabled the formulation of a hypothesis of persistence (Fig. 41). Persistent ABs are enlarged RBs that reactivate and resume the developmental cycle when the persistence stimulus is removed (Brockett & Liechti 2021). Every reported persistence inducer leads to this phenotype. What is the reason for the enlarged growth of the chlamydial membrane? Is there a correlation with chlamydial lipid metabolism? Reduced or depleted sphingomyelin hinders entry into persistence by early conversion into EBs and subsequent host cell lysis (section 3.3.5.2.2.4, D. K. Robertson et al. 2009). Sphingomyelin, ceramide and lipids are necessary for chlamydial development in general. Fatty acid biosynthetic enzymes (Yao et al. 2014) remain unchanged in acute and persistent infection (Fig. 30). The subsequent infection leads to the generation of smaller progeny. Concentration-dependent (Chiarelli et al. 2020) and size-dependent signals (G. W. Liechti 2021) initiate the differentiation into EBs. These enzymes are not associated with persistence. Nevertheless, levels of TCA cycle enzymes and transporter proteins are slightly increased in persistence but markedly increased in acute infection, alongside glucose starch metabolic enzymes. They are supposed to maintain and stabilise the Na^+ gradient during persistence necessary for metabolic import, K^+ homeostats and putative Na^+-dependent ATPase generation. Investigation of ion distribution in inclusions has shown accumulation of Na^+ (Liang et al. 2018) and K^+ (Andrew et al. 2021) in RBs. Ionic homeostasis presumably plays a fundamental during persistence because ABs are derived from RBs.

Andrew et al. (2021) demonstrated induction of persistence upon incubation with the ionophores nigericin and valinomycin that are highly selective for K^+ over Na^+. They selectively chelated Ca^{2+} with ionomycin and found no effect on infectivity, demonstrating the relevance of K^+ homeostasis for chlamydial development. Liang et al. (2018) treated *C. trachomatis* serovar L2b at 1 and 12 hpi with monensin, an ionophore with a 10-fold higher affinity for Na^+ than K^+, and observed a reduction in inclusion size and infection rate in immunofluorescence at 36 hpi for both conditions. The interference with chlamydial ion homeostasis induces persistence. Therefore, ion homeostasis is essential for acute infection. S. Grieshaber et al. (2002) showed that the inclusion membrane is permeable to molecules < 520 Da, but distinct metabolites require active import via symporters (e.g. Na^+-dependent amino acid transporter

CT_231, sodium:dicarboxylate symport protein CT_401). A reduced Na^+ gradient might negatively affect or even hinder the import of metabolites and amino acids. Amino acid imbalance, such as an excess of a single amino acid (Gussmann et al. 2008), a lack of nutrients or amino acids (Harper et al. 2000) as well as IFN-γ-mediated iron depletion (Raulston 1997, Thompson & Carabeo 2011) and L-tryptophan starvation (Ouellette et al. 2016, Pokorzynski et al. 2019, Reveneau et al. 2005) lead to chlamydial persistence. N. D. Hatch & Ouellette (2020) induced persistence by mimicking amino acid starvation via inhibition of tRNA synthetase. As a result, the diminished levels of amino acids allow only minimal metabolism and reduced protein translation. The persistence inducer doxycycline also inhibits translation, thereby showing significant downregulation of tRNA pseudouridine synthase A. Other translation inhibitors that induce persistence are azithromycin (Reveneau et al. 2005, Xue et al. 2017) and chloramphenicol (Hobson et al. 1982). A commonality amongst these persistence inducers is that translation seems to be the limiting step leading to the AB phenotype. In contrast, the β-lactam antibiotic penicillin is also known to induce persistence (Skilton et al. 2009) but does not interfere with metabolism or translation. Bacteria require peptidoglycan for cellular stabilisation to compensate for the environmental osmotic pressure. Without peptidoglycan, the synthesis of which is inhibited by penicillin, gram-negative bacteria grow a fragile spheroplast that cannot withstand osmotic pressure, thereby bursting and dying. The actual bactericidal effect is lost in *Chlamydia* because they synthesise peptidoglycan only for cell division (G. Liechti et al. 2016). Therefore, they grow until cells divide but continue when penicillin inhibits cell division until they fill the entire inclusion lumen. S. Grieshaber et al. (2002) showed that the inclusion lumen mimics the cytosolic pH and ion concentrations (K^+, Na^+ and Ca^{2+}) because it is permeable to molecules < 520 Da. Due to this physiological equilibrium, chlamydial bacteria are not exposed to osmotic pressure that would require a peptidoglycan sacculus. However, penicillin and other persistence inducers commonly lead to only a few aberrantly enlarged bodies. This similarity might indicate that persistent *Chlamydia*, in general, are incapable of cell division. Chlamydial cell division is carried out by septal synthesis of peptidoglycan (G. W. Liechti 2021), similarly to the Z-ring of *E. coli* (Dewachter et al. 2018). MreB, an ortholog of FtsZ from *E. coli*, polymerises at the septum in an ATP-independent manner and organises components of the lipid II biosynthesis, including MurF, MraY and MurG (Gaballah et al. 2011). Peptidoglycan precursors are flipped into the periplasm by FtsW (Gaballah et al. 2011) and then further processed and cross-linked by amidase AmiA (CT_268), transpeptidases PBP2/3 and muramidase (NlpD, CT_759). The hydrolase AmiC (= AmiA, CT_268) degrades peptidoglycan and thus separates the daughter cells (Ouellette et al. 2020). The proteomic investigation of the current work revealed a reduction in AmiA and an increase in MreB in doxycycline-treated *C. trachomatis* serovar D, indicating a disequilibrium and disturbed cell division. Dysregulated peptidoglycan synthesis is consistent with Brockett &

Liechti (2021), who tested several persistence inducers and showed that peptidoglycan synthesis occurs only when treated with the β-lactam antibiotic ampicillin. Furthermore, MreB interact with FtsK (Ouellette et al. 2012, 2014), an ATPase that translocates double-stranded DNA in the final step of chromosome segregation (Ouellette et al. 2020), right after genomic DNA replication. The complexity of replication and segregation has been well described for *E. coli* (Dewachter et al. 2018), with orthologues existing for *C. trachomatis*. This bacterium encodes DnaA1 and DnaA2 with conserved amino acid sequences similar to *E. coli* DnaA, whereas DnaA2 shares more similarities. In brief, the ATPase DnaA is activated by ATP and binds sequence-specific DNA boxes. As soon as all boxes are occupied, genomic DNA is unwound at oriC simultaneously with the recruitment of replisome components for DNA replication, which leads to ATP hydrolysis to the inactive form DnaA-ADP. Initiation is highly controlled by the concentration of activated DnaA-ATP to avoid re-initiation in the same cell cycle. Activated DnaA-ATP initiates replication if it represents 80% of the total amount of DnaA. DnaA-ATP of the active complex is then hydrolysed immediately to inactive DnaA-ADP, leaving 20% active DnaA-ATP behind. Several mechanisms lead to dissociation of ADP from DnaA and binding of new ATP, thereby reactivating DnaA, but the largest proportion of DnaA-ATP results from *de novo* synthesis of DnaA with subsequent ATP binding. Treatment of *Chlamydia* with the quinolone antibiotics nalidixic acid or ciprofloxacin lead to persistence (Dreses-Werringloer et al. 2000). They inhibit ATP-dependent type II topoisomerase gyrase, which unwinds and relaxes positive supercoiled DNA during replication. Near the end of replication, proteins related to chromosome segregation and septum formation are organised. Experiments with the chlamydial temperature-sensitive mutant DnaE(P852S), the catalytic subunit of DNA polymerase III, showed temperature-dependent inhibition of replication termination (Brothwell et al. 2021). This inhibition led to persistent enlarged ABs and the absence of peptidoglycan synthesis.

All the above-mentioned persistence stimuli lead to disturbed metabolism and an altered amino acid reservoir. Due to this interference, ATP acquisition is restricted, and proteins are barely expressed. This limitation is supposed to affect replication initiation because this process requires a high level of *de novo* synthesised DnaA and a high level of ATP to form DnaA-ATP (Dewachter et al. 2018). Even upon successful replication initiation despite restriction, cell division requires a regulatory system to organise chromosome segregation, its positioning and divisome recruitment with precise synchronisation. Systems as Noc/ParB (Adams et al. 2015) presumably require a lot of nutrients and intense translation that are directly or indirectly limited due to the persistence-inducing stimulus. The segregation of the daughter chromosomes correlates tightly with the Z-ring (*E. coli*) or peptidoglycan ring (*Chlamydia*).

The success and completion of replication is a prerequisite for MreB polymerisation, thereby organising the divisome with subsequent peptidoglycan synthesis (Brothwell et al. 2021). Brockett & Liechti (2021) showed starvation stimuli had an inhibitory effect on peptidoglycan synthesis. Shutdown of replication termination via DnaE(P852S) inhibits peptidoglycan synthesis (Brothwell et al. 2021).

In formulating the explanatory model based on the results of this work, the review of Eisenreich et al. (2020) and the experimental investigations of Brockett & Liechti (2021) came to a similar conclusion that persistence is a phenotype resulting from different stimuli that converge and limit cell division. Eisenreich et al. (2020) discussed bacterial persistence in general and argued that the DnaA-ATP level is the limiting step, while Brockett & Liechti (2021) focussed on the inhibition of peptidoglycan synthesis in chlamydial persistence. The reasons for their conclusions differ from this work. The results of this work led to the conclusion that persistence is not limited to either replication initiation or peptidoglycan synthesis but rather is an interplay of many inhibiting factors that interferes with cell division in general.

The explanation model of this work describes that 1) any stimulus that causes inhibition or imbalance can lead to persistence, 2) successful persistence-induction depends on the concentration of the stimulus and treatment timing, and 3) *Chlamydia* require integrity and stability of the bacterial and inclusion membrane to survive the persistent state.

According to point 1) chlamydial persistence can be described in a bottom-to-top model with interfering events starting from imbalanced metabolism and ending in the final steps of the cell division through impaired chromosome segregation or peptidoglycan synthesis.

One core factor is the disruption of chlamydial metabolism. Iron depletion or chelation of K^+/Na^+ disturbs the ionic homeostasis that reduces the import of metabolites driven by ion-dependent symporter and antiporter. The reduced import leads to a disequilibrium of the metabolome that can be also achieved by excess of distinct nutrients or depletion. This imbalance can shift the metabolism to enhance and decrease distinct pathways that, in turn, negatively affect fatty acid metabolism (growths), protein translation, transcription, replication and peptidoglycan synthesis. A subsequential factor is the imbalance of amino acids such as depletion, starvation or excess, which restricts protein translation. Protein translation can also be restricted directly by inhibition of tRNA synthase or translation inhibition via antibiotics such as doxycycline. The direct inhibition of protein translation restricts the proteomic reservoir that is required to initiate replication and septum formation. For the case that replication was successfully initiated, the replication can be still inhibited by reduced nucleotide import or directly by inhibition of gyrase. This active interference into genomic replication prevents chromosome segregation, a prerequisite for septum formation and cell division. Finally, direct inhibition of peptidoglycan

synthesis by β-lactam antibiotics or by depletion of precursor actively blocks the separation of the bacterium into daughter cells during cell division. Overall, these inhibitions and interferences cause *Chlamydia* to stagnate in the cell division

2) All persistence inducers ultimately block cell division. Observations during *C. trachomatis* serovar D recovery in this work and by Skilton et al. (2009) have shown that progeny from ABs are formed by budding, a process assumed to rely on the enlarged growth of ABs. This demonstrates that persistent *Chlamydia* are prepared for immediate cell division upon removal of the stimulus. T3SS inhibition by C1 (Brockett & Liechti 2021) abolishes secretion of Inc proteins, and bacteria display weak recovery after removing the inhibitor. This observation demonstrates that a repertoire of Inc proteins is required for host cell interaction to survive, persist and prepare for immediate cell division, underscoring the relevance of the time of infection at the time of treatment. Furthermore, the success of persistence depends on the stimulus concentration. In this study, the azithromycin concentration was too high, and *C. trachomatis* serovar D was unable to become persistent. *Chlamydia* cannot progress to cell division if the concentration of the persistence-inducing stimulus is initially too high (except for β-lactam antibiotics). Thus, once the stimulus is removed, *Chlamydia* are in a state where they cannot divide and are devoid of metabolites and proteins. In this state, *Chlamydia* are unable to express proteins and enzymes at a level sufficient for metabolic stabilisation, inclusion integrity and host cell manipulation. This inability prevents survival and leads to death.

According to point 3), an essential prerequisite to ensure survival during persistence is membrane integrity and stability. The negative affection of chlamydial sphingomyelin homeostasis seems to be lethal and hinders proper entry into persistence through early EB formation leading to early egress. Therefore, IncD upregulation in doxycycline-induced persistence is necessary to stabilise CERT recruitment to maintain lipid transfer.

In sum, chlamydial persistence is the consequence of stalled cell division. Any kind of stimulus can lead to persistence. The success of persistence depends on time of infection, stimulus concentration and treatment timing, allowing basal activity to prepare for cell division. Finally, the integrity and stability of the inclusion and bacterial membrane ensures survival during the persistence.

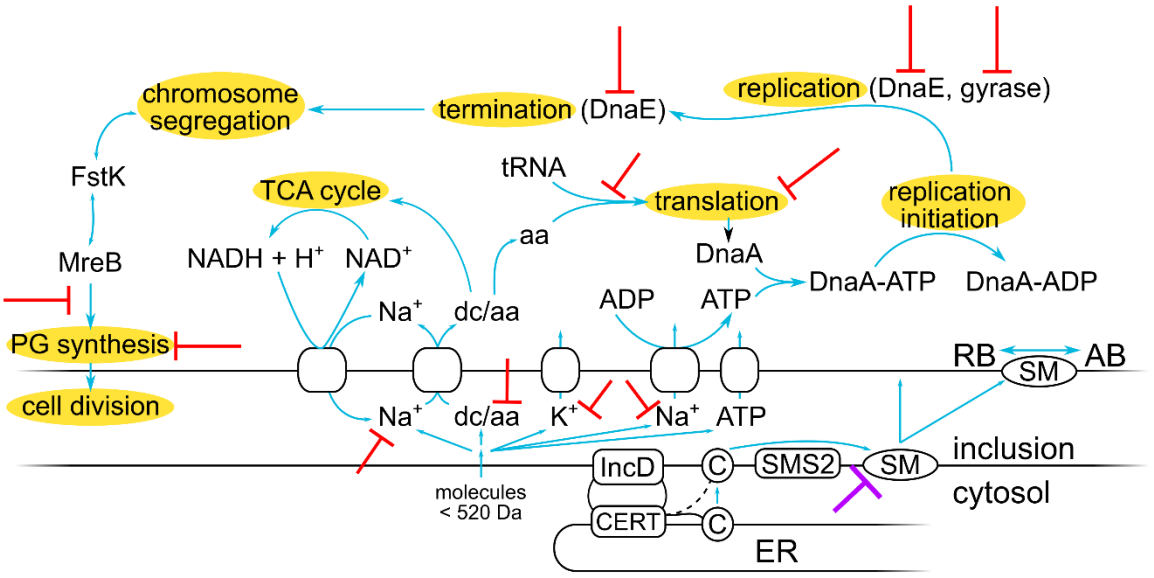

Fig. 41 The path to persistence.

Interaction with CERT supports the acquisition of ceramide (C) and then sphingomyelin (SM), which is important for pathogenesis. Interference (purple stamp) blocks persistence entry and leads to early EB formation. Small molecules diffuse across the inclusion membrane. Na^+/K^+ are important to generate a gradient for the import of dicarboxylate (dc)/amino acids (aa)/ATP and for Na^+-dependent ATP generation. Dicarboxylates are necessary for the TCA cycle and thus the Na^+ gradient. tRNAs are loaded with amino acids for translation, yielding DnaA. DnaA binds ATP and initiates DNA replication, hydrolysing ATP to ADP. DnaE and gyrase proceed replication. Termination of DNA replication initiates chromosome segregation. The segregation complex simultaneously interacts with FstK and MreB. MreB polymerises and recruits proteins for the divisome and peptidoglycan (PG) synthesis. *C. trachomatis* then proceeds with vital cell division. The red stamps show possible interference in the pathway that ultimately leads to stalled cell division and thus persistence.

5 Conclusions and outlook

In this work, interactions of *Chlamydia* spp. with the human host cell and basic mechanisms of chlamydial persistence in the human pathogen *C. trachomatis* serovar D were investigated. The zoonotic pathogen *C. psittaci* can infect both, humans and birds. *C. psittaci* interacts with the human host cell with Inc proteins, although no similarity of amino acid sequences exists with the obligatory human pathogen *C. trachomatis*. The question was addressed, how *C. psittaci* maintains infection in human epithelial cells focusing on Inc proteins. *In silico* analysis revealed 11 putative Inc proteins, of which 8 were further investigated. A new approach was established during the work. Solubilised and fluorescently labelled Inc proteins, the split-Inc proteins, facilitated visual and quantitative identification of host cellular interaction partners. Using the split-Inc, interaction partners of CP0355, CP0856, CP0857, CP0558 and CP0598 were determined. These interactions were concluded to participate in interference of host cell expression and cytokinesis, cytoskeletal rearrangements, fatty acid metabolism and supply of nutrients such as amino acids, respectively. An important role in organisation and inclusion membrane integrity was extrapolated for CP0534, CP0535 and CP0181. Future investigations are required to decipher the direct mechanism of interaction and the particular role of those host cells for chlamydial development. The replication of these experiments in avian cells will be valuable and clarify interspecies correlations.

Furthermore, using split-Inc proteins, the hypothesis could be proven that the interplay of all cytosolic domains is required to mimic native interactions. Future studies must consider the cytosolic domains of Inc proteins. The newly established method also offers an adaptation to Inc proteins with multiple cytosolic domains but requires further optimisation for faster reassembly of eGFP and enhanced fluorescence. The mitochondria-anchored adaptation of split-Inc proteins also provides mimicry of membranous chlamydial interaction that could be used for quick detection of interactions in western blot by isolation of mitochondria.

The aim of this work was to identify the persistence mechanism that helps *C. trachomatis* survive antibiotic pressure. The aberrant phenotype was characterised morphologically via EM. The subsequent experiments focussed on maintaining expression despite translation inhibition. The first hypothesis that trans-translation is the antibiotic-counteracting force that enables chlamydial persistence could not be proven. The results indicate that the mechanism could support persistence, but further investigations are required. However, this led to a change of view. First, selected host proteins were expressed individually and characterised during acute and persistent *C. trachomatis* serovar D infection. Upon realising the limitation of this kind of investigation, proteomics were performed to identify abundant host cell proteins or Inc proteins that are selectively expressed in the presence of doxycycline. These Inc proteins

were assumed to interact with host proteins to enable survival during persistence. The results revealed the fundamental importance to ensure inclusion integrity during the persistence: IncD is upregulated in doxycycline-induced persistence and recruits CERT to the inclusion membrane proposing maintenance of sphingomyelin uptake. Interestingly, Rab12 accumulated at the inclusion membrane of persistent *C. trachomatis* serovar D. Investigation showed that Rab12 plays a role in chlamydial development and EB formation of acute *C. trachomatis* serovar D, suggesting a function in iron uptake by Tfr degradation. Furthermore, Rab12 KD enhanced chlamydial recovery. The recruitment of Rab12 to the inclusion membrane during the persistence is proposed to interfere with autophagy regulation, which ensures chlamydial survival. Furthermore, SNX5 and SNX6 KO, thus interfering with the retrograde trafficking of the host cell, enhanced recovery from doxycycline-induced persistence. Surprisingly, the chlamydial proteome showed reduced metabolic regulation and revealed disturbed cell division via a stoichiometric imbalance in proteins for peptidoglycan synthesis and the divisome. Finally, the results of this work enabled the elucidation of doxycycline-induced persistence in *C. trachomatis* serovar D: chlamydial persistence is the consequence of stalled cell division. Depending on the concentration, time of infection and treatment timing, any stimulus can induce persistence. The survival of persistence, thus successful recovery, relies on the integrity and stability of the bacterial and inclusion membrane.

In this work, new *C. psittaci* Inc proteins were identified and characterised. The newly established split-Inc protein method allowed the determination of host cellular interaction partners with the *C. psittaci* Inc proteins that help to understand the biology of *C. psittaci*. Finally, this work extended the knowledge about chlamydial persistence and provided new information about the acute infection of *C. trachomatis* serovar D.

6 Literature

AbdelRahman, Y. M., & Belland, R. J. 2005. The chlamydial developmental cycle. *FEMS Microbiology Reviews*, *29*5, 949–959. https://doi.org/10.1016/j.femsre.2005.03.002

Adams, D. W., Wu, L. J., & Errington, J. 2015. Nucleoid occlusion protein Noc recruits DNA to the bacterial cell membrane. *The EMBO Journal*, *34*4, 491–501. https://doi.org/10.15252/embj.201490177

Aeberhard, L., Banhart, S., Fischer, M., Jehmlich, N., Rose, L., Koch, S., Laue, M., Renard, B. Y., Schmidt, F., & Heuer, D. 2015. The Proteome of the Isolated Chlamydia trachomatis Containing Vacuole Reveals a Complex Trafficking Platform Enriched for Retromer Components. *PLoS Pathogens*, *11*6, e1004883. https://doi.org/10.1371/journal.ppat.1004883

Agacfidan, A., Moncada, J., & Schachter, J. 1993. In vitro activity of azithromycin (CP-62,993) against Chlamydia trachomatis and Chlamydia pneumoniae. *Antimicrobial Agents and Chemotherapy*, *37*9, 1746–1748.

Agaisse, H., & Derré, I. 2014. Expression of the Effector Protein IncD in Chlamydia trachomatis Mediates Recruitment of the Lipid Transfer Protein CERT and the Endoplasmic Reticulum-Resident Protein VAPB to the Inclusion Membrane. *Infection and Immunity*, *82*5, 2037–2047. https://doi.org/10.1128/IAI.01530-14

Agaisse, H., & Derré, I. 2015. STIM1 Is a Novel Component of ER-Chlamydia trachomatis Inclusion Membrane Contact Sites. *PloS One*, *10*4, e0125671. https://doi.org/10.1371/journal.pone.0125671

Agwuh, K. N., & MacGowan, A. 2006. Pharmacokinetics and pharmacodynamics of the tetracyclines including glycylcyclines. *Journal of Antimicrobial Chemotherapy*, *58*2, 256–265. https://doi.org/10.1093/jac/dkl224

Albert-Weissenberger, C., Cazalet, C., & Buchrieser, C. 2007. Legionella pneumophila - a human pathogen that co-evolved with fresh water protozoa. *Cellular and Molecular Life Sciences: CMLS*, *64*4, 432–448. https://doi.org/10.1007/s00018-006-6391-1

Alegun, O., Pandeya, A., Cui, J., Ojo, I., & Wei, Y. 2021. Donnan Potential across the Outer Membrane of Gram-Negative Bacteria and Its Effect on the Permeability of Antibiotics. *Antibiotics*, *10*6, 701. https://doi.org/10.3390/antibiotics10060701

Alonso, M. A., & Millán, J. 2001. The role of lipid rafts in signalling and membrane trafficking in T lymphocytes. *Journal of Cell Science*, *114*22, 3957–3965. https://doi.org/10.1242/jcs.114.22.3957

Altschul, S. F., Madden, T. L., Schäffer, A. A., Zhang, J., Zhang, Z., Miller, W., & Lipman, D. J. 1997. Gapped BLAST and PSI-BLAST: a new generation of protein database search programs. *Nucleic Acids Research*, *25*17, 3389–3402.

Andini, N., & Nash, K. A. 2011. Expression of tmRNAin Mycobacteria is Increased by Antimicrobial Agents that Target the Ribosome. *FEMS Microbiology Letters*, *322*2, 172–179. https://doi.org/10.1111/j.1574-6968.2011.02350.x

Andrew, S. C., Dumoux, M., & Hayward, R. D. 2021. Chlamydia Uses K+ Electrical Signalling to Orchestrate Host Sensing, Inter-Bacterial Communication and Differentiation. *Microorganisms*, *9*1, 173. https://doi.org/10.3390/microorganisms9010173

Angrand, P.-O., Segura, I., Völkel, P., Ghidelli, S., Terry, R., Brajenovic, M., Vintersten, K., Klein, R., Superti-Furga, G., Drewes, G., Kuster, B., Bouwmeester, T., & Acker-Palmer, A. 2006. Transgenic mouse proteomics identifies new 14-3-3-associated proteins involved in cytoskeletal rearrangements and cell signaling. *Molecular & Cellular Proteomics: MCP*, *5*12, 2211–2227. https://doi.org/10.1074/mcp.M600147-MCP200

Baek, M., DiMaio, F., Anishchenko, I., Dauparas, J., Ovchinnikov, S., Lee, G. R., Wang, J., Cong, Q., Kinch, L. N., Schaeffer, R. D., Millán, C., Park, H., Adams, C., Glassman, C. R., DeGiovanni, A., Pereira, J. H., Rodrigues, A. V., van Dijk, A. A., Ebrecht, A. C., … Baker, D. 2021. Accurate prediction of protein structures and interactions using a three-

track neural network. *Science*, *373*6557, 871–876. https://doi.org/10.1126/science.abj8754

Balla, A., & Balla, T. 2006. Phosphatidylinositol 4-kinases: old enzymes with emerging functions. *Trends in Cell Biology*, *16*7, 351–361. https://doi.org/10.1016/j.tcb.2006.05.003

Balsamo, G., Maxted, A. M., Midla, J. W., Murphy, J. M., Wohrle, R., Edling, T. M., Fish, P. H., Flammer, K., Hyde, D., Kutty, P. K., Kobayashi, M., Helm, B., Oiulfstad, B., Ritchie, B. W., Stobierski, M. G., Ehnert, K., & Tully, T. N. 2017. Compendium of Measures to Control Chlamydia psittaci Infection Among Humans (Psittacosis) and Pet Birds (Avian Chlamydiosis), 2017. *Journal of Avian Medicine and Surgery*, *31*3, 262–282. https://doi.org/10.1647/217-265

Banhart, S., Saied, E. M., Martini, A., Koch, S., Aeberhard, L., Madela, K., Arenz, C., & Heuer, D. 2014. Improved Plaque Assay Identifies a Novel Anti-Chlamydia Ceramide Derivative with Altered Intracellular Localization. *Antimicrobial Agents and Chemotherapy*, *58*9, 5537–5546. https://doi.org/10.1128/AAC.03457-14

Banhart, S., Schäfer, E. K., Gensch, J.-M., & Heuer, D. 2019. Sphingolipid Metabolism and Transport in Chlamydia trachomatis and Chlamydia psittaci Infections. *Frontiers in Cell and Developmental Biology*, *7*, 223. https://doi.org/10.3389/fcell.2019.00223

Bannantine, J. P., Rockey, D. D., & Hackstadt, T. 1998. Tandem genes of Chlamydia psittaci that encode proteins localized to the inclusion membrane. *Molecular Microbiology*, *28*5, 1017–1026. https://doi.org/10.1046/j.1365-2958.1998.00867.x

Barbour, A. G., Amano, K., Hackstadt, T., Perry, L., & Caldwell, H. D. 1982. Chlamydia trachomatis has penicillin-binding proteins but not detectable muramic acid. *Journal of Bacteriology*, *151*1, 420–428. https://doi.org/10.1128/jb.151.1.420-428.1982

Basovskiy, Y. I., Shkarupeta, M. M., Levitskiy, S. A., Kostryukova, E. S., Lazarev, V. N., & Govorun, V. M. 2008. Hydrophobic domains determine localization of IncC and IncG full-length proteins of C. trachomatis during their expression in cultured HeLa cells.

Bulletin of Experimental Biology and Medicine, *145*4, 425–429. https://doi.org/10.1007/s10517-008-0108-4

Bavoil, P., Ohlin, A., & Schachter, J. 1984. Role of disulfide bonding in outer membrane structure and permeability in Chlamydia trachomatis. *Infection and Immunity*, *44*2, 479–485. https://doi.org/10.1128/iai.44.2.479-485.1984

Bayramova, F., Jacquier, N., & Greub, G. 2018. Insight in the biology of Chlamydia-related bacteria. *Microbes and Infection*, *207*, 432–440. https://doi.org/10.1016/j.micinf.2017.11.008

Beatty, K. E., Liu, J. C., Xie, F., Dieterich, D. C., Schuman, E. M., Wang, Q., & Tirrell, D. A. 2006. Fluorescence Visualization of Newly Synthesized Proteins in Mammalian Cells. *Angewandte Chemie International Edition*, *45*44, 7364–7367. https://doi.org/10.1002/anie.200602114

Beatty, W. L., Morrison, R. P., & Byrne, G. I. 1994. Persistent chlamydiae: from cell culture to a paradigm for chlamydial pathogenesis. *Microbiological Reviews*, *58*4, 686.

Belland, R. J., Nelson, D. E., Virok, D., Crane, D. D., Hogan, D., Sturdevant, D., Beatty, W. L., & Caldwell, H. D. 2003. Transcriptome analysis of chlamydial growth during IFN-γ-mediated persistence and reactivation. *Proceedings of the National Academy of Sciences of the United States of America*, *100*26, 15971–15976. https://doi.org/10.1073/pnas.2535394100

Belland, R. J., Zhong, G., Crane, D. D., Hogan, D., Sturdevant, D., Sharma, J., Beatty, W. L., & Caldwell, H. D. 2003. Genomic transcriptional profiling of the developmental cycle of Chlamydia trachomatis. *Proceedings of the National Academy of Sciences of the United States of America*, *100*14, 8478–8483. https://doi.org/10.1073/pnas.1331135100

Benamri, I., Azzouzi, M., Sanak, K., Moussa, A., & Radouani, F. 2021. An overview of genes and mutations associated with Chlamydiae species' resistance to antibiotics. *Annals of Clinical Microbiology and Antimicrobials*, *20*, 59. https://doi.org/10.1186/s12941-021-00465-4

Bindea, G., Mlecnik, B., Hackl, H., Charoentong, P., Tosolini, M., Kirilovsky, A., Fridman, W.-H., Pagès, F., Trajanoski, Z., & Galon, J. 2009. ClueGO: a Cytoscape plug-in to decipher functionally grouped gene ontology and pathway annotation networks. *Bioinformatics*, *25*8, 1091–1093. https://doi.org/10.1093/bioinformatics/btp101

Böcker, S., Heurich, A., Franke, C., Monajembashi, S., Sachse, K., Saluz, H. P., & Hänel, F. 2014. Chlamydia psittaci inclusion membrane protein IncB associates with host protein Snapin. *International Journal of Medical Microbiology: IJMM*, *3045*–6, 542–553. https://doi.org/10.1016/j.ijmm.2014.03.005

Borel, N., Leonard, C., Slade, J., & Schoborg, R. V. 2016. Chlamydial Antibiotic Resistance and Treatment Failure in Veterinary and Human Medicine. *Current Clinical Microbiology Reports*, *3*, 10–18. https://doi.org/10.1007/s40588-016-0028-4

Borth, N., Litsche, K., Franke, C., Sachse, K., Saluz, H. P., & Hänel, F. 2011. Functional Interaction between Type III-Secreted Protein IncA of Chlamydophila psittaci and Human G3BP1. *PLoS ONE*, *6*1, e16692. https://doi.org/10.1371/journal.pone.0016692

Bragina, E., Gomberg, M., & Dmitriev, G. 2001. Electron microscopic evidence of persistent chlamydial infection following treatment. *Journal of the European Academy of Dermatology and Venereology*, *15*5, 405–409. https://doi.org/10.1046/j.1468-3083.2001.00342.x

Brandman, O., Liou, J., Park, W. S., & Meyer, T. 2007. STIM2 is a feedback regulator that stabilizes basal cytosolic and endoplasmic reticulum Ca2+ levels. *Cell*, *131*7, 1327–1339. https://doi.org/10.1016/j.cell.2007.11.039

Brockett, M. R., & Liechti, G. W. 2021. Persistence Alters the Interaction between Chlamydia trachomatis and Its Host Cell. *Infection and Immunity*. https://doi.org/10.1128/IAI.00685-20

Brothwell, J. A., Brockett, M., Banerjee, A., Stein, B. D., Nelson, D. E., & Liechti, G. W. 2021. Genome Copy Number Regulates Inclusion Expansion, Septation, and Infectious Developmental Form Conversion in Chlamydia trachomatis. *Journal of Bacteriology*. https://doi.org/10.1128/JB.00630-20

Brumell, J. H., & Scidmore, M. A. 2007. Manipulation of Rab GTPase Function by Intracellular Bacterial Pathogens. *Microbiology and Molecular Biology Reviews : MMBR*, *71*4, 636–652. https://doi.org/10.1128/MMBR.00023-07

Brunel, R., & Charpentier, X. 2016. Trans-translation is essential in the human pathogen Legionella pneumophila. *Scientific Reports*, *6*, 37935. https://doi.org/10.1038/srep37935

Brunham, R. C., Binns, B., Guijon, F., Danforth, D., Kosseim, M. L., Rand, F., McDowell, J., & Rayner, E. 1988. Etiology and outcome of acute pelvic inflammatory disease. *The Journal of Infectious Diseases*, *158*3, 510–517. https://doi.org/10.1093/infdis/158.3.510

Bugalhão, J. N., & Mota, L. J. 2019. The multiple functions of the numerous Chlamydia trachomatis secreted proteins: the tip of the iceberg. *Microbial Cell*, *6*9, 414–449. https://doi.org/10.15698/mic2019.09.691

Caldwell, H. D., Wood, H., Crane, D., Bailey, R., Jones, R. B., Mabey, D., Maclean, I., Mohammed, Z., Peeling, R., Roshick, C., Schachter, J., Solomon, A. W., Stamm, W. E., Suchland, R. J., Taylor, L., West, S. K., Quinn, T. C., Belland, R. J., & McClarty, G. 2003. Polymorphisms in Chlamydia trachomatis tryptophan synthase genes differentiate between genital and ocular isolates. *Journal of Clinical Investigation*, *111*11, 1757–1769. https://doi.org/10.1172/JCI200317993

Capmany, A., Gambarte Tudela, J., Alonso Bivou, M., & Damiani, M. T. 2019. Akt/AS160 Signaling Pathway Inhibition Impairs Infection by Decreasing Rab14-Controlled Sphingolipids Delivery to Chlamydial Inclusions. *Frontiers in Microbiology*, *10*, 666. https://doi.org/10.3389/fmicb.2019.00666

Carabeo, R. A., Mead, D. J., & Hackstadt, T. 2003. Golgi-dependent transport of cholesterol to the Chlamydia trachomatis inclusion. *Proceedings of the National Academy of Sciences of the United States of America*, *100*11, 6771–6776. https://doi.org/10.1073/pnas.1131289100

Caven, L., & Carabeo, R. A. 2019. Pathogenic Puppetry: Manipulation of the Host Actin Cytoskeleton by Chlamydia trachomatis. *International Journal of Molecular Sciences*, *21*1, 90. https://doi.org/10.3390/ijms21010090

Chen, X., Cao, K., Wei, Y., Qian, Y., Liang, J., Dong, D., Tang, J., Zhu, Z., Gu, Q., & Yu, W. 2020. Metagenomic next-generation sequencing in the diagnosis of severe pneumonias caused by Chlamydia psittaci. *Infection*, *48*4, 535–542. https://doi.org/10.1007/s15010-020-01429-0

Chesnokov, V. N., & Mertvetsov, N. P. 1990. [The effect of translation inhibitor cycloheximide on expression of mammalian genes]. *Biokhimiia (Moscow, Russia)*, *55*7, 1276–1278.

Chiarelli, T. J., Grieshaber, N. A., Omsland, A., Remien, C. H., & Grieshaber, S. S. 2020. Single-Inclusion Kinetics of Chlamydia trachomatis Development. *MSystems*, *5*5. https://doi.org/10.1128/mSystems.00689-20

Chin, E., Kirker, K., Zuck, M., James, G., & Hybiske, K. 2012. Actin Recruitment to the Chlamydia Inclusion Is Spatiotemporally Regulated by a Mechanism That Requires Host and Bacterial Factors. *PLoS ONE*, 710, e46949. https://doi.org/10.1371/journal.pone.0046949

Chopra, I., & Roberts, M. 2001. Tetracycline Antibiotics: Mode of Action, Applications, Molecular Biology, and Epidemiology of Bacterial Resistance. *Microbiology and Molecular Biology Reviews*, *65*2, 232–260. https://doi.org/10.1128/MMBR.65.2.232-260.2001

Chow, E. P. F., Camilleri, S., Ward, C., Huffam, S., Chen, M. Y., Bradshaw, C. S., & Fairley, C. K. 2016. Duration of gonorrhoea and chlamydia infection at the pharynx and rectum among men who have sex with men: a systematic review. *Sexual Health*, *13*3, 199–204. https://doi.org/10.1071/SH15175

Chow, J. M., Yonekura, M. L., Richwald, G. A., Greenland, S., Sweet, R. L., & Schachter, J. 1990. The association between Chlamydia trachomatis and ectopic pregnancy. A matched-pair, case-control study. *JAMA*, *263*23, 3164–3167.

Christensen, S., Halili, M. A., Strange, N., Petit, G. A., Huston, W. M., Martin, J. L., & McMahon, R. M. 2019. Oxidoreductase disulfide bond proteins DsbA and DsbB form an active redox pair in Chlamydia trachomatis, a bacterium with disulfide dependent infection and development. *PLoS ONE*, *14*9. https://doi.org/10.1371/journal.pone.0222595

Clausen, J. D., Christiansen, G., Holst, H. U., & Birkelund, S. 1997. Chlamydia trachomatis utilizes the host cell microtubule network during early events of infection. *Molecular Microbiology*, *25*3, 441–449. https://doi.org/10.1046/j.1365-2958.1997.4591832.x

Clemens, D. L., & Horwitz, M. A. 1995. Characterization of the Mycobacterium tuberculosis phagosome and evidence that phagosomal maturation is inhibited. *The Journal of Experimental Medicine*, *181*1, 257–270. https://doi.org/10.1084/jem.181.1.257

Clifton, D. R., Fields, K. A., Grieshaber, S. S., Dooley, C. A., Fischer, E. R., Mead, D. J., Carabeo, R. A., & Hackstadt, T. 2004. A chlamydial type III translocated protein is tyrosine-phosphorylated at the site of entry and associated with recruitment of actin. *Proceedings of the National Academy of Sciences of the United States of America*, *101*27, 10166–10171. https://doi.org/10.1073/pnas.0402829101

Costerton, J. W., Poffenroth, L., Wilt, J. C., & Kordová, N. 1976. Ultrastructural studies of the nucleoids of the pleomorphic forms of Chlamydia psittaci 6BC: a comparison with bacteria. *Canadian Journal of Microbiology*, *22*1, 16–28. https://doi.org/10.1139/m76-003

Cronan, J. E. 2005. Targeted and proximity-dependent promiscuous protein biotinylation by a mutant Escherichia coli biotin protein ligase. *The Journal of Nutritional Biochemistry*, *16*7, 416–418. https://doi.org/10.1016/j.jnutbio.2005.03.017

Dedhar, S. 2000. Cell-substrate interactions and signaling through ILK. *Current Opinion in Cell Biology*, *12*2, 250–256. https://doi.org/10.1016/s0955-0674(99)00083-6

Dehoux, P., Flores, R., Dauga, C., Zhong, G., & Subtil, A. 2011. Multi-genome identification and characterization of chlamydiae-specific type III secretion substrates: the Inc proteins. *BMC Genomics*, *12*, 109. https://doi.org/10.1186/1471-2164-12-109

Delevoye, C., Nilges, M., Dehoux, P., Paumet, F., Perrinet, S., Dautry-Varsat, A., & Subtil, A. 2008. SNARE Protein Mimicry by an Intracellular Bacterium. *PLoS Pathogens*, *4*3. https://doi.org/10.1371/journal.ppat.1000022

Derré, I., Swiss, R., & Agaisse, H. 2011. The Lipid Transfer Protein CERT Interacts with the Chlamydia Inclusion Protein IncD and Participates to ER-Chlamydia Inclusion Membrane Contact Sites. *PLoS Pathogens*, *7*6, e1002092. https://doi.org/10.1371/journal.ppat.1002092

Dessus-Babus, S., Moore, C. G., Whittimore, J. D., & Wyrick, P. B. 2008. Comparison of Chlamydia trachomatis serovar L2 growth in polarized genital epithelial cells grown in three-dimensional culture with non-polarized cells. *Microbes and Infection / Institut Pasteur*, *10*5, 563–570. https://doi.org/10.1016/j.micinf.2008.02.002

Dewachter, L., Verstraeten, N., Fauvart, M., & Michiels, J. 2018. An integrative view of cell cycle control in Escherichia coli. *FEMS Microbiology Reviews*, *42*2, 116–136. https://doi.org/10.1093/femsre/fuy005

Dickinson, M. S., Anderson, L. N., Webb-Robertson, B.-J. M., Hansen, J. R., Smith, R. D., Wright, A. T., & Hybiske, K. 2019. Proximity-dependent proteomics of the Chlamydia trachomatis inclusion membrane reveals functional interactions with endoplasmic reticulum exit sites. *PLoS Pathogens*, *15*4, e1007698. https://doi.org/10.1371/journal.ppat.1007698

Dombrowski, J. C., Wierzbicki, M. R., Newman, L. M., Powell, J. A., Miller, A., Dithmer, D., Soge, O. O., & Mayer, K. H. 2021. Doxycycline Versus Azithromycin for the Treatment of Rectal Chlamydia in Men Who Have Sex With Men: A Randomized Controlled Trial. *Clinical Infectious Diseases: An Official Publication of the Infectious Diseases Society of America*, *73*5, 824–831. https://doi.org/10.1093/cid/ciab153

Dreses-Werringloer, U., Padubrin, I., Jürgens-Saathoff, B., Hudson, A. P., Zeidler, H., & Köhler, L. 2000. Persistence of Chlamydia trachomatis Is Induced by Ciprofloxacin and Ofloxacin In Vitro. *Antimicrobial Agents and Chemotherapy*, *44*12, 3288–3297.

Drozdetskiy, A., Cole, C., Procter, J., & Barton, G. J. 2015. JPred4: a protein secondary structure prediction server. *Nucleic Acids Research*, *43*W1, W389–W394. https://doi.org/10.1093/nar/gkv332

Dugan, J., Rockey, D. D., Jones, L., & Andersen, A. A. 2004. Tetracycline Resistance in Chlamydia suis Mediated by Genomic Islands Inserted into the Chlamydial inv-Like Gene. *Antimicrobial Agents and Chemotherapy*. https://journals.asm.org/doi/abs/10.1128/AAC.48.10.3989-3995.2004

Dukers-Muijrers, N. H. T. M., Wolffs, P. F. G., De Vries, H., Götz, H. M., Heijman, T., Bruisten, S., Eppings, L., Hogewoning, A., Steenbakkers, M., Lucchesi, M., Schim van der Loeff, M. F., & Hoebe, C. J. P. A. 2019. Treatment Effectiveness of Azithromycin and Doxycycline in Uncomplicated Rectal and Vaginal Chlamydia trachomatis Infections in Women: A Multicenter Observational Study (FemCure). *Clinical Infectious Diseases: An Official Publication of the Infectious Diseases Society of America*, *69*11, 1946–1954. https://doi.org/10.1093/cid/ciz050

Efergan, A., Azouz, N. P., Klein, O., Noguchi, K., Rothenberg, M. E., Fukuda, M., & Sagi-Eisenberg, R. 2016. Rab12 Regulates Retrograde Transport of Mast Cell Secretory Granules by Interacting with the RILP-Dynein Complex. *Journal of Immunology (Baltimore, Md.: 1950)*, *196*3, 1091–1101. https://doi.org/10.4049/jimmunol.1500731

Eisenreich, W., Rudel, T., Heesemann, J., & Goebel, W. 2020. Persistence of Intracellular Bacterial Pathogens-With a Focus on the Metabolic Perspective. *Frontiers in Cellular and Infection Microbiology*, *10*, 615450. https://doi.org/10.3389/fcimb.2020.615450

Eissenberg, L. G., Wyrick, P. B., Davis, C. H., & Rumpp, J. W. 1983. Chlamydia psittaci elementary body envelopes: ingestion and inhibition of phagolysosome fusion. *Infection and Immunity*, *40*2, 741–751. https://doi.org/10.1128/iai.40.2.741-751.1983

Elwell, C. A., Czudnochowski, N., von Dollen, J., Johnson, J. R., Nakagawa, R., Mirrashidi, K., Krogan, N. J., Engel, J. N., & Rosenberg, O. S. 2017. Chlamydia interfere with an interaction between the mannose-6-phosphate receptor and sorting nexins to counteract host restriction. *ELife*, *6*, e22709. https://doi.org/10.7554/eLife.22709

Elwell, C. A., Jiang, S., Kim, J. H., Lee, A., Wittmann, T., Hanada, K., Melancon, P., & Engel, J. N. 2011. Chlamydia trachomatis Co-opts GBF1 and CERT to Acquire Host Sphingomyelin for Distinct Roles during Intracellular Development. *PLoS Pathogens*, *7*9, e1002198. https://doi.org/10.1371/journal.ppat.1002198

Elwell, C., Mirrashidi, K., & Engel, J. 2016. Chlamydia cell biology and pathogenesis. *Nature Reviews. Microbiology*, *14*6, 385–400. https://doi.org/10.1038/nrmicro.2016.30

Ennis, H. L., & Lubin, M. 1964. Cycloheximide: Aspects of Inhibition of Protein Synthesis in Mammalian Cells. *Science*. https://doi.org/10.1126/science.146.3650.1474

Fadel, S., & Eley, A. 2008. Differential glycosaminoglycan binding of Chlamydia trachomatis OmcB protein from serovars E and LGV. *Journal of Medical Microbiology*, *57*Pt 9, 1058–1061. https://doi.org/10.1099/jmm.0.2008/001305-0

Fernandez-Prada, C. M., Zelazowska, E. B., Nikolich, M., Hadfield, T. L., Roop, R. M., Robertson, G. L., & Hoover, D. L. 2003. Interactions between Brucella melitensis and human phagocytes: bacterial surface O-Polysaccharide inhibits phagocytosis, bacterial killing, and subsequent host cell apoptosis. *Infection and Immunity*, *71*4, 2110–2119. https://doi.org/10.1128/IAI.71.4.2110-2119.2003

Filardo, S., Skilton, R. J., O'Neill, C. E., Di Pietro, M., Sessa, R., & Clarke, I. N. 2019. Growth kinetics of Chlamydia trachomatis in primary human Sertoli cells. *Scientific Reports*, *9*1, 5847. https://doi.org/10.1038/s41598-019-42396-3

Fisher, D. J., Fernández, R. E., & Maurelli, A. T. 2013. Chlamydia trachomatis transports NAD via the Npt1 ATP/ADP translocase. *Journal of Bacteriology*, *195*15, 3381–3386. https://doi.org/10.1128/JB.00433-13

Fraser, D. W., Tsai, T. R., Orenstein, W., Parkin, W. E., Beecham, H. J., Sharrar, R. G., Harris, J., Mallison, G. F., Martin, S. M., McDade, J. E., Shepard, C. C., & Brachman, P. S. 1977. Legionnaires' disease: description of an epidemic of pneumonia. *The New England Journal of Medicine*, *297*22, 1189–1197. https://doi.org/10.1056/NEJM197712012972201

Friis, R. R. 1972. Interaction of L cells and Chlamydia psittaci: entry of the parasite and host responses to its development. *Journal of Bacteriology*, *110*2, 706–721. https://doi.org/10.1128/jb.110.2.706-721.1972

Gaballah, A., Kloeckner, A., Otten, C., Sahl, H.-G., & Henrichfreise, B. 2011. Functional Analysis of the Cytoskeleton Protein MreB from Chlamydophila pneumoniae. *PLoS ONE*, *6*10. https://doi.org/10.1371/journal.pone.0025129

Gambarte Tudela, J., Buonfigli, J., Luján, A., Alonso Bivou, M., Cebrián, I., Capmany, A., & Damiani, M. T. 2019. Rab39a and Rab39b Display Different Intracellular Distribution and Function in Sphingolipids and Phospholipids Transport. *International Journal of Molecular Sciences*, *20*7, 1688. https://doi.org/10.3390/ijms20071688

Garrett, A. J., Harrison, M. J., & Manire, G. P. 1974. A search for the bacterial mucopeptide component, muramic acid, in Chlamydia. *Journal of General Microbiology*, *80*1, 315–318. https://doi.org/10.1099/00221287-80-1-315

Gasteiger, E., Hoogland, C., Gattiker, A., Duvaud, S., Wilkins, M. R., Appel, R. D., & Bairoch, A. 2005. Protein Identification and Analysis Tools on the ExPASy Server. In J. M. Walker Ed., *The Proteomics Protocols Handbook* pp. 571–607. Humana Press. https://doi.org/10.1385/1-59259-890-0:571

Geisler, W. M., Uniyal, A., Lee, J. Y., Lensing, S. Y., Johnson, S., Perry, R. C. W., Kadrnka, C. M., & Kerndt, P. R. 2015. Azithromycin versus Doxycycline for Urogenital Chlamydia trachomatis Infection. *The New England Journal of Medicine*, *373*26, 2512–2521. https://doi.org/10.1056/NEJMoa1502599

Gitsels, A., Sanders, N., & Vanrompay, D. 2019. Chlamydial Infection From Outside to Inside. *Frontiers in Microbiology*, *10*, 2329. https://doi.org/10.3389/fmicb.2019.02329

Giudice, E., Macé, K., & Gillet, R. 2014. Trans-translation exposed: understanding the structures and functions of tmRNA-SmpB. *Frontiers in Microbiology*, *5*, 113. https://doi.org/10.3389/fmicb.2014.00113

Gohla, A., & Bokoch, G. M. 2002. 14-3-3 regulates actin dynamics by stabilizing phosphorylated cofilin. *Current Biology: CB*, *12*19, 1704–1710. https://doi.org/10.1016/s0960-9822(02)01184-3

Gokmenoglu, C., Ozmeric, N., Sungur, C., Sahin Bildik, R., Erguder, I., & Elgun, S. 2018. Nitric oxide and arginase levels in peri-implant tissues after delayed loading. *Archives of Oral Biology*, *85*, 207–211. https://doi.org/10.1016/j.archoralbio.2017.10.019

Gordon, M. A., Graham, S. M., Walsh, A. L., Wilson, L., Phiri, A., Molyneux, E., Zijlstra, E. E., Heyderman, R. S., Hart, C. A., & Molyneux, M. E. 2008. Epidemics of invasive Salmonella enterica serovar enteritidis and S. enterica Serovar typhimurium infection associated with multidrug resistance among adults and children in Malawi. *Clinical Infectious Diseases: An Official Publication of the Infectious Diseases Society of America*, *46*7, 963–969. https://doi.org/10.1086/529146

Grieshaber, S., Grieshaber, N., Yang, H., Baxter, B., Hackstadt, T., & Omsland, A. 2018. Impact of Active Metabolism on Chlamydia trachomatis Elementary Body Transcript Profile and Infectivity. *Journal of Bacteriology*, *200*14. https://doi.org/10.1128/JB.00065-18

Grieshaber, S. S., Grieshaber, N. A., & Hackstadt, T. 2003. Chlamydia trachomatis uses host cell dynein to traffic to the microtubule-organizing center in a p50 dynamitin-independent process. *Journal of Cell Science*, *116*Pt 18, 3793–3802. https://doi.org/10.1242/jcs.00695

Grieshaber, S., Swanson, J. A., & Hackstadt, T. 2002. Determination of the physical environment within the Chlamydia trachomatis inclusion using ion-selective ratiometric probes. *Cellular Microbiology*, *4*5, 273–283. https://doi.org/10.1046/j.1462-5822.2002.00191.x

Griffin, M. O., Fricovsky, E., Ceballos, G., & Villarreal, F. 2010. Tetracyclines: a pleitropic family of compounds with promising therapeutic properties. Review of the literature. *American Journal of Physiology - Cell Physiology*, *299*3, C539–C548. https://doi.org/10.1152/ajpcell.00047.2010

Gussmann, J., Al-Younes, H. M., Braun, P. R., Brinkmann, V., & Meyer, T. F. 2008. Long-term effects of natural amino acids on infection with Chlamydia trachomatis. *Microbial Pathogenesis*, *44*5, 438–447. https://doi.org/10.1016/j.micpath.2007.11.009

Hackstadt, T., Baehr, W., & Ying, Y. 1991. Chlamydia trachomatis developmentally regulated protein is homologous to eukaryotic histone H1. *Proceedings of the National Academy of Sciences of the United States of America*, *88*9, 3937–3941. https://doi.org/10.1073/pnas.88.9.3937

Hackstadt, T., Scidmore, M. A., & Rockey, D. D. 1995. Lipid metabolism in Chlamydia trachomatis-infected cells: directed trafficking of Golgi-derived sphingolipids to the chlamydial inclusion. *Proceedings of the National Academy of Sciences of the United States of America*, *92*11, 4877–4881.

Haeusser, D. P., & Margolin, W. 2016. Splitsville: structural and functional insights into the dynamic bacterial Z ring. *Nature Reviews. Microbiology*, *14*5, 305–319. https://doi.org/10.1038/nrmicro.2016.26

Hammerschlag, M. R. 2002. The intracellular life of chlamydiae. *Seminars in Pediatric Infectious Diseases*, *13*4, 239–248. https://doi.org/10.1053/spid.2002.127201

Hanada, K., Kumagai, K., Tomishige, N., & Yamaji, T. 2009. CERT-mediated trafficking of ceramide. *Biochimica Et Biophysica Acta*, *1791*7, 684–691. https://doi.org/10.1016/j.bbalip.2009.01.006

Hannigan, G. E., Leung-Hagesteijn, C., Fitz-Gibbon, L., Coppolino, M. G., Radeva, G., Filmus, J., Bell, J. C., & Dedhar, S. 1996. Regulation of cell adhesion and anchorage-dependent growth by a new beta 1-integrin-linked protein kinase. *Nature*, *379*6560, 91–96. https://doi.org/10.1038/379091a0

Harper, A., Pogson, C. I., Jones, M. L., & Pearce, J. H. 2000. Chlamydial Development Is Adversely Affected by Minor Changes in Amino Acid Supply, Blood Plasma Amino Acid Levels, and Glucose Deprivation. *Infection and Immunity*, *68*3, 1457–1464.

Harris, S. R., Clarke, I. N., Seth-Smith, H. M. B., Solomon, A. W., Cutcliffe, L. T., Marsh, P., Skilton, R. J., Holland, M. J., Mabey, D., Peeling, R. W., Lewis, D. A., Spratt, B. G.,

Unemo, M., Persson, K., Bjartling, C., Brunham, R., de Vries, H. J. C., Morré, S. A., Speksnijder, A., … Thomson, N. R. 2012. Whole-genome analysis of diverse Chlamydia trachomatis strains identifies phylogenetic relationships masked by current clinical typing. *Nature Genetics*, *44*4, 413–419, S1. https://doi.org/10.1038/ng.2214

Hatch, N. D., & Ouellette, S. P. 2020. Inhibition of tRNA Synthetases Induces Persistence in Chlamydia. *Infection and Immunity*, *88*4, e00943-19. https://doi.org/10.1128/IAI.00943-19

Hatch, T. P. 1976. Utilization of exogenous thymidine by Chlamydia psittaci growing in the thymidine kinase-containing and thymidine kinase-deficient L cells. *Journal of Bacteriology*, *125*2, 706–712. https://doi.org/10.1128/jb.125.2.706-712.1976

He, M., Pei, Z., Mohsen, A.-W., Watkins, P., Murdoch, G., Van Veldhoven, P. P., Ensenauer, R., & Vockley, J. 2011. Identification and Characterization of New Long Chain Acyl-CoA Dehydrogenases. *Molecular Genetics and Metabolism*, *102*4, 418–429. https://doi.org/10.1016/j.ymgme.2010.12.005

He, Z., Xiao, J., Wang, J., Lu, S., Zheng, K., Yu, M., Liu, J., Wang, C., Ding, N., Liang, M., & Wu, Y. 2021. The Chlamydia psittaci Inclusion Membrane Protein 0556 Inhibits Human Neutrophils Apoptosis Through PI3K/AKT and NF-κB Signaling Pathways. *Frontiers in Immunology*, *12*, 694573. https://doi.org/10.3389/fimmu.2021.694573

Herweg, J.-A., & Rudel, T. 2016. Interaction of Chlamydiae with human macrophages. *The FEBS Journal*, *283*4, 608–618. https://doi.org/10.1111/febs.13609

Heuer, D., Rejman Lipinski, A., Machuy, N., Karlas, A., Wehrens, A., Siedler, F., Brinkmann, V., & Meyer, T. F. 2009. Chlamydia causes fragmentation of the Golgi compartment to ensure reproduction. *Nature*, *4577*230, 731–735. https://doi.org/10.1038/nature07578

Hitchcock-DeGregori, S. E., & Barua, B. 2017. Tropomyosin Structure, Function, and Interactions: A Dynamic Regulator. In D. A. D. Parry & J. M. Squire Eds., *Fibrous Proteins: Structures and Mechanisms* pp. 253–284. Springer International Publishing. https://doi.org/10.1007/978-3-319-49674-0_9

Hobson, D., Stefanidis, D., Rees, E., & Tait, I. A. 1982. Effects of chloramphenicol on Chlamydia trachomatis infection in neonatal conjunctivitis and in McCoy cell cultures. *The Journal of Hygiene*, *89*3, 457–466.

Hogerwerf, L., DE Gier, B., Baan, B., & VAN DER Hoek, W. 2017. Chlamydia psittaci (psittacosis) as a cause of community-acquired pneumonia: a systematic review and meta-analysis. *Epidemiology and Infection*, *145*15, 3096–3105. https://doi.org/10.1017/S0950268817002060

Hölzer, M., Barf, L.-M., Lamkiewicz, K., Vorimore, F., Lataretu, M., Favaroni, A., Schnee, C., Laroucau, K., Marz, M., & Sachse, K. 2020. Comparative Genome Analysis of 33 Chlamydia Strains Reveals Characteristic Features of Chlamydia Psittaci and Closely Related Species. *Pathogens*, *9*11, 899. https://doi.org/10.3390/pathogens9110899

Hutagalung, A. H., & Novick, P. J. 2011. Role of Rab GTPases in membrane traffic and cell physiology. *Physiological Reviews*, *91*1, 119–149. https://doi.org/10.1152/physrev.00059.2009

Hybiske, K., & Stephens, R. S. 2007. Mechanisms of host cell exit by the intracellular bacterium Chlamydia. *Proceedings of the National Academy of Sciences of the United States of America*, *104*27, 11430–11435. https://doi.org/10.1073/pnas.0703218104

Iliffe-Lee, E. R., & McClarty, G. 2000. Regulation of carbon metabolism in Chlamydia trachomatis. *Molecular Microbiology*, *38*1, 20–30. https://doi.org/10.1046/j.1365-2958.2000.02102.x

Jeffrey, B. M., Suchland, R. J., Quinn, K. L., Davidson, J. R., Stamm, W. E., & Rockey, D. D. 2010. Genome sequencing of recent clinical Chlamydia trachomatis strains identifies loci associated with tissue tropism and regions of apparent recombination. *Infection and Immunity*, *78*6, 2544–2553. https://doi.org/10.1128/IAI.01324-09

Johnson, R. M., & Kerr, M. S. 2015. Modeling the transcriptome of genital tract epithelial cells and macrophages in healthy mucosa versus mucosa inflamed by Chlamydia muridarum infection. *Pathogens and Disease*, *73*9, ftv100. https://doi.org/10.1093/femspd/ftv100

Kanaji, S., Iwahashi, J., Kida, Y., Sakaguchi, M., & Mihara, K. 2000. Characterization of the Signal That Directs Tom20 to the Mitochondrial Outer Membrane. *The Journal of Cell Biology*, *151*2, 277–288.

Kaul, R., Hoang, A., Yau, P., Bradbury, E. M., & Wenman, W. M. 1997. The chlamydial EUO gene encodes a histone H1-specific protease. *Journal of Bacteriology*, *179*18, 5928–5934.

Kebbi-Beghdadi, C., Pilloux, L., Martin, V., & Greub, G. 2020. Eukaryotic Cell Permeabilisation to Identify New Putative Chlamydial Type III Secretion System Effectors Secreted within Host Cell Cytoplasm. *Microorganisms*, *8*3, 361. https://doi.org/10.3390/microorganisms8030361

Knittler, M. R., & Sachse, K. 2015. Chlamydia psittaci: update on an underestimated zoonotic agent. *Pathogens and Disease*, *73*1, 1–15. https://doi.org/10.1093/femspd/ftu007

Koch-Edelmann, S., Banhart, S., Saied, E. M., Rose, L., Aeberhard, L., Laue, M., Doellinger, J., Arenz, C., & Heuer, D. 2017. The cellular ceramide transport protein CERT promotes Chlamydia psittaci infection and controls bacterial sphingolipid uptake. *Cellular Microbiology*, *19*10. https://doi.org/10.1111/cmi.12752

Koirala, S., Guo, Q., Kalia, R., Bui, H. T., Eckert, D. M., Frost, A., & Shaw, J. M. 2013. Interchangeable adaptors regulate mitochondrial dynamin assembly for membrane scission. *Proceedings of the National Academy of Sciences of the United States of America*, *110*15, E1342-1351. https://doi.org/10.1073/pnas.1300855110

Kokes, M., Dunn, J. D., Granek, J. A., Nguyen, B. D., Barker, J. R., Valdivia, R. H., & Bastidas, R. J. 2015. Integrating chemical mutagenesis and whole-genome sequencing as a platform for forward and reverse genetic analysis of Chlamydia. *Cell Host & Microbe*, *17*5, 716–725. https://doi.org/10.1016/j.chom.2015.03.014

Kong, F. Y. S., Tabrizi, S. N., Law, M., Vodstrcil, L. A., Chen, M., Fairley, C. K., Guy, R., Bradshaw, C., & Hocking, J. S. 2014. Azithromycin versus doxycycline for the treatment of genital chlamydia infection: a meta-analysis of randomized controlled trials. *Clinical*

Infectious Diseases: An Official Publication of the Infectious Diseases Society of America, *59*2, 193–205. https://doi.org/10.1093/cid/ciu220

Kostryukova, E. S., Korobova, F. V., Lazarev, V. N., Shkarupeta, M. M., Titova, G. A., Akopian, T. A., & Govorun, V. M. 2005. Location of C. trachomatis Inc Proteins during Expression of Their Genes in HeLa Cell Culture. *Bulletin of Experimental Biology and Medicine*, *139*5, 600–604. https://doi.org/10.1007/s10517-005-0355-6

Kumagai, K., Cherilyn, E. A., Ando, S., Engel, J. E., & Hanada, K. 2018. Both the N- and C-terminal regions of the Chlamydial inclusion protein D are required for interaction with the pleckstrin homology domain of the ceramide transport protein CERT. *Biochemical and Biophysical Research Communications*, *505*4, 1070–1076. https://doi.org/10.1016/j.bbrc.2018.09.168

Lamoth, F., & Greub, G. 2010. Amoebal pathogens as emerging causal agents of pneumonia. *FEMS Microbiology Reviews*, *34*3, 260–280. https://doi.org/10.1111/j.1574-6976.2009.00207.x

Lau, C.-Y., & Qureshi, A. K. 2002. Azithromycin versus doxycycline for genital chlamydial infections: a meta-analysis of randomized clinical trials. *Sexually Transmitted Diseases*, *29*9, 497–502. https://doi.org/10.1097/00007435-200209000-00001

Lawn, A. M., Blyth, W. A., & Taverne, J. 1973. Interactions of TRIC agents with macrophages and BHK-21 cells observed by electron microscopy. *The Journal of Hygiene*, *71*3, 515–528. https://doi.org/10.1017/s0022172400046507

Lee, Y.-H., Campbell, H. D., & Stallcup, M. R. 2004. Developmentally Essential Protein Flightless I Is a Nuclear Receptor Coactivator with Actin Binding Activity. *Molecular and Cellular Biology*, *24*5, 2103–2117. https://doi.org/10.1128/MCB.24.5.2103-2117.2004

Leiva, N., Capmany, A., & Damiani, M. T. 2013. Rab11-Family of Interacting Protein 2 associates with chlamydial inclusions through its Rab-binding domain and promotes bacterial multiplication. *Cellular Microbiology*, *15*1, 114–129. https://doi.org/10.1111/cmi.12035

Lemmon, M. A. 2008. Membrane recognition by phospholipid-binding domains. *Nature Reviews. Molecular Cell Biology*, *9*2, 99–111. https://doi.org/10.1038/nrm2328

Lenart, J., Andersen, A. A., & Rockey, D. D. 2001. Growth and Development of Tetracycline-Resistant Chlamydia suis. *Antimicrobial Agents and Chemotherapy*, *45*8, 2198–2203. https://doi.org/10.1128/AAC.45.8.2198-2203.2001

Lenz, G., Doron-Faigenboim, A., Ron, E. Z., Tuller, T., & Gophna, U. 2011. Sequence Features of E. coli mRNAs Affect Their Degradation. *PLOS ONE*, *6*12, e28544. https://doi.org/10.1371/journal.pone.0028544

Lev, S., Ben Halevy, D., Peretti, D., & Dahan, N. 2008. The VAP protein family: from cellular functions to motor neuron disease. *Trends in Cell Biology*, *18*6, 282–290. https://doi.org/10.1016/j.tcb.2008.03.006

Lewis, M. E., Belland, R. J., AbdelRahman, Y. M., Beatty, W. L., Aiyar, A. A., Zea, A. H., Greene, S. J., Marrero, L., Buckner, L. R., Tate, D. J., McGowin, C. L., Kozlowski, P. A., O'Brien, M., Lillis, R. A., Martin, D. H., & Quayle, A. J. 2014. Morphologic and molecular evaluation of Chlamydia trachomatis growth in human endocervix reveals distinct growth patterns. *Frontiers in Cellular and Infection Microbiology*, *4*, 71. https://doi.org/10.3389/fcimb.2014.00071

Li, J., Ji, L., Shi, W., Xie, J., & Zhang, Y. 2013. Trans-translation mediates tolerance to multiple antibiotics and stresses in Escherichia coli. *Journal of Antimicrobial Chemotherapy*, *68*11, 2477–2481. https://doi.org/10.1093/jac/dkt231

Liang, P., Rosas-Lemus, M., Patel, D., Fang, X., Tuz, K., & Juárez, O. 2018. Dynamic energy dependency of Chlamydia trachomatis on host cell metabolism during intracellular growth: Role of sodium-based energetics in chlamydial ATP generation. *The Journal of Biological Chemistry*, *293*2, 510–522. https://doi.org/10.1074/jbc.M117.797209

Liechti, G., Kuru, E., Packiam, M., Hsu, Y.-P., Tekkam, S., Hall, E., Rittichier, J. T., VanNieuwenhze, M., Brun, Y. V., & Maurelli, A. T. 2016. Pathogenic Chlamydia Lack a Classical Sacculus but Synthesize a Narrow, Mid-cell Peptidoglycan Ring, Regulated

by MreB, for Cell Division. *PLoS Pathogens*, *125*, e1005590. https://doi.org/10.1371/journal.ppat.1005590

Liechti, G. W. 2021. Localized Peptidoglycan Biosynthesis in Chlamydia trachomatis Conforms to the Polarized Division and Cell Size Reduction Developmental Models. *Frontiers in Microbiology*, *12*, 733850. https://doi.org/10.3389/fmicb.2021.733850

Liou, J., Kim, M. L., Heo, W. D., Jones, J. T., Myers, J. W., Ferrell, J. E., & Meyer, T. 2005. STIM is a Ca2+ sensor essential for Ca2+-store-depletion-triggered Ca2+ influx. *Current Biology: CB*, *15*13, 1235–1241. https://doi.org/10.1016/j.cub.2005.05.055

Litwin, J. 1959. The growth cycle of the psittacosis group of micro-organisms. *The Journal of Infectious Diseases*, *105*, 129–160. https://doi.org/10.1093/infdis/105.2.129

Loewen, C. J. R., Roy, A., & Levine, T. P. 2003. A conserved ER targeting motif in three families of lipid binding proteins and in Opi1p binds VAP. *The EMBO Journal*, *22*9, 2025–2035. https://doi.org/10.1093/emboj/cdg201

Lu, J., Wu, T., Zhang, B., Liu, S., Song, W., Qiao, J., & Ruan, H. 2021. Types of nuclear localization signals and mechanisms of protein import into the nucleus. *Cell Communication and Signaling*, *19*1, 60. https://doi.org/10.1186/s12964-021-00741-y

Lutter, E. I., Barger, A. C., Nair, V., & Hackstadt, T. 2013. Chlamydia trachomatis inclusion membrane protein CT228 recruits elements of the myosin phosphatase pathway to regulate release mechanisms. *Cell Reports*, *3*6, 1921–1931. https://doi.org/10.1016/j.celrep.2013.04.027

Lutter, E. I., Martens, C., & Hackstadt, T. 2012. Evolution and Conservation of Predicted Inclusion Membrane Proteins in Chlamydiae. *Comparative and Functional Genomics*, *2012*. https://doi.org/10.1155/2012/362104

Luu, W., Hart-Smith, G., Sharpe, L. J., & Brown, A. J. 2015. The terminal enzymes of cholesterol synthesis, DHCR24 and DHCR7, interact physically and functionally. *Journal of Lipid Research*, *56*4, 888–897. https://doi.org/10.1194/jlr.M056986

Madeira, F., Park, Y. M., Lee, J., Buso, N., Gur, T., Madhusoodanan, N., Basutkar, P., Tivey, A. R. N., Potter, S. C., Finn, R. D., & Lopez, R. 2019. The EMBL-EBI search and

sequence analysis tools APIs in 2019. *Nucleic Acids Research*, *47*W1, W636–W641. https://doi.org/10.1093/nar/gkz268

Malhotra, M., Sood, S., Mukherjee, A., Muralidhar, S., & Bala, M. 2013. Genital Chlamydia trachomatis: an update. *The Indian Journal of Medical Research*, *138*3, 303–316.

Manor, U., Bartholomew, S., Golani, G., Christenson, E., Kozlov, M., Higgs, H., Spudich, J., & Lippincott-Schwartz, J. 2015. A mitochondria-anchored isoform of the actin-nucleating spire protein regulates mitochondrial division. *ELife*, *4*, e08828. https://doi.org/10.7554/eLife.08828

Marangoni, A., Zalambani, C., Marziali, G., Salvo, M., Fato, R., Foschi, C., & Re, M. C. 2020. Low-dose doxycycline induces Chlamydia trachomatis persistence in HeLa cells. *Microbial Pathogenesis*, *147*, 104347. https://doi.org/10.1016/j.micpath.2020.104347

Maslow, A. S., Davis, C. H., Choong, J., & Wyrick, P. B. 1988. Estrogen enhances attachment of Chlamydia trachomatis to human endometrial epithelial cells in vitro. *American Journal of Obstetrics and Gynecology*, *159*4, 1006–1014. https://doi.org/10.1016/s0002-9378(88)80189-3

Massey, J. B. 2001. Interaction of ceramides with phosphatidylcholine, sphingomyelin and sphingomyelin/cholesterol bilayers. *Biochimica Et Biophysica Acta*, *1510*1–2, 167–184. https://doi.org/10.1016/s0005-2736(00)00344-8

Matsui, T., & Fukuda, M. 2013. Rab12 regulates mTORC1 activity and autophagy through controlling the degradation of amino-acid transporter PAT4. *EMBO Reports*, *14*5, 450–457. https://doi.org/10.1038/embor.2013.32

Matsui, T., & Fukuda, M. 2014. Methods of analysis of the membrane trafficking pathway from recycling endosomes to lysosomes. *Methods in Enzymology*, *534*, 195–206. https://doi.org/10.1016/B978-0-12-397926-1.00011-1

Matsui, T., Itoh, T., & Fukuda, M. 2011. Small GTPase Rab12 regulates constitutive degradation of transferrin receptor. *Traffic (Copenhagen, Denmark)*, *12*10, 1432–1443. https://doi.org/10.1111/j.1600-0854.2011.01240.x

Matsui, T., Noguchi, K., & Fukuda, M. 2014. Dennd3 Functions as a Guanine Nucleotide Exchange Factor for Small GTPase Rab12 in Mouse Embryonic Fibroblasts. *The Journal of Biological Chemistry*, *289*20, 13986–13995. https://doi.org/10.1074/jbc.M113.546689

Mauvezin, C., & Neufeld, T. P. 2015. Bafilomycin A1 disrupts autophagic flux by inhibiting both V-ATPase-dependent acidification and Ca-P60A/SERCA-dependent autophagosome-lysosome fusion. *Autophagy*, *11*8, 1437–1438. https://doi.org/10.1080/15548627.2015.1066957

McCray, B. A., Skordalakes, E., & Taylor, J. P. 2010. Disease mutations in Rab7 result in unregulated nucleotide exchange and inappropriate activation. *Human Molecular Genetics*, *19*6, 1033–1047. https://doi.org/10.1093/hmg/ddp567

McDade, J. E., Shepard, C. C., Fraser, D. W., Tsai, T. R., Redus, M. A., & Dowdle, W. R. 1977. Legionnaires' disease: isolation of a bacterium and demonstration of its role in other respiratory disease. *The New England Journal of Medicine*, *297*22, 1197–1203. https://doi.org/10.1056/NEJM197712012972202

Mehlitz, A., Eylert, E., Huber, C., Lindner, B., Vollmuth, N., Karunakaran, K., Goebel, W., Eisenreich, W., & Rudel, T. 2017. Metabolic adaptation of Chlamydia trachomatis to mammalian host cells. *Molecular Microbiology*, *103*6, 1004–1019. https://doi.org/10.1111/mmi.13603

Mestrovic, T., & Ljubin-Sternak, S. 2018. Molecular mechanisms of Chlamydia trachomatis resistance to antimicrobial drugs. *Frontiers in Bioscience (Landmark Edition)*, *23*, 656–670. https://doi.org/10.2741/4611

Meyer, C., Garzia, A., Morozov, P., Molina, H., & Tuschl, T. 2020. The G3BP1-Family-USP10 Deubiquitinase Complex Rescues Ubiquitinated 40S Subunits of Ribosomes Stalled in Translation from Lysosomal Degradation. *Molecular Cell*, *77*6, 1193-1205.e5. https://doi.org/10.1016/j.molcel.2019.12.024

Michalska, K., Wellington, S., Maltseva, N., Jedrzejczak, R., Selem-Mojica, N., Rosas-Becerra, L. R., Barona-Gómez, F., Hung, D. T., & Joachimiak, A. 2021. Catalytically impaired

TrpA subunit of tryptophan synthase from Chlamydia trachomatis is an allosteric regulator of TrpB. *Protein Science : A Publication of the Protein Society*, *30*9, 1904–1918. https://doi.org/10.1002/pro.4143

Mirrashidi, K. M., Elwell, C. A., Verschueren, E., Johnson, J. R., Frando, A., Von Dollen, J., Rosenberg, O., Gulbahce, N., Jang, G., Johnson, T., Jager, S., Gopalakrishnan, A. M., Sherry, J., Dunn, J. D., Olive, A., Penn, B., Shales, M., Starnbach, M. N., Derre, I., … Engel, J. 2015. Global Mapping of the Inc-Human Interactome Reveals that Retromer Restricts Chlamydia Infection. *Cell Host & Microbe*, *18*1, 109–121. https://doi.org/10.1016/j.chom.2015.06.004

Mital, J., Miller, N. J., Fischer, E. R., & Hackstadt, T. 2010. Specific chlamydial inclusion membrane proteins associate with active Src family kinases in microdomains that interact with the host microtubule network. *Cellular Microbiology*, *12*9, 1235–1249. https://doi.org/10.1111/j.1462-5822.2010.01465.x

Molano, M., Meijer, C. J. L. M., Weiderpass, E., Arslan, A., Posso, H., Franceschi, S., Ronderos, M., Muñoz, N., & van den Brule, A. J. C. 2005. The natural course of Chlamydia trachomatis infection in asymptomatic Colombian women: a 5-year follow-up study. *The Journal of Infectious Diseases*, *191*6, 907–916. https://doi.org/10.1086/428287

Moulder, J. W. 1985. Comparative biology of intracellular parasitism. *Microbiological Reviews*, *49*3, 298–337.

Moulder, J. W., Levy, N. J., & Schulman, L. P. 1980. Persistent infection of mouse fibroblasts (L cells) with Chlamydia psittaci: evidence for a cryptic chlamydial form. *Infection and Immunity*, *30*3, 874–883. https://doi.org/10.1128/iai.30.3.874-883.1980

Mpiga, P., & Ravaoarinoro, M. 2006. Chlamydia trachomatis persistence: an update. *Microbiological Research*, *161*1, 9–19. https://doi.org/10.1016/j.micres.2005.04.004

Nagahama, M., Ohnishi, M., Kawate, Y., Matsui, T., Miyake, H., Yuasa, K., Tani, K., Tagaya, M., & Tsuji, A. 2009. UBXD1 is a VCP-interacting protein that is involved in ER-

associated degradation. *Biochemical and Biophysical Research Communications*, *382*2, 303–308. https://doi.org/10.1016/j.bbrc.2009.03.012

Ness, R. B., Soper, D. E., Richter, H. E., Randall, H., Peipert, J. F., Nelson, D. B., Schubeck, D., McNeeley, S. G., Trout, W., Bass, D. C., Hutchison, K., Kip, K., & Brunham, R. C. 2008. Chlamydia antibodies, chlamydia heat shock protein, and adverse sequelae after pelvic inflammatory disease: the PID Evaluation and Clinical Health (PEACH) Study. *Sexually Transmitted Diseases*, *35*2, 129–135. https://doi.org/10.1097/olq.0b013e3181557c25

Newhall, W. J., & Jones, R. B. 1983. Disulfide-linked oligomers of the major outer membrane protein of chlamydiae. *Journal of Bacteriology*, *154*2, 998–1001. https://doi.org/10.1128/jb.154.2.998-1001.1983

O'Loughlin, T., Masters, T. A., & Buss, F. 2018. The MYO6 interactome reveals adaptor complexes coordinating early endosome and cytoskeletal dynamics. *EMBO Reports*, *19*4, e44884. https://doi.org/10.15252/embr.201744884

Olson, M. G., Ouellette, S. P., & Rucks, E. A. 2020. A Meta-Analysis of Affinity Purification-Mass Spectrometry Experimental Systems Used to Identify Eukaryotic and Chlamydial Proteins at the Chlamydia trachomatis Inclusion Membrane. *Journal of Proteomics*, *212*, 103595. https://doi.org/10.1016/j.jprot.2019.103595

Omar, J., Rosenbaum, E., Efergan, A., Sneineh, B. A., Yeheskel, A., Maruta, Y., Fukuda, M., & Sagi-Eisenberg, R. 2021. Biochemical and structural insights into Rab12 interactions with RILP and its family members. *Scientific Reports*, *11*. https://doi.org/10.1038/s41598-021-89394-y

Omasits, U., Ahrens, C. H., Müller, S., & Wollscheid, B. 2014. Protter: interactive protein feature visualization and integration with experimental proteomic data. *Bioinformatics*, *30*6, 884–886. https://doi.org/10.1093/bioinformatics/btt607

Østergaard, O., Follmann, F., Olsen, A. W., Heegaard, N. H., Andersen, P., & Rosenkrands, I. 2016. Quantitative Protein Profiling of Chlamydia trachomatis Growth Forms Reveals

Defense Strategies Against Tryptophan Starvation. *Molecular & Cellular Proteomics : MCP*, *15*12, 3540–3550. https://doi.org/10.1074/mcp.M116.061986

Ouellette, S. P., & Carabeo, R. A. 2010. A Functional Slow Recycling Pathway of Transferrin is Required for Growth of Chlamydia. *Frontiers in Microbiology*, *1*, 112. https://doi.org/10.3389/fmicb.2010.00112

Ouellette, S. P., Hatch, T. P., AbdelRahman, Y. M., Rose, L. A., Belland, R. J., & Byrne, G. I. 2006. Global transcriptional upregulation in the absence of increased translation in Chlamydia during IFNgamma-mediated host cell tryptophan starvation. *Molecular Microbiology*, *62*5, 1387–1401. https://doi.org/10.1111/j.1365-2958.2006.05465.x

Ouellette, S. P., Karimova, G., Subtil, A., & Ladant, D. 2012. Chlamydia co-opts the rod shape-determining proteins MreB and Pbp2 for cell division. *Molecular Microbiology*, *85*1, 164–178. https://doi.org/10.1111/j.1365-2958.2012.08100.x

Ouellette, S. P., Lee, J., & Cox, J. V. 2020. Division without Binary Fission: Cell Division in the FtsZ-Less Chlamydia. *Journal of Bacteriology*, *202*17, e00252-20. https://doi.org/10.1128/JB.00252-20

Ouellette, S. P., Rueden, K. J., Gauliard, E., Persons, L., Boer, P. A. de, & Ladant, D. 2014. Analysis of MreB interactors in Chlamydia reveals a RodZ homolog but fails to detect an interaction with MraY. *Frontiers in Microbiology*, *5*. https://doi.org/10.3389/fmicb.2014.00279

Ouellette, S. P., Rueden, K. J., & Rucks, E. A. 2016. Tryptophan Codon-Dependent Transcription in Chlamydia pneumoniae during Gamma Interferon-Mediated Tryptophan Limitation. *Infection and Immunity*, *84*9, 2703–2713. https://doi.org/10.1128/IAI.00377-16

Páez-Canro, C., Alzate, J. P., González, L. M., Rubio-Romero, J. A., Lethaby, A., & Gaitán, H. G. 2019. Antibiotics for treating urogenital Chlamydia trachomatis infection in men and non-pregnant women. *The Cochrane Database of Systematic Reviews*, *1*, CD010871. https://doi.org/10.1002/14651858.CD010871.pub2

Page, L. A. 1959. Experimental Ornithosis in Turkeys. *Avian Diseases*, *3*1, 51–66. https://doi.org/10.2307/1587757

Panzetta, M. E., Valdivia, R. H., & Saka, H. A. 2018. Chlamydia Persistence: A Survival Strategy to Evade Antimicrobial Effects in-vitro and in-vivo. *Frontiers in Microbiology*, *9*, 3101. https://doi.org/10.3389/fmicb.2018.03101

Parnham, M. J., Erakovic Haber, V., Giamarellos-Bourboulis, E. J., Perletti, G., Verleden, G. M., & Vos, R. 2014. Azithromycin: mechanisms of action and their relevance for clinical applications. *Pharmacology & Therapeutics*, *143*2, 225–245. https://doi.org/10.1016/j.pharmthera.2014.03.003

Partridge, S. R., Kwong, S. M., Firth, N., & Jensen, S. O. 2018. Mobile Genetic Elements Associated with Antimicrobial Resistance. *Clinical Microbiology Reviews*, *31*4, e00088-17. https://doi.org/10.1128/CMR.00088-17

Paul, B., Kim, H. S., Kerr, M. C., Huston, W. M., Teasdale, R. D., & Collins, B. M. 2017. Structural basis for the hijacking of endosomal sorting nexin proteins by Chlamydia trachomatis. *ELife*, *6*, e22311. https://doi.org/10.7554/eLife.22311

Pickens, C. J., Johnson, S. N., Pressnall, M. M., Leon, M. A., & Berkland, C. J. 2018. Practical Considerations, Challenges, and Limitations of Bioconjugation via Azide-Alkyne Cycloaddition. *Bioconjugate Chemistry*, *29*3, 686–701. https://doi.org/10.1021/acs.bioconjchem.7b00633

Pokorzynski, N. D., Brinkworth, A. J., & Carabeo, R. 2019. A bipartite iron-dependent transcriptional regulation of the tryptophan salvage pathway in Chlamydia trachomatis. *ELife*, *8*, e42295. https://doi.org/10.7554/eLife.42295

Pokorzynski, N. D., Hatch, N. D., Ouellette, S. P., & Carabeo, R. A. 2020. The iron-dependent repressor YtgR is a tryptophan-dependent attenuator of the trpRBA operon in Chlamydia trachomatis. *Nature Communications*, *11*, 6430. https://doi.org/10.1038/s41467-020-20181-5

Ponting, C. P., & Aravind, L. 1999. START: a lipid-binding domain in StAR, HD-ZIP and signalling proteins. *Trends in Biochemical Sciences*, *24*4, 130–132. https://doi.org/10.1016/s0968-0004(99)01362-6

Pooley, R. D., Moynihan, K. L., Soukoulis, V., Reddy, S., Francis, R., Lo, C., Ma, L.-J., & Bader, D. M. 2008. Murine CENPF interacts with syntaxin 4 in the regulation of vesicular transport. *Journal of Cell Science*, *121*Pt 20, 3413–3421. https://doi.org/10.1242/jcs.032847

Puri, C., Renna, M., Bento, C. F., Moreau, K., & Rubinsztein, D. C. 2013. Diverse Autophagosome Membrane Sources Coalesce in Recycling Endosomes. *Cell*, *154*6, 1285–1299. https://doi.org/10.1016/j.cell.2013.08.044

Qin, L., Guo, J., Zheng, Q., & Zhang, H. 2016. BAG2 structure, function and involvement in disease. *Cellular & Molecular Biology Letters*, *21*1, 18. https://doi.org/10.1186/s11658-016-0020-2

Ramos-Morales, F. 2012. Impact of Salmonella enterica Type III Secretion System Effectors on the Eukaryotic Host Cell. *ISRN Cell Biology*, *2012*, e787934. https://doi.org/10.5402/2012/787934

Raulston, J. E. 1997. Response of Chlamydia trachomatis serovar E to iron restriction in vitro and evidence for iron-regulated chlamydial proteins. *Infection and Immunity*, *65*11, 4539–4547. https://doi.org/10.1128/iai.65.11.4539-4547.1997

Recuero-Checa, M. A., Sharma, M., Lau, C., Watkins, P. A., Gaydos, C. A., & Dean, D. 2016. Chlamydia trachomatis growth and development requires the activity of host Long-chain Acyl-CoA Synthetases (ACSLs). *Scientific Reports*, *6*, 23148. https://doi.org/10.1038/srep23148

Rejman Lipinski, A., Heymann, J., Meissner, C., Karlas, A., Brinkmann, V., Meyer, T. F., & Heuer, D. 2009. Rab6 and Rab11 Regulate Chlamydia trachomatis Development and Golgin-84-Dependent Golgi Fragmentation. *PLoS Pathogens*, *5*10, e1000615. https://doi.org/10.1371/journal.ppat.1000615

Reveneau, N., Crane, D. D., Fischer, E., & Caldwell, H. D. 2005. Bactericidal Activity of First-Choice Antibiotics against Gamma Interferon-Induced Persistent Infection of Human Epithelial Cells by Chlamydia trachomatis. *Antimicrobial Agents and Chemotherapy*. https://doi.org/10.1128/AAC.49.5.1787-1793.2005

Reymond, N., Borg, J. P., Lecocq, E., Adelaide, J., Campadelli-Fiume, G., Dubreuil, P., & Lopez, M. 2000. Human nectin3/PRR3: a novel member of the PVR/PRR/nectin family that interacts with afadin. *Gene*, *255*2, 347–355. https://doi.org/10.1016/s0378-1119(00)00316-4

Ritz, D., Vuk, M., Kirchner, P., Bug, M., Schütz, S., Hayer, A., Bremer, S., Lusk, C., Baloh, R. H., Lee, H., Glatter, T., Gstaiger, M., Aebersold, R., Weihl, C. C., & Meyer, H. 2011. Endolysosomal sorting of ubiquitylated caveolin-1 is regulated by VCP and UBXD1 and impaired by VCP disease mutations. *Nature Cell Biology*, *13*9, 1116–1123. https://doi.org/10.1038/ncb2301

Robertson, D. K., Gu, L., Rowe, R. K., & Beatty, W. L. 2009. Inclusion Biogenesis and Reactivation of Persistent Chlamydia trachomatis Requires Host Cell Sphingolipid Biosynthesis. *PLoS Pathogens*, *5*11, e1000664. https://doi.org/10.1371/journal.ppat.1000664

Robertson, J. N., Ward, M. E., Conway, D., & Caul, E. O. 1987. Chlamydial and gonococcal antibodies in sera of infertile women with tubal obstruction. *Journal of Clinical Pathology*, *40*4, 377–383. https://doi.org/10.1136/jcp.40.4.377

Roche, E. D., & Sauer, R. T. 1999. SsrA-mediated peptide tagging caused by rare codons and tRNA scarcity. *The EMBO Journal*, *18*16, 4579–4589. https://doi.org/10.1093/emboj/18.16.4579

Rockey, D. D., Fischer, E. R., & Hackstadt, T. 1996. Temporal analysis of the developing Chlamydia psittaci inclusion by use of fluorescence and electron microscopy. *Infection and Immunity*, *64*10, 4269–4278.

Rockey, D. D., Grosenbach, D., Hruby, D. E., Peacock, M. G., Heinzen, R. A., & Hackstadt, T. 1997. Chlamydia psittaci IncA is phosphorylated by the host cell and is exposed on the

cytoplasmic face of the developing inclusion. *Molecular Microbiology*, *24*1, 217–228. https://doi.org/10.1046/j.1365-2958.1997.3371700.x

Rockey, D. D., Heinzen, R. A., & Hackstadt, T. 1995. Cloning and characterization of a Chlamydia psittaci gene coding for a protein localized in the inclusion membrane of infected cells. *Molecular Microbiology*, *15*4, 617–626. https://doi.org/10.1111/j.1365-2958.1995.tb02371.x

Rodnina, M. V. 2018. Translation in Prokaryotes. *Cold Spring Harbor Perspectives in Biology*, *10*9, a032664. https://doi.org/10.1101/cshperspect.a032664

Ronzone, E., & Paumet, F. 2013. Two coiled-coil domains of Chlamydia trachomatis IncA affect membrane fusion events during infection. *PloS One*, *8*7, e69769. https://doi.org/10.1371/journal.pone.0069769

Roundtree, I. A., Luo, G.-Z., Zhang, Z., Wang, X., Zhou, T., Cui, Y., Sha, J., Huang, X., Guerrero, L., Xie, P., He, E., Shen, B., & He, C. 2017. YTHDC1 mediates nuclear export of N6-methyladenosine methylated mRNAs. *ELife*, *6*, e31311. https://doi.org/10.7554/eLife.31311

Roux, K. J., Kim, D. I., Raida, M., & Burke, B. 2012. A promiscuous biotin ligase fusion protein identifies proximal and interacting proteins in mammalian cells. *The Journal of Cell Biology*, *196*6, 801–810. https://doi.org/10.1083/jcb.201112098

Rydell, G. E., Renard, H.-F., Garcia-Castillo, M.-D., Dingli, F., Loew, D., Lamaze, C., Römer, W., & Johannes, L. 2014. Rab12 localizes to Shiga toxin-induced plasma membrane invaginations and controls toxin transport. *Traffic (Copenhagen, Denmark)*, *15*7, 772–787. https://doi.org/10.1111/tra.12173

Rzomp, K. A., Moorhead, A. R., & Scidmore, M. A. 2006. The GTPase Rab4 Interacts with Chlamydia trachomatis Inclusion Membrane Protein CT229. *Infection and Immunity*, *74*9, 5362–5373. https://doi.org/10.1128/IAI.00539-06

Rzomp, K. A., Scholtes, L. D., Briggs, B. J., Whittaker, G. R., & Scidmore, M. A. 2003. Rab GTPases Are Recruited to Chlamydial Inclusions in Both a Species-Dependent and

Species-Independent Manner. *Infection and Immunity*, *71*10, 5855–5870. https://doi.org/10.1128/IAI.71.10.5855-5870.2003

Saka, H. A., Thompson, J. W., Chen, Y.-S., Kumar, Y., Dubois, L. G., Moseley, M. A., & Valdivia, R. H. 2011. Quantitative proteomics reveals metabolic and pathogenic properties of Chlamydia trachomatis developmental forms. *Molecular Microbiology*, *82*5, 1185–1203. https://doi.org/10.1111/j.1365-2958.2011.07877.x

Schachter, J., & Caldwell, H. D. 1980. Chlamydiae. *Annual Review of Microbiology*, *34*, 285–309. https://doi.org/10.1146/annurev.mi.34.100180.001441

Schneider-Poetsch, T., Ju, J., Eyler, D. E., Dang, Y., Bhat, S., Merrick, W. C., Green, R., Shen, B., & Liu, J. O. 2010. Inhibition of Eukaryotic Translation Elongation by Cycloheximide and Lactimidomycin. *Nature Chemical Biology*, *6*3, 209–217. https://doi.org/10.1038/nchembio.304

Schöfl, G., Voigt, A., Litsche, K., Sachse, K., & Saluz, H. P. 2011. Complete Genome Sequences of Four Mammalian Isolates of Chlamydophila psittaci▿. *Journal of Bacteriology*, *193*16, 4258. https://doi.org/10.1128/JB.05382-11

Schroder, K., Hertzog, P. J., Ravasi, T., & Hume, D. A. 2004. Interferon-γ: an overview of signals, mechanisms and functions. *Journal of Leukocyte Biology*, *75*2, 163–189. https://doi.org/10.1189/jlb.0603252

Scidmore, M. A., & Hackstadt, T. 2001. Mammalian 14-3-3β associates with the Chlamydia trachomatis inclusion membrane via its interaction with IncG. *Molecular Microbiology*, *39*6, 1638–1650. https://doi.org/10.1046/j.1365-2958.2001.02355.x

Scidmore-Carlson, M. A., Shaw, E. I., Dooley, C. A., Fischer, E. R., & Hackstadt, T. 1999. Identification and characterization of a Chlamydia trachomatis early operon encoding four novel inclusion membrane proteins. *Molecular Microbiology*, *33*4, 753–765. https://doi.org/10.1046/j.1365-2958.1999.01523.x

Semenkov, Yu. P., Makarov, E. m., Makhno, V. i., & Kirillov, S. v. 1982. Kinetic aspects of tetracycline action on the acceptor (A) site of Escherichia coli ribosomes. *FEBS Letters*, *144*1, 125–129. https://doi.org/10.1016/0014-5793(82)80584-X

Shannon, P., Markiel, A., Ozier, O., Baliga, N. S., Wang, J. T., Ramage, D., Amin, N., Schwikowski, B., & Ideker, T. 2003. Cytoscape: a software environment for integrated models of biomolecular interaction networks. *Genome Research*, *13*11, 2498–2504. https://doi.org/10.1101/gr.1239303

Shaw, E. I., Dooley, C. A., Fischer, E. R., Scidmore, M. A., Fields, K. A., & Hackstadt, T. 2000. Three temporal classes of gene expression during the Chlamydia trachomatis developmental cycle. *Molecular Microbiology*, *37*4, 913–925. https://doi.org/10.1046/j.1365-2958.2000.02057.x

Shkarupeta, M. M., Kostrjukova, E. S., Lazarev, V. N., Levitskii, S. A., Basovskii, Yu. I., & Govorun, V. M. 2008. Localization of C. trachomatis inc proteins in expression of their genes in HeLa cell culture. *Bulletin of Experimental Biology and Medicine*, *146*2, 237–242. https://doi.org/10.1007/s10517-008-0254-8

Sixt, B. S. 2020. Host cell death during infection with Chlamydia: a double-edged sword. *FEMS Microbiology Reviews*, *45*1, fuaa043. https://doi.org/10.1093/femsre/fuaa043

Skilton, R. J., Cutcliffe, L. T., Barlow, D., Wang, Y., Salim, O., Lambden, P. R., & Clarke, I. N. 2009. Penicillin Induced Persistence in Chlamydia trachomatis: High Quality Time Lapse Video Analysis of the Developmental Cycle. *PLoS ONE*, *4*11, e7723. https://doi.org/10.1371/journal.pone.0007723

Soboloff, J., Spassova, M. A., Hewavitharana, T., He, L.-P., Xu, W., Johnstone, L. S., Dziadek, M. A., & Gill, D. L. 2006. STIM2 is an inhibitor of STIM1-mediated store-operated Ca2+ Entry. *Current Biology: CB*, *16*14, 1465–1470. https://doi.org/10.1016/j.cub.2006.05.051

Soupene, E., Wang, D., & Kuypers, F. A. 2015. Remodeling of host phosphatidylcholine by Chlamydia acyltransferase is regulated by acyl-CoA binding protein ACBD6 associated with lipid droplets. *MicrobiologyOpen*, *4*2, 235–251. https://doi.org/10.1002/mbo3.234

Stanhope, R., Flora, E., Bayne, C., & Derré, I. 2017. IncV, a FFAT motif-containing Chlamydia protein, tethers the endoplasmic reticulum to the pathogen-containing vacuole.

Proceedings of the National Academy of Sciences of the United States of America, *114*45, 12039–12044. https://doi.org/10.1073/pnas.1709060114

Stephens, R. S., Kalman, S., Lammel, C., Fan, J., Marathe, R., Aravind, L., Mitchell, W., Olinger, L., Tatusov, R. L., Zhao, Q., Koonin, E. V., & Davis, R. W. 1998. Genome sequence of an obligate intracellular pathogen of humans: Chlamydia trachomatis. *Science (New York, N.Y.)*, *282*5389, 754–759. https://doi.org/10.1126/science.282.5389.754

Stephens, R. S., Koshiyama, K., Lewis, E., & Kubo, A. 2001. Heparin-binding outer membrane protein of chlamydiae. *Molecular Microbiology*, *40*3, 691–699. https://doi.org/10.1046/j.1365-2958.2001.02418.x

Su, H., & Caldwell, H. D. 1998. Sulfated Polysaccharides and a Synthetic Sulfated Polymer Are Potent Inhibitors of Chlamydia trachomatis Infectivity In Vitro but Lack Protective Efficacy in an In Vivo Murine Model of Chlamydial Genital Tract Infection. *Infection and Immunity*, *66*3, 1258–1260.

Su, H., Raymond, L., Rockey, D. D., Fischer, E., Hackstadt, T., & Caldwell, H. D. 1996. A recombinant Chlamydia trachomatis major outer membrane protein binds to heparan sulfate receptors on epithelial cells. *Proceedings of the National Academy of Sciences of the United States of America*, *93*20, 11143–11148.

Suchland, R. J., Dimond, Z. E., Putman, T. E., & Rockey, D. D. 2017. Demonstration of Persistent Infections and Genome Stability by Whole-Genome Sequencing of Repeat-Positive, Same-Serovar Chlamydia trachomatis Collected From the Female Genital Tract. *The Journal of Infectious Diseases*, *215*11, 1657–1665. https://doi.org/10.1093/infdis/jix155

Suchland, R. J., Sandoz, K. M., Jeffrey, B. M., Stamm, W. E., & Rockey, D. D. 2009. Horizontal Transfer of Tetracycline Resistance among Chlamydia spp. In Vitro. *Antimicrobial Agents and Chemotherapy*, *53*11, 4604–4611. https://doi.org/10.1128/AAC.00477-09

Sun, Q., Yong, X., Sun, X., Yang, F., Dai, Z., Gong, Y., Zhou, L., Zhang, X., Niu, D., Dai, L., Liu, J.-J., & Jia, D. 2017. Structural and functional insights into sorting nexin 5/6

interaction with bacterial effector IncE. *Signal Transduction and Targeted Therapy*, *2*, 17030. https://doi.org/10.1038/sigtrans.2017.30

Tamura, A., & Manire, G. P. 1967. Preparation and Chemical Composition of the Cell Membranes of Developmental Reticulate Forms of Meningopneumonitis Organisms. *Journal of Bacteriology*, *944*, 1184–1188.

Tang, T., Wu, H., Chen, X., Chen, L., Liu, L., Li, Z., Bai, Q., Chen, Y., & Chen, L. 2021. The Hypothetical Inclusion Membrane Protein CPSIT_0846 Regulates Mitochondrial-Mediated Host Cell Apoptosis via the ERK/JNK Signaling Pathway. *Frontiers in Cellular and Infection Microbiology*, *11*, 607422. https://doi.org/10.3389/fcimb.2021.607422

Tao, S., Kaul, R., & Wenman, W. M. 1991. Identification and nucleotide sequence of a developmentally regulated gene encoding a eukaryotic histone H1-like protein from Chlamydia trachomatis. *Journal of Bacteriology*, *173*9, 2818–2822. https://doi.org/10.1128/jb.173.9.2818-2822.1991

Taraktchoglou, M., Pacey, A. A., Turnbull, J. E., & Eley, A. 2001. Infectivity of Chlamydia trachomatis Serovar LGV but Not E Is Dependent on Host Cell Heparan Sulfate. *Infection and Immunity*, *69*2, 968–976. https://doi.org/10.1128/IAI.69.2.968-976.2001

Thomas, S., Kumar, R. S., & Brumeanu, T.-D. 2004. Role of lipid rafts in T cells. *Archivum Immunologiae Et Therapiae Experimentalis*, *52*4, 215–224.

Thompson, C. C., & Carabeo, R. A. 2011. An optimal method of iron starvation of the obligate intracellular pathogen, Chlamydia trachomatis. *Frontiers in Microbiology*, *2*, 20. https://doi.org/10.3389/fmicb.2011.00020

Todd, W. J., & Caldwell, H. D. 1985. The Interaction of Chlamydia trachomatis with Host Cells: Ultrastructural Studies of the Mechanism of Release of a Biovar II Strain from HeLa 229 Cells. *The Journal of Infectious Diseases*, *151*6, 1037–1044. https://doi.org/10.1093/infdis/151.6.1037

Trousdale, C., & Kim, K. 2015. Retromer: Structure, function, and roles in mammalian disease. *European Journal of Cell Biology*, *94*11, 513–521. https://doi.org/10.1016/j.ejcb.2015.07.002

Turpin-Nolan, S. M., & Brüning, J. C. 2020. The role of ceramides in metabolic disorders: when size and localization matters. *Nature Reviews Endocrinology*, *16*4, 224–233. https://doi.org/10.1038/s41574-020-0320-5

van Hoek, A. H. A. M., Mevius, D., Guerra, B., Mullany, P., Roberts, A. P., & Aarts, H. J. M. 2011. Acquired Antibiotic Resistance Genes: An Overview. *Frontiers in Microbiology*, *2*, 203. https://doi.org/10.3389/fmicb.2011.00203

Van Lent, S., Piet, J. R., Beeckman, D., van der Ende, A., Van Nieuwerburgh, F., Bavoil, P., Myers, G., Vanrompay, D., & Pannekoek, Y. 2012. Full Genome Sequences of All Nine Chlamydia psittaci Genotype Reference Strains. *Journal of Bacteriology*, *194*24, 6930–6931. https://doi.org/10.1128/JB.01828-12

van Ooij, C., Kalman, L., van Ijzendoorn, null, Nishijima, M., Hanada, K., Mostov, K., & Engel, J. N. 2000. Host cell-derived sphingolipids are required for the intracellular growth of Chlamydia trachomatis. *Cellular Microbiology*, *2*6, 627–637. https://doi.org/10.1046/j.1462-5822.2000.00077.x

Vanrompay, D., Ducatelle, R., & Haesebrouck, F. 1995. Chlamydia psittaci infections: a review with emphasis on avian chlamydiosis. *Veterinary Microbiology*, *45*2, 93–119. https://doi.org/10.1016/0378-1135(95)00033-7

Vaughn, B., & Abu Kwaik, Y. 2021. Idiosyncratic Biogenesis of Intracellular Pathogens-Containing Vacuoles. *Frontiers in Cellular and Infection Microbiology*, *11*, 722433. https://doi.org/10.3389/fcimb.2021.722433

Wasylnka, J. A., Bakowski, M. A., Szeto, J., Ohlson, M. B., Trimble, W. S., Miller, S. I., & Brumell, J. H. 2008. Role for Myosin II in Regulating Positioning of Salmonella-Containing Vacuoles and Intracellular Replication. *Infection and Immunity*, *76*6, 2722–2735. https://doi.org/10.1128/IAI.00152-08

Watabe-Uchida, M., John, K. A., Janas, J. A., Newey, S. E., & Van Aelst, L. 2006. The Rac activator DOCK7 regulates neuronal polarity through local phosphorylation of stathmin/Op18. *Neuron*, *51*6, 727–739. https://doi.org/10.1016/j.neuron.2006.07.020

Witkin, S. S., Minis, E., Athanasiou, A., Leizer, J., & Linhares, I. M. 2017. Chlamydia trachomatis: the Persistent Pathogen. *Clinical and Vaccine Immunology : CVI*, *24*10. https://doi.org/10.1128/CVI.00203-17

Wojnacki, J., & Galli, T. 2018. A new actin-binding domain glues autophagy together. *The Journal of Biological Chemistry*, *293*12, 4575–4576. https://doi.org/10.1074/jbc.H118.002041

Wolf, K., Fischer, E., & Hackstadt, T. 2000. Ultrastructural Analysis of Developmental Events in Chlamydia pneumoniae-Infected Cells. *Infection and Immunity*, *68*4, 2379–2385.

Wong, C.-H., Chan, H., Ho, C.-Y., Lai, S.-K., Chan, K.-S., Koh, C.-G., & Li, H.-Y. 2009. Apoptotic histone modification inhibits nuclear transport by regulating RCC1. *Nature Cell Biology*, *11*1, 36–45. https://doi.org/10.1038/ncb1810

Workowski, K. A., Bachmann, L. H., Chan, P. A., Johnston, C. M., Muzny, C. A., Park, I., Reno, H., Zenilman, J. M., & Bolan, G. A. 2021. Sexually Transmitted Infections Treatment Guidelines, 2021. *MMWR Recommendations and Reports*, *70*4, 1–187. https://doi.org/10.15585/mmwr.rr7004a1

Wright, H. R., Turner, A., & Taylor, H. R. 2008. Trachoma. *Lancet (London, England)*, *371*9628, 1945–1954. https://doi.org/10.1016/S0140-6736(08)60836-3

Wu, H., Wang, C., Jiang, C., Xie, Y., Liu, L., Song, Y., Ma, X., & Wu, Y. 2016. Localization and characterization of two putative TMH family proteins in Chlamydia psittaci. *Microbiological Research*, *183*, 19–25. https://doi.org/10.1016/j.micres.2015.11.005

Wylie, J. L., Hatch, G. M., & McClarty, G. 1997. Host cell phospholipids are trafficked to and then modified by Chlamydia trachomatis. *Journal of Bacteriology*, *179*23, 7233–7242. https://doi.org/10.1128/jb.179.23.7233-7242.1997

Wyrick, P. B. 2010. Chlamydia trachomatis Persistence in Vitro – An Overview. *The Journal of Infectious Diseases*, *201*Suppl 2, S88–S95. https://doi.org/10.1086/652394

Xu, C., Wang, X., Liu, K., Roundtree, I. A., Tempel, W., Li, Y., Lu, Z., He, C., & Min, J. 2014. Structural basis for selective binding of m6A RNA by the YTHDC1 YTH domain. *Nature Chemical Biology*, *10*11, 927–929. https://doi.org/10.1038/nchembio.1654

Xu, J., Fotouhi, M., & McPherson, P. S. 2015. Phosphorylation of the exchange factor DENND3 by ULK in response to starvation activates Rab12 and induces autophagy. *EMBO Reports*, *16*6, 709–718. https://doi.org/10.15252/embr.201440006

Xu, J., Kozlov, G., McPherson, P. S., & Gehring, K. 2018. A PH-like domain of the Rab12 guanine nucleotide exchange factor DENND3 binds actin and is required for autophagy. *The Journal of Biological Chemistry*, *293*12, 4566–4574. https://doi.org/10.1074/jbc.RA117.001446

Xue, Y., Zheng, H., Mai, Z., Qin, X., Chen, W., Huang, T., Chen, D., & Zheng, L. 2017. An in vitro model of azithromycin-induced persistent Chlamydia trachomatis infection. *FEMS Microbiology Letters*, *364*14, fnx145. https://doi.org/10.1093/femsle/fnx145

Yao, J., Abdelrahman, Y. M., Robertson, R. M., Cox, J. V., Belland, R. J., White, S. W., & Rock, C. O. 2014. Type II Fatty Acid Synthesis Is Essential for the Replication of Chlamydia trachomatis*. *Journal of Biological Chemistry*, *289*32, 22365–22376. https://doi.org/10.1074/jbc.M114.584185

Yasir, M., Pachikara, N. D., Bao, X., Pan, Z., & Fan, H. 2011. Regulation of Chlamydial Infection by Host Autophagy and Vacuolar ATPase-Bearing Organelles ▿. *Infection and Immunity*, *79*10, 4019–4028. https://doi.org/10.1128/IAI.05308-11

Yoon, Y., Krueger, E. W., Oswald, B. J., & McNiven, M. A. 2003. The mitochondrial protein hFis1 regulates mitochondrial fission in mammalian cells through an interaction with the dynamin-like protein DLP1. *Molecular and Cellular Biology*, *23*15, 5409–5420. https://doi.org/10.1128/MCB.23.15.5409-5420.2003